

---

DIRECTED DIFFERENTIATION OF  
HUMAN EMBRYONIC STEM CELLS  
TO MICROGLIAL-LIKE CELLS

---



A thesis

submitted in fulfilment of the requirements for the degree

of

**Doctor of Philosophy (PhD)**

at the

**School of Biosciences, Cardiff University**

by

**Emma Louise Cope**

**2014**

---

# ABSTRACT

---

Protein aggregations of  $\beta$ -Amyloid ( $A\beta$ ) and Tau are alone not sufficient to account for all the symptoms and progression of Alzheimer's Disease (AD), as such there is much emphasis upon the immune component of the disease. The cells of the brain that are capable of initiating an immune response are microglia; these are derivatives of hematopoietic cells and they have the capacity to phagocytose and clear  $A\beta$  aggregates or release cytokines such as  $TNF-\alpha$ , in a neurotoxic role, promoting apoptosis of the surrounding neurons and hence aiding disease progression.

To uncover the precise role of microglia in terms of AD we propose a protocol to enable differentiation of microglia from human embryonic stem cells (hESCs). The protocol we propose is a two-step differentiation procedure i) hESCs to monocytes followed by ii) ES-derived monocytes to microglia.

**Chapter 3:** Exogenous over-expression of PU.1, a transcription factor vital in both the onset of haematopoiesis and the terminal differentiation of monocytes and microglia, was revealed to enable differentiation to a hematopoietic fate.

**Chapter 4:** hESCS were differentiated to monocyte-like cells ( $CD45^+/CD11b^+$ ) through culture in the presence of the hematopoietic growth factors; M-CSF and IL-3.

**Chapter 5:** focuses on the differentiation of ES-derived monocytes to microglia. It shows that monocytes cultured in astrocyte conditioned medium give rise to cells that are  $IBA-1^+/Glut5^+/CD45^{low}/NG2^{low}/CD80^+/CD11c^+$  and have a ramified

microglial phenotype, which upon stimulation with  $A\beta_{(1-42)}$  can become activated to the amoeboid phenotype.

The development of the protocol for the generation of microglia holds great importance in terms of creating *in vitro* models for AD research as a whole and can be extended to the differentiation of patient iPSCs that contain mutations in genes associated with innate immunity or SNPs associated with AD risk, disease onset and progression.



---

# ACKNOWLEDGEMENTS

---

*To all at Alzheimer's Research UK, thank you for all of your hard work to be able to support this research, it's been a pleasure working with you and let's hope we are now one step, however small, closer to defeating dementia.*

I would first of all like to thank my supervisor Prof. Nick Allen, without whom none of this work would have been possible. I sincerely thank you for all the wonderful opportunities that you have given me over the years and for all of your thoughts and your feedback that enabled me to complete this thesis. Similarly I'd also like to thank Prof. Paul Kemp for all your input in the recent years, it's been greatly appreciated. I would also like to extend my gratitude to Dr. Sally Cowley, for kindly sharing her protocols for monocyte differentiation prior to publication.

I also wanted to thank the members of the lab, both past and present; Shona, Susannah, Sali, Shun-Ming, Rachel and Charlie. Thank you for making the long days, late nights and weekends in the lab enjoyable and unforgettable. I especially wanted to acknowledge Shona and Susannah, from whom I've learned so much!

To Dr. Julia Griffiths, thank you for all of your input with the electrophysiology section of the thesis, I really couldn't have done that without your expertise.

Finally I would like to acknowledge all of my family and friends who have supported me unequivocally throughout the whole process. In particular I'd like to thank my parents, I know it hasn't been easy but through the hardest times and the greatest moments you were, and are still, always there. Thank you!

---

# ABBREVIATIONS

---

AB	Amyloid $\beta$
ACM	Astrocyte Conditioned Media
AD	Alzheimer's Disease
ADF	Advanced DMEM F12
AGM	Aorta Gonad Mesonephros
APC	Allophycocyanin
APP	Amyloid Precursor Protein
BBB	Blood Brain Barrier
BDNF	Brain-Derived Neurotrophic Factor
bFGF	Basic Fibroblast Growth Factor
BMP4	Bone Morphogenetic Protein 4
BrdU	Bromodeoxyuridine
C/EBP $\alpha$	CCAAT/Enhancer Binding Protein $\alpha$
Casp	Caspase
CD	Cluster of Differentiation
CFU-G	Colony Forming Unit – Granulocyte
CFU-M	Colony Forming Unit – Monocyte
CLP	Common Lymphoid Precursor
CNS	Central Nervous System
DAPT	N-[N-(3,5-difluorophenacetyl)-L-alanyl]-S-phenylglycine-t-butylester

DMEM	Dulbecco's Modified Eagle Media
EAE	Experimental Autoimmune Encephalomyelitis
EGF	Epidermal Growth Factor
Egr-1	Early Growth Response Protein 1
EM	Electron Microscopy
EMT	Epithelial to mesenchyme transition
EPO	Erythropoietin
ESdM	ES-derived Monocytes
ESdMG	ES-derived Microglia
fAB	Fibrillar Amyloid $\beta$
FBS	Fetal Bovine Serum
FITC	Fluorescein Isothiocyanate
FLK1	Fetal Liver Kinase 1 ( <i>Also known as VEGFR</i> )
GATA-1	Globin Transcription Factor 1
G-CSF	Granulocyte Colony Stimulating Factor
GFAP	Glial Fibrillary Acidic Protein
Gfi-1	Growth Factor Independent 1 Transcription Repressor
GFP	Green Fluorescent Protein
GM-CSF	Granulocyte Macrophage Colony Stimulating Factor
GM-CSFR $\alpha$	Granulocyte Macrophage Colony Stimulating Factor Receptor $\alpha$
GMP	Granulocyte Macrophage Precursors
HAND	HIV Associated Neurocognitive Disorder
hESC	Human Embryonic Stem Cell
HIV	Human Immunodeficiency Virus
HSC	Haematopoietic Stem Cell

IBA-1	Ionised Calcium-Binding Adapter Molecule 1
ICAM-1	Intracellular Adhesion Molecule 1
IFN	Interferon
IGF-1	Insulin-like Growth Factor 1
IL	Interleukin
IPSC	Induced pluripotent Stem Cell
JAK	Janus Kinase
KSR	Knockout Serum Replacement
LIF	Leukemia Inhibitory Factor
LMP	Lymphoid Myeloid Precursor
LN	Melanophillin
LPS	Lipopolysaccharide
Mac-1	Macrophage -1 Antigen
M-CSF	Macrophage Colony Stimulating Factor
MEF	Mouse Embryonic Fibroblasts
MEFi	Irradiated Mouse Embryonic Fibroblasts
MEP	Megakaryocyte – Erythrocyte Progenitor
mESC	Mouse Embryonic Stem Cell
MHC-II	Major Histocompatibility Complex Class II
MS	Multiple Sclerosis
NADPH	Nicotinamide Adenine Dinucleotide Phosphate
NFT	Neurofibrillary Tangles
NFkB	Nuclear Factor kappa-light-chain-enhancer of Activated B Cells
NG2	Chondroitin Sulfate Proteoglycan 4
NGF	Nerve Growth Factor

NLR	NOD-Like Receptor
NLRP3	NLR family Pyrin domain 3
NMDA	N-Methyl-D-Aspartic Acid
NSAID	Non-Steroidal Anti-Inflammatory Drug
PE	Phycoerythrin
PHL	Paired Helical Filaments
PRR	Pattern Recognition Receptors
PS	Phosphatidylserine
PSEN	Presenillin
RAGE	Receptor for Advanced Glycation Endproducts
RFD7	Macrophage Antibody
RGCs	Radial Glial Cells
RUNX1	Runt Related Transcription Factor 1
sAPP	Soluble Amyloid Precursor Protein
SCF	Stem Cell Factor
SCID	Severe Combined Immunodeficiency
SOD	Superoxide Dismutase
SRA	Scavenger Receptor
SSEA	Stage Specific Embryonic Antigen
STAT	Signal Transducer and Activator of Transcription
TGF $\beta$	Transforming Growth Factor $\beta$
TH	T Helper Cell
THPO	Thrombopoietin
TLR	Toll Like Receptor
TPA	Tissue Plasminogen Activator

TREM2      Triggering Receptor Expressed on Myeloid cells 2

VEGF      Vascular Endothelial Growth Factor

---

# CONTENTS

---

1.	INTRODUCTION .....	1
1.1	MICROGLIA .....	1
1.1.1	GLIAL CELLS .....	1
1.1.2	MICROGLIAL ORIGIN .....	4
1.1.3	MICROGLIA AND THEIR HEMATOPOIETIC PRECURSORS .....	7
1.1.4	ION CHANNELS IN MICROGLIA .....	14
1.1.5	PHENOTYPES OF MICROGLIA .....	19
1.1.6	MICROGLIAL FUNCTION IN HEALTH AND DISEASE .....	22
1.2	ALZHEIMER'S DISEASE .....	25
1.2.1	ALZHEIMER'S DISEASE .....	25
1.2.2	MECHANISMS OF ALZHEIMER'S DISEASE .....	26
1.2.3	MICROGLIAL ROLES IN ALZHEIMER'S DISEASE .....	29
1.2.4	CURRENT MODELS OF ALZHEIMER'S DISEASE .....	33
1.3	STEM CELLS .....	35
1.3.1	HUMAN EMBRYONIC STEM CELLS .....	35
1.3.2	<i>IN VITRO</i> DIFFERENTIATION POTENTIAL OF ES CELLS .....	39
1.3.3	INDUCED PLURIPOTENT STEM CELLS .....	39
1.3.4	EMBRYONIC AND INDUCED PLURIPOTENT STEM CELLS IN DISEASE .....	40
1.4	AIMS .....	42
2.	MATERIALS AND METHODS .....	45
2.1	MATERIALS .....	45
2.1.1	CELL CULTURE REAGENTS .....	45
2.1.2	SOLUTIONS, BUFFERS AND ENZYMES .....	48
2.1.3	PRIMERS .....	52
2.1.4	ANTIBODIES .....	53
2.1.5	CONSUMABLES .....	55
2.1.6	KITS .....	56
2.1.7	EQUIPMENT .....	56
2.1.8	SOFTWARE .....	57

2.2 MEFI FEEDER LAYER .....	58
2.2.1 GROWING AND IRRADIATING MEFS .....	58
2.2.2 PLATING IRRADIATED MEFS .....	59
2.3 MAINTENANCE OF ES CELLS .....	59
2.4 GENERATION AND MAINTENANCE OF HSCS .....	59
2.5 MAINTENANCE OF THP-1 MONOCYTES .....	60
2.6 NEURAL PROGENITOR CELL CULTURE .....	60
2.7 NUCLEOFECTION .....	61
2.7.1 CREATING THE PCAGG-PU.1-IRES-GFP CONSTRUCT .....	61
2.7.3 AMAXA NUCLEOFECTION .....	63
2.7.3 SELECTION .....	64
2.7.4 DIFFERENTIATION TO MONOCYTIC PRECURSORS .....	64
2.8 MONOCYTE DIFFERENTIATION TO MICROGLIAL-LIKE CELLS .....	64
2.8.1 ASTROCYTE CONDITIONED MEDIA .....	64
2.8.2 MONOCYTE DIFFERENTIATION TO MICROGLIAL-LIKE CELL .....	65
2.8.3 ADDITION OF AB .....	65
2.11 IMMUNOCYTOCHEMISTRY .....	65
2.12 FACS .....	66
2.12.1 SINGLE COLOUR STAINING .....	66
2.12.2 TRIPLE COLOUR STAINING .....	66
2.13 HISTOLOGY .....	67
2.13.1 CYTOCENTRIFUGATION .....	67
2.13.2 STAINING .....	67
2.14 PHAGOCYTOSIS ASSAY .....	67
2.15 QPCR .....	68
2.16 WESTERN BLOT .....	70
2.17 ELECTROPHYSIOLOGY .....	71
2.18 CYTOKINE/CHEMOKINE ARRAYS .....	71
2.19 STATISTICS .....	72
3. GENERATION OF MONOCYTES BY ECTOPIC OVER- EXPRESSION OF PU.1 .....	73
3.1 INTRODUCTION .....	73
3.2 AIM .....	74
3.3 VECTOR CONSTRUCTION .....	75
3.4 NEURAL PRECURSOR DIFFERENTIATION .....	77
3.5 NUCLEOFECTION OF NEURAL PROGENITORS .....	79

3.6 DIFFERENTIATION OF TRANSFECTED CELLS .....	84
3.7 NON-ADHERENT CELL CHARACTERISATION .....	89
3.8 DATA SUMMARY .....	94
3.9 DISCUSSION .....	95
4. M-CSF/IL-3 DIRECTED DIFFERENTIATION .....	99
4.1 INTRODUCTION.....	99
4.1 AIM .....	102
4.2 THE NON-HAEMATOPOIETIC NATURE OF HESCS .....	104
4.3 THE MONOCYTE PRODUCING COLONIES .....	108
4.4 ES-DERIVED MONOCYTES.....	114
4.5 FUNCTIONALITY OF ES-DERIVED MONOCYTES .....	121
4.6 DATA SUMMARY .....	125
4.7 DISCUSSION .....	126
5. DIFFERENTIATION OF ES-DERIVED MONOCYTES TO MICROGLIAL-LIKE CELLS .....	126
5.1 INTRODUCTION.....	126
5.2 AIM .....	130
5.3 MONOCYTE DIFFERENTIATION TO MICROGLIAL-LIKE CELLS .....	131
5.4 ELECTROPHYSIOLOGICAL PROFILE OF ES-DERIVED MICROGLIAL- LIKE CELLS.....	140
5.5 FUNCTIONALITY OF ES-DERIVED MICROGLIAL-LIKE CELLS .....	145
5.6 DATA SUMMARY .....	154
5.7 DISCUSSION .....	155
6. GENERAL DISCUSSION .....	161
6.1 MONOCYTE DIFFERENTIATION .....	161
6.1.1 PU.1 OVEREXPRESSION.....	161
6.1.2 MCSF/IL3 DIRECTED DIFFERENTIATION.....	163
6.2 MONOCYTE DIFFERENTIATION TO MICROGLIAL-LIKE CELLS .....	165
6.2.1 ASTROCYTE CONDITIONED MEDIA (ACM).....	165
6.3 LEGITIMACY OF STUDY .....	167
6.3.1 DIFFERENTIATION STRATEGY .....	167
6.3.2 MICROGLIAL MARKERS .....	168
6.3.3 THP1 MONOCYTIC CELLS AS A CONTROL CELL LINE .....	169
6.3.4 THE EFFECT OF NEUROBREW 21 IN THE ACM.....	170
6.4 IMPACT OF STUDY.....	172
6.5 FURTHER WORK.....	174

7. REFERENCES .....	177
APPENDICES .....	195
APPENDIX I .....	195
I.I PU.1 SEQUENCED REGION (825BP) .....	195
I.II PCAGIG .....	196
I.III PIRES2-EGFP .....	197
I.IV PCAGG-IRES-GFP .....	198
I.V PCAGG-PU.1-IRES-GFP .....	199
APPENDIX II .....	200
II.I QPCR PRIMER DATA SHEETS .....	200

---

# 1. INTRODUCTION

---

---

## 1.1 MICROGLIA

---

---

### 1.1.1 GLIAL CELLS

---

The brain tissue is composed of two groups of cells, neurons and glia, the former are cells capable of initiating action potentials, synthesizing neurotransmitters and using the synthesized neurotransmitters to transmit signals across synapses. The latter are a group of cells that, unlike neurons, are unable to transduce action potentials but are vital for the correct functioning of neurons and in the maintenance of brain homeostasis. Glia encompass both macroglia and microglia, two functionally and developmentally distinct groups of cells.

Although diverse in their function, neurons and macroglia are intricately linked through cell lineage and their differentiation during the development of the embryonic central nervous system (CNS) and in adult neurogenesis. During development of the brain, a portion of the embryonic ectoderm becomes specialized forming the neuroectoderm. These signals include noggin and chordin, which function through the inhibition of BMP4, a TGF $\beta$  family protein that represses a neural fate (Spörle & Schughart, 1997, Bronner-Fraser & Fraser, 1997).

The neuroepithelial cells of the neuroectoderm differentiate into radial glial cells (RGCs) and acquire features common to astrocytes, including; the presence of glycogen granules and glial fibrillary acidic protein (GFAP), and act as progenitors for both neurons and glia during development (Costa et al. 2010; Doetsch 2003). RGCs

are elongated between the ventricular and pial surfaces, these cells then undergo expansion through symmetrical division to increase the stem cell pool, but at the onset of neurogenesis they divide asymmetrically generating a stem cell that remains in the ventricular zone and a neuron, which migrates radially, utilising the radial glia as a scaffold, thickening the structure of the brain (Merkle and Alvarez-Buylla 2006). Due to the increased complexity of the human cerebral cortex there is a second set of progenitors within the outer subventricular zone, which enables neurogenesis to occur at both the ventricular zone and the outer subventricular zone, during mid gestation (Hansen et al. 2010). When neurogenesis is near completion the RGCs revert to symmetrical divisions resulting in the formation of glial cells (Sun et al. 2003). At birth, in mammals, the RGCs differentiate into astrocyte-like cells and oligodendrocytes, in the ventral regions. The astrocytes, in particular, are thought to provide the stem cell niche for adult neurogenesis in the olfactory bulb and hippocampus through asymmetric divisions (Doetsch 2003).

Macroglial cells were first described by Virchow, in the middle of the 19<sup>th</sup> century, as neuroectoderm-derived non-neuronal cells (Virchow 1846). They are numerous, diverse cells and although intricately linked to neurons their functions are far from analogous. Later in the 19<sup>th</sup> century it was deduced that macroglia comprise both the oligodendrocytes and astrocytes along with ependymal cells that line the brain ventricles (Merrill 1987).

Oligodendrocytes are the central nervous system equivalent of the peripheral Schwann cells, their profuse processes wrap around the closely associated neurons forming the insulating myelin sheath surrounding axons and increasing the transduction velocity of action potentials (Heneka et al. 2010). The importance of the

oligodendrocyte myelin sheath is evident in diseases where the myelination of axons is disrupted. Multiple sclerosis (MS) for instance is an autoimmune disease, but during the initial progressive stage loss of myelination in MS lesions is due to oligodendrocyte cell death, rather than inflammation (De Keyser et al. 2008).

Astrocytes are the most abundant cells of the human brain, they are characteristically star shaped cells that are organised into vast networks, which not only maintain the Blood Brain Barrier (BBB) and provide structural and metabolic support to neurons, but actively influence neurotransmission through calcium dependent glutamate release (Bushong et al. 2004; Parpura et al. 1994). Astrocytes are so fundamental in the maintenance of brain homeostasis that they are implicated in many pathologies, from migraines to epilepsy, where  $Ca^{2+}$  levels in astrocytes are key in causing excessive depolarization of surrounding neurons, and astrocytes are also fundamental in the progression of many neurodegenerative diseases (De Keyser et al. 2008).

Whereas astrocytes and oligodendrocytes derive from neuroepithelium, microglia are now thought to have a mesodermal origin, invading the developing brain from embryonic blood islands and bone marrow in the adult. Microglia are thought of as brain macrophages and their physiological function extends beyond immunity to glutamate-dependent release of neurotrophic factors; BDNF and NGF and monitoring the function of neurons as well as removal of cellular debris and pathogens, much like tissue macrophages (Liang et al. 2010). Microglia are also implicated in pathologies including HIV associated neurocognitive disorder (HAND) and multiple sclerosis, as well as Parkinson's and Alzheimer's disease.

---

### 1.1.2 MICROGLIAL ORIGIN

---

Microglia were first described within the third element, neither neuron nor astrocyte, by Cajal (1913) before his student del Rio-Hortega (1919) unearthed microglia from the oligodendrocyte – microglial composite of the third element in the early twentieth century where their origin has been debated ever since. There are many hypotheses regarding microglial derivation in early development; (1) a neuroectodermal origin from glioblasts in the same manner as astrocytes and oligodendrocytes, (2) yolk sac derived mesenchymal tissue associated with neuroepithelium or (3) invasion of blood monocytes (Chan, Kohsaka, & Rezaie, 2007).

Although a haematopoietic nature of microglia is generally now accepted, several studies have shown evidence that at least some of the microglial population could be of neuroectodermal origin. Autoradiographic studies by Kitamura et al. (1984) showed that there is continuous differentiation of microglia from the glioblasts in the grey matter, which are also the source of astrocytes and oligodendrocytes. Labeling of neuroepithelial and microglial fractions taken from the developing rat brain showed cells positive for lipocortin-I, a protein responsible for mediating anti-inflammatory responses induced by glucocorticoids, within both fractions indicating a potential neuroepithelial origin (Fredoroff 1995; Flower and Rothwell 1994). Further evidence for their neuroectodermal origin came from culturing mouse neuroepithelial cells, free of Mac-I+ microglial precursors, which lead to the production of microglia and macrophage-like cells (Hao et al. 1991).

The neuroectodermal theory of microglial origin has been contested by the more likely haematopoietic route. Much evidence is in support of the latter hypothesis as it was determined that microglia share not only function but also marker and enzyme expression with tissue macrophages (Ling et al. 1982; Boya et al. 1979; Cuadros

and Navascués 1998). This overwhelming similarity to macrophages leads to the conclusion that microglia are indeed members of the mononuclear phagocyte family and moreover, closely related to monocytes and macrophages (Cuadros and Navascués 1998). This is by no means a modern idea, it was suggested by del Rio-Hortega, soon after their discovery, that microglia were of mesodermal rather than neuroectodermal origin (del Rio-Hortega 1932).

A close link has been made between the yolk sac and microglial precursors. Alliot et al. (1999) showed that the number and appearance of microglial precursors in the neural folds is preceded by their appearance in the yolk sac where their numbers continue to outnumber those in the brain (Figure 1.1). Work by Ginhoux et al. (Ginhoux et al. 2010), suggests that microglial cells are visible in the neuroepithelium in mice from day E10.5, Theiler stage 16, equivalent to Carnegie stage 13 or day 28 in human embryogenesis, whilst others suggest that human microglia are present from the second trimester. From birth and throughout adult life renewal of microglial cells can occur via invasion of circulating blood monocytes across a permeable BBB or through microglial self-renewal (Davoust et al. 2008).

Upon accepting that microglial cells could originate from outside of the nervous system, the question became how and when do haematopoietic cells enter nervous tissue? There are three possible routes of mesodermal cell entry to the brain; 1) from the meninges through the pial surface, 2) from the ventricles through the ventricular layer and 3) from the blood stream through the BBB. The meninges, the membrane surrounding the CNS, were the first proposed route of entry by del-Rio-Hortega who described the pial margins as a sizeable source of microglia (del Rio-Hortega 1932). The ventricles also pose as entry sites of microglia into the brain, macrophage cells

have been found within the ventricle along with evidence to show microglial cells in the process of crossing the ventricular layer (Jordan & Thomas 1988; Navascués et al. 1996). Finally the blood stream, which although more problematic in the mature brain, due to the BBB, it is a route that provides entry to large numbers of microglial precursors during development prior to the formation of the BBB proper and could be the route of entry during pathologies and in old age where the BBB becomes permeable. Here the invading microglial precursors attach to vessel walls through the ICAM-I homing and adhesion system, which as has been implicated in monocyte

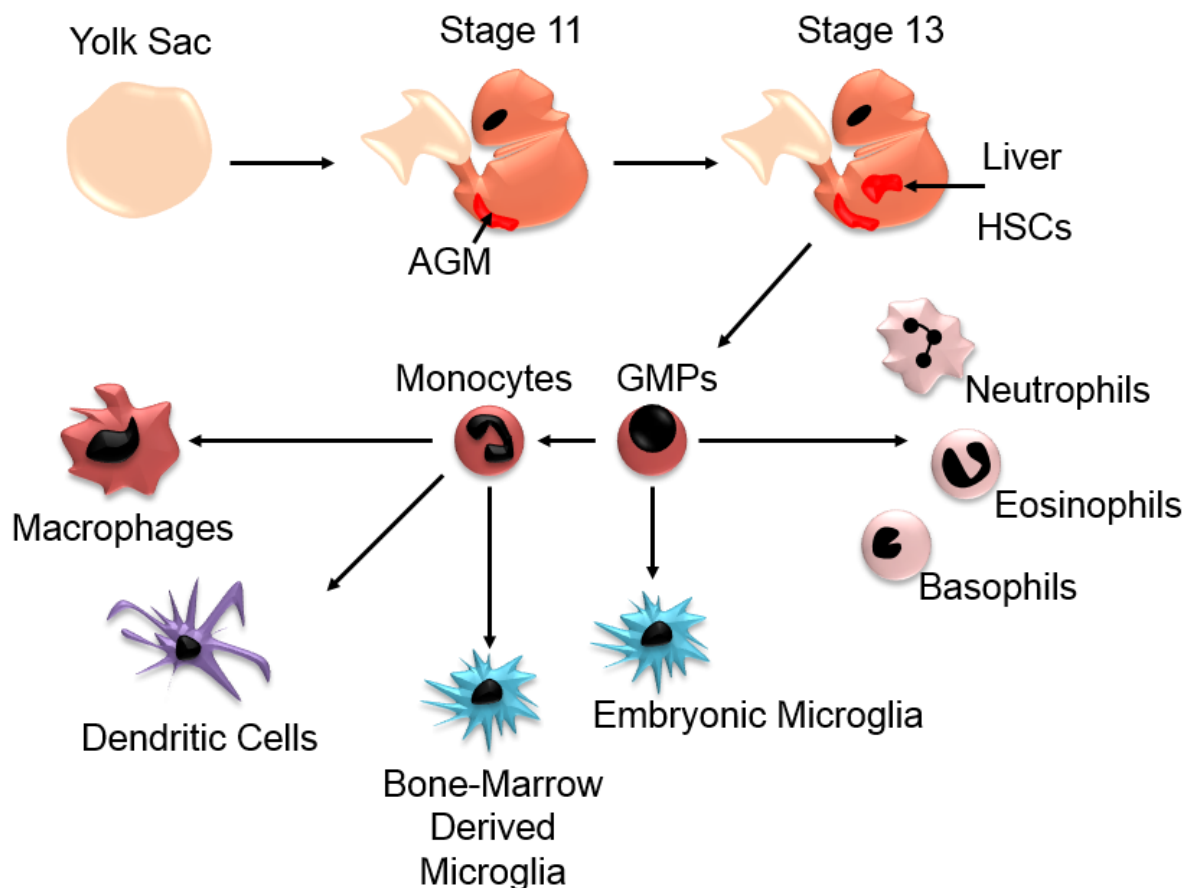


**Figure 1.1. Origin of Microglia**

At Carnegie stage 11 the Aorta-Gonad-Mesonephros (AGM) develops and is the site of primitive haematopoiesis until the liver adopts the role at stage 13 in development. It is at this stage that a large number of CD34+ haematopoietic stem cells (HSCs) are observed. These HSCs further differentiate into Granulocyte Macrophage precursors (GMPs) which allow for the formation of many cells of the haematopoietic system, including monocytes and microglia which enter the developing brain prior to the formation of the BBB proper and proliferate *in situ* until birth. Monocytes have the capacity to form macrophages and dendritic cells and also microglia, by the invasion of circulating monocytes into the adult brain especially under pathological conditions where the BBB is not fully intact.

---

### 1.1.3 MICROGLIA AND THEIR HEMATOPOIETIC PRECURSORS

---

Embryonic haematopoiesis provides the necessary precursors for microglia. The process begins in the yolk sac where hematopoietic precursors migrate into the mesenchyme and are subsequently surrounded by epithelial cells, which aggregate and form the blood islands of early embryonic haematopoiesis enabling survival of the fetus until haematopoiesis at the AGM is initiated (McGrath and Palis 2005; Palis and Yoder 2001). The blood islands are thought to contain the haemangioblast, a cell type with the capability to differentiate into blood or endothelial cells in the absence or presence of the VEGF receptor, FLK1, respectively. It has been shown that FLK1 deficient mice are unable to form primitive embryonic blood cells (Palis and Yoder 2001). FLK1 is not required for their definitive differentiation, which is instead dependent on RUNX1, a transcription factor that is up regulated at the haemangioblast stage, which has the ability to bind to the downstream regulatory elements of CD34, thus promoting the formation of the Haematopoietic Stem Cell, HSC (Lacaud et al. 2002; Yokomizo et al. 2008; Levantini et al. 2011).

The yolk sac is primarily utilized in erythrocyte production to oxygenate the developing fetus prior to hematopoiesis in the AGM, liver and ultimately bone marrow; but there are also limited numbers of macrophages produced (Sasaki & Matsamura 1986). These fetal macrophages differ from their adult counterparts, as they do not derive from monocytes but instead, derive from their own macrophage precursor (Moore and Metcalf 1970). It has also been seen in mice that yolk sac derived cells, whether distinct from the macrophage precursor is unknown, migrate to the CNS and form microglia (Palis et al. 1999). This is known as the first wave of microglial engraftment during the non-vascular period, forming embryonic microglia.

The resultant HSC colonizes the liver and spleen, followed by the bone marrow where normal hematopoiesis ensues and the focus becomes granulopoiesis rather than erythropoiesis, with the formation of neutrophils, eosinophils and basophils along with monocytes and lymphocytes (Figure 1.2). These monocytes are then able to traverse the developing BBB where they differentiate into bone-marrow derived microglia, forming the adult microglial population. There is a lack of distinction from the literature as to whether fetal haematopoiesis and the formation of this HSC is primitive or definitive in nature, but this could be the reason that there seem to be two distinct populations of microglia, which could be divided based on their expression of HOXB8. Chen et al. (2010) showed that only the bone marrow derived microglia were HOXB8<sup>+</sup>, which represented only 40% of the total microglial pool, whilst the remaining 60% of microglia were HOXB8<sup>-</sup> and thus have an origin outside of the bone marrow, potentially the yolk sac.

Microglial maintenance in adult life is quite different to that of the colonization of microglial of the CNS in the foetus. Microglia, unlike their tissue macrophage counterparts, have the ability to self-renew enabling the microglial pool to be replenished even though the blood brain barrier is intact. Microglial engraftment from bone marrow derived cells has long been a source for study by many groups. Ablation of native immune cells followed by the transplantation of GFP marked donor cells leads to invasion of the choroid plexus, leptomeninges and perivascular regions by donor cells (Tanaka et al. 2003). But few donor cells have been seen infiltrating the brain parenchyma proper (Kennedy 1997). A study by Priller et al. (2001) showed that 4 months post-transplantation 25% of the microglial pool was donor derived. Kinetic studies of microglia recruitment have shown that although derived from bone marrow cells, microglia are engrafted much more slowly than other

macrophages where 89% of splenic macrophages were found to be of donor origin after just 4 weeks and nearly two thirds of alveolar macrophages were donor derived by 12 months post-transplantation (Kennedy and Abzowitz 1997).

Invasion of donor cells to the inner regions of the brain can be enhanced by brain injury, where these cells become indistinguishable from endogenous microglia and develop into a major mechanism of the disease pathology. Under certain conditions, in models of bacterial meningitis for example, bone marrow derived microglia recruitment can occur after the onset of disease, where their function is largely skewed toward tissue repair rather than the inflammation associated with disease pathology (Djukic et al. 2006). Conversely Ajami et al. (2011) suggested that although microglia can be derived from the bone marrow in their model of EAE due to the normal mechanism for their exclusion failing, these cells do not remain in the endogenous microglial pool subsequent to the pathology instead they suggest that microglia are maintained *in situ* through a process of self-renewal via a small number of precursor cells. But engraftment of donor cells to the brain during injury has posed as an attractive route for the delivery of genetically modified cells to the CNS to prevent further damage caused by the pathology and to aid recovery.

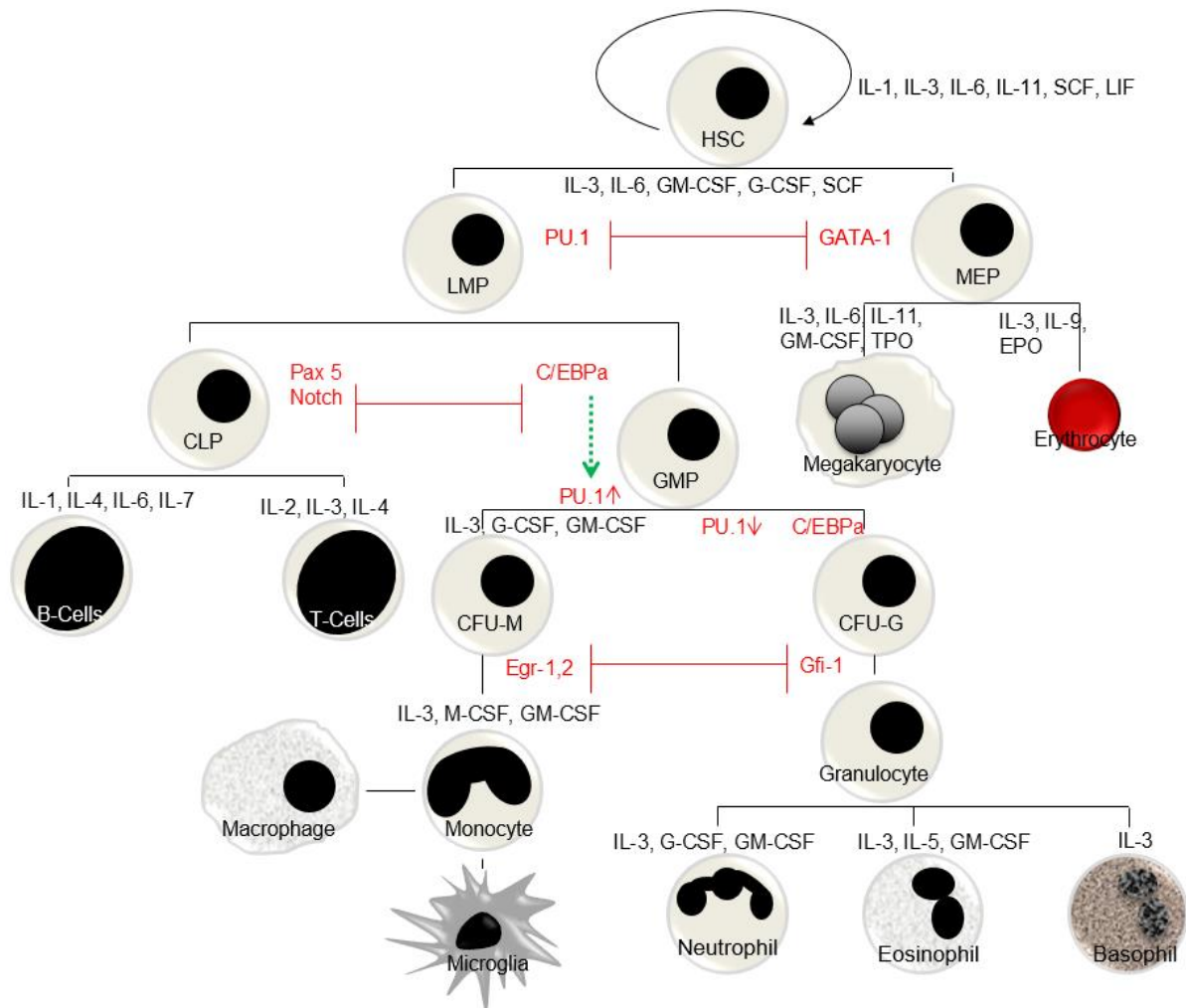


**Figure 1.2. Adult Hematopoiesis**

Haematopoietic stem cells (HSCs) are capable of self renewal, in order to keep a pool of pluripotent cells, and this occurs under the influence of IL-1, IL-3, IL-6, IL-11, SCF and LIF. The transcription factor GATA-1 induces lineage commitment to a Megakaryocyte-Erythrocyte Progenitor (MEP). The cytokines IL-3, IL-6, IL-11, GM-CSF and TPO induce meagakaryocyte differentiation whereas IL-3, IL-9 and EPO result in the formation of erythrocytes. PU.1, on the other hand, induces the differentiation of a lymphoid myeloid precursor (LMP) from the HSC. PU.1 and GATA-1 antagonise each other which keep the HSC differentiation fates unbiased. Expression of the transcription factors Pax5 and Notch result in the formation of a Common Lymphoid Precursor (CLP). B-cells are formed under the influence of IL-1, IL-4, IL-6 and IL-7 or IL-2, IL-3 and IL-4 result in the formation of T-cells. Pax5 and Notch are inhibitors of C/EBP $\alpha$ , the transcription factor required for the development of the Granulocyte Monocyte Progenitor (GMP). The GMP can differentiate into either granulocytic or monocytic precursors, which depends on the level of PU.1 expression. Low levels of PU.1 and C/EBP $\alpha$  commit the GMPs to granulocytic precursors (CFU-G) whereas high levels of PU.1, induced by C/EBP $\alpha$ , along with IL-3, G-CSF and GM-CSF result in monocytic precursors (CFU-M). CFU-G are able to, under the influence of Gfi-1, differentiate into neutrophils, eosinophils or basophils. Egr-1,2 expression and secretion of IL-3, M-CSF and GM-CSF results in CFU-M differentiation to monocytes, which ultimately mature into macrophages or microglia (*Modified from Friedman 2006 and Dale 2008*).

As suggested microglia can be derived from monocytes, both during development and throughout adult life, monocytes are also the precursors to macrophages and as such both macrophages and microglia behave similarly, with a capacity to phagocytose and present antigens to T-cells. They also express many of the same surface markers, making it extremely difficult to distinguish between the two populations of cells. A list of markers (Table 1.1) that showed differential expression between macrophages and microglia was compiled by Guilleman and Brew (2004) but they concluded that only under Electron Microscopy (EM) could the cells be truly distinguished. Scanning EM showed that microglia were identifiable by a surface covered in spines compared to the smooth exterior of the macrophage, but a consensus profile of marker expression was also determined for the identification of microglia; CD68+, CD45<sup>low</sup>, CD11c<sup>high</sup>, MHC-II+, CD14+, IBA-1+ (Guillemin and Brew 2004).

The most universally utilised stain for microglial identification is IBA-1, a protein that has a role within the histocompatibility complex and in calcium binding. IBA-1 is expressed exclusively by microglia in brain slices, but when removed from the remit of the brain, expression is found in monocytic lineage cells in other organs (Ito et al. 1998; Imai et al. 1996). The search for a specific marker for the characterization of microglia found that antibodies against the human glucose transporter, GLUT5, could be used in the place of IBA-1 for identifying microglia (Sasaki et al. 2003). GLUT5, in human tissue, is advantageous over IBA-1 as it is able to stain microglia specifically, even over the other closely related cells such as the perivascular macrophage ( Kettenmann et al. 2011).

Kettenmann et al. (1993) also describe another means of macrophage and microglia distinction; electrophysiology. They found that microglia only express inwardly rectifying potassium channels making them highly susceptible to depolarization events whereas macrophages are less prone to depolarization as they possess outwardly rectifying potassium channels.

**Table 1.1. Comparison of Marker Expression in Early Haematopoietic Cells, Macrophages and Microglia**

The expected expression profile for each stage of differentiation can be used to identify the generated cell type. Although a specific marker for the identification of microglia is difficult to find, the difference in the presence of numerous markers compared to macrophages can lead to a positive identification of microglia. Of note are the differences in proliferation (Ki-67), CD11c and CD45. Asterisks denote expression only when the cell is activated.

(Modified from Guillemin and Brew 2004)

<b>Marker</b>	<b>Early Haematopoietic Precursor</b>	<b>Macrophage</b>	<b>Microglia</b>
<b>FLK1</b>	++	+*	+*
<b>RUNX1</b>	++	-	+*
<b>CD34</b>	++	-	+*
<b>PU.1</b>	+++	++	++
<b>Ki-67</b>	+	-	+
<b>CD11c</b>	-	+	+++
<b>CD11b</b>	-	++	++
<b>CD14</b>	-	+	-
<b>CD45</b>	+	+++	+
<b>CD80</b>	-	-	+
<b>NG2</b>	-	++	-
<b>IBA-1</b>	-	+*	++
<b>GLUT5</b>	-	+*	++
<b>Kir2.1</b>	-	+	++
<b>NaV1.5</b>	-	+	+
<b>NaV1.6</b>	-	+	++
<b>RFD7</b>	-	+++	-
<b>Substance P</b>	-	+	+++
<b><math>\alpha</math>1-chymotrypsin</b>	-	++	-

---

#### 1.1.4 ION CHANNELS IN MICROGLIA

---

Microglia express numerous ion channels from  $\text{Cl}^-$  to  $\text{H}^+$  as well as  $\text{K}^+$  and  $\text{Na}^+$  channels that are fundamental in their correct functioning. The most controversial of which are the voltage-gated  $\text{Na}^+$  channels. Such channels open only in response to a current, where the activation gate in the  $\alpha$ -subunit can open to allow  $\text{Na}^+$  ions to flow into the cell causing depolarization. At the peak of depolarization the pore is plugged by the inactivation gate to prevent reactivation. The channel has a built in filter to only allow passage of  $\text{Na}^+$  ions, in the form of the negatively charged amino acid lining of the pore and the pore size; large enough to enable a single  $\text{Na}^+$  ion and an associated water molecule. This family of channels has numerous isoforms with the majority being expressed in the nervous system during development. Microglia on the other hand only express three of the ten isoforms, Nav1.1, 1.5 and 1.6, with Nav1.6 being the most prominent in cultured rodent microglia (Black and Waxman, 2009). Controversy lays with the tetrodotoxin (TTX) insensitive Nav1.5 channels, which seem to be the focus of human microglial studies, but neglected in rodent experiments (Nicholson 2009). These channels have been found to be linked to the activation state of the cells, those challenged with Lipopolysaccharide (LPS) or CNS damage show an increase in expression of those channels. Blocking the channels with TTX or phenytoin leads to a reduction in microglial activation.

Rodent microglia also have a distinctive pattern of  $\text{K}^+$  channel expression, which enables ramified microglia to be distinguished from macrophage. When inactive and immature, microglia show activity of only inwardly rectifying  $\text{K}^+$  channels, with very little activity of the outward or voltage gated channels (Kettenman et al. 1993). Inwardly rectifying channels are able to pass positively charged ions, current, into the cell much more easily than out. This enables the cell to maintain a negative resting

membrane potential. In microglia the inwardly rectifying  $K^+$  channels resemble those of the  $K_{ir}2.1$  channels and enable the maintenance of a negative membrane potential, which facilitates the influx of  $Ca^{2+}$  ions that are required for proliferation. When activated by either hypoxia, CNS damage or immune onslaught, the cells transform from the quiescent ramified cell to the amoeboid form, a state very similar if not indistinguishable from a macrophage, there is then activity from the voltage gated  $K^+$  channels. In rodents there has been a proposed link between  $K_v1.3$  and the production of the pro-inflammatory cytokines IL-1 $\beta$  and TNF $\alpha$ . In the case of IL-1 $\beta$  a decrease in the concentration of intracellular potassium, through efflux via  $K_v$  channels, is required to facilitate the functioning of ICE/Caspase 1, the enzyme required to cleave pro-IL-1 $\beta$  to the active cytokine.  $K_v$  channels are also present in microglia subsequent to attachment to a substratum due to changes in the structure of the membrane (McLarnon et al. 1997). Although a valuable marker for rodent microglia the presence of  $K_{ir}$  channel activity and the absence of activity from  $K_v$  channels is less pronounced in human microglia where the majority of cells possess activity from both channels (McLarnon et al. 1997).

Another proposed important  $K^+$  channel in microglia is the small conductance  $Ca^{2+}$ /calmodulin activated  $K^+$  channel (KCNN4/KCa3.1/SK4/IK1). Cell hyperpolarisation leads to an influx of  $Ca^{2+}$  through voltage-gated  $Ca^{2+}$  channels, which binds to the calmodulin (CaM). CaM binds to its binding domain within the intracellular portion of the KCa3.1 channel, which causes a conformational change and the subsequent mechanical opening of the pore to allow  $K^+$  ions to move out of the cell. Treating microglial with TRAM-34, a KCa3.1 inhibitor, was shown to decrease microglial activation and the resultant neuronal death (Reushal et al 2007). It is hypothesized that the KCa3.1 microglial activation is mediated by the p38 MAPK

pathway, which could be initiated through the osmotic shock of  $K^+$  efflux or due to the increased production of  $IL-1\beta$ , since ICE functions when the concentration of intracellular potassium decreases.

Work specific to AD showed that the P2X7 ATP gated cation channel is up regulated around the sites of amyloid plaques in murine models of the disease. There are several P2X receptors expressed in microglia; P2X1 and P2X4 are seen in embryonic immature microglia, their expression then decreases with maturity coinciding with the up-regulation of P2X7. Much work with P2X7 receptors has shown that they increase the release of pro-inflammatory cytokines and are involved in neuropathic pain, another area of interest in microglia research. Along with the P2X receptors are the P2Y family, these are metabotropic G-protein coupled receptors and of particular interest to microglia is the P2Y12 receptor. ATP addition causes a multitude of responses based upon its concentration. A low concentration of ATP would initiate chemotaxis to the site of injury, where the concentration of ATP increases causing phagocytosis and cytokine secretion. These responses are mediated through influx of cations through P2X7, causing migration and a later efflux of  $K^+$  ions through P2Y12 responsible for the secretion of cytokines. P2X7 has also been shown to be up regulated in activated microglia after injury and during MS and ALS. It has been proposed to be vital in the mediation of microglial lead neuronal injury (Skaper 2011).

CLIC1 a chloride channel is also seen to translocate from its intracellular cytosolic location to the plasma membrane upon exposure to  $A\beta$ . The physiological function of CLIC1 in microglia is grounded within proliferation, which is dependent upon chloride conductance. But in rodent models a challenge by  $A\beta$  leads to an increase in both

protein level and functionality of CLIC1, which simultaneously leads to the production of reactive oxygen species and TNF $\alpha$ . Blocking of these channels by a specific inhibitor leads to the prevention of TNF $\alpha$  release and thus neuronal apoptosis (Novarivo et al. 2004).

Certain microglial functions are dependent on the co-operation of multiple channels (Figure 1.3). Proliferation is a process that is dependent on Ca<sup>2+</sup>, as such inwardly rectifying K<sup>+</sup> channels maintain the negative membrane potential to increase the driving force of Ca<sup>2+</sup> across the membrane through Ca<sup>2+</sup> release – activated Ca<sup>2+</sup> channels (CRACs). Migration is also controlled through two different ion channels; voltage independent Cl<sup>-</sup> channels and Ca<sup>2+</sup> -dependent K<sup>+</sup> channels, the efflux of KCl leads to water efflux through osmosis and the retraction of the rear end of the cell. Activation to the ameboid phenotype is also dependent on multiple channels. Cation channels in the cell body and K<sup>+</sup>/Cl<sup>-</sup> co-transporters in the processes result in an increase in osmolarity in the cell body due to cation influx causing water to enter the cell and the cell body to swell. KCl efflux from the processes, decreases osmolarity and water leaves, causing shrinkage and retraction of the processes.

As such ion channels can be used as a tool to monitor the activation state of microglial cells and whilst less valuable for human microglia macrophage distinction they do pose the potential to be therapeutic targets for neurodegenerative diseases and other cognitive or CNS impairments that are linked to microglia.

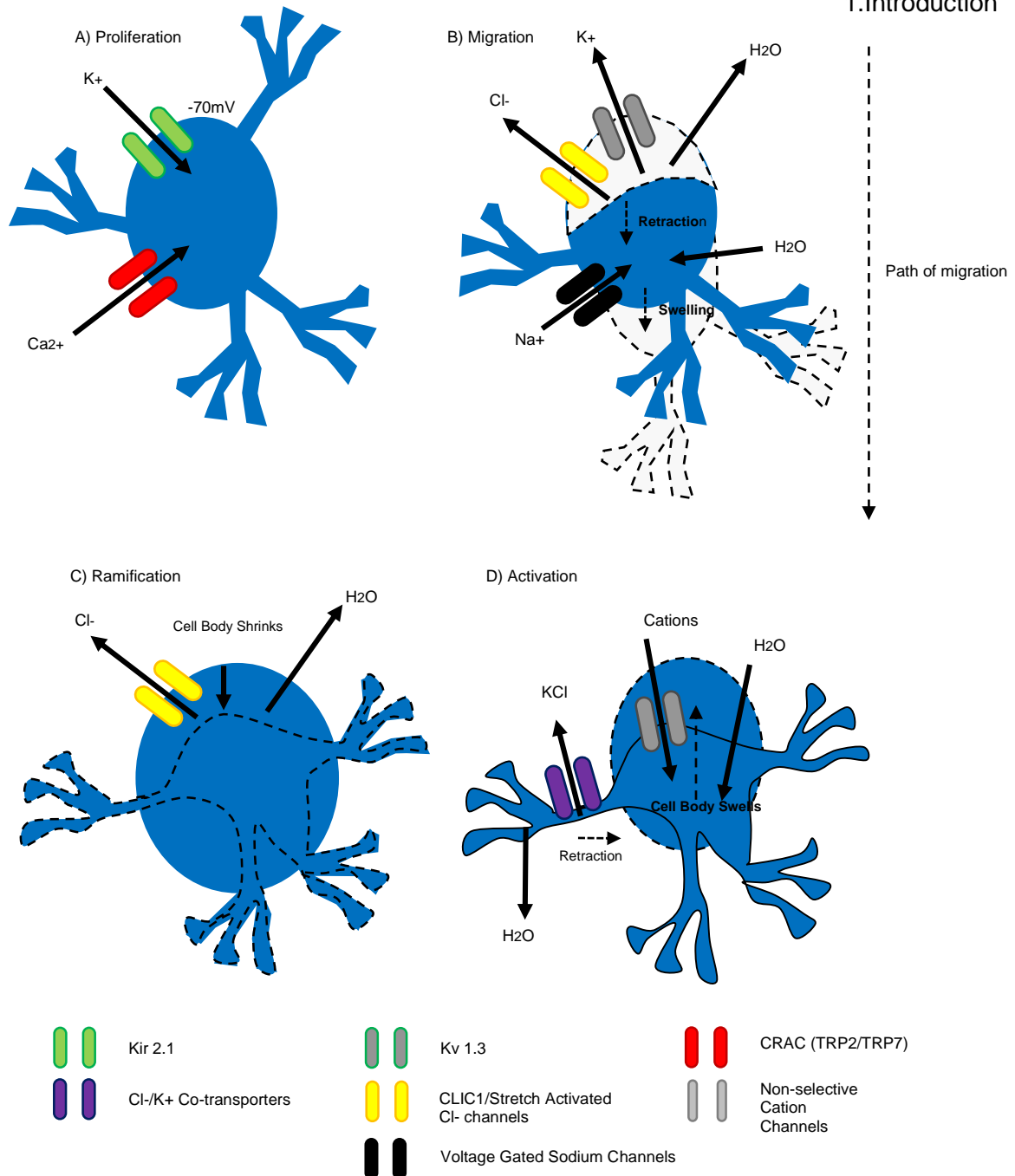


**Figure 1.3. Function of Ion Channels in Microglia**

(A) Proliferation requires  $\text{Ca}^{2+}$ , to increase the flow of  $\text{Ca}^{2+}$  CRAC channels a negative membrane potential is required and is created by the inward flow of  $\text{K}^{+}$  through channels such as Kir2.1.

(B) Migration is a process of retraction and swelling regulated by voltage independent  $\text{Cl}^{-}$  channels and  $\text{Ca}^{2+}$  -dependent  $\text{K}^{+}$  channels. The loss of  $\text{KCl}$  leads to the loss of water through osmosis and the retraction of the rear end of the cell. The swelling of the leading edge of the cell is controlled by voltage gated sodium channels, flow of  $\text{Na}^{+}$  into the cell causes the uptake of water through osmosis and the swelling of the cell. Similarly to retraction (C) ramification is the result of shrinkage caused by the efflux of  $\text{Cl}^{-}$  through CLIC1 channels and the loss of water, forming the characteristic processes of the ramified cell.

(D) Activation from ramified to ameboid, due to cation channels in the cell body and that result in influx of cations so water enter the cell leading to the cell body swelling.  $\text{K}^{+}/\text{Cl}^{-}$  co-transporters in the processes lead to  $\text{KCl}$  efflux, decreasing the osmolarity so water leaves, and the processes retract.

### 1.1.5 PHENOTYPES OF MICROGLIA

Microglia can further be subdivided based on their phenotype, generally either ramified or ameboid (Figure 1.4). Ameboid cells are the first phenotype to colonise the developing brain from their monocyte precursors, where they proliferate in situ throughout gestation and development before differentiating into the mature ramified cells during the postnatal period (Perry et al. 1985). The ameboid cells are rounded with extremely short processes, highly motile and capable of phagocytosis, functioning as fully activated tissue macrophages (Rezaie & Male 2002). It is thought that these ameboid cells shape the evolving brain by phagocytosing the excess neurons produced during development (Killackey 1984).

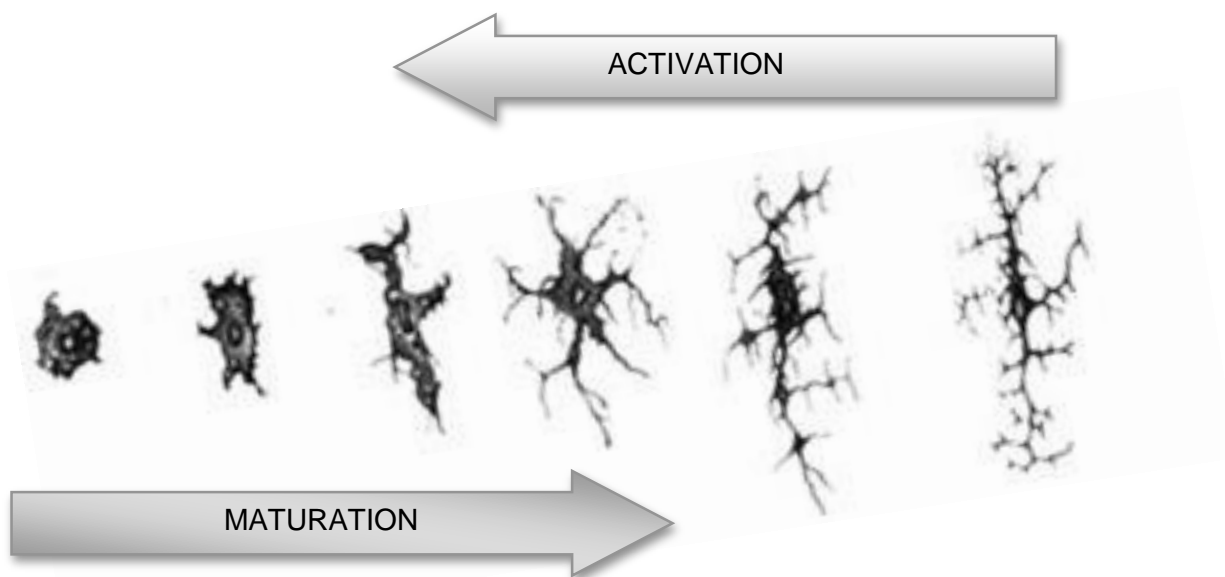


**Figure 1.4. Microglial phenotypes**

Microglia can be seen in various phenotypic forms, from the activated rounded ameboid cell to the resting or surveying process laden ramified cell. Ameboid cells are able to mature into those of a ramified nature and ramified cells are able to undergo activation to an ameboid cell.

Adapted from Kim & de Vellis (2005)

In the developed brain the ameboid cells give rise to an immune dampened version of microglia; the ramified microglial cells. The cell body becomes smaller and the processes increase in length and complexity (Davis et al. 1994). Since their proliferative capacity has ceased and motility decreased they survey the brain parenchyma through building, withdrawing and re-building their processes into new, unchecked areas. This enables the large microglial network to survey the entire milieu within only a few hours (Hanisch and Kettenmann 2007).

The functionality of both phenotypes of microglia was confirmed through genome wide transcriptome analysis by Parakalan et al. (2012). They were able to conclude that ameboid microglia expressed genes required for the development of the nervous and immune system, as well as genes for cell migration; suggesting that they are the first to arrive during development and are also motile. Ameboid cells also have an active cell cycle with the expression of myc genes and cyclinA2, B2 and D1, so are proliferative but are also able to undergo apoptosis with high expression of caspase genes; casp2 and casp3. Conversely the immune dampened ramified cells show high levels of expression of genes involved in myelination, antigen presentation and were also shown to express CamK2, Grin2c and S100b all of which are involved in the modulation of synaptic transmission (Parakalan et al. 2012).

The processes of monocyte maturation through the transient ameboid state to the down regulated brain macrophage, the ramified cell and their re-activation to an immune competent cell is still not fully understood. It has been suggested that the transition is aided by differential septin expression, where ameboid cells express Sept7 compared to the expression of Sept4 in ramified cells. The ramification of

microglia could also be caused by the expression of Lsp1 found in ramified cells but absent in the ameboid state. Over-expression of Lsp1 in highly motile melanoma cell lines was shown to dramatically decrease motility and lead to the formation of hair like projections as seen in the transition from motile rounded ameboid cells to dormant spiky ramified cells.

It is known however, that microglia are maintained in a quiescent, ramified state through the 'calming' influence of receptor ligand pairs situated on the membranes of neurons and microglia. Interactions between these pairs; neuronal CD200 and microglial CD200-R and neuronal CX3CR1 and microglial CX3CR1-R, dampen microglial activation (Vilhardt 2005). Disruptions between these signals, due to neuronal damage, cause activation of ramified cells to an activated, ameboid phenotype. Other activating factors have been discovered, such as IFN- $\gamma$ , LPS and tPA, although the mechanism behind their function has yet to be found (Suzumura et al. 1991). The same study by Suzumura et al. (1991) showed that rod shaped microglial cells found around lesioned areas, with a presumptively active role, did not produce superoxide anions but did incorporate BrdU to a greater extent than the other phenotypes, suggesting that the rod shaped cells are the proliferative intermediate phenotype of microglia and this phenotype could be induced through the addition of GM-CSF.

Another phenotype of microglia has also been suggested, although not found in the normal healthy brain. These are the giant multinucleated cells found during viral infections in particular HIV-1 and is considered a hallmark of the immunodeficiency virus. Their function is even less well understood than the ramified and ameboid phenotypes, with suggestions ranging from conglomeration of several activated cells,

collection of exhausted cells with no beneficial or detrimental function to an abnormal cell produced as a by-product of the disease state (Davis et al. 1994).

---

#### 1.1.6 MICROGLIAL FUNCTION IN HEALTH AND DISEASE

---

Although microglia are the resident immune cells of the brain, they have a vast range of functions beyond those of pathogen removal. They are able to secrete cytokines IGF-1, NGF and BDNF, in a glutamate dependent manner, promoting oligodendrocyte functioning and neurogenesis (Liang et al. 2010). In an anti-inflammatory role they can secrete IL-10 and TGF $\beta$  which induce a neuroprotective effect on neurons, as shown in traumatic injury and stroke models (Neumann et al. 2006). Conversely they can also secrete pro-inflammatory cytokines; IL-1 $\beta$  and TNF $\alpha$ , which are thought to be neurotoxic.

Phagocytosis by microglia is essential for the maintenance of brain homeostasis, by removing cellular debris as well as pathogens. Phagocytosis occurs subsequent to chemotaxis to the site of concern due to the presence of two receptor types; Toll-like receptors (TLRs) and phosphatidylserine (PS) recognising receptors (Schiegelmich et al. 2011). TLRs recognise microbial patterning and lead to phagocytosis of pathogens along with the secretion of pro-inflammatory cytokines (Lehnardt 2010). PS recognising receptors such as TREM2, recognise PS 'eat-me' signals on apoptotic cells resulting in anti-inflammatory phagocytosis with the release of IL-10 and TGF $\beta$  (Neher et al. 2011; Schiegelmich et al. 2011). The phagocytic function of microglia is also important in structuring synapses. The complement component C3 is expressed on all synapses and microglia enabled with the C3 receptor target certain synapses for removal in order to organise neuronal connections (Martin et al. 2007).

Besides their physiological functions microglia have been implicated in pathological states including many neurodegenerative diseases, from those specifically with immunological links such as HIV associated neurocognitive disorder (HAND) and multiple sclerosis to those without; Parkinson's and Alzheimer's disease.

The HIV virus targets mononuclear cells, such as monocytes and macrophages along with CD4+ T cells (Deeks 2011). Since microglia are derivatives of primitive monocytes they are also a target of HIV once it crosses the BBB (Strazza et al. 2011). The result of microglia infection is an innate immune response and the production of neurotoxic factors that lead to both the dementia symptoms and neuropsychiatric disorders found in HAND (Deeks 2011).

Multiple sclerosis is an autoimmune disease that leads to attack on the myelin sheaths of neurons in the CNS. It has been known for many years that TH17, TH1 and B cells have major pathological roles in the progression of the disease, but more recently a microglial role emerged in the EAE mouse model of the disease (Priller et al. 2001). Here it was found that microglia played two important roles in the disease; antigen presentation to T-cells and secretion of IL-6, IL-23, IL-1 $\beta$  and TGF $\beta$  aiding the differentiation and activation of TH17 cells (Saijo and Glass 2011).

In Parkinson's disease there is a characteristic loss of dopaminergic neurons from the substantia nigra and accumulations of  $\alpha$ -synuclein which leads to both astrogliosis and microglial activation (Mattson 2000). The activation of microglia occurs through the Pattern Recognition Receptors (PRRs) and purinergic receptors leading to the secretion of toxic cytokines leading to neuronal loss.

Similarly, Alzheimer's disease results in the loss of neurons in the frontal cortex and limbic system as a result of protein aggregations; extracellular aggregations of

Amyloid  $\beta$  ( $A\beta$ ) and intracellular tau tangles created from hyperphosphorylated tau. Microglial activation results through TLRs, NLRP3 and RAGE in response to the aggregations, leading to secretion of cytotoxic cytokines and neuronal death but microglia can also phagocytose aggregated  $A\beta$  in a neuroprotective role (Heneka et al. 2010).

## 1.2 ALZHEIMER'S DISEASE

---

### 1.2.1 ALZHEIMER'S DISEASE

---

Alzheimer's disease (AD) is a progressive neurodegenerative disease that was first noted by German neurologist Alois Alzheimer, after whom the disease is named. AD leads to neuronal atrophy in the frontal cortex and many areas of the limbic system including the hippocampus and amygdala (Findeis 2007; Heneka 2006). These areas are most associated with memory, learning and emotions, the abilities most affected in sufferers of the disease. Along with the characteristic symptoms involving memory defects, many sufferers also experience problems with speech, obsessive behavior is established, along with incontinence and disturbed sleep. These symptoms develop in advanced stages of the disease into dysphagia accompanied by loss of appetite and consequent weight loss. This can coincide with hallucinations and an increase in violent behavior that is worsened at night. Severe AD patients are also more prone to infection due and as such death is often attributed to factors other than AD. Medications currently prescribed in the UK focus on delaying the development of AD to minimize the severity of symptoms for as long as possible, most commonly acetylcholine esterase inhibitors; donepezil, galantamine and rivastigmine, are prescribed in the early stages of the disease and NMDA-type glutamate receptor inhibitor memantine is given during the latter stages, but there is no current cure.

AD is considered by many a disease of old age, but sufferers can be divided into two groups depending on age at onset. Early onset or familial AD affects an individual prior to old age, and is associated with genetic mutations situated within genes coding for elements of the Amyloid Precursor Protein (APP) processing pathway (Tanzi and Bertram 2001). More common are afflictions later in life, subsequent the

seventh decade of life, and are classed as late or sporadic onset AD (Simard et al. 2006). In these cases an accumulation of risk factor gene variants, environmental influences and age play the biggest roles.

---

### 1.2.2 MECHANISMS OF ALZHEIMER'S DISEASE

---

The mechanisms that underpin onset and progression of Alzheimer's disease are not fully understood in the sporadic onset cases, what is known is that there are two hallmarks of the disease; Amyloid plaques and Neurofibrillary tangles, whose relationship with each other and with AD are not, as of yet, clear.

Much insight into the amyloid hypothesis has come from studies involving early onset sufferers, where genetics play the most fundamental role. From these studies it was found that many of the genetic mutations revolved around the production of Amyloid Precursor Protein (APP) and its processing via the Presenillin (PSEN) 1 and 2  $\gamma$ -secretase components (Tanzi and Bertram 2001). The physiological function of APP is thought to be in the formation of synapses, around which the protein is localized (Priller et al. 2006). In the healthy brain APP is digested by  $\alpha$ -secretase, a non-amyloidogenic route, which results in soluble APP (sAPP) production. Alternatively  $\beta$ -secretase and subsequent  $\gamma$ -secretase digestion results in the release of  $A\beta$ , the amyloidogenic path (Figure 1.5) (LaFerla et al. 2006). The formation of  $A\beta$  is not, on its own, pathological. It is released constantly in non-AD individuals but the difference lays in the rate of clearance, which physiologically equals the rate of production. It is only when the balance is tipped that  $A\beta$  will aggregate. A slowing in  $A\beta$  clearance is seen with age; hence the age relation to AD, but the production of  $A\beta$  can also increase through mutation so that there are greater amounts of  $A\beta$  present than can be cleared. These aggregations form senile or amyloid plaques that

are composed of, in the main, two forms of  $A\beta$ ,  $A\beta_{40}$  and  $A\beta_{42}$ . The difference between each fragment lies in the number of amino acid residues, with the latter being more hydrophobic and most inclined to aggregate.

The alternative hypothesis is that of neurofibrillary or tau tangles (NFTs). Tau is an intracellular protein associated with the microtubules and functions in their stabilization (Cleveland et al. 1977). In Alzheimer's disease there is hyperphosphorylation of Tau leading to the formation of paired helical filaments (PHL) which result in NFTs. The underlying cause of the phosphorylation can be explained by either an imbalance in the protein kinases and phosphatases in the cell or by a mutation in the MAPT gene that encodes the tau protein (Pittman et al. 2006). The aggregations accumulate, destabilizing the microtubules and disrupting neuronal axon transport, making the cell less functional until the neuron ultimately dies, aiding AD progression.

The Amyloid Hypothesis has been disputed as the cause of AD and instead more emphasis has been placed on the NFTs as the underlying mechanism of disease. However, both aggregations occur during disease progression and which precedes the other is still unclear. It is also suggested that both amyloid plaques and NFTs are required for the onset of AD. But this said, amyloid plaques have been found in the postmortem brains of non-AD sufferers and NFTs alone are seen in familial pre-senile dementia cases (Sumi et al. 1992).

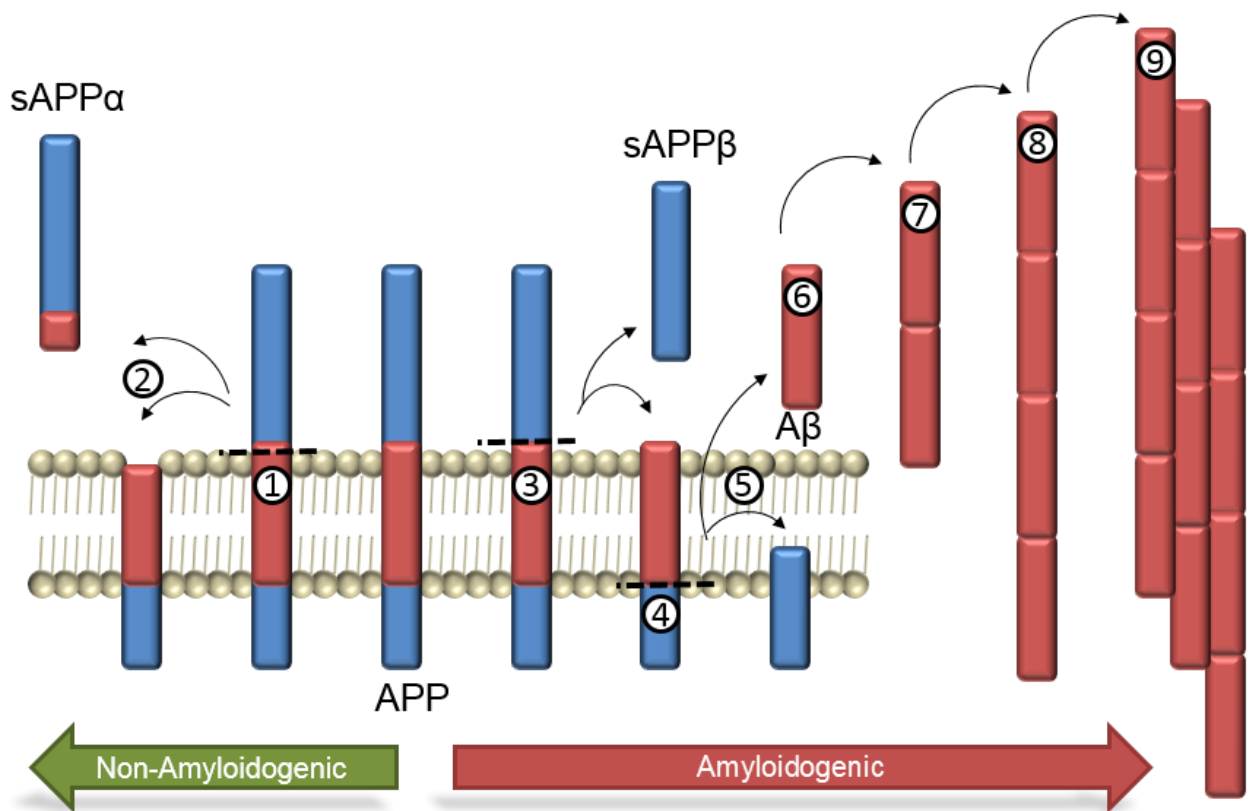


**Figure 1.5. APP Processing and Aggregation**

Amyloid Precursor Protein (APP) can be acted upon by either  $\alpha$  – secretase or  $\beta$  – secretase in a non – amyloidogenic or amyloidogenic process. In the non – amyloidogenic process, APP is cleaved by  $\alpha$  – secretase (1) to release sAPP $\alpha$  from the membrane (2). sAPP $\alpha$  contains the C-terminal region of the  $\beta$ -Amyloid protein meaning that subsequent cleavage will not result in a protein fragment capable of aggregation. During the amyloidogenic process though APP is cleaved by  $\beta$  – secretase (3) resulting in the release of the soluble sAPP $\beta$  fragment from the membrane. The protein remaining in the membrane is cut by  $\gamma$  – secretase (4) and  $\beta$  – Amyloid (A $\beta$ ) (6). Due to its small size and hydrophobic nature the only stable conformation available for the protein is for it to aggregate with other A $\beta$  fragments forming dimers (7) then oligomers (8) and finally plaques (9), which are the characteristic feature of AD.

Thus the intimate link between aggregated A $\beta$  and Tau can be explained through one of three theories. 1) Amyloid aggregation, due to a slowing of A $\beta$  clearance with age, causes an imbalance between intracellular protein kinases and phosphatases that leads to tau hyper-phosphorylation and ultimately the formation of NFTs. 2) Mutations in the MAPT gene cause an increased likelihood of hyper-phosphorylation and tangle formation that disrupts the neuronal axon transport system, along which APP is transported to the synapses where it functions, so the cleavage products of the APP are now in close proximity increasing the chance of aggregation and plaque formation, as well as disturbing synapse function. 3) Both aggregations could occur independently but when amyloid plaques and NFTs are in the same susceptible region of the brain, the cortex or limbic system, their effects synergise leading to the symptoms associated with AD. This latter hypothesis gives the possibility that both aggregations are separate entities and also can be of distinct origin, whether genetic or environmental in nature, but are able to propagate each other in the case of AD.

---

### 1.2.3 MICROGLIAL ROLES IN ALZHEIMER'S DISEASE

---

The role of the immune system in AD progression has been speculated upon for many years, as mentioned both Amyloid plaques and NFTs can be found in the brains of non-AD patients and many of the classical AD symptoms cannot be explained solely by aggregation. As well as this treatment of AD sufferers with Non-Steroidal Anti-Inflammatory Drugs (NSAIDs) and the immunization of patients against A $\beta$  had beneficial consequences on halting memory loss (McGeer et al. 1996; Wisniewski and Konietzko 2008). The possible benefits of antibody therapy has also been speculated upon, there is much evidence that suggests the immune system plays a major role in this disease.

As mentioned, the immune cells of the brain are microglia and they, like macrophages, have many cell surface receptors for the detection and presentation of foreign proteins to T cells. Amongst these receptors is a receptor complex comprising of CD36, CD47 and  $\beta_1$ -integrin for the recognition of fibrillar A $\beta$  (fA $\beta$ ) (Bamberger et al. 2003). This complex along with CD14 and Toll-Like Receptors (TLRs) 2 and 4 are responsible for the activation and motility of microglia, in their response to senile plaques (Reed-Geaghan et al. 2009). It was recently shown that TREM2, a mononuclear phagocyte surface receptor expressed by microglia and is involved in the phagocytosis of apoptotic cells and the inhibition of inflammatory responses, has six variants (Guerreiro et al. 2013). The presence of these variants drastically increase the risk of AD through impaired TREM2 function leading to a decrease in phagocytosis and an increase in inflammation, which not only adds evidence to the theory of inflammation in AD but also links microglial function in the disease onset and progression.

Further GWAS studies highlighted HLA-DRB1, HLA-DRB5, ABCA7 and CD33 as comprising variants that increase the risk of AD (Lambert et al. 2013; Rosenthal and Kamboh 2014). All of these play a role in the immune system with the HLA genes encoding for the MHCII gene, vital for the presentation of antigens on lymphocytes and macrophages as well as microglia. Genetic variants of the HLA-DRB genes could lead to a down regulation of MHC-II leading to an increase in cytotoxicity and an increase in inflammation (Butovsky et al. 2005). ABCA7 is an ATP-binding cassette gene involved in lipid transport. It was noted that the expression of ABCA7 was amongst the highest in the microglia within the hippocampus where it functions to aid the phagocytosis of A $\beta$  (Kim et al. 2005). Variants of the gene, as seen in AD, would result in less A $\beta$  clearance and increased plaque formation. CD33 encodes for

a sialic acid binding immunoglobulin-like lectin, which is able to initiate cell-cell interactions in immune cells. Studies have shown that there is an increase in the expression of CD33 on the microglia of AD brains, where it inhibits the uptake of  $A\beta_{(1-42)}$  and thus plaque clearance (Griciuc et al. 2014).

The GWAS studies and the resultant risk factor genes associated with microglia highlight their two major functions with regard to AD; inflammation and phagocytosis and it is here that their role in AD is disputed (Figure 1.6). They are able to phagocytose and clear  $A\beta$  in a neuroprotective role but conversely they are also capable of secreting cytokines, such as  $TNF\alpha$ , IL-4 and IL-1 $\beta$ , of which some are neurotoxic, in response to the senile plaque (El Khoury and Luster 2008). These cytokines are not only toxic to neurons but they are also able to influence the phagocytic capacity and thus the neuroprotective effect of the microglia themselves. IL-4 rich environments promote both the phagocytic and neurogenesis capacity of microglia whereas the presence of IL-1 $\beta$ , during inflammation, inhibits phagocytosis. Therefore newly invading microglial cells, from the bone marrow, may have a greater neuroprotective role in AD as they have not been subjected to the inhibitory IL-1 $\beta$  environment (Koeingsknecht-Talboo and Landreth 2005; Simard et al. 2006).

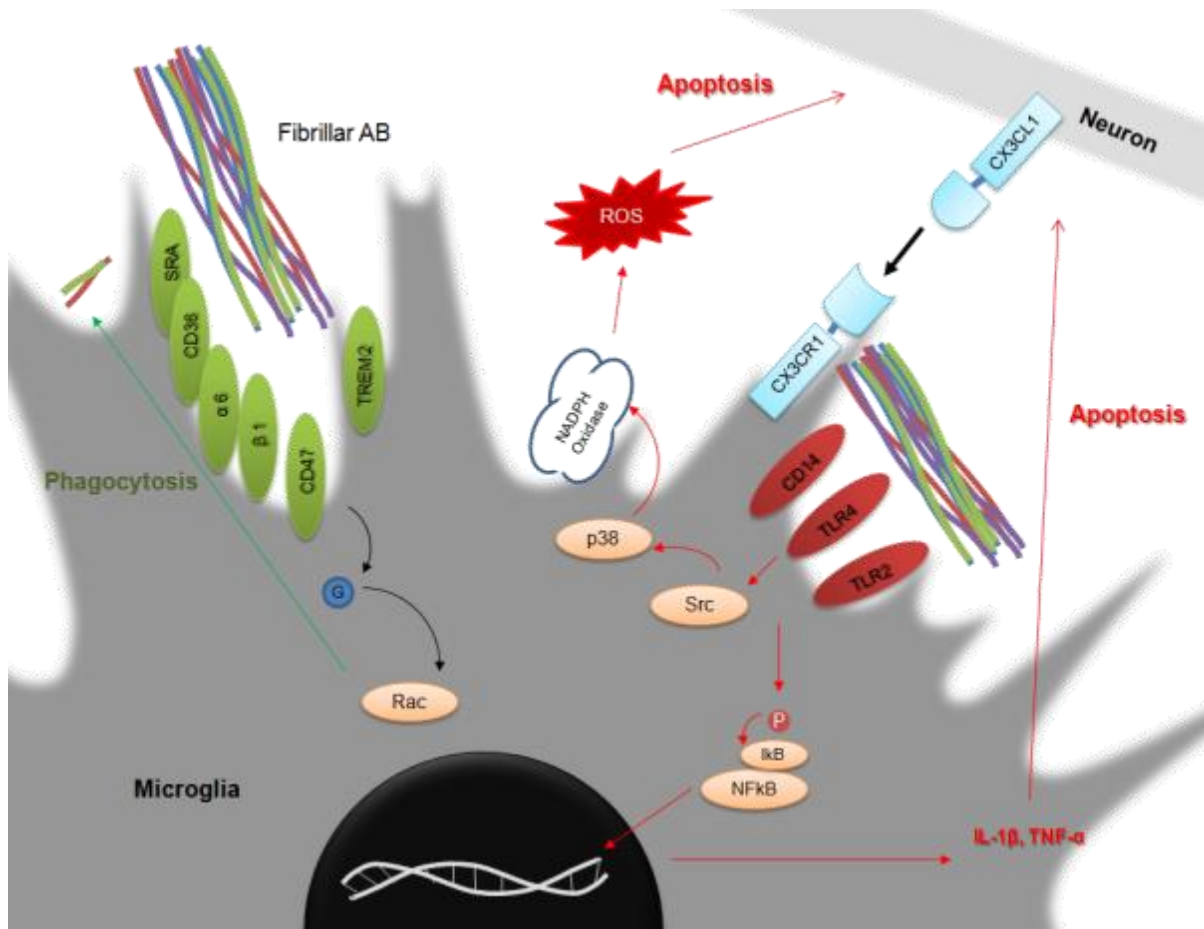


**Figure 1.6. Microglial Roles in Alzheimer's Disease**

Microglia are able to contact and communicate with neighbouring neurons through the CX3CR1/CX3CL1 receptor ligand complex, enabling microglia to verify the status of the neuron in their physiological role and retaining the ramified state. Microglia also have a SRA, CD36, integrin  $\alpha 6/\beta 1$ , CD47 complex, which along with CD14 and TLR2 and 4, recognize and bind A $\beta$ . This activates a three parallel cascades beginning with Src activation followed by the activation of i) NF $\kappa$ B leading to the production of pro-inflammatory cytokines IL-1 $\beta$  and TNF $\alpha$ , ii) p38 and the production of reactive oxygen species from NADPH Oxidase and iii) Vav, followed by Rac and the phagocytosis of Amyloid plaques. The former processes result in apoptosis of the surrounding neurons, aiding AD progression, whereas the latter results in the clearance of the aggregations and the decrease of amyloid load.

---

## 1.2.4 CURRENT MODELS OF ALZHEIMER'S DISEASE

---

Although mouse models are by far the most common animal model of AD, other non-mammalian models also exist such as; those of the fruit fly, *Drosophila sp*, and worm *Caenorhabditis elegans* (Chan & Bonini 2000; Link 2005). Mouse models of AD have been largely based on the genetic disturbances in early onset disease rather than the accumulation of risk factors that underpins the more common sporadic form. There are transgenic models (PDAPP, Tg2576, APP23, TgCRND8 and J20), expressing the mutant human forms of the APP processing gene, to knock-in and knock-out models whereby the APP processing enzyme  $\gamma$ -secretase activity and gene expression are affected respectively (Reviewed in (Mineur et al. 2005)) .

Work on PDAPP mice and m266 antibody treatment to decrease amyloid burden and reverse memory deficits paved the way for the bapineuzumab antibody clinical trial some ten years later (Dodart et al. 2002). The Semagacestat  $\gamma$ -secretase inhibitor development and phase III clinical trials in 2010 were undoubtedly influenced by experiments carried out on mouse models such as those by Comery et al. (2005) where inhibition of  $\gamma$ -secretase by *N*-[*N*-(3,5-difluorophenacetyl)-*L*-alanyl]-*S*-phenylglycine-*t*-butylester (DAPT) in Tg2576 mice showed improved fear conditioning and thus better hippocampal function. Although none of these clinical trials were successful as there was no significant difference between drug treated and placebo treated patients, models of AD are vital for the emergence of new therapeutic strategies.

Animal models, even non-mammalian models, of the disease have proved valuable in the study of AD in earlier years and, mouse models in particular, will always have their place in whole animal drug testing but however close the mouse model comes to paralleling AD onset and progression such models will never serve as the best

model for a human disease. The alternative lies in modeling a human disease with human cells *in vitro*, with the advent of Induced pluripotent Stem cell (IPS) technology, fibroblasts from AD sufferers can be re-programmed to stem cell like cells and then re-differentiated into any cell type of the body, enabling Alzheimer's specific and even patient specific culture models to be created.

---

## 1.3 STEM CELLS

---

---

### 1.3.1 HUMAN EMBRYONIC STEM CELLS

---

Stem cells can be classified as either adult stem cells or embryonic stem cells (hESCs). The former are generally multipotent, and can give rise to only a limited range of cell types i.e. hematopoietic stem cells that are committed to producing only blood cells. hESCs, on the other hand are pluripotent, that is, they are taken from the inner cell mass of a blastocyst and are capable of differentiating into any of the various cell types within the three germ layers; endoderm, mesoderm or ectoderm. Although their differentiation capacity is vast, pluripotent hESCs are unable to differentiate into extra-embryonic tissue, which is the role of the outer trophoblast (Figure 1.7).

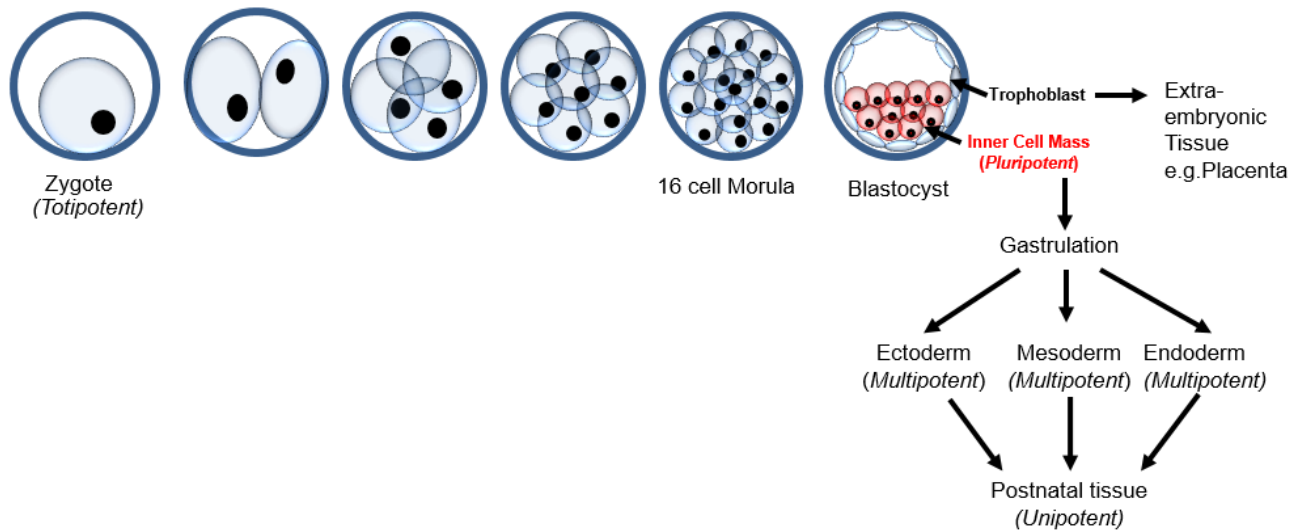


**Figure 1.7. Totipotency, Pluripotency, Multipotency and Unipotency in Embryogenesis**

The fertilized ovum or zygote is totipotent (able to form embryonic and extra-embryonic tissue). It undergoes multiple mitotic cleavages to result in the formation of a spherical mass of 16 cells, the morula. The final cleavage creates 128 cells that form the blastocyst. The blastocyst is composed of the outer trophoblast and the pluripotent inner cell mass. Before gastrulation the trophoblast differentiates into the outer syncytiotrophoblast and the inner cytotrophoblast, which is responsible for the formation of the placenta. Several inner mass cells quickly differentiate into endoderm cells that form the space for the yolk sac, which ultimately becomes the amniotic cavity. The floor of the cavity is formed composed of the embryonic disk. The morphology of the disk changes from oval to pear shaped and there is the formation of the primitive streak, formed by a thickening of the ectoderm. At the sides of the primitive streak the mesoderm cells differentiate. These three layers are the multipotent progenitors responsible for the formation of unipotent embryonic tissue.

During the 1980s it was shown by both Martin and Evans, independently, that the inner cell mass can be cultured *in vitro*. Many groups had previously struggled to achieve the same result due to the lack of inner cell mass cells within the blastocyst at the time of harvest. To counter this Evans et al. (1981) delayed the implantation of blastocysts for several days, allowing inner mass cells to accumulate, by increasing progesterone levels and removing the ovaries post-fertilisation. Martin (1981) used a carcinoma cell line to condition media and cultured inner cell mass cells from late blastocysts on feeder layers. Both methods resulted in the formation of colonies that were comparable to an embryonic carcinoma cell and were capable of forming teratomas containing all three germ layers, indicative of pluripotent cells. More than a decade later hESC lines were derived, using cleavage stage embryos that were created via *in vitro* fertilization. Methods similar to those carried out by Evans et al. (1981) were used to initially form five different cell lines; H1, 13, 14, 7 and 9. The latter two lines were of a normal XX karyotype, whereas the remainder were of a normal XY karyotype. All the lines were positive for the surface markers; SSEA3, SSEA4, TRA-1-60 and TRA-1-81, which are known to also characterize the ES cells from non-human primates (Thomson et al. 1998).

Since their discovery the mechanisms behind the maintenance of pluripotency in ESCs has been a source of interest. It is now known that ESCs require a feeder layer of irradiated mouse embryonic fibroblasts (MEFi) in order to sustain pluripotency and in feeder-free conditions mESCs require the addition of LIF to maintain an undifferentiated state (Williams et al. 1988). LIF functions through a JAK/STAT pathway that utilizes the LIF-R and gp130 cell surface receptors. Activation of these receptors ultimately leads to the dimerisation of STATs, predominantly STAT3, and their translocation to the nucleus leading to gene

transcription (Niwa et al. 1998). Interestingly one binding element of this STAT3 is within the Nanog promoter region leading to up regulation of this gene (Suzuki et al. 2006). Although important in mESC maintenance the LIF/STAT3 pathway, fundamental for diapause in the mouse embryo, is not activated under the maintenance conditions for hESC pluripotency where bFGF and soluble factors from MEFs are required for the activation of TGF $\beta$  signaling through Smads (Dahéron et al. 2013).

Nanog, along with Oct4 and Sox2 are indispensable in the regulation of the inner cell mass and are critical in early cell fate decisions, where the loss of Oct4 for example leads to the inner cell mass reverting to trophoblast and over-expression leading to the cells joining the extra embryonic endoderm lineage (Loh et al. 2006; Suzuki et al. 2006). Nanog has also been shown to bind Smad1 and inhibit BMP induced differentiation, confirming the importance of the TGF $\beta$  signaling through Smad2/3 in the maintenance of pluripotency (Suzuki et al. 2006; James et al. 2005).

These groundbreaking discoveries regarding ESCs and maintaining their pluripotent state and the understanding of signaling pathways that lead to their differentiation enabled the *in vivo* differentiation of cells to be mimicked *in vitro*. This allowed a cell type of interest to be created, through chemically defined media, environmental conditions and through exogenous over-expression of the required genes. This inherent plasticity in hESCs has proved most useful in modeling both tissues and diseases, but for the latter hESCs have their limitations, in that they do not contain the problematic features of the cells afflicted by the disease such as genetic mutations.

---

### 1.3.2 *IN VITRO* DIFFERENTIATION POTENTIAL OF ES CELLS

---

An important marker of pluripotent embryonic stem cells is their ability to differentiate into any of the three germ layers. This capacity has been harnessed by many groups in order to create a supply of the cell type of interest. An example of ectodermal differentiation is the development of protocols for the production of neural lineage cells. The addition of retinoic acid, NGF and EGF to cultures or culturing in the presence of stromal cell lines or on matrigel all enhance the neural differentiation potential of ES cells and such techniques have yielded dopaminergic neurons to create a Parkinson's disease model (Freed and Greene 2001).

Groups have also succeeded in the formation of blood cells by culturing cystic embryoid bodies that form the blood islands from which blood cells emanate during development (Karlsson et al. 2008). Feeder layers have again been important in the mesoderm differentiation and OP9 cells are common place for the development of all types of haematopoietic cells (Lim et al. 2013). Finally endoderm differentiation of hESCs has been able to yield some insulin secreting cells with the characteristics of pancreatic docrine cells, which holds great hope for the treatment of diabetes (Kroon et al. 2008).

---

### 1.3.3 INDUCED PLURIPOTENT STEM CELLS

---

Once a somatic cell has reached terminal differentiation, they no longer have the capacity to differentiate and take on the role of the mature cell type. But several years ago Takahashi et al. (2007), produced the first human induced pluripotent stem cells (iPSCs), which enabled terminally differentiated somatic cells to be 're-programmed' to a stem cell like state. This was achieved by the transfection of pluripotency genes; Oct4, Sox2, c-Myc and Klf4, into human fibroblasts, which

reverted to stem cell morphology in less than four weeks (Takahashi et al. 2007). The cells could then be treated in the same way as a hESC allowing subsequent differentiation to any other cell type allowing the formation of disease specific models and with patient specific cells.

---

#### 1.3.4 EMBRYONIC AND INDUCED PLURIPOTENT STEM CELLS IN DISEASE

---

With the advent of hESCs dawned a new wave of excitement due to the endless supply of cells of interest and the possibility of transplantation to cure the incurable? Pathological conditions such as myocardial infarction, vascular damage, neuro-repair and diabetes have been improved by introducing ES cells into mouse models of these diseases.

There have been improvements in rat models of myocardial infarction on transplantation of beating ES-derived cells cardiomyocytes (Min et al. 2002). Vascular structures have been made by the isolation of PECAM-1<sup>+</sup> cells from hES endothelium differentiation and seeding on scaffolds that are then grown subcutaneously in SCID mice (Levenberg et al. 2002; Putnam and Mooney 1996). Brustle et al. (1997 and 1999) made two discoveries upon differentiation of ES cells into neuronal cells and also glial precursors. The former cells were shown to be functional and differentiate into region specific cells when transplanted into the developing mouse brain, whilst the latter were able to reverse the pathological phenotype found in the demyelinating disease Pelizaeus-Merzbacher. Positive strides towards Parkinson's treatment were made in rat models of the disease when partial recovery was witnessed upon transplantation of mES-derived dopaminergic neurons (Kim et al. 2002). Unfortunately this was not the outcome when neural cells from human fetal brain were introduced into Parkinson's patients. There was no

significant improvement in disease and some two years later many developed dyskinesia (Freed et al. 2001). Although largely unsuccessful this study did prove that these embryonic neural progenitors could survive in a human host, which none the less shows that there is an impending for the future for ES transplantation. Taken together all these studies show that ES cells have a potential to successfully model human disease and ultimately aid recovery through drug development and transplantation genetically modified ES-derived cells.

## 1.4 AIMS

---

A protocol for deriving microglia from human embryonic stem cells has, as of yet, not been published but methods for their derivation from mouse embryonic stem cells has been successful. Groups have utilised the five step method devised by Lee et al. (2000) for the differentiation of neural cells from ES cells. Tsuchiya et al (2005) produced a neuronal culture via this method and then by the addition of GM-CSF Mac1+ cells were formed and isolated for microglial culture. Napoli et al (2009) and Buetner et al (2010) both utilised the five step method to first create neuroectoderm and then a mixed brain culture from which Napoli et al isolated the IBA-1+ cells whereas Buetner et al isolated the myeloid precursors and cultured further to differentiate to microglia. All these methods are indeed very similar and require differentiation to a neuronal lineage prior to the formation of microglia and all use large number of growth factors and expensive medium to achieve their goal.

Forsberg et al. (2008) and others including Sievers et al. (1994) produced microglia from monocytes. A logical step since microglia are most likely derivatives of monocytic cells. Forsberg et al. (2008) was able to reprogram murine adult neural stem cells to monocytes by the over-expression of the myeloid transcription factor, PU.1. These were then transplanted into mouse brain and further differentiated into microglia due to the influence of the surrounding cells. Along the lines of environmental influence Sievers et al. (1994) showed that it was possible to create microglial-like cells from blood monocytes and splenic macrophages by co-culturing them with astrocytes, they also found that direct contact with astrocytes was unnecessary and using medium conditioned by astrocytes functioned just as well indicating that factors secreted by astrocytes are key in the transition from monocyte to microglia.

As monocyte to microglia transition is relatively straightforward in the case of astrocyte conditioned medium then a method that includes hES to monocyte followed by microglia transition would seem useful. Many of the published methods for the production of haematopoietic cells are growth factor, and so cost, intensive. Evseenko et al. (2010) used a basal induction medium containing VEGF, bFGF, BMP4 and Activin A to induce mesoderm followed by their culture on OP9 feeder cells to result in the differentiation of mesoderm to haematopoietic cells. Chadwick et al. (2003) cultured EBs in a differentiation medium that contained six growth factors; SCF, Flt3-ligand, IL-3, IL-6, GM-CSF and BMP4 for haematopoietic commitment. One method that differed from the growth factor demanding protocols was that of Karlsson et al. (2008), where EBs are cultured in the presence of bFGF and plated down using medium containing only MCSF and IL3 to form 'factory' like structures that result in the formation on non-adherent monocytic cells.

The definitive aim of the project is to devise a protocol for the differentiation of hESCs to microglial-like cells. Since we have established protocols for the differentiation of hESCs to neural precursors and the over-expression of PU.1 in the work by Forsberg et al. requires little growth factor intervention this also poses an attractive route to monocyte formation.

A second strategy in the effort to differentiate hESCs to monocytes is a method similar to that of Karlsson et al. (2008) and the more recent adaptation of that work by van Wilgenburg et al. (2013). These studies show that monocytes can be produced from hESCs and iPSCs with minimal growth factors. This said, the cell lines available for differentiation in this project differ from those used previously.

For the final differentiation step to microglial-like cells, the ES-derived monocytes will be cultured in astrocyte conditioned media (ACM) to mimic the environmental cues that bombard monocytes that cross the BBB *in vivo*, and has been described by Sievers et al. (1994). Once the protocol is established the functionality of the resulting microglial-like cells will be examined through phagocytosis, chemotaxis and cytokine secretion.

## 2. MATERIALS AND METHODS

### 2.1 MATERIALS

#### 2.1.1 CELL CULTURE REAGENTS

- **Cell Lines**

<b>Name</b>	<b>Source</b>
<i>H9 hESCs</i>	WiCell
<i>THP-1 Monocytes</i>	Dr. Dipak Ramji, Cardiff University

- **MEF Media**

<b>Components</b>	<b>Amount</b>	<b>Company (Cat #)</b>
<i>DMEM GlutaMAX</i>	450ml	GIBCO (31965080)
<i>Fetal Bovine Serum</i>	10% (50ml)	GIBCO (10439024)
<i>Penicillin/Streptomycin</i> (5000U/5000µg)	50U/50µg (5ml)	GIBCO (15070063)

- **H9 Media**

<b>Components</b>	<b>Amount</b>	<b>Company (Cat #)</b>
<i>Knockout DMEM</i>	425ml	GIBCO (10829018)
<i>Knockout Serum Replacement</i>	15% (75ml)	GIBCO (10828028)
<i>Non-Essential Amino Acids</i>	1% (5ml)	GIBCO (11140035)
<i>L-Glutamine (200mM)</i>	2mM (5ml)	GIBCO (25030024)
<i>Penicillin/Streptomycin</i> (5000U/5000µg)	50U/50µg (5ml)	GIBCO (15070063)
<i>B-Mercaptoethanol</i>	0.1mM (3.5µl)	Sigma (M3148)
<i>FGF<sub>2</sub></i>	10ng/ml	Peptrotech (100-18B)

- **XVIVO Factory Media**

<b>Components</b>	<b>Amount</b>	<b>Company (Cat #)</b>
<i>XVIVO 15 media</i>	500ml	Lonza (BE04-418)
<i>L-Glutamine (200mM)</i>	2mM (5ml)	GIBCO (25030024)
<i>Penicillin/Streptomycin</i> (5000U/5000µg)	50U/50µg (5ml)	GIBCO (15070063)
<i>B-Mercaptoethanol</i>	50µM (1.75µl)	Sigma (M3148)

- **XVIVO Factory Complete Media**

<b>Components</b>	<b>Amount</b>	<b>Company (Cat #)</b>
<i>XVIVO Factory Media</i>	50ml	
<i>M-CSF</i>	100ng/ml	Miltenyi (130-096-491)
<i>IL-3</i>	50ng/ml	Miltenyi (130-093-909)

- **Monocyte Maintenance Media**

<b>Components</b>	<b>Amount</b>	<b>Company (Cat #)</b>
<i>RPMI1640 ( No Glutamine)</i>	450ml	GIBCO (31870025)
<i>Fetal Bovine Serum</i>	50ml	GIBCO (10439024)
<i>L-Glutamine (200mM)</i>	2mM (5ml)	GIBCO (25030024)
<i>Penicillin/Streptomycin (5000U/5000µg)</i>	50U/50µg (5ml)	GIBCO (15070063)

- **ADF Media**

<b>Components</b>	<b>Amount</b>	<b>Company (Cat #)</b>
<i>Advanced DMEM/F12 (1:1)</i>	500ml	GIBCO (12634028)
<i>CD Lipid Concentrate</i>	5ml	GIBCO (11905031)
<i>L-Glutamine (200mM)</i>	2mM (5ml)	GIBCO (25030024)
<i>Insulin</i>	14µg/ml	Sigma (I6634)
<i>Transferrin</i>	7.5µg/ml	Sigma (T8158)
<i>B-Mercaptoethanol</i>	0.1mM (3.5µl)	Sigma (M3148)
<i>Penicillin/Streptomycin (5000U/5000µg)</i>	50U/50µg (5ml)	GIBCO (15070063)

- **ADF/SB/LDN (EB Culture)**

<b>Components</b>	<b>Amount</b>	<b>Company (Cat #)</b>
<i>ADF media</i>	50ml	
<i>SB431542</i>	10µM	AbCam (ab120163)
<i>LDN 193189</i>	0.5µM	Stemgent (04-0019)

- **ADF/FGF (Adherent Rosette Culture)**

<b>Components</b>	<b>Amount</b>	<b>Company (Cat #)</b>
<i>ADF media</i>	50ml	
<i>FGF<sub>2</sub></i>	5ng/ml	Peptotech (100-18B)

- **Astrocyte Conditioned Media**

<b>Components</b>	<b>Amount</b>	<b>Company (Cat #)</b>
<i>DMEM/F12 (1:1)</i>	500ml	GIBCO (11330057)
<i>NeuroBrew 21</i>	10ml	Miltenyi (130093566)
<i>L-Glutamine</i>	20mM (5ml)	GIBCO (25030024)
<i>Penicillin/Streptomycin (5000U/5000µg)</i>	50U/50µg	GIBCO (15070063)

- **Other Cell Culture Reagents**

0.05% Trypsin	(GIBCO 25300054)
1x PBS pH7.4	(GIBCO 10010015)
Accutase	(PAA Laboratories L11-007)
Antibiotic-Antimycotic	(GIBCO 15240062)
BD Matrigel	(BD Biosciences 354230)
Bovine Serum Albumin	(Sigma A9418)
Collagenase type IV	(GIBCO 17104019)
dH <sub>2</sub> O	(GIBCO 15230188)
DMSO	(Sigma D2650)
EmbryoMax 0.1% Gelatin Solution	(Millipore ES-006-B)
FBS	(GIBCO 26140079)
Ficoll-Paque PLUS	(Stem Cell Technologies 07957)
G418 Geneticin	(GIBCO 1011-027)
Human Plasma Fibronectin	(Millipore FC010-10MG)
Methylcellulose Media with GFs Minus EPO	(RnD Systems HSC004)
Mouse Laminin	(Stemgent 06-0002)
Poly-L-Lysine Hydrobromide	(Sigma P5899)
Trypan blue	(Sigma T8154)
Y-27632 Rho Kinase Inhibitor	(Abcam ab120129)

## 2.1.2 SOLUTIONS, BUFFERS AND ENZYMES

- 1X TAE buffer

<b>Components</b>	<b>Amount</b>	<b>Company (Cat #)</b>
50x TAE Buffer	20ml	MPBIO (11TAE50X01)
dH <sub>2</sub> O	Up to 1 L	

- 1% Agarose gel

<b>Components</b>	<b>Amount</b>	<b>Company (Cat #)</b>
Agarose	1g	Melford Laboratories (MB1200)
Safeview	250µl	NBS Bio (NBS-SV1)
Guanosine	1mM	Sigma (G6264)
1xTAE Buffer	100ml	

- Orange G Loading buffer

<b>Components</b>	<b>Amount</b>	<b>Company (Cat #)</b>
Glycerol	25ml	Sigma (G9012)
10X TAE	25ml	MPBIO (11TAE50X01)
Orange G	0.175g	Sigma (O3756)

- Platinum Taq PCR

<b>Components</b>	<b>Amount</b>	<b>Company (Cat #)</b>
cDNA from monocytes	60ng	
Primer Pair	0.5µl	MWG (See Below)
Platinum Taq Buffer (10x)	2.5µl	Invitrogen (11304-011)
MgSO <sub>4</sub> (50mM)	1µl	Invitrogen (11304-011)
DMSO	0.6µl	Sigma ( <u>D9170</u> )
dNTPs (25mM)	1µl	Promega (U1420)
Platinum Taq - HF	0.25µl	Invitrogen (11304-011)
RNAse Free dH <sub>2</sub> O	Up to 25µl	Ambion (AM9937)

- Kanamycin LB Agar

<b>Components</b>	<b>Amount</b>	<b>Company (Cat #)</b>
LB	4g	Invitrogen (12780-052)
Agar	3g	Invitrogen (22700-025)
dH <sub>2</sub> O	200ml	
Kanamycin	50mg/ml	Sigma (K400)

- Kanamycin LB Media

<b>Components</b>	<b>Amount</b>	<b>Company (Cat #)</b>
LB	4g	Invitrogen (12780-052)
dH <sub>2</sub> O	200ml	
Kanamycin	50mg/ml	Sigma (K400)

- Restriction Digest Enzymes

<b>Enzyme</b>	<b>(Recognition Site (5'-3'))</b>	<b>Company(Cat #)</b>	<b>Supplied Buffer(s)</b>
<i>Bam</i> HI – HF	(G <sup>^</sup> GATCC)	NEB (R3136)	NEB 4
<i>Eco</i> RI – HF	(G <sup>^</sup> AATTC)	NEB (R3101)	NEB 4
<i>Xho</i> I	(C <sup>^</sup> TCGAG)	NEB (R0146)	NEB 4 + BSA
<i>Asc</i> I	(GG <sup>^</sup> CGCGCC)	NEB (R0558)	NEB 4
<i>Sal</i> I – HF	(G <sup>^</sup> TCGAC)	NEB (R3138)	NEB 4
<i>Asc</i> I	(AT <sup>^</sup> TAAT)	NEB (R0526)	NEB 3
<i>Bgl</i> II	(A <sup>^</sup> GATCT)	NEB (R0144)	NEB 3

- Double Restriction Digest

<b>Components</b>	<b>Amount</b>	<b>Company (Cat #)</b>
DNA	5 -10µl	
5x Restriction Buffer (3/4)	5µl	NEB (See Above)
Restriction Enzyme (1)	1µl	NEB (See Above)
Restriction Enzyme (2)	1µ	NEB (See Above)
BSA	0.1µl	NEB (See Above)
dH <sub>2</sub> O	Up to 25µl	GIBCO (15230-188)

- T4 DNA Ligase Ligation

<b>Components</b>	<b>Amount</b>	<b>Company (Cat #)</b>
Vector: Insert	1:3	
T4 DNA Ligase Buffer (10x)	2µl	NEB (M0202)
T4 DNA Ligase	1µl	NEB (M0202)
dH <sub>2</sub> O	Up to 20µl	GIBCO (15230-188)

- 4% Paraformaldehyde (PFA), pH 7-8

<b>Components</b>	<b>Amount</b>	<b>Company (Cat #)</b>
Paraformaldehyde	5g	Sigma (P5148)
1x PBS (pH7.4)	25ml	GIBCO (10010-015)
dH <sub>2</sub> O	50ml	GIBCO (15230-188)

- Immunocytochemistry Blocking Solution For External Markers

<b>Components</b>	<b>Amount</b>	<b>Company (Cat #)</b>
Bovine Serum Albumin (BSA)	3%	Sigma (A9418)
Normal Serum (Goat/Rabbit)	2%	Dako (X0907/X0902)
1x PBS (pH7.4)	Up to 50ml	GIBCO (10010-015)

- Immunocytochemistry Blocking Solution For Internal Markers

<b>Components</b>	<b>Amount</b>	<b>Company (Cat #)</b>
<i>Bovine Serum Albumin (BSA)</i>	3%	Sigma (A9418)
<i>Normal Serum (Goat/Rabbit)</i>	2%	Dako (X0907/X0902)
<i>Triton X-100</i>	0.1%	Sigma (T8787)
<i>1x PBS (pH7.4)</i>	Up to 50ml	GIBCO (10010-015)

- Histology - Sorenson's Buffer, pH 6.8

<b>Components</b>	<b>Amount</b>	<b>Company (Cat #)</b>
<i>KH<sub>2</sub>PO<sub>4</sub></i>	3.33g	Sigma (P9791)
<i>Na<sub>2</sub>HPO<sub>4</sub></i>	1.28g	Sigma (S3264)
<i>dH<sub>2</sub>O</i>	500ml	

- Histology - 5% Giemsa

<b>Components</b>	<b>Amount</b>	<b>Company (Cat #)</b>
<i>Giemsa Stain</i>	2.5ml	BDH (35086)
<i>Sorenson's Buffer</i>	Up to 50ml	

- Reverse Transcription (RT) Mix

<b>Components</b>	<b>Amount</b>	<b>Company (Cat #)</b>
<i>RNA</i>	1-10µl	
<i>Random Primers (1/12 dilution)</i>	1µl	Invitrogen (48190011)
<i>dNTPS (10mM)</i>	1µl	Invitrogen (18427013)
<i>First Strand Buffer (5x)</i>	4µl	Invitrogen (18080044)
<i>DTT (10mM)</i>	2µl	Invitrogen (18080044)
<i>RNase Out</i>	1µl	Invitrogen (10777019)
<i>RNase-free dH<sub>2</sub>O</i>	Up to 19µl	Ambion (AM9937)
<i>SuperScript III</i>	1µl	Invitrogen (18080044)

- QPCR Mix

<b>Components</b>	<b>Amount</b>	<b>Company (Cat #)</b>
<i>cDNA</i>	1µl	
<i>Primer Mix (1/100 dilution)</i>	1µl	MWG (Section 2.1.3)
<i>SYBR Green Master Mix (2x)</i>	10µl	Finnzymes (F-470L)
<i>RNase-Free dH<sub>2</sub>O</i>	8µl	Ambion (AM9937)

- **Western Blot - 10% Acrylamide Gel (Resolving Gel)**

<b>Components</b>	<b>Amount</b>	<b>Company (Cat #)</b>
30% Acrylamide/Bis (37.5:1)	3.3ml	BioRad (161-0158)
1.5mM Tris pH8.8	2.5ml	Roche (10708976001)
10% SDS	100µl	Sigma (L4390)
10% APS	100µl	Sigma (A3678)
TEMED	20µl	Sigma (T7024)
ddH <sub>2</sub> O	4ml	

- **Western Blot - Acrylamide Gel (Stacking Gel)**

<b>Components</b>	<b>Amount</b>	<b>Company (Cat#)</b>
30% Acrylamide/Bis (37.5:1)	1.67ml	BioRad (161-0158)
0.5mM Tris pH6.6	2.5ml	Roche (10708976001)
10% SDS	100µl	Sigma (L4390)
10% APS	100µl	Sigma (A3678)
TEMED	20µl	Sigma (T7024)
ddH <sub>2</sub> O	5.83ml	

- **Western Blot - Running Buffer (10x) pH8.3**

<b>Components</b>	<b>Amount</b>	<b>Company (Cat #)</b>
Tris Base	30.2g	Roche (10708976001)
Glycine	144g	Sigma (G8898)
SDS	10g	Sigma (L4390)
ddH <sub>2</sub> O	Up to 1L	

- **Western Blot - Transfer Buffer (1x)**

<b>Components</b>	<b>Amount</b>	<b>Company (Cat #)</b>
Tris Base	3.03g	Roche (10708976001)
Glycine	14.4g	Sigma (G8898)
Methanol	200ml	FisherScientific (M400017)
ddH <sub>2</sub> O	Up to 1L	

- **Western Blot Blocking Solution**

<b>Components</b>	<b>Amount</b>	<b>Company (Cat #)</b>
Powdered Milk	5%	Marvel
1x PBS (pH7.4)	50ml	GIBCO (10010-015)
Tween	0.1%	Sigma (P9416)

## 2.1.3 PRIMERS

**PU.1 Amplification Primers (Purchased from MWG)**

Primer	Forward	Reverse
<b>PU.1</b>	AACGGATCCATGTTACAGGCTGCAAAAT	AACGGATCCTCAGTGGGGCGGGTGGCGC

**QPCR Primers (Purchased from MWG)**

Primer	Forward	Reverse
<b>Oct4</b>	GCAGCTCGGAAGGCAGAT	TGGATTTTAAAAGGCAGAGACTTG
<b>Nanog</b>	CAGCCCCGATTCTTCCACCAGTCCC	CGGAAGATTCCCAGTCGGGTTCCACC
<b>Fik1</b>	GGCCCAATAATCAGAGTGGCA	CCAGTGTCAATTCGGATCACTTT
<b>RUNX1</b>	CTGCCCATCGCTTTCAAGGT	GCCGAGTAGTTTTTCATCATTGCC
<b>CD34</b>	TGGACCGCGGCTTTGCT	CCCTGGGTAGGTAACCTCTGGG
<b>CD45</b>	CATTTGGCTTTGCCTTTCTG	TTCTCTTTCAAAGGTGCTTGC
<b>PU.1</b>	CCAGCTCAGATGAGGAGGAG	CAGGTCCAACAGGAAGTGGT
<b>NG2</b>	AGAAGCAAGTGCTCCTCTCG	CCACTCAGCAGTCAGACCCT
<b>CD11c</b>	GGAAGACCCTTCTCCAAAGC	CAGAGGAGCTGACAGCCTTC
<b>CD80</b>	AGGGAACATCACCATCCAG	CAAACCTCGCATCTACTGGCA
<b>IBA-1</b>	GCTGAGCTATGAGCCAAACC	TCATCCAGCCTCTCTTCCTG
<b>IL-1B</b>	ACAGATGAAGTGCTCCTTCCA	GTCGGAGATTCGTAGCTGGAT
<b>TNF-a</b>	CCCAGGGACCTCTCTAATC	ATGGGCTACAGGCTTGCTCACT
<b>Kir2.1</b>	GGTTTGCTTTGGCTCAGTCG	GAACATGTCCTGTTGCTGGC

<b>NaV1.5</b>	CATTCAGGGCTGAAGACCA	GGCAGAAGACTGTGAGGACC
<b>NaV1.6</b>	GGCAATGTTTCAGCTCTACGC	ATTGTCTTCAGGCCTGGGATT

#### 2.1.4 ANTIBODIES

- **Immunocytochemistry Antibodies**

<b>1° Antibody (ICC)</b>	<b>Supplier (Cat #)</b>	<b>Host</b>	<b>Dilution</b>
<b>Oct4</b>	Santa Cruz (SC-5279)	Mouse Mono (IgG <sub>2A</sub> )	1/100
<b>SOX2</b>	Millipore (AB5603)	Rabbit Poly (IgG)	1/200
<b>PU.1</b>	Santa-Cruz (SC-352)	Rabbit Poly (IgG)	1/50
<b>RUNX1</b>	Abcam (ab61753)	Rabbit Poly (IgG)	1/267
<b>FLK1</b>	Abcam (ab2349)	Rabbit Poly (IgG)	1/80
<b>CD34</b>	Abcam (ab6330)	Mouse Mono (IgG <sub>1</sub> )	1/100
<b>CD45</b>	RnD (MAB1430)	Mouse Mono (IgG <sub>1</sub> )	1/100
<b>CD11b</b>	Abcam (ab8878)	Rat Mono (IgG <sub>2b</sub> )	1/50
<b>IBA-1</b>	Abcam (ab5076)	Goat Poly (IgG)	1/100
<b>B-Tubulin III</b>	Sigma (T8660)	Mouse Mono (IgG <sub>2B</sub> )	1/400
<b>ZO-1</b>	BD Bioscience (610966)	Mouse Mono (IgG <sub>1</sub> )	1/500
<b>GLUT5</b>	RnD (MAB1349)	Mouse Mono (IgG <sub>2A</sub> )	1/100
<b>A<math>\beta</math></b>	Abcam(ab2539)	Rabbit Poly (IgG)	1/100

<b>2° Antibody (ICC)</b>	<b>Supplier</b>	<b>Dilution</b>
<b>Alexa Fluor Goat Anti-Mouse IgG 488</b>	Invitrogen (A11001)	1/400
<b>Alexa Fluor Goat Anti-Mouse IgG 594</b>	Invitrogen (A11032)	1/400
<b>Alexa Fluor Goat Anti-Rabbit IgG 488</b>	Invitrogen (A11034)	1/400
<b>Alexa Fluor Goat Anti – Rabbit IgG 594</b>	Invitrogen (A11037)	1/400

<b>Alexa Fluor Chicken Anti-Rat IgG 594</b>	Invitrogen (A21471)	1/400
<b>Alexa Fluor Donkey Anti-Goat IgG 488</b>	Invitrogen (A11055)	1/400

- **FACS Antibodies**

<b>Conjugated Antibody</b>	<b>Company (Cat#)</b>
<b>CD34 – PECy7</b>	e-Bioscience (25-0349-42)
<b>CD45 – FITC</b>	e-Bioscience (11-9459-42)
<b>CD11b - APC</b>	e-Bioscience (17-0118-42)

- **Western Blot Antibodies**

<b>1° Antibody (WB)</b>	<b>Company (Cat#)</b>	<b>Host</b>	<b>Dilution</b>
<b>B-Actin</b>	Sigma (A2228)	Mouse Mono (IgG <sub>2A</sub> )	1/10000
<b>PU.1</b>	Santa-Cruz (SC-352)	Rabbit Poly (IgG)	1/200
<b>2° Antibody (WB)</b>	<b>Company (Cat#)</b>	<b>Host</b>	<b>Dilution</b>
<b>ECL α-Mouse HRP</b>	GE Healthcare (NA931V)	Mouse IgG	1/10000
<b>ECL α-Rabbit HRP</b>	GE Healthcare (NIF824)	Rabbit IgG	1/10000

---

2.1.5 CONSUMABLES

---

0.2ml thin wall dome cap tube	(Alpha Labs LW2130AS)
1.5ml plastic tube	(Alpha Labs LW2410)
10 cm non-adherent culture plates	(Sterilin PDS-140-050F)
10cm adherent culture plates	(NUNC 150350)
10µl, 20µl, 200µl, 1000µl pipette tips	(Fisher scientific FB781-00, 06,10,12)
14 gauge needles	(Monoject 200011)
15ml tubes	(Corning 430766)
18mm (0.16mm Thickness) Glass Cover Slips	(VWR 631-0153)
20ml, 60ml eccentric tip syringes	(BD Bio 300613, 300866)
24 well plates	(NUNC TKT-190-010Y)
3.5cm culture plates	(NUNC IVF-150-255T)
50ml tubes	(Corning 430897)
5ml round bottom tubes	(BD Falcon 352058)
5ml, 10ml, 25ml stripettes	(Corning CC109, CC114, CC116)
6 well plates	(NUNC TKT-190-110E)
6cm adherent culture plates	(NUNC TKT-110-0105)
6cm non-adherent culture plates	(Sterilin 101RT/IRR)
Amersham Hybond – ECL	(GE Healthcare RPN203D)
Cell Scraper	(Corning 3008)
Cryovials	(Fisher Scientific FB74414)
Histobond Glass Slides 75x25x1mm	(RALamb E27.5HB)
Low Profile 96 well unskirted PCR plates	(BioRad MLL-9651)
Minisart plus Syringe Filters 0.2µm	(Sartorius Stedim Biotech 17823--Q)
Super Rx Medical X-ray film	(FujiFilm 4741008389)
T25 flasks	(NUNC TKT-130-150L)
T75 flasks	(NUNC TKT-130-190W)

## 2.1.6 KITS

Amaya Mouse Neural Stem Cell Nucleofection kit	(Lonza VPG 1004)
BCA Protein Assay kit	(Thermo Scientific 23227)
DNAase	(QIAGEN 79254)
Endofree Maxi Prep kit (10)	(QIAGEN 12362)
Gene Clean Gel Extraction	(MP BIO 1001-400)
RNEasy mini (50) Kit	(QIAGEN 74104)
SuperSignal West Dura Extended Exposure Kit	(Thermo Scientific 34076)

## 2.1.7 EQUIPMENT

<b>Centrifuges</b>	Rotanta 460R ( <i>Hettich Zentrifugen</i> )
	Biofuge Pico ( <i>Heraeus</i> )
<b>Electrophoresis Tank</b>	Electrophoresis Tank ( <i>Flowgen</i> )
<b>Power Supply</b>	Power Pac 200 ( <i>BioRad</i> )
<b>Water Bath</b>	BS5 with ET100 controller ( <i>Fisher Scientific</i> )
<b>Incubators</b>	CB 150 ( <i>Binder</i> )
	Jeio Tech SI-900 ( <i>Medline Scientific UK</i> )
<b>Laminar Flow Hood</b>	MicroFlow Peroxide Advanced BioSafety Cabinet ClassIII ( <i>BioQuell</i> )
<b>Microscopes</b>	AMG ( <i>EVOS</i> )
	IX71 ( <i>Olympus</i> )
	IX81 ( <i>Olympus</i> )
	BX61 ( <i>Olympus</i> )
<b>pH Meter</b>	pH Meter 240 ( <i>Corning</i> )
<b>QPCR Thermocycler</b>	CFX Connect Real Time System ( <i>Bio-Rad</i> )
<b>Thermocycler</b>	TC-412 ( <i>Techne</i> )
	TC-512 ( <i>Techne</i> )
<b>Vortex</b>	Vortex Genie-2 ( <i>Scientific Industries</i> )
<b>FACS Machine</b>	FACS Canto ( <i>BD Biosciences</i> )

**Western Blot Rig**Mini-Protean III (*Bio Rad*)**Cytocentrifuge**CYT04 (*Centurion Scientific*)

---

**2.1.8 SOFTWARE**

---

Analysis 3.2	( <i>Soft Imaging System GmbH</i> )
BD FACs DIVA	( <i>BD Biosciences</i> )
Cylogic	( <i>CyFlo LTD</i> )
FlowJo 7.6.4	( <i>Tree Star</i> )
Mendeley	( <i>Glyph &amp; Cog</i> )
Microsoft Office 2007	( <i>Microsoft</i> )
Photoshop 7	( <i>Adobe</i> )
GraphPad Prism v6	( <i>GraphPad Software Ltd</i> )

## 2.2 MEFI FEEDER LAYER

---

### 2.2.1 GROWING AND IRRADIATING MEFS

---

B16 mouse embryos were harvested at 12 to 13 days post-coitum. The uterus, containing the embryos, was then removed into 1x PBS. The head and internal organs of the embryos were removed and transferred to a sterile petri dish. The embryos were then minced using a sterile blade and incubated in 0.05% trypsin for 5 minutes at 37°C. Following trypsinisation, MEF medium (See Section 2.1.1) was added and the mixture vigorously homogenized with a pipette before centrifugation at 1000rpm for 5 minutes. The supernatant was removed by aspiration and the pellet was re-suspended in MEF medium (containing 1% Antibiotic-Antimycotic (*GIBCO 15240062*)) and plated as one embryo per 14cm plate. The cells were fed with fresh MEF medium every other day until they reached confluence. At this stage the cells were split (1:5) using 0.05% trypsin as passage 1. When these plates reached confluence 80% were used for irradiation, the remaining 20% were split with trypsin to give rise to passage 2. At passage 2 confluence all plates were irradiated and frozen. Irradiation was achieved by centrifugation of the trypsinised cells at 1000rpm for 5 minutes, followed by aspiration of the supernatant and the combination of all cell pellets to a single 50ml tube in 20ml of MEF media. These cells were irradiated for 30 minutes at 216 Rads/min. The cells were frozen at -1°C/minute overnight in cryovials at a density of  $1 \times 10^6$  cells/vial in 1ml of freezing medium (MEF medium + 10% DMSO) and stored at -80°C.

---

### 2.2.2 PLATING IRRADIATED MEFS

---

Irradiated Mouse embryonic Fibroblasts (MEFi) were thawed and plated in MEF Media (See Section 2.1.1) at a density of  $12.5 \times 10^4$  cells onto 6cm culture dishes, that were pre-coated with EmbryoMax 0.1% gelatin solution (*Millipore ES-006-B*) for 30 minutes, and allowed to attach for a minimum 24 hours prior to use as a feeder layer.

---

### 2.3 MAINTENANCE OF ES CELLS

---

Human Embryonic Stem Cells (hESCs), H9 cell line, were maintained on feeder plates of MEFi, in H9 Media (See Section 2.1.1). The medium was changed daily, by aspiration, and the cells were passaged with 1mg/ml collagenase type IV (*GIBCO 17104019*) in KO-DMEM (*GIBCO 10829018*), every three days (or at 80% confluence) onto a MEFi feeder layer, as above in H9 medium with 10 $\mu$ M Rho Kinase inhibitor (*Abcam ab120129*)

---

### 2.4 GENERATION AND MAINTENANCE OF HSCS

---

H9 cells on a feeder layer of MEFi in a 6cm dish (*Nunc TKT-110-0105*) at a confluence of 70-80% were scored into a 10x10 grid using a 14 gauge needle (*Monoject 200011*) and lifted from the plate using a cell scraper (*Corning 3008*). Cells were allowed to settle by gravity before aspirating the supernatant medium and resuspending in fresh H9 medium with 10ng/ml bFGF to a 6cm low attachment plate to form embryoid bodies. At day 2 there was a 50% medium change with the addition of fresh H9 medium + 10ng/ml bFGF. The EBs were plated 15 EBs per well of a 6-well tissue culture plate in XVIVO 15 factory medium (See Section 2.1.1) with M-CSF and IL-3 at day 4. The medium was changed every 5 days or when the medium began to yellow and the supernatant cells were collected by centrifugation at

1500rpm for 3 minutes. The pellet of cells was resuspended, assayed for viability through trypan blue staining and plated at a maximum density of  $1 \times 10^6$  cells per well of a 6-well tissue culture plate in XVIVO complete factory medium (See Section 2.1.1).

---

### 2.5 MAINTENANCE OF THP-1 MONOCYTES

---

THP-1 monocytes (a cell line obtained from an acute monocytic leukemia patient) were acquired from Dr. Dipak Ramji (Cardiff University). The cells were maintained in non-adherent culture in a T75 flask (*Nunc TKT-130-190W*) in monocyte maintenance medium (MMM) (See 2.1.1). Every fourth day the cells were recovered from the medium by centrifugation (1500rpm for 3 minutes), re-suspended in MMM and split in a 1:2 ratio into T75 flasks (*Nunc TKT-130-190W*).

---

### 2.6 NEURAL PROGENITOR CELL CULTURE

---

H9 cells, at 80% confluence, were dissociated from the plate and Mefi feeder layer with 1mg/ml collagenase type IV (*GIBCO 17104019*) in KO-DMEM (*GIBCO 10829018*) and the resulting cells were centrifuged for 3 minutes at 1000rpm. The colonies were dissociated into smaller aggregations of cells by manual passaging with a pipette. Embryoid bodies (EBs) were created by plating the cell suspension in 10cm non-adherent culture plates (*Sterelin PDS-140-050F*) in ADF/SB/LDN medium (See Section 2.1.1) for 8 days. The medium was replaced every other day and on the eighth day the EBs were dissociated with Accutase (*PAA L11-007*) for 5 minutes at 37°C and centrifuged (1000rpm for 3minutes) to recover the cells. The cells were dissociated to a single cell suspension by repeat pipetting and plated onto Poly-L-Lysine (*Sigma P5899*)/Laminin (*Stemgent 06-0002*) coated glass cover slips (*VWR 631-0153*) in a 24 well plate (*Nunc TKT-190-010Y*) at a density of  $5 \times 10^4$  cells per

well in ADF/FGF medium (See Section 2.1.1). The medium was changed every other day until neural precursor formation, with characteristic rosette morphology. At day 12 the neural precursors were nucleofected (See Section 2.7).

---

## 2.7 NUCLEOFECTION

---

---

### 2.7.1 CREATING THE PCAGG-PU.1-IRES-GFP CONSTRUCT

---

The vector backbone was pIRES2-EGFP which was, through four steps; (1) Amplifying human PU.1 by PCR, (2) Inserting a CAG promoter from pCAGIG, (3) Inserting PU.1 and (4) Removing the CMV promoter, converted the plasmid into a PU.1 expression vector (*for vector maps and PU.1 sequence, see Appendix I*).

PU.1 was amplified from human primary macrophage cDNA, using primers that were specifically designed to amplify with BamHI restriction sites to the ends of the gene. The PCR was carried out using Platinum high fidelity DNA polymerase (See Section 2.1.2) with the addition of DMSO to aid strand separation.

The PCR product was inserted into a Zero Blunt TOPO PCR vector (*Invitrogen K2875-20*), which was transformed into the supplied TOP10 competent cells and streaked onto 50mg/ml kanamycin sulfate agar plates (See Section 2.1.2). The resulting colonies were grown in LB medium containing 50mg/ml kanamycin sulfate (See Section 2.1.2) and mini-preped using the alkaline lysis procedure (as described in Maniatis et al. 1982). The DNA was analysed by BamHI restriction digest for the presence of the PU.1 insert and those colonies found to contain the gene were sequenced to ensure proper gene amplification and true replication.

The original CMV promoter from pIRES2-EGFP was then removed and replaced with the CAG promoter from pCAGIG. Compatible restriction sites within the MCS of

pIRES2-EGFP (XhoI, EcoRI) and surrounding the CAG promoter in pCAGIG (Sall, EcoRI) were used to give directionality to the promoter on ligation of the fragments. The plasmid DNA preparations were digested with the required enzymes for 30 minutes at 37°C in the appropriate buffer, before running the digest on a 1% TAE agarose gel containing 1 mM guanosine (See Section 2.1.2) to protect DNA from UV damage. The fragments were extracted from the gel using gene clean II kit (MP Bio 1001-400) and the concentration and purity (260/280 value) of the sample was determined by spectrophotometry (Nanodrop). The fragments were ligated in a 3:1 ratio of insert to plasmid based on molecular weight using the formula;

$$\frac{((Vector (ng))(Insert (Kb)))}{((Vector (Kb))(ratio))} = Insert (ng)$$

T4 DNA ligase was used for the ligation (See Section 2.1.2), which occurred at 25°C for 2 hours. The ligated product was then transformed into Sub Cloning Efficiency DH5α *E. coli* cells (Invitrogen 18265-017), which were streaked onto agar plates containing 50 mg/ml kanamycin sulfate (See Section 2.1.2). The colonies were selected and grown in LB medium with 50 mg/ml kanamycin sulfate (See Section 2.1.2) and were subsequently used in alkaline lysis to extract the DNA. Restriction digest reactions were run using several combinations of enzymes to ensure correct ligation of the fragments had occurred.

The PU.1 gene (with verified sequence) was removed from the TOPO vector by Bam HI (NEB) digestion along with the newly formed pCAGG-IRES-GFP vector and both were gel extracted, ligated and transformed as above. The resulting colonies were grown in LB medium containing 50 mg/ml kanamycin sulfate (See Section 2.1.2), alkaline lysed to extract the DNA and screened for both the presence and correct orientation of PU.1 insert by multiple restriction digestions.

Finally, the redundant CMV promoter within pCAGG-PU.1-IRES-GFP was removed by digestion with *AseI* (*NEB*) and *BglIII* (*NEB*) followed by Klenow (*NEB M0210*) blunt ending of the non-compatible ends, gel extracting and re-ligating the vector (as above). The ligation was again transformed into sub cloning efficiency DH5 $\alpha$  cells, colonies were picked, grown and lysed to extract DNA (as above) before restriction digest analysis to ensure proper removal of the CMV promoter and correct re-ligation of the vector.

---

### 2.7.3 AMAXA NUCLEOFECTATION

---

Neural rosettes, created from H9 cells (described in Section 2.6) were dissociated from the plate with *Accutase* (*PAA Laboratories L11-007*) and washed in PBS pH7.4 (*GIBCO 10010015*); cells were centrifuged for 3 minutes at 1000rpm and re-suspended in Mouse Neural Stem Cell nucleofection solution (*Lonza VPG-1004*) with either 10 $\mu$ g of pCAGG-PU.1-IRES-GFP or control (pCAGG-IRES-GFP) and gently mixed before they were transferred to a transfection cuvette. The cells were transfected using the Amaxa Nucleofection machine and program A-023. Post transfection the cells were re-suspended in 1ml of pre-warmed ADF medium (See Section 2.1.1) and removed from the cuvette with the provided plastic Pasteur pipette and counted, using a haemocytometer, prior to plating on matrigel (*BD Biosciences 354230*) coated glass cover slips in a 24 well plate at a density of 5x10<sup>4</sup> cells per well.

---

### 2.7.3 SELECTION

---

Expression of the GFP marker is evident in the positively nucleofected cells 48 hours post nucleofection this was observed under the Olympus IX71 microscope using the FITC filter. Selection of the GFP+ cells was achieved by the addition of 200µg/ml G418 (*GIBCO 1011-027*) to the culture medium, which was changed every other day, until only GFP+ cells remained.

---

### 2.7.4 DIFFERENTIATION TO MONOCYTIC PRECURSORS

---

On presence of only GFP+ cells, the G418 (*GIBCO 1011-027*) was removed from the medium and cells were fed every other day in ADF/FGF medium (*See Section 2.1.1*). The supernatant was collected and the non-adherent cells were recovered by centrifugation at 1000rpm for 3 minutes. The non-adherent cells were re-suspended in MMM, cell viability was assessed by trypan blue exclusion and they were plated on to 5µg/cm<sup>2</sup> fibronectin (*Millipore FC010-10MG*) coated glass cover slips (*VWR 631-0153*) in a 24-well plate (*NUNC TKT-190-010Y*).

---

## 2.8 MONOCYTE DIFFERENTIATION TO MICROGLIAL-LIKE CELLS

---

---

### 2.8.1 ASTROCYTE CONDITIONED MEDIA

---

ACM was produced as according to Rushton et al. (2013) and all animal work was carried out by Professor Nick Allen. Striata from newborn C57B1/6J mice were dissected into cold Hank's Buffered Salt Solution (HBSS, *Life Technologies 14025092*) and digested by incubation with Accutase (*PAA Laboratories L11-007*) and DNase1 (0.1mg/ml, *Sigma D7291*) for 30 minutes at 37°C. The digestion was terminated and the cells were resuspended by the addition of MEF media (*See Section 2.1.1*). The cells were washed twice and plated into T75 culture flasks (*NUNC TKT-130-190W*) in MEF media. Upon confluence astrocytes were passaged

1:6 and confluent cultures from P1 and P2 were used to condition the base medium (DMEM/F12 (1:1), 2% Neurobrew 21, 1% L-Glutamine, 1% Penicillin/Streptomycin). After the 48h of conditioning the medium was collected filtered and frozen, whilst the astrocytes were washed in PBS and cultured in MEF medium for 24h for recovery before conditioning re-started.

---

### 2.8.2 MONOCYTE DIFFERENTIATION TO MICROGLIAL-LIKE CELL

---

The monocytes were plated at a density of  $1 \times 10^5$  onto coverslips that were coated with  $5 \mu\text{g}/\text{cm}^2$  fibronectin (*Millipore FC010-10MG*) as a  $100 \mu\text{l}$  droplet and allowed to attach for several hours prior to flooding the wells with  $250 \mu\text{l}$  of Astrocyte Conditioned Media (ACM) (*See Section 2.1.1*). The medium was changed every third day for up to 14 days, until differentiation to a ramified microglial-like cell. Assays took place on day 7 of the differentiation.

---

### 2.8.3 ADDITION OF AB

---

Prior to addition to cultures  $A\beta_{(1-42)}$  (*Tocris 1428*) and  $rA\beta_{(42-1)}$  (*Tocris 3391*) were prepared by a 1 hour incubation at  $37^\circ\text{C}$ .  $A\beta_{(1-42)}$  or  $rA\beta_{(42-1)}$  were then added to day 7 microglial-like cells resulting from culture in ACM, or the control cells cultured in the unconditioned base medium at a final concentration of  $5 \mu\text{M}$ . Phenotypic and immunological studies preceded after a 2 hour incubation, studies involving gene expression resulted from cultures 8 hours post incubation.

---

## 2.11 IMMUNOCYTOCHEMISTRY

---

Cells on glass cover slips were fixed in 4% PFA (*See Section 2.2.1*), or cytospin on to glass slides (*See Section 2.13.1*) and washed in PBS pH7.4 (*GIBCO 10010-015*) before being blocked in the appropriate solution for the marker, either internal or

external (See Section 2.9.1). The primary antibodies (See Section 2.3) were diluted in the appropriate block (+/- Triton X) and incubated overnight at 4°C. After washing with PBS pH7.4 (GIBCO 10010015) the fluorescent secondary antibodies (See Section 2.3) were added and incubated for an hour at room temperature before washing and counterstaining the nucleus with 0.1µg/ml Hoechst and mounting in PBS:Glycerol (1:1) onto glass microscope slides.

---

### 2.12 FACS

---

#### 2.12.1 SINGLE COLOUR STAINING

---

Live non-adherent cells were washed in 0.1% BSA (*Sigma A9418*) in PBS (*GIBCO 10010015*) and centrifuged at 300rpm for 1 minute. The cell pellet was re-suspended in 100µl 0.1% BSA in PBS with 5ul of the appropriate conjugated antibody (See Section 2.1.4) for the test samples, and 100µl 0.1% BSA in PBS without any antibody for the control sample, for 20 minutes at room temperature in the dark. This was followed by gentle centrifugation (300rpm for 1 minute) and a final wash in 0.1% BSA in PBS. The cells were then transferred to 5ml round bottom tubes (*BD Falcon*) in an appropriate volume 0.1% BSA in PBS. The samples were then run using a BD Bioscience FACS Canto machine and analysed using FlowJo (Version 6.3.2; [www.FlowJo.com](http://www.FlowJo.com))

---

#### 2.12.2 TRIPLE COLOUR STAINING

---

As for the single staining above, with the addition of single stained samples and an unstained sample for controls and to allow for any compensation. The triple stained sample was then incubated with 0.1% BSA (*Sigma A9418*) in PBS (*GIBCO 10010015*) with 5ul of three antibodies conjugated to fluorophores (See Section

2.1.4) chosen to limit spill over into adjacent channels and thus the need for compensation and for their intensity compared to the expression level of the marker.

---

## 2.13 HISTOLOGY

---

---

### 2.13.1 CYTOCENTRIFUGATION

---

Non-adherent cells were collected and spun at 800rpm for 1 minute through pre-wet filters onto glass slides using a Centurion CYT04 cytocentrifuge.

---

### 2.13.2 STAINING

---

Slides were incubated with 5% Giemsa stain (See Section 2.1.2) or haematoxylin for 10 minutes. Giemsa stained samples were then washed in Sorenson's buffer pH6.8 (See Section 2.1.2) followed by washes in tap water to remove the excess stain before viewing. Haematoxylin stained samples were washed for 5minutes under a running tap to remove the excess stain. Both were viewed on an Olympus IX61 microscope.

---

## 2.14 PHAGOCYTOSIS ASSAY

---

Optimal time and temperature were determined by FACS analysis using fluorescent Alexa Fluor® 594 labelled E.coli bioparticles (*Invitrogen E23370*) and staining the non-adherent cells with CD45. The optimal results were then used to chart phagocytosis by time-lapse microscopy. For time lapse monocytes were plated at a density of  $2 \times 10^4$  per well of a 24 well plate and allowed to attach to the tissue culture plastic for several hours. On initiation of microscopy the medium was changed by aspiration and washing to an extracellular solution to enable cells to maintain function outside of a gas controlled incubator and 40ng/µl of beads were added. An Olympus IX61 fluorescent microscope was used in conjunction with SimplePCI

software to capture an image in both brightfield and using the TRITC filter to visualise the beads every 15 seconds for 90 minutes.

### 2.15 QPCR

Cells were washed and lysed in RLT buffer (*QIAGEN 74104, as part of RNEasy Mini Kit*) containing 10 $\mu$ l/ml  $\beta$ -Mercaptoethanol (*Sigma A9418*) and stored at -80°C. On thawing the RNA was extracted using an RNEasy Mini Kit (*QIAGEN 74104*), the lysate was diluted (1:1) in 70% ethanol (*Fisher Scientific E0650DF17*) and loaded on to the provided column. The column was centrifuged for 15 seconds; the column was washed with the provided buffer and re-centrifuged for 15 seconds and on-column DNase digestion was performed by incubating the sample on the column in 80 $\mu$ l of DNase in RDD buffer (*QIAGEN 79254*) for 20 minutes at room temperature. Then column was then washed and centrifuged before the sample was eluted in RNase free dH<sub>2</sub>O. The concentration of the sample and its purity (260/280 value) were assessed by Spectrophotometry (*Nanodrop*).

cDNA was created by the addition of the collected RNA, random primers (*Invitrogen 48190011*), first strand buffer and the reverse transcriptase SuperScript III (*Invitrogen 18080044*), as described in section 2.1.2, before being placed in a thermocycler (*Techne TC-512*) with the program detailed below.

Temperature	Time
25°C	10 minutes
42°C	50 minutes
70°C	15 minutes

To enable quantification of gene expression QPCR was carried out on the cDNA. This was achieved by using primers specifically designed for QPCR with a T<sub>m</sub> close

to 60°C, which resulted in a product of between 80 and 120bp, optimal for the QPCR program (below). The primer efficiencies were first established by serial dilution of cDNA using the formula  $\%E = \left(10^{\left(-\frac{1}{M}\right)} - 1\right) \times 100$ . Only primers with efficiencies between 90 and 105% were used in the downstream reactions (*for primer efficiency data see Appendix II*).

The QPCR mix, described above in section 2.1.2, was added to a 96 well plate (*BioRad MLL-9651*) before being centrifuged for 1 minute at 1500rpm and was cycled through the program below. For analysis the  $\Delta\Delta C_t$  Livak method was used on 3 biological replicates, where each biological sample was analysed in triplicate as technical replicates (Livak and Schmittgen 2001). To further define, in this case biological replicates are identical cells grown separately but treated in the same manner to ascertain that the difference witnessed is representative of a biological difference. Technical replicates are defined as the same biological replicate analysed multiple times, in this case run in triplicate, to establish technical variability.

<b>Step</b>	<b>Temperature</b>	<b>Time</b>	<b>Repeat</b>
<b>Initial Denaturation</b>	95°C	15 minutes	1X
<b>Denaturation</b>	95°C	30 seconds	40X
<b>Annealing</b>	60°C	30 seconds	
<b>Extension</b>	72°C	30 seconds	
	<b>Plate Read</b>	-	1X
<b>Melt Curve</b>	53-95°C (+0.5°C/Plate Read)	2 seconds/ +0.5°C	1X

## 2.16 WESTERN BLOT

---

Samples were collected in lysis buffer (See 2.13.1) for 30 minutes at 4°C before being centrifuged at high speed for 20 minutes. The supernatant was then assayed for protein concentration by using a BCA Protein Assay kit (*Thermo Scientific 23227*) and colorimetric analysis.

Stacking and resolving (10%) Acrylamide gels (See Section 2.1.2) were made and allowed to set before the samples were diluted, to the concentration determined in the BCA assay, in loading buffer (See Section 2.1.2). The samples were then denatured and loaded onto the gel along with a Novex Sharp protein standard (*Invitrogen LC5800*). The gel was run at 100V for an hour in 1x running buffer. After which the glass plates were removed, the stacking gel cut away and the gel carefully placed onto the membrane (*GE Healthcare RPN 203D*), in a bath of transfer buffer. The transfer cassettes were then constructed using pre-soaked sponges and filter paper along with the gel and membrane. The tank was filled with transfer buffer (See Section 2.1.2), set on a magnetic stirrer and run overnight at 25V at 4°C. After the transfer, the membrane was removed from the cassette washed in 0.1% PBS/Tween (See Section 2.1.2) and blocked (See Section 2.1.2) for 1 hour before incubating for 1 hour in primary antibody diluted in block (See Section 2.1.4). Following the incubation, the membranes were washed in 0.1% PBS/Tween then the membrane was incubated with the secondary antibody (See Section 2.1.4) for 1 hour. The membrane was then washed in 0.1% PBS/Tween before placing in the developing cassette and adding SuperSignal West Dura Exposure solutions (*Thermo Scientific 34076*) onto the membrane for 5 minutes in the dark before placing the

chemiluminescent detection film (*Roche 11666916001*) on top of the membrane for the desired length of time and then developing the image.

### 2.17 ELECTROPHYSIOLOGY

---

Whole cell voltage clamp was performed by Dr. J. Griffiths on H9 derived cells perfused with a HEPES- buffered solution containing, in mM: 135 NaCl; 5 KCl; 5 HEPES; 1.2 MgCl<sub>2</sub>; 1.25 mM CaCl<sub>2</sub>; 10 Glucose; pH 7.4. The pipette solution contained, in mM: 117 KCl; 10 NaCl; 2 MgCl<sub>2</sub>; 1 CaCl<sub>2</sub>; 11 EGTA; 2 Na.ATP; 11 HEPES; pH 7.2. Filled with this solution, borosilicate pipettes pulled on a Narishige (PP-81) 2-stage puller, demonstrated resistances of 5-7 MΩ. Following capacitance and series resistance compensation, cells were voltage clamped at -70 mV and currents were evoked by a voltage step protocol (from -170 to +60 mV in 10 mV increments, each 200ms, at 2Hz Hz, P/N = 4 on-line subtraction). All electrophysiology experiments were conducted at ambient room temperature. All current recordings were made using an Axopatch 200A amplifier and Digidata 13320 A/D interface (*Axon Instruments, Forster City, CA, USA*). Currents were digitized at 10 kHz and Bessel low-pass filtered at 5 kHz.

### 2.18 CYTOKINE/CHEMOKINE ARRAYS

---

Cell culture supernatants were collected 8h post incubation with Aβ<sub>(1-42)</sub> or rAβ<sub>(42-1)</sub> and centrifuged to remove particles and debris. The membranes (as part of the cytokine array (*RnD Systems ARY005*) or the chemokine array (*RnD Systems ARY017*)) were blocked for 1 hour in 2ml Array Buffer 4 (*Included in ARY005 and ARY017*). During the incubation the samples were prepared as follows; 250μl supernatant, 500μl Array Buffer 4 and 750μl Array Buffer 5, finally the antibody cocktail was added and incubated for 1 hour. Array Buffer 4 was then removed from

the membranes and the supernatant/antibody mix was added and incubated overnight at 4°C on a rocking platform. The membranes were then washed 3 times with 1x Wash Buffer (*Included in ARY005 and ARY017*) for 10 minutes per wash, after the final wash 2ml Streptavidin-HRP (*Included in ARY005 and ARY017*) was added to each membrane and incubated for 30 minutes on a rocking platform.

Following the incubation the membranes were washed a further 3 times in 1xWash Buffer. The membranes were then removed from the wash and the excess buffer was allowed to drain from the membrane before placing it onto a plastic sheet within a developing cassette and adding 1ml Chemi Reagent Mix (*Included in ARY005 and ARY017*). The top plastic sheet was placed over the membranes and the air bubbles were smoothed out and the Chemi Reagent Mix was evenly spread out over each membrane before incubating for 1 minute, after which the excess Chemi Reagent Mix was removed. Chemiluminescent detection film (*Roche 11666916001*) was placed on top of the membranes and exposed for the desired length of time. The developed image was analysed using ImageJ for the pixel density.

## 2.19 STATISTICS

---

Statistical analysis of QPCR data was carried out using GraphPad Prism 6.05. The means were compared using ANOVA and significant differences were compared using the Bonferroni Post-Hoc test at a 95% confidence interval, which were also denoted on graphs as asterics representing the significance summary provided by GraphPad Prism and are defined as follows; \*  $\leq 0.05$ , \*\*  $\leq 0.01$ , \*\*\*  $\leq 0.001$ , \*\*\*\*  $\leq 0.0001$ .

---

## 3. GENERATION OF MONOCYTES BY ECTOPIC OVER-EXPRESSION OF PU.1

---

---

### 3.1 INTRODUCTION

---

Terminal differentiation to monocytes is dependent on the timely expression of lineage restricted transcription factors and release of cytokines that regulate a haematopoietic niche (Figure 2; Section 1.1.3). One essential transcription factor in this regard is PU.1, which is required in a dose-dependent manner throughout hematopoiesis and at high levels for the final differentiation of haematopoietic precursors to monocytes. Since microglia are derived from a monocytic lineage, PU.1 is also vital for microglial differentiation. This was proven in PU.1 knock-out mouse models, where a lack of both circulating monocytes and CNS microglia were observed (Walton et al. 2000).

Work by Forsberg et al. (2008) showed that murine adult neural stem cells could be reprogrammed easily into monocytes, an unrelated lineage, by introducing an exogenous source of PU.1 through lentiviral transduction. When these cells were transplanted into the brain *in vivo* they migrated and differentiated into microglia, which were indistinguishable, with the exception of GFP expression, from the native microglia. Beutner et al. (2010) have also used a modified five step method for the production of neuronal cells as the basis of their differentiation strategy of mESCs to microglia.

PU.1 is the 270 amino acid, 31kDa protein product from the SPI1 gene. It exists in two isoforms due to alternative splicing; (1) the canonical form and (2) the alternative form, which has a glutamine insertion at position 15 (Ray et al. 1990). PU.1 is a transcription factor of the E-twenty six (Ets) family, which binds to the purine rich 5'-GAGGAA-3' sequence (Klemsz et al. 1990). It is a key regulator of haematopoiesis with downstream targets that include; *c-fms* (M-CSF receptor), CD45, CD11b, GM-CSFR $\alpha$  and CEBP/ $\alpha$  and is regarded as the main director of myelo- and lympho-genesis.

PU.1 is required both for a cell to enter haematopoiesis, as PU.1 is under the control of RUNX1, and also throughout the haematopoietic process in a dose-dependent manner (Huang et al. 2008). PU.1 expression levels are low at the onset of haematopoiesis, enabling self-renewal of HSCs but levels increase to induce differentiation toward Granulocyte Monocyte Precursors (GMPs) (Dakic et al. 2007). PU.1 is also accredited as the transcription factor in neutrophil or monocyte fate determination. High levels of PU.1 in the granulocyte myeloid precursor (GMP) stage repress *Gif-1* the neutrophil transcription factor, leading to monocyte differentiation, conversely low PU.1 levels allow full *Gif-1* function and subsequent neutrophil differentiation (McIvor et al. 2003).

---

#### 3.2 AIM

---

Work described in this chapter aimed to construct a human PU.1 expression vector to drive overexpression of PU.1 in hES-derived neural progenitors, for the purpose of inducing a lineage switch to either a monocyte or microglial-like fate, in a similar means to Forsberg et al. (2008).

### 3.3 VECTOR CONSTRUCTION

---

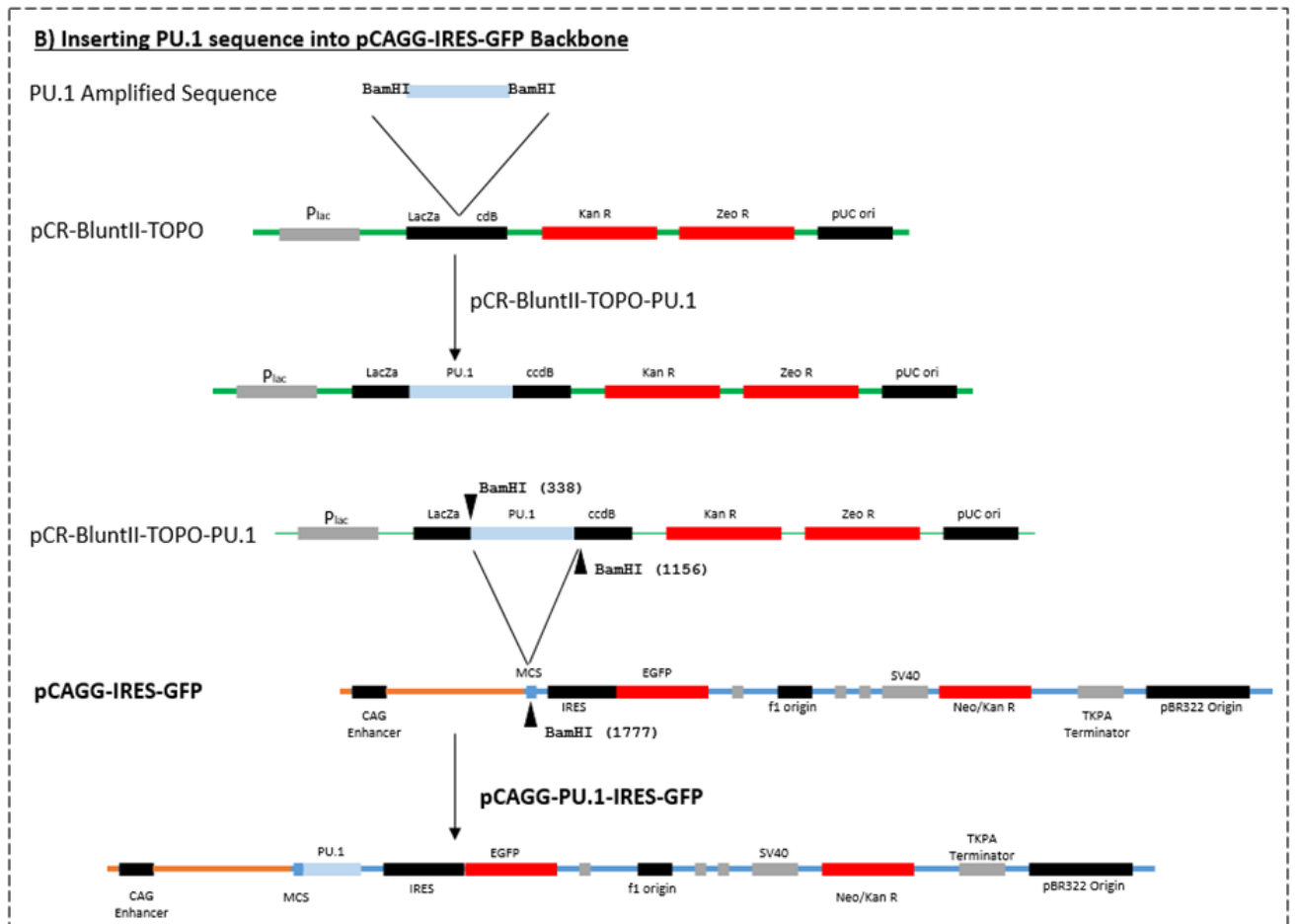
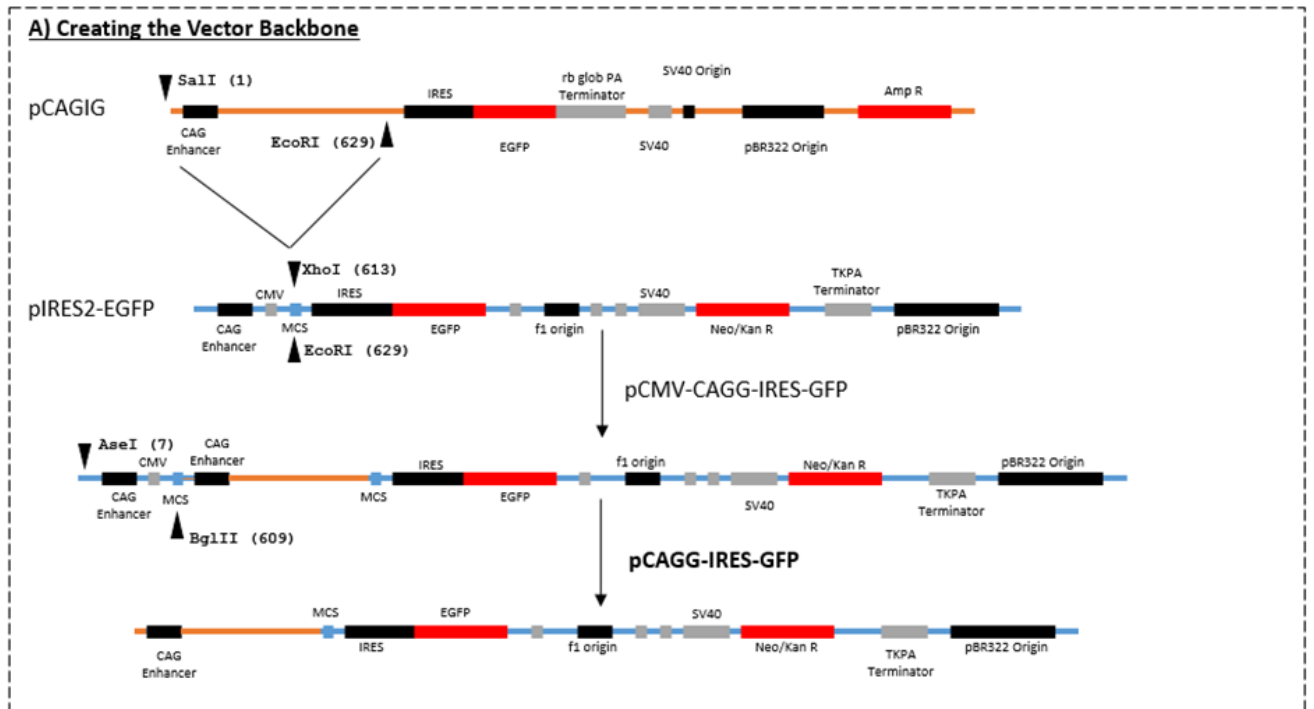
The exogenous source of PU.1 was amplified by PCR from Human monocyte cDNA with primers designed specifically to introduce flanking BamHI restriction sites to enable ligation into the mammalian expression vector, pIRES2-EGFP. pIRES2-EGFP drives gene expression from the cytomegalovirus (CMV) promoter. It also provides GFP reporter gene expression to visualise the positively transfected cells, and a Neomycin/Kanamycin resistance cassette to allow bacterial (Kanamycin) and mammalian (Neomycin/G418) selection. Since the CMV promoter has been shown to be susceptible to transcriptional inactivation by cytosine methylation in human stem cells (Prosch et al 1996), this was replaced with a more robust CAGG promoter (a CMV enhancer combined with a chicken  $\beta$ -actin promoter), from pCAGIG (*Addgene*). The CAGG promoter has been shown to increase gene expression by almost 10-fold when compared to the CMV alone and to be less susceptible to epigenetic silencing (Xu et al. 2001). The strategy for vector construction is shown below in Figure 3.1.

#### **Figure 3.1. Vector Construction (Overleaf)**

(A) The vector bone was created by removing the CAGG promoter region from pCAGIG via digestion with Sall and EcoRI. This was ligated into pIRES2-EGFP, which had been digested with XhoI and EcoRI, creating pCMV-CAGG-IRES-GFP. The CMV promoter was removed through digestion with AseI and BglII and the re-ligated vector generated was pCAGG-IRES-GFP, the control vector.

(B) To insert the PU.1 sequence, PU.1 was amplified from monocyte cDNA with BamHI sticky ends and cloned into pCR-BluntII-TOPO. The PU.1 sequence was excised from pCR-BluntII-TOPO and inserted into pCAGG-IRES-GFP, which had been linearised by BamHI digestion. The ligated vector produced was pCAGG-PU.1-IRES-GFP.

### 3. Over-expression of PU.1



## 3.4 NEURAL PRECURSOR DIFFERENTIATION

In a similar means to the Forsberg et al. (2008) protocol the created vectors; pCAGG-PU.1-IRES-GFP or the control pCAGG-IRES-GFP, were transfected into neural progenitors to initiate a lineage switch to a monocytic fate (Figure 3.2).

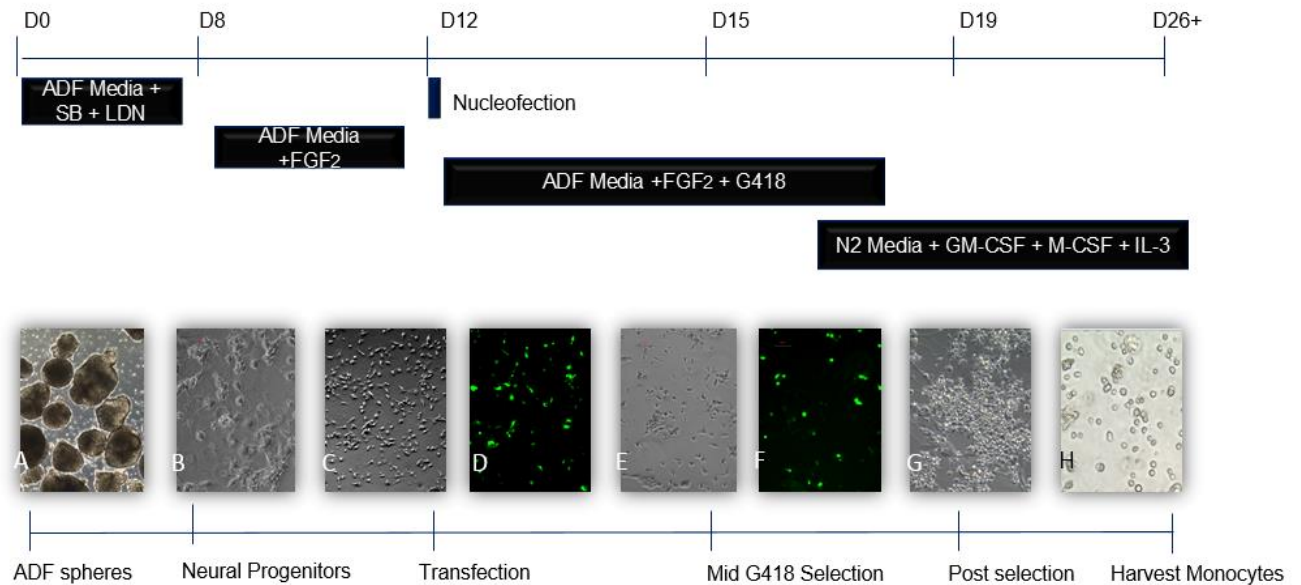


### Figure 3.2. Schematic Representation of the Differentiation Protocol

(A) Embryoid bodies were formed from H9 hES cells in ADF medium with dual SMAD inhibition using SB (SB431542) and LDN (LDN193189) for 8 days. (B) hES-derived neural precursors were cultured to day 12 (D12) in ADF medium with FGF2. The neural progenitor cells were then transfected with either PU.1 or control constructs (C/D). The positively transfected cells GFP+ and neomycin resistant and were selected using G418 (E/F) until only GFP+ cells remained at D19 (G). Post selection non-adherent cells are formed and harvested from D26 (H).

Neurogenic cultures were established from H9 hESCs by forming EBs in serum and TGF $\beta$ /BMP-free chemically defined medium (ADF) using a protocol of dual SMAD inhibition (Figure 3.3 A) (Chambers et al. 2009). Day 8 neuralised EBs were then dissociated to a single cell suspension and re-plated to form neural rosettes in adherent monolayer culture (Figure 3.3 B). Neural precursor formed rosette structures that stained positively for nestin with centrally localised ZO-1 staining at day 12, markers for neuron specific intermediate filament and tight junctions respectively (Figure 3.3 C and D).

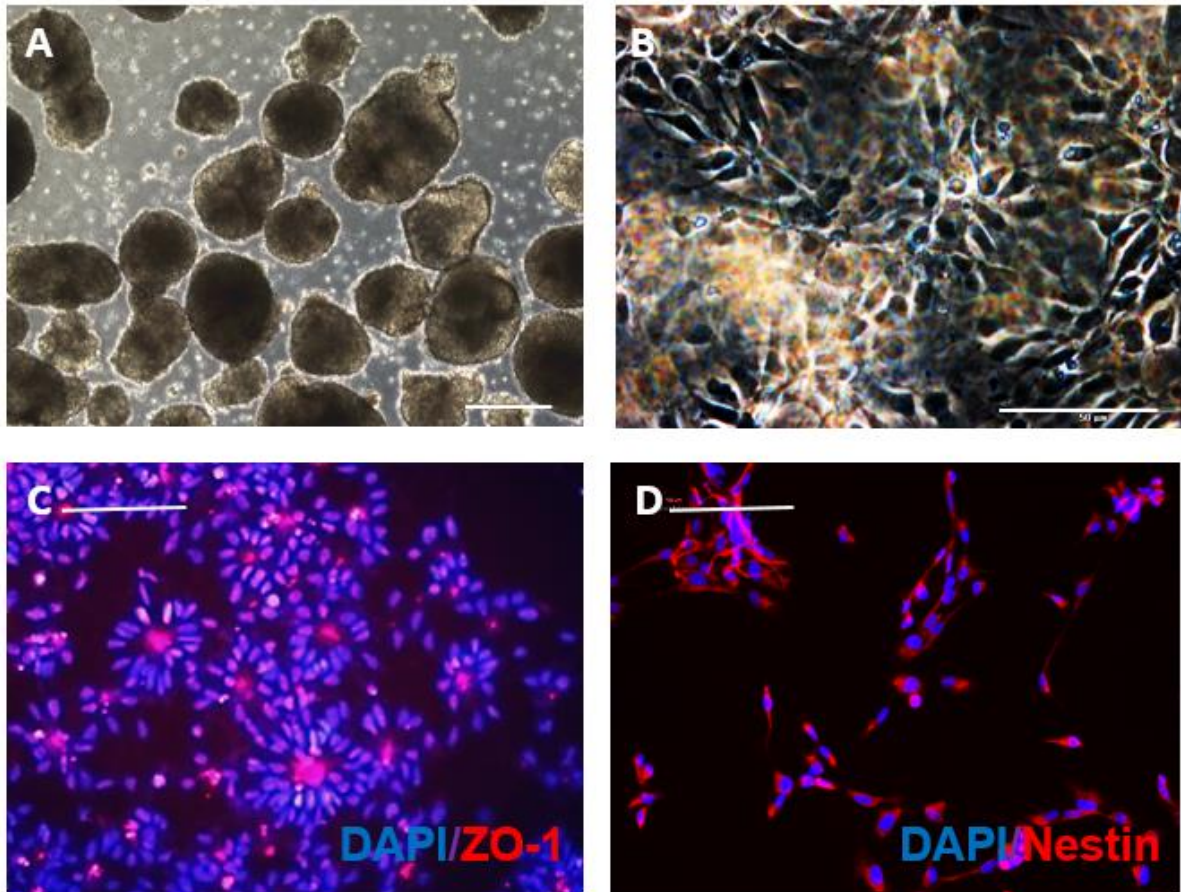


**Figure 3.3. Neuronal Precursor Differentiation**

(A) Phase contrast image of the embryoid bodies produced from H9 cells in ADF media. (B) Phase contrast image of the neural precursor cells at D12. (C) Immunocytochemistry of the D12 neural precursors stained with ZO-1 (red). (D) Immunocytochemistry of the D12 neural precursors at D12 stained with Nestin (red).

Scale bar represents 50 $\mu$ m

## 3.5 NUCLEOFECTION OF NEURAL PROGENITORS

The neural rosette cultures nucleofected with either the pCAGG-PU.1-IRES-GFP construct (Figure 3.4 A) or the control construct pCAGG-IRES-GFP (Figure 3.4 D), exhibited GFP expression 48h post-transfection (Figure 3.4 C and F).

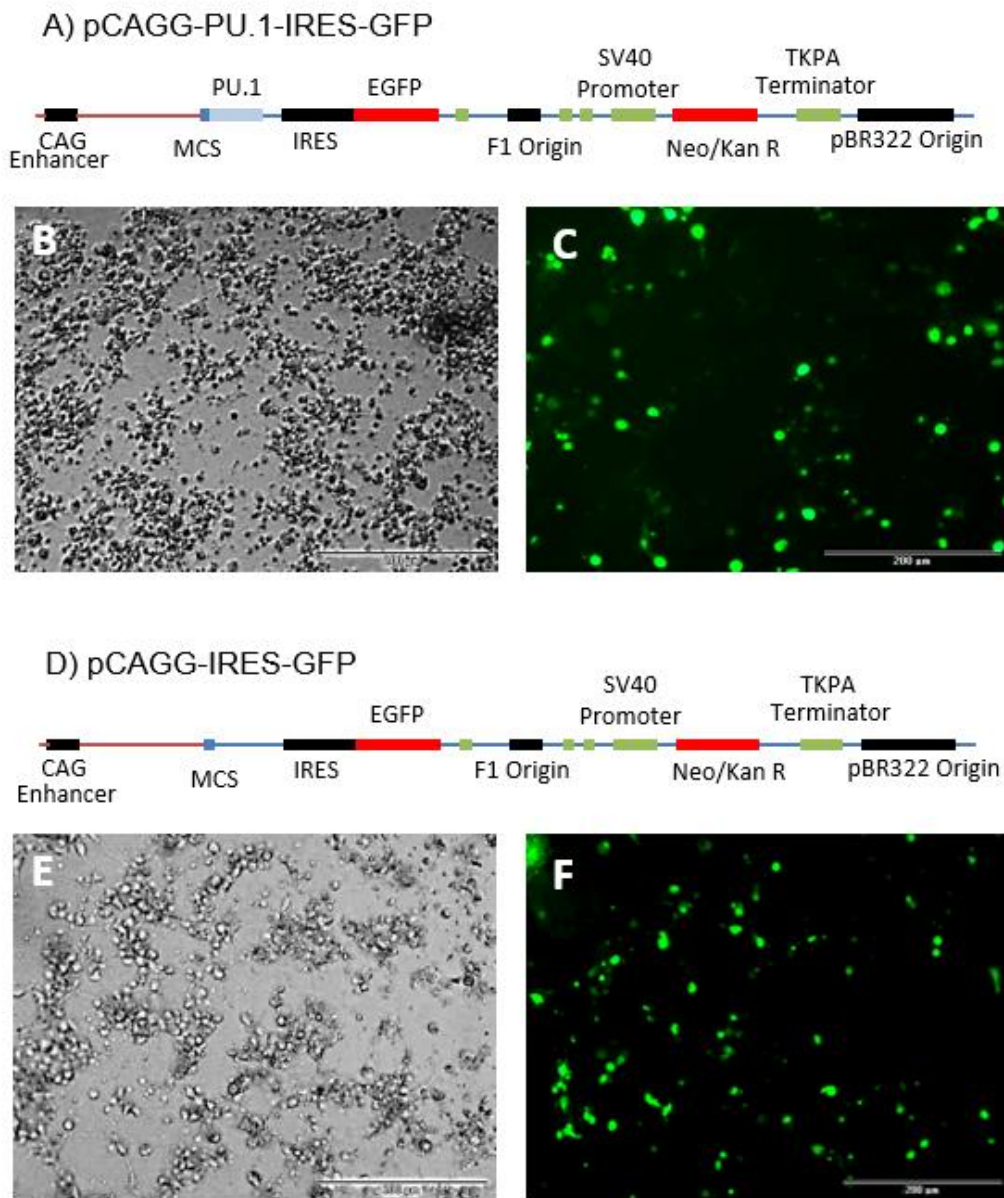


**Figure 3.4. pCAGG-PU.1-IRES-GFP and Control Vectors Express GFP Post-Transfection**

(A) The pCAGG-PU.1-IRES-GFP construct with a CAG promoter, EGFP and Kanamycin/Neomycin resistance cassette and PU.1. (B) Phase contrast image of the neural progenitors 48h post transfection (PT). (C) The corresponding GFP expression in the neural progenitors 48h PT. (D) The control pCAGG-IRES-GFP construct. (E) Phase contrast image of the neural progenitors 48h PT. (F) GFP expression in the neural progenitors 48h PT with the control construct.

Scale bars represent 200μm

Post-nucleofection the survival rates of the cells and the %GFP+ cells were calculated for several available Amaxa nucleofection programs. The maximal transection efficiencies achieved were a 23% survival rate with 31% of the surviving cells expressing GFP for those transfected with pCAGG-PU.1-IRES-GFP with similar results (25% and 36%, respectively) obtained for the control construct (Figure 3.5). Following seven days of G418 selection all remaining cells expressed GFP at a level that remained high throughout the differentiation from its onset 24h post nucleofection (Figure 3.5).

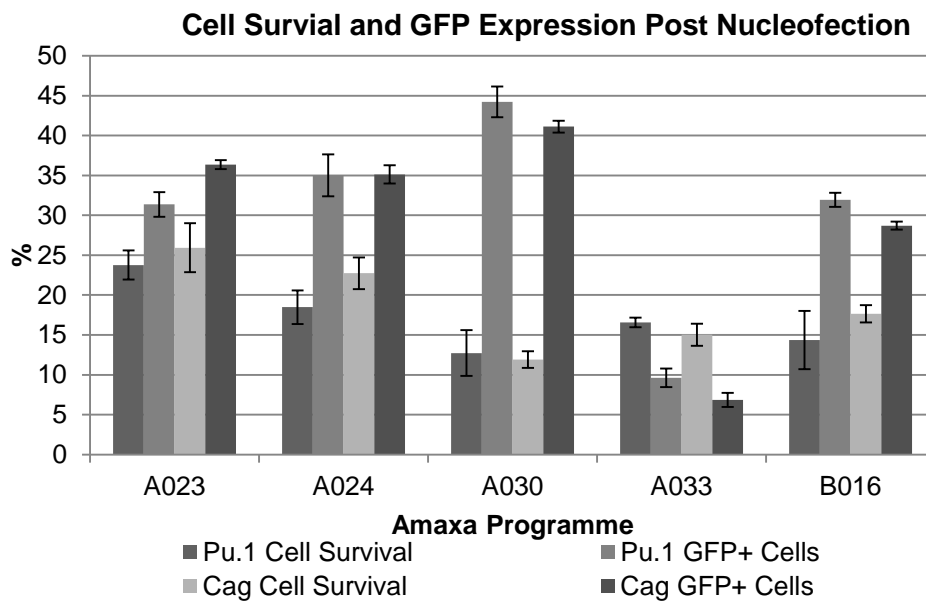


**Figure 3.5. pCAGG-IRES-GFP Nucleofection**

The efficiency of nucleofection was determined through cell survival and GFP expression, which show similar values in both the PU.1 construct transfection and the control. The neural precursors 24h post transfection using program A023 with the Pu.1 construct, shows GFP+ cells with a 31% transfection efficiency.

PU.1 protein expression from the pCAGG-PU.1-IRES-GFP vector was initially confirmed by western-blotting following transient transfection and expression in HEK293 cells (Figure 3.6 A). PU.1 expression in H9-derived neural precursor cells (NPCs) transfected with pCAGG-PU.1-IRES-GFP was also confirmed by QRT-PCR (Figure 3.6 B and C). ANOVA was conducted to compare the effect of pCAGG-PU.1-IRES-GFP transfection on PU.1 expression to non-transfected cells, which revealed that there was a significant increase in PU.1 expression at the 95% confidence level [ $F(3,8)=263.3$ ,  $p<0.001$ ]. Post-hoc comparisons using the Bonferroni test indicated that the mean for the non-transfected NPCs ( $M=0.0003$ ,  $SD=7.497e^{-005}$ ) was significantly different to the mean of the transfected samples (PU.1 PT ( $M=4.469$ ,  $SD=0.1088$ ), PU.1 PS ( $M=2.788$ ,  $SD=0.4073$ )).

When the control vector, pCAGG-IRES-GFP, was analysed by ANOVA there was no significant difference in PU.1 expression when the NPCs were transfected with the control construct [ $F(2,6)=2.362$ ,  $p=0.1751$ ]. The increase in PU.1 expression observed is thus deemed to represent the effect of transfection with the pCAGG-PU.1-IRES-GFP vector.

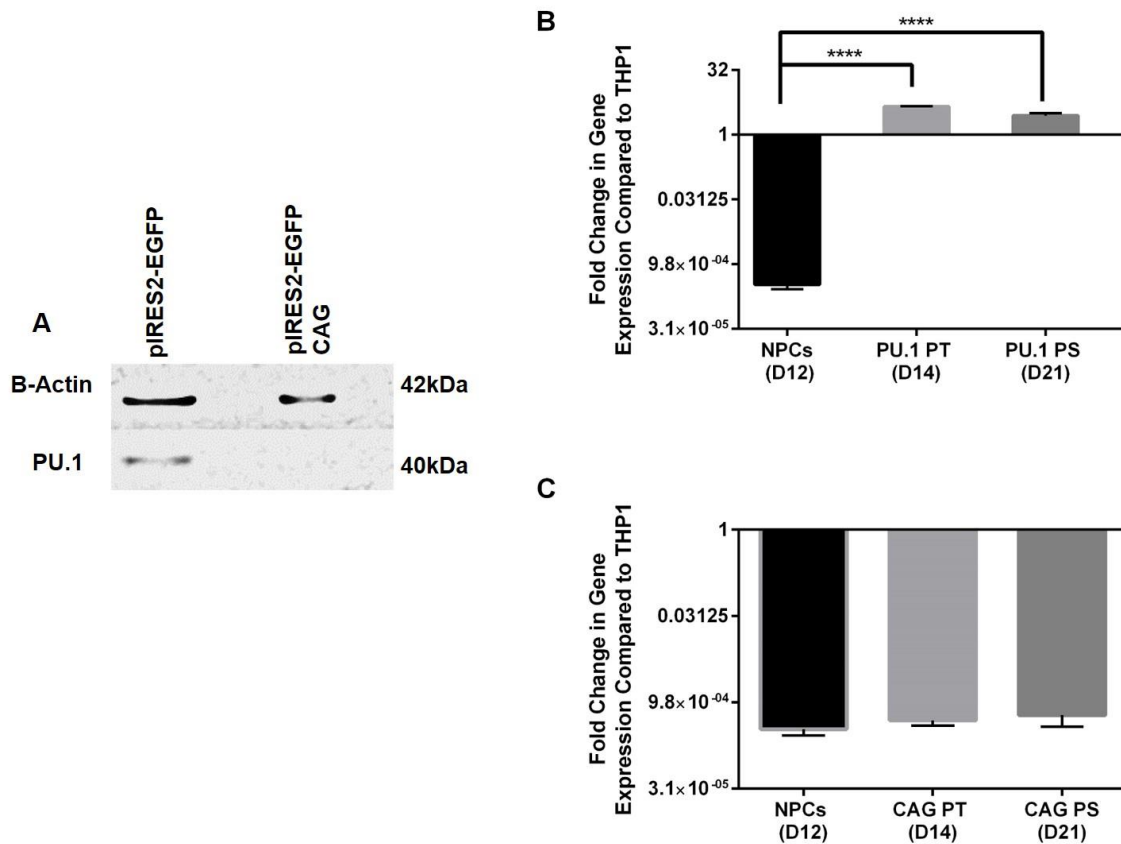


**Figure 3.6. PU.1 Expression is Up-regulated Post-Transfection with pCAGG-PU.1-IRES-GFP**

(A) Western blot showed PU.1 expression in HEK293 cells, when transfected with pCAGG-PU.1-IRES-GFP and no expression in the control transfection

(B) PU.1 Expression in Neural Precursor Cells (NPCs) was shown to be increased 4.5-fold compared to THP1 cells post-transfection (PT) and almost 3-fold in cells post-selection (PS). ANOVA showed that these increases were significant [ $F(3,8)=263.3$ ,  $p<0.001$ ]. Post Hoc Bonferroni test revealed significant differences between the means of the NPCs ( $M=0.0003$ ,  $SD=7.497e^{-005}$ ) and PT ( $M=4.469$ ,  $SD=0.1088$ ) and PS ( $M=2.788$ ,  $SD=0.4073$ ) samples.

(C) PU.1 expression in NPCs transfected with pCAGG-IRES-GFP was shown to be similar both PT and PS to the un-transfected NPCs. There was no significant difference in the means after ANOVA [ $F(2,6)=2.362$ ,  $p=0.1751$ ]

QRTPCR data was normalised to  $\beta$ -Actin and taken from 3 technical replicates of 3 biological replicates

Asterisks denote statistical significance; \*  $\leq 0.05$ , \*\*  $\leq 0.01$ , \*\*\*  $\leq 0.001$ , \*\*\*\*  $\leq 0.0001$

Immunocytochemistry was carried out to show that PU.1 expression originated from only GFP<sup>+</sup>, successfully transfected cells. This showed that PU.1 and GFP expression and co-localised in the NPCs transfected with pCAGG-PU.1-IRES-GFP 48h post-transfection, but no PU.1 expression was evident in the NPCs transfected with the control construct (Figure 3.7).

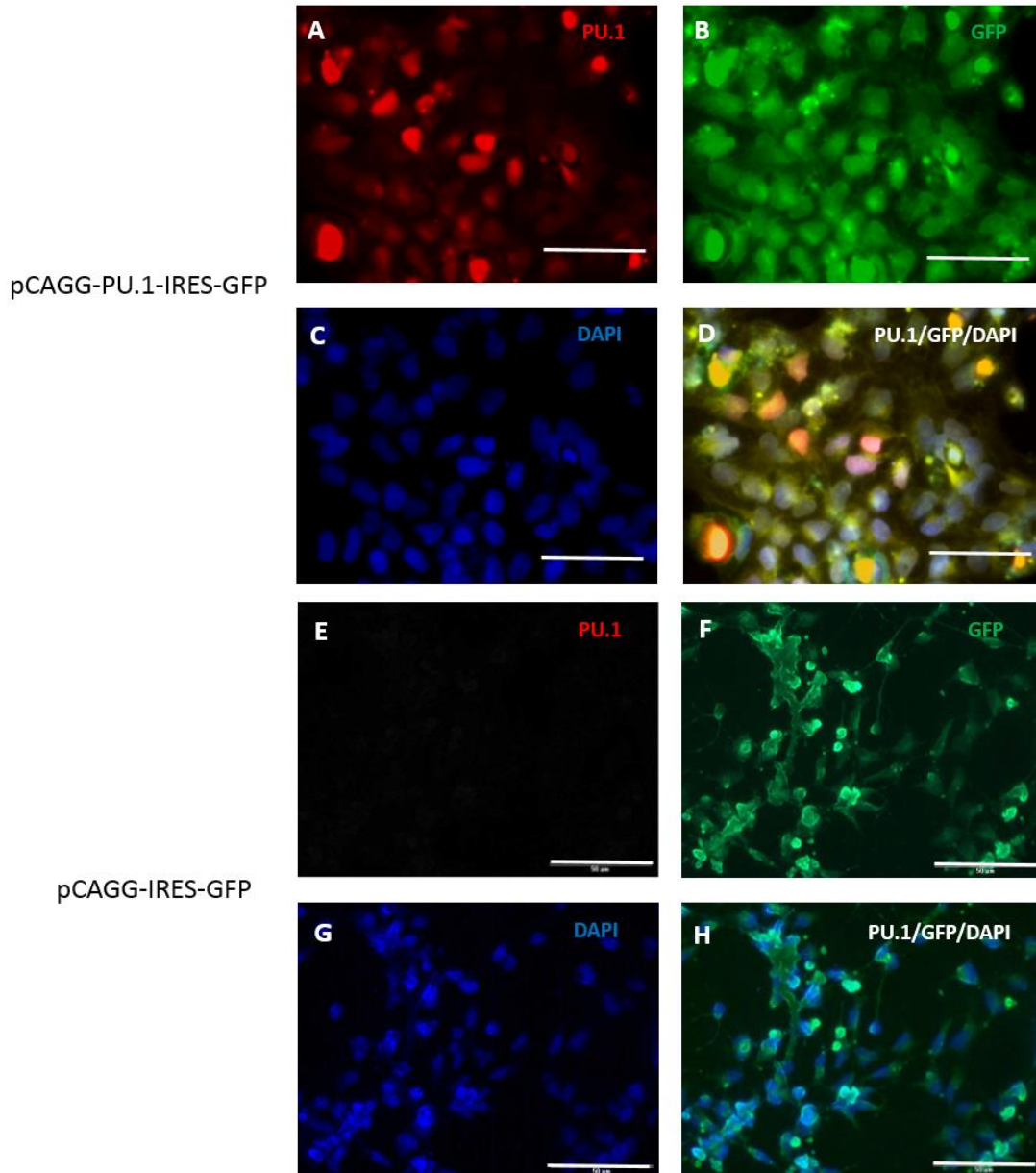


**Figure 3.7. PU.1 and GFP Co-Localisation in Neural Progenitors**

(A) NPCs transfected with pCAGG-PU.1-IRES-GFP were stained with PU.1 (red), (B) GFP (green) and (C) DAPI. The images were merged (D) to show co-localisation and expression of PU.1 and GFP. (E) NPCs transfected with the control construct were stained with PU.1 (red), (F) GFP (green) and DAPI (G). Co-localisation via the merged image is shown in H.

Scale bars represent 50  $\mu$ m

### 3.6 DIFFERENTIATION OF TRANSFECTED CELLS

To confirm the loss of neuronal identity post transfection during differentiation. QRTPCR was performed for the neural intermediate filament, Nestin, both pre- and post- transfection (Figure 3.8). One way ANOVA was carried out to compare nestin expression the pCAGG-PU.1-IRES-GFP transfected cells over time. This showed that the difference between the means was statistically significant [ $F(2,6)=176.6$ ,  $p<0.0001$ ]. Post-hoc comparisons with the Bonferroni test showed that there was a statistically significant decrease in nestin expression both post-selection ( $M=1.087$ ,  $SD=0.3224$ ) and once integrated at D60 ( $M=0.9679$ ,  $SD=0.0711$ ) compared to the level of nestin expression in the post-transfected cells at D14 ( $M=14.17$ ,  $SD=1.6827$ ). This indicated that the cells were undergoing a lineage switch from their neural precursor origins during differentiation. Whether this is due to time in culture or transfection with PU.1 or both is not clear.

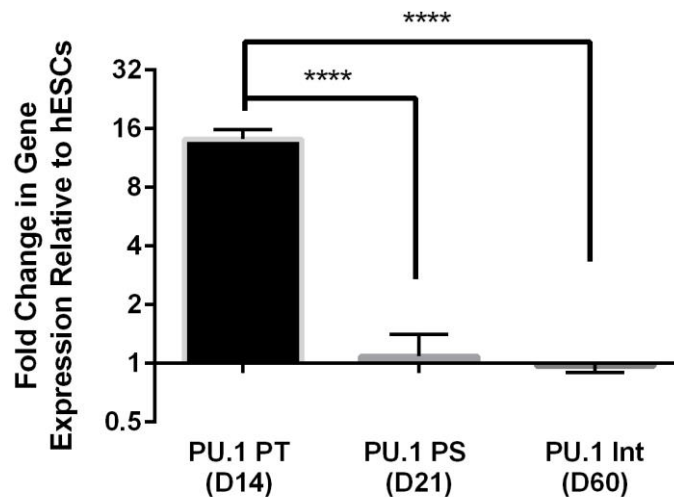


**Figure 3.8. Nestin Expression is down-regulated upon transfection with pCAGG-PU.1-IRES-GFP**

48h post-transfection at differentiation D14 there was a 14-fold increase in Nestin expression relative to undifferentiated H9 hESCs. ANOVA showed that there was a significant decrease in nestin expression [ $F(2,6)=176.6$ ,  $p<0.001$ ]. Post-selection at D21 and later on at differentiation D60, when the PU.1 construct has integrated, there is a statistically significant down-regulation of nestin (PU.1 PS ( $M=1.087$ ,  $SD=0.3224$ ), PU.1 Int ( $M=0.9679$ ,  $SD=0.0711$ )).

QRTPCR data was normalised to  $\beta$ -Actin and taken from 3 technical replicates of 3 biological replicates.

Asterisks denote statistical significance; \*  $\leq 0.05$ , \*\*  $\leq 0.01$ , \*\*\*  $\leq 0.001$ , \*\*\*\*  $\leq 0.0001$

Since there was a loss of expression of the nestin and thus neuronal identity post-transfection, the effect of PU.1 overexpression in transfected neural progenitors (Day 14 and Day 21 post-transfection) on the regulation of developmental haematopoietic genes was monitored by Q-RTPCR. This was carried out using primers for genes involved in haematopoietic induction; both primitive (FLK1) and definitive (RUNX1), and haematopoiesis via PU.1, CD34 and CD45 (Figure 3.9). Where CD34 is a marker for the apex of haematopoeisis, the HSC and early haematopoeitic progenitors, whilst CD45 is the leukocyte common antigen found in more committed leukocyte cells and is situated downstream of PU.1.

A comparison of the means via ANOVA showed that transfection with PU.1 resulted in a statistically significant difference [ $F(3,30)=906.3$ ,  $p<0.0001$ ]. Bonferroni's multiple comparison test revealed several differences between the NPCs and the PU.1 transfected cells.

PU.1 expression is increased when cells are transfected with the pCAGG-PU.1-IRES-GFP construct at both D14 and D21 (PU.1 PT (M=3.996, SD=0.686), PU.1 PS (M=2.513, SD=0.103)) compared to NPCs at D12 (M=0.00027, SD=0.00006). PU.1 transfected cells also showed an increase in FLK1 expression of around 3-fold in post-transfected cells (M=3.057, SD=0.375) and a 12-fold increase in post-selected cells (M=12.47, SD=0.375). FLK1 expression in NPCs remained negligible (M=0.1165, SD=0.01595). RUNX1 was not significantly different in the post-transfected cells (M=0.08115, SD=0.017) but was significantly up-regulated in the post-selected cells (M=0.7771, SD=0.072) compared to the NPCs (M=0.01513, SD=0.00293). The haematopoietic stem cell marker, CD34, showed no significant difference at either of the transfected cell time points (PU.1 PT (M=1.597,

SD=0.154), PU.1 PS (M=1.866, SD=0.297)) when compared to the NPCs (M=1.637, SD=0.09464). QRTPCR finally revealed that transfection of neural precursors with the PU.1 construct resulted in an increase in expression of CD45, to a level comparable to THP1 monocytes, in both post-transfected cells (M=0.9688, SD=0.217) and the post-selected cells (M=1.031, SD=0.026) compared to NPCs (M=0.03157, SD=0.00238).

Post-selection, at day 21, the QRTPCR showed that there is an increase in the expression of all the haematopoietic markers of interest, with the obvious exception of PU.1. This indicates that there is a lineage switch towards a monocytic or microglial-like fate occurring upon PU.1 overexpression.

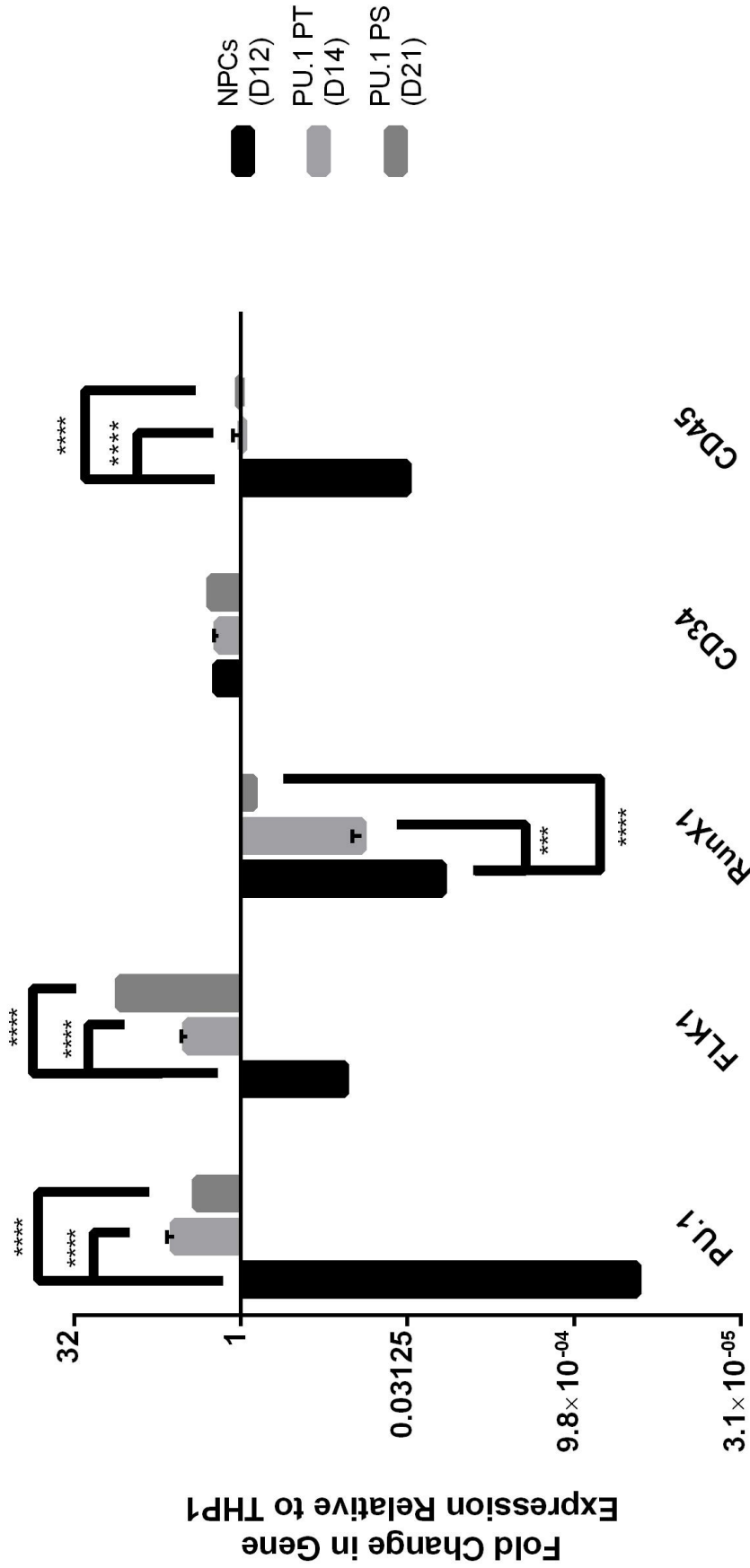


**Figure 3.9. Haematopoietic Gene Expression in PU.1 Transfected Cells (Overleaf)**

Expression of PU.1 is increased in cells transfected with the PU.1 construct both post-transfection and post-selection (PU.1 PT (M=3.996, SD=0.686), PU.1 PS (M=2.513, SD=0.103)). PU.1 expression in neural stage cells is negligible, down-regulated in comparison to the control THP1 monocyte cells. Post selection there is an increase in the expression of the primitive haematopoietic gene, FLK1 (M=12.47, SD=0.144). There is also less down-regulation of the definitive haematopoietic marker RUNX1 (M=0.7771, SD=0.072), which is at a similar level to that of the control cells. CD34 remained constant, with levels similar to both NPCs and THP1 cells. CD45 was also shown to be increased to a level that resembles the control THP1 cell line post selection (M=1.031, SD=0.026).

QRT-PCR data was normalised to  $\beta$ -Actin and taken from 3 technical replicates of 3 biological replicates

Asterisks denote statistical significance; \*  $\leq 0.05$ , \*\*  $\leq 0.01$ , \*\*\*  $\leq 0.001$ , \*\*\*\*  $\leq 0.0001$

To investigate the consequences of ectopic PU.1 expression immunocytochemistry was performed post G418 selection. This showed that all selected cells were positive for CD45. Groups of CD11b+ cells were also visible but there were very few visible CD34+ (Figure 3.10). CD34+ cells would lead to the conclusion of the presence of HSCs or early, non-committed, haematopoietic progenitors found at the beginning of haematopoiesis. The presence of CD45+ and CD11b+ cells suggests that the cells are more committed leukocytes with at least some of which being committed CD11b+ monocytes.

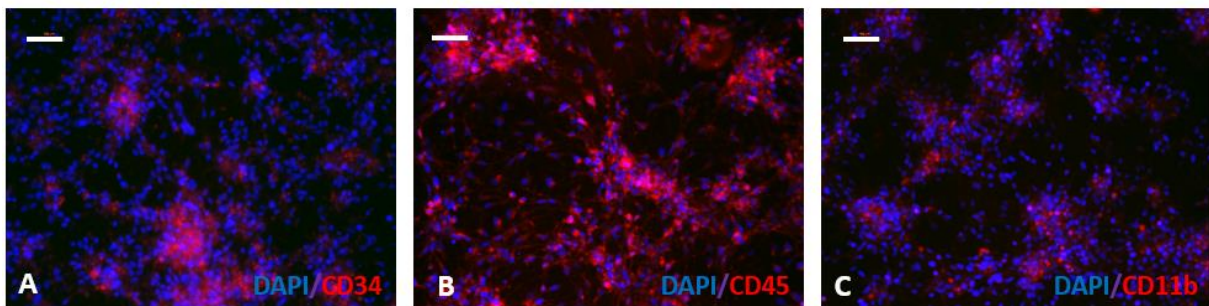


**Figure 3.10. Hematopoietic Marker Localisation in the Adherent Population**

Post-selection (D29) the adherent population, resulting from transfection with pCAGG-PU.1-IRES-GFP were stained for CD34 (A), CD45 (B) and CD11b (C).

Scale bars represent 100µm

### 3.7 NON-ADHERENT CELL CHARACTERISATION

With extended culture the transfected adherent cells gave rise to a phase-bright non-adherent cell population. It is expected that this non-adherent population would contain the desired monocytic cell type. The non-adherent cells that were generated post-selection were assayed for cell viability using trypan-blue exclusion to ensure that these were not a result of increased cell death. The number of viable cells steadily increased post-selection in the PU.1 transfected cells, peaking at day 25 at over  $9 \times 10^5$  cells/ml (Figure 3.11 A). This was compared to the viability of the non-adherent cells produced from the cells that were transfected with the CAG control, which produced significantly fewer viable non-adherent cells (Figure 3.11 B). This showed that PU.1 overexpression generated in a greater number of viable, phase bright, non-adherent cells.

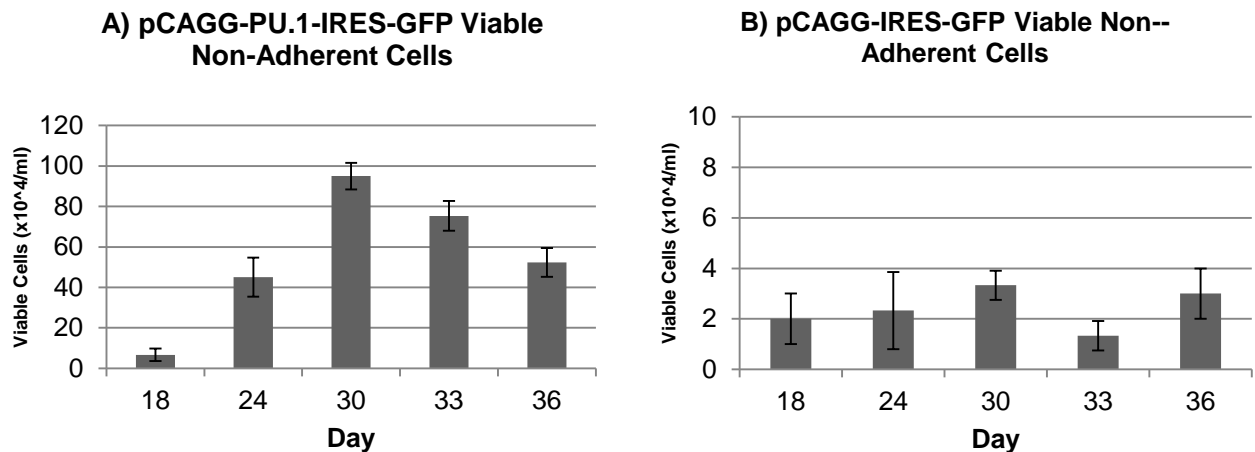


**Figure 3.11. Viability of non-adherent cells**

Subsequent to the removal of the selective pressure at D18 the viability of non-adherent cells harvested from culture medium was determined. Cells over-expressing PU.1 generated  $>9 \times 10^5$  cells/ml at D25 before beginning to decline (A). For the control sample, the viability of cells never exceeds  $3.5 \times 10^4$  cells/ml (B).

The viable non-adherent cells collected at day 30 from the nucleofected samples were examined immunologically for markers of haematopoiesis; CD45 and CD11b (Figure 3.12). This revealed that forced expression of PU.1 induced expression of CD45 and CD11b in non-adherent cells, whilst little staining was evident in cell transfected with the CAG only control vector, which would indicate that it is PU.1 overexpression rather than culture conditions that is the driving force behind the differentiation.

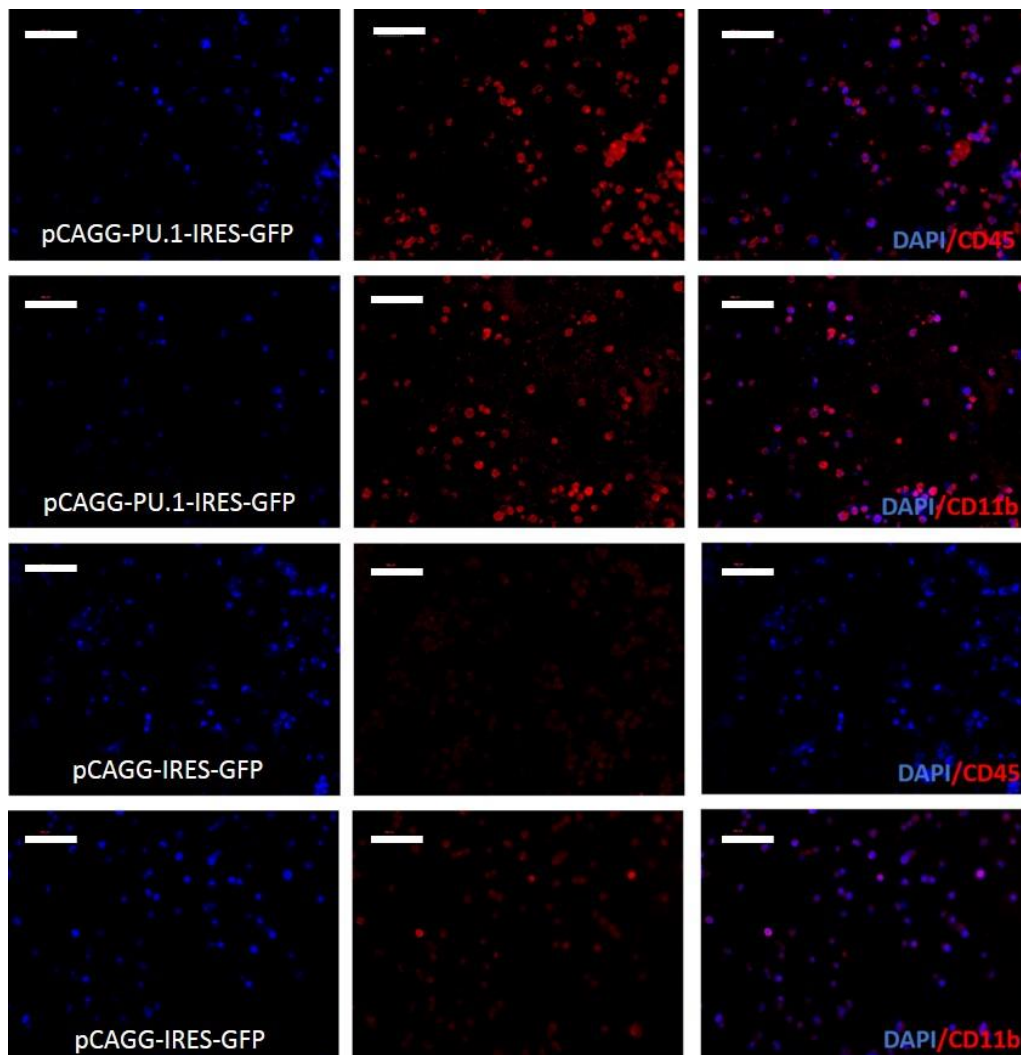


**Figure 3.12. Hematopoietic Marker Expression In the Non-Adherent Cells**

(A) Day 30 supernatant cells from cultures transfected with pCAGG-PU.1-IRES-GFP stained for CD45 and (B) CD11b. CD45 (C) and CD11b (D) in day 30 supernatant cells harvested from cultures transfected with control vector pCAGG-IRES-GFP

Scale bars represent 100µm

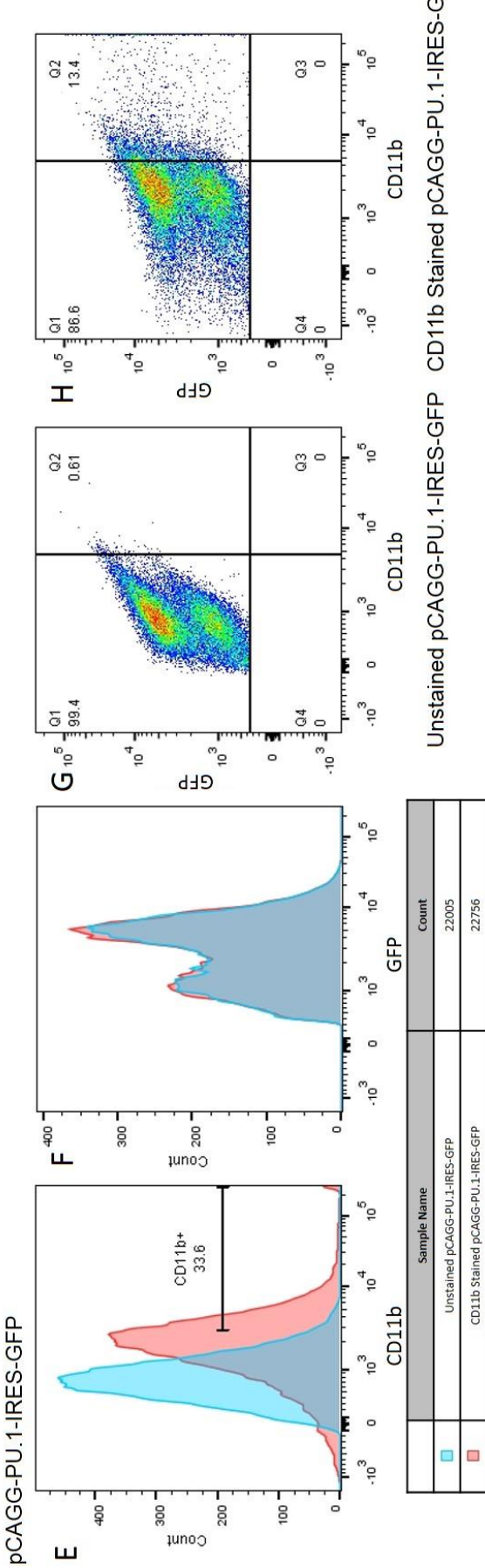
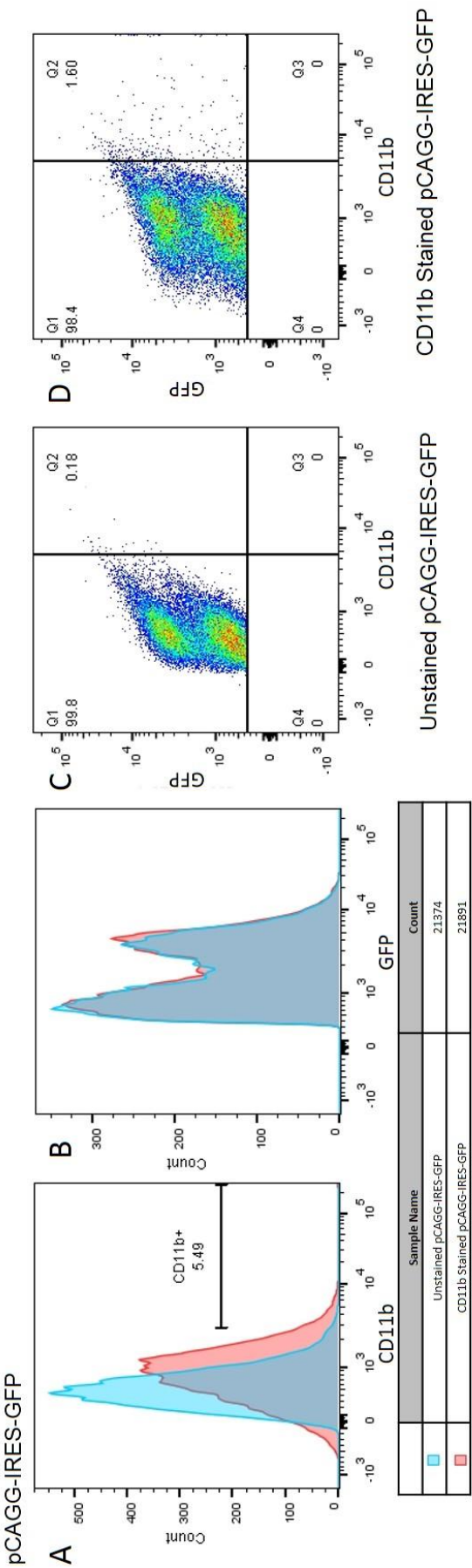
The non-adherent cell populations from both transfections, with the PU.1 containing construct and the control, were also analysed by flow cytometry to quantify CD11b expression as a marker of myelopoiesis and also of microglia along with its co-expression of GFP.

Flow cytometry revealed that there was a small population of ~5% CD11b<sup>+</sup> cells in control transfected cultures, whilst the population was 6 times larger in cells differentiated following pCAGG-PU.1-IRES-GFP transfection, where over 33% of the non-adherent cells were CD11b<sup>+</sup> (Figure 3.13).

The GFP<sup>+</sup> cells were similar in both the control pCAGG-IRES-GFP and pCAGG-PU.1-IRES-GFP supernatant cells whether stained or isotype control. The histogram for GFP<sup>+</sup> cells shows two clear peaks and so two distinct populations of cells. This is potentially due to the integration of one or two copies of the GFP expressing plasmid into the genome. Cells were also analysed for their co-expression of GFP and CD11b, as shown in the quadrant plots where CD11b<sup>+</sup>/GFP<sup>+</sup> cells are seen in the upper right quadrant. This showed that only 1.6% of the control transfected cells resided within this quadrant, whilst over 13% appeared in the quadrant when transfected with pCAGG-PU.1-IRES-GFP, which also equates to around half of the CD11b<sup>+</sup> population. This confirms that the expression of CD11b is largely due to transfection and subsequent expression of PU.1, rather than culture conditions.

#### **Figure 3.13. Quantification of GFP and CD11b Expression in PU.1 and control vector transfected cells (Overleaf)**

(A) The supernatant cells arising from transfection with the control construct showed only 5.49% of the cells were CD11b<sup>+</sup>. (B) The GFP<sup>+</sup> cells were also similar in both the isotype control and the test sample but show two distinct populations. (C) Co-expression of CD11b and GFP in the unstained control was only 0.61%, which remained low (D) at 1.60% CD11b<sup>+</sup>/GFP<sup>+</sup> cells in the stained test sample. (E) Supernatant cells resulting from the transfection of the pCAGG-PU.1-IRES-GFP construct showed a population of over 33% CD11b<sup>+</sup>. (F) The isotype control and the stained sample showed the same population of GFP<sup>+</sup> cells, again with two distinct populations. (G) Co-expression of CD11b and GFP in the isotype control was 0.18% whilst (H) the co-expression was markedly increased in the PU.1 transfected cells with 13.4% CD11b<sup>+</sup>/GFP<sup>+</sup> cells.



PU.1 overexpression yielded cells that express both CD45 and CD11b, markers commonly used to identify monocytes. The functionality of these cells were assayed using time lapse microscopy for the phagocytosis of opsonised *E. coli* bioparticles (Figure 3.14). This showed that over a 60 minute incubation period with the particles, none of the cells were shown to have taken up the particles as would have been expected by functional monocytes.

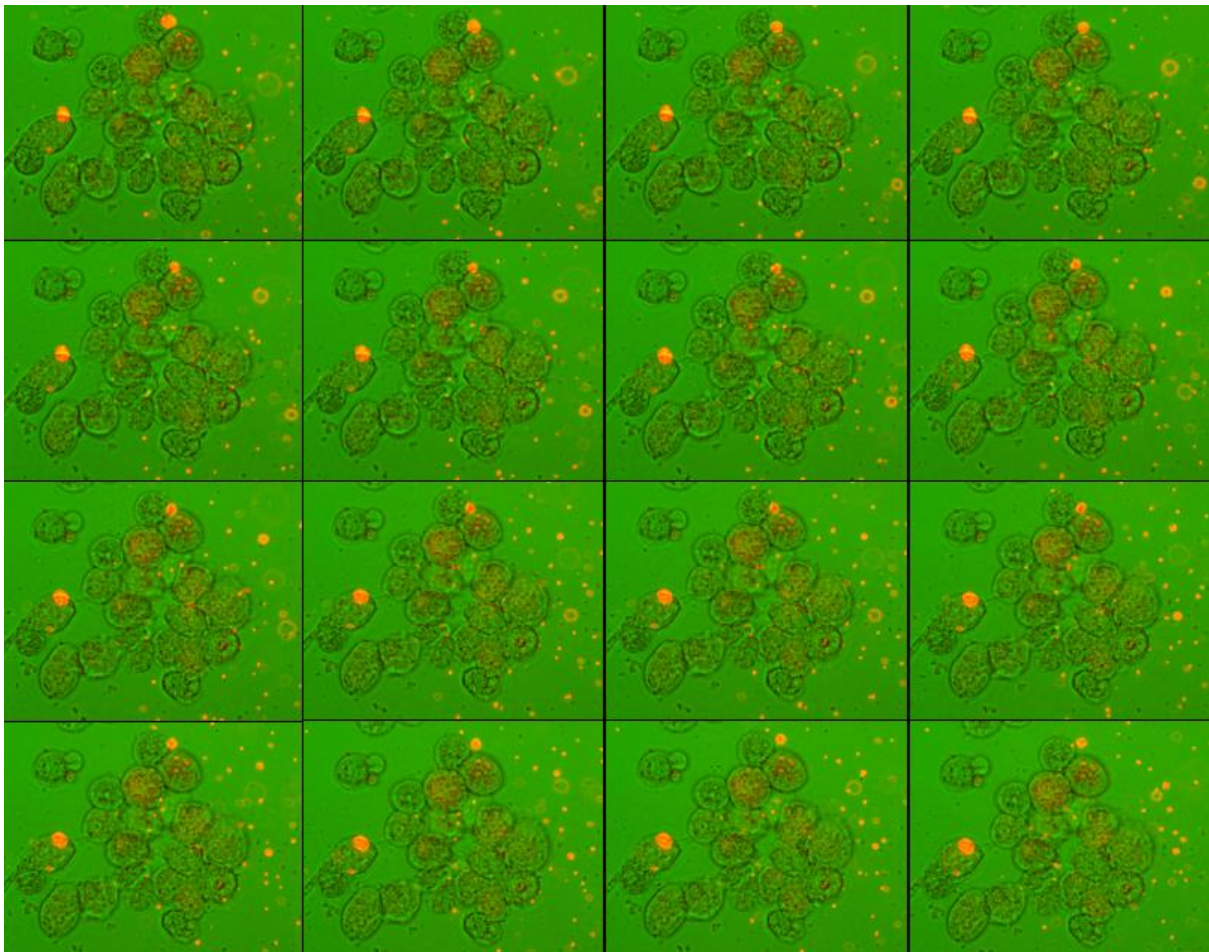


**Figure 3.14. Time Lapse Microscopy of *E. coli* Bioparticle Phagocytosis**

Non – adherent cells that arose from transfection with pCAGG-PU.1-IRES-GFP were incubated with fluorescent *E.coli* bioparticles (red) for 60 minutes, with images taken at 3 minute intervals. This shows that, although the bioparticles contact the surface of the cells they are not phagocytosed.

### 3.8 DATA SUMMARY

---

Neuronal precursor cells differentiated from hESCs formed characteristic neural rosette structures, the *in vitro* 2D equivalent to the neural tube, and were positive for both nestin and ZO-1.

A reproducible transfection protocol was established and both the control and PU.1 containing plasmids functioned to express GFP. Transfection with pCAGG-PU.1-IRES-GFP was also shown to lead to expression of PU.1, which was not expressed in the cells prior to transfection nor in those cells transfected with the control plasmid. Transfection of the PU.1 construct lead to a down-regulation of the neuronal intermediate filament Nestin, and thus a loss of neuronal identity. Differentiation of cells transfected with PU.1 derived an adherent population of principally CD45+ cells, with little or no CD34 expression, but with some pockets of CD11b expression post selection. This indicates that PU.1 promotes the differentiation of cells to express markers associated with leukocytes (CD45) and monocytes (CD11b) rather than those of primitive HSCs (CD34).

With extended culture, non-adherent cells shed into the culture supernatant stained for both CD45 and CD11b when transfected with the PU.1 vector. Cells transfected with control vector showed little or no staining for CD45, although a small population of CD11b+ cells was detected when analysed by flow cytometry. Although the cells that resulted from the transfections were not deemed to be functional monocytes due to their lack of ability to phagocytose *E.coli* bioparticles. Their lack of functionality was also confirmed through their inability to differentiate in the presence of astrocyte conditioned medium (data not shown).

### 3.9 DISCUSSION

---

PU.1 has various roles in hematopoiesis, from cell-cycle regulation to avoid exhaustion of the HSC niche and the onset of hematopoiesis to fate determination between monocytes and neutrophils. It has been shown previously that the over-expression of this transcription factor alone is able to 're-programme' a neural stem cell to a lineage, far removed from their ectodermal origins, to monocyte and ultimately a microglial cell, which would naturally arise from the mesoderm. Neural stem cells or progenitors are attributed with significant nuclear plasticity and potential for reprogramming, requiring only exogenous Oct4 to enable them to be reprogrammed to iPSCs (Kim et al. 2009). It is for this reason that neural stem cells were chosen by Forsberg et al. (2008) to be 're-programmed' to monocytes by overexpression of exogenous PU.1. A five step protocol for the differentiation of neuronal cells can also be adapted for the formation of microglia by Beutner et al. (2010). Since neural precursors have been used successfully in the differentiation of microglia in murine cells and a robust protocol is established for the formation of neural precursors from hESCs these were used in place of the adult neural stem cells in the publication by Forsberg et al. (2008).

The transfection protocol established is one that is reproducible and has maximal efficiency for neural progenitors. Efficiencies of transfection using the Amaxa nucleofection system in Human neural stem cells has been shown to be 35% by Marchenke and Flanagan (2007). Amaxa transfection can be more efficient as shown by Maasho et al. (2004) where efficiencies were 40% with viability reaching 85%, but these figures were gained in natural killer cells, rather than the delicate neural progenitors required for the current protocol. This not only confirms the

functionality of the protocol used for transfection, but also the functionality of the vector through its expression of GFP.

Under the control of the CAG promoter PU.1 expression was increased over 3-fold in G418 selected cells, whilst cells transfected and selected using the control plasmid showed little expression of PU.1 when compared to THP1 monocytes. The co-expression and thus localisation of PU.1 and GFP was shown but in some cases only GFP expression was evident, although not ideal this is not unexplainable, the GFP gene is part of the IRES-GFP cassette, which has been shown to interfere with the translation of certain small genes (Mansha et al. 2012). At just over 800bp PU.1 is small and could be a target for such translational interference in some cells, hence the GFP only cells found after selection.

PU.1 expressing cells showed a significant increase in the levels of FLK1 both post-transfection and post-selection. FLK1 can be upregulated depending on cellular activation and proliferation (Yang et al. 2004). PU.1 is able to increase the level of proliferation via the expression of MCSFR, so it is unsurprising that cells that overexpress PU.1 also have increased FLK1 expression. These cells also show a significant increase in the expression of the leukocyte common antigen, CD45, expression, evidenced by immunostaining and QRTPCR. CD45 is a receptor tyrosine phosphatase vital for leukocyte function. The same techniques showed that there was little expression of CD34 and only some CD11b expression. This is most likely due to the PU.1 binding sites within the CD45 promoter region, making CD45 a downstream target of PU.1 (Anderson 2000). Although likely that the lineage switch is due, at least, in part to PU.1 overexpression the length of time in the differentiation and the differentiation conditions can not be overlooked. Since post-selection cells

are cultured with IL-3, M-CSF and GM-CSF in a media similar to that used in the 5-step protocol for mouse ES to microglia differentiation. As mentioned previously PU.1 also targets the M-CSF and GM-CSF receptor genes along with CD11b. CD11b is an integrin that regulates the adhesion and migration of monocytes as well as serving a role in the complement system as the C3bi receptor. Since all of these induce monocytic commitment it is unsurprising that the resultant cells are expressing largely leukocytic markers. M-CSFR, levels of which increase during monocyte differentiation, has a binding site for PU.1 upstream of the 5' promoter elements and functions to increase proliferation of monocytic cells through actions on cyclin D and E to induce the transition from G1 to S-phase in the cell cycle (Rhoades et al. 1996). This is consistent with the finding that those cells transfected with PU.1 produce over 20-fold more viable supernatant cells than those transfected with the control construct.

The non-adherent supernatant cells were shown to be haematopoietic in the presence of PU.1, expressing both CD45 and CD11b, whilst the control cultures were largely negative for these markers. This is again unsurprising since PU.1 is able to bind to the CD45 gene promoter region and influence transcription of CD45. As mentioned PU.1 is also able to influence CD11b expression, accounting for the CD11b+ cells seen within the supernatant of the cultures transfected with the PU.1 construct. Another major difference between the cultures lies in the number of supernatant cells produced, due to the proliferative action of PU.1.

Improvements to the system though could be made in an effort to increase the efficiency of the differentiation. The vector, once integrated, is susceptible to silencing so PU.1 would no longer be expressed. Although not hugely problematic

since the lineage switch to leukocytes, through the initial overexpression of PU.1, the high levels of PU.1 required for terminal monocyte differentiation could be assisted further by the contribution of endogenous PU.1. To combat this potential problem the vector could be supplemented with insulator sequences to prevent transgene silencing. Also it is known that transgene expression is most effective when under selection, which was not the case here (Alexopoulou et al. 2008). Seven days of selection was sufficient to enable stable transfection, after which G418 was removed. Increased PU.1 expression after stable transfection could be induced by the addition of a minimal concentration of G418 within the culture medium throughout the differentiation protocol.

The monocyte-like cells produced via this protocol were deemed non-functional since they were unable to undergo phagocytosis and differentiate to microglial-like cells. PU.1 can be bound by various factors including; CBP, HDAC1, RUNX1, which under the conditions of PU.1 overexpression could lead to sequestration of these and other genes required for differentiation and phagocytosis (Takahashi 2011). An important factor in the differentiation of microglia is the interferon regulatory factor 8 (IRF8), which heterodimerises with PU.1 and leads to the differentiation of microglia and the formation of mature phagocytes (Kierdorf et al. 2013; Marquis et al. 2011).

PU.1 overexpression in hES derived neural progenitors shows much promise for switching the lineage to a monocytic one, although there is still room to improve the protocol for increased monocyte production.

---

## 4. M-CSF/IL-3 DIRECTED DIFFERENTIATION

---

### 4.1 INTRODUCTION

---

Microglia are the immune cells of the brain, which are derived from haematopoietic precursors during embryogenesis. They infiltrate the brain prior to the formation of the BBB and proliferate *in situ* until birth. These infiltrating cells are initially ameboid cells, which function in the phagocytosis of excess apoptotic neurons produced during development to help shape the developing brain, whilst also having the ability to provoke cell death of developing cells via a superoxide-dependent mechanism (Vilharat, 2005). A sub-population of microglia are suggested to derive from bone marrow cells that migrate into the CNS during pathogenesis throughout postnatal and adult life. To this extent it is plausible to hypothesise that *in vitro* differentiation of hESCs to monocytes and subsequent differentiation to microglia poses an attractive route to producing Human ES-derived microglial-like cells.

Generation of hematopoietic cells from hESCs has been established using many protocols (reviewed in (Orlovskaya et al. 2008)). Evseenko et al. (2010) utilized an adherent method to create hematopoietic cells by culturing in the presence of multiple growth factors (SCF, FLt3, TPO, VEGF, IL-3, Epo) and a small molecule TGF $\beta$  antagonist (SB-431542) supplemented with the use of murine bone marrow stromal OP9 feeder layers. Although the focus of their work was tracking and mapping the process of epithelial to mesenchymal transition (EMT), they were able

to produce CD34+ hematopoietic precursors, which could be further cultured to derive monocytes and microglial-like cells. Chadwick et al. (2003) created hematopoietic cells through an embryoid body based protocol by culturing for 15 days, again in the presence of a similar set of growth factors; SCF, FLt3, IL-3, IL-6, G-CSF and BMP4. They showed a mechanism for mimicking the events of early differentiation of hematopoietic precursors in the embryo resulting in the production of a CD34+CD45+ population of cells.

Both methods, and many of the other protocols discussed by Orlovskaya et al. (2008), use multiple growth factors in order to achieve haematopoietic differentiation. A more recent report published in PLOS One by van Wilgenburg et al. (2013) and its predecessor published in Experimental Haematology by Karlsson et al. (2008) showed that hESCs could be differentiated into monocytes utilising only two growth factors, M-CSF and IL-3, throughout the differentiation. Due to the smaller number of growth factors required and the lack of possible feeder layer contamination, this protocol is the most attractive and as such is replicated in this chapter with H9 HESCs in order to achieve hematopoietic differentiation, the foundation of microglial differentiation.

Macrophage – Colony Stimulating Factor (M-CSF) is a haematopoietic cytokine whose actions are directed specifically towards macrophages (Rambaldi et al. 1987). It was found to be a homodimeric protein, with its two subunits linked via disulphide bonds with different isoforms produced through alternative splicing (Cerretti et al. 1988). M-CSF can also induce differentiation of haematopoietic stem cells (HSCs) to macrophages through synergising with other cytokines, in particular those of the interleukin family, but its main role remains closely connected to macrophages by

extending the growth and survival rate of the macrophage precursor, the monocyte (Metcalf et al. 1992).

The other growth factor used in the differentiation protocol described by van Wilgenburg et al (2013) is IL-3. Interleukins are a large family of cytokines that are defined as being produced by leukocytes; mainly T-cells and macrophages. Interleukins have been shown to promote growth and differentiation of cells within the haematopoietic system and also play key roles in inflammation (Frendel 1992). IL-3 is a small protein that supports the differentiation of HSCs due to its interactions with colony stimulating factors, such as M-CSF, resulting in colony forming granulocytes, macrophages, erythroid, megakaryocyte and mast cells, whilst also being able to signal and effect non-haematopoietic stromal cells in the bone marrow (Ihne 1992).

Hematopoiesis, is a complex process that involves successive loss of multipotency and self-renewal of HSCs, the derivation of lineage-restricted progenitors and subsequent terminal differentiation to the various blood cells. Amongst the defined progenitor populations the Granulocyte Monocyte Progenitor (GMP) is the first to form within the AGM of the embryo. GMPs are characterised by expression of both CD34 and CD45 and can ultimately give rise to granulocytes, monocytes and microglia (Manz et al. 2002). Monocyte-like precursors are the foundation for microglial formation and prior to birth microglia proliferate *in situ*, undergoing differentiation from a monocyte-like cell due to the environmental cues secreted from the surrounding glial and neuronal cells. Microglial engraftment to the brain during pathogenesis in adult life is likely to result from bone marrow derived cells crossing a compromised BBB and also differentiating based on the similar cues that signal to

embryonic precursors with regard to their subsequent differentiation to microglia, although the type of microglial cell produced, whether pro-inflammatory or phagocytic is dependent on the inflammatory status of the tissue. Environments rich in IL-4 will lead to cells with a greater capacity for phagocytosis, whilst environments that have high levels of TNF- $\alpha$  yield a greater proportion of neurotoxic, inflammatory microglia.

---

### 4.1 AIM

---

The aim of this chapter was to direct the differentiation of hESCs into monocytic precursors through the application of the growth factor combination utilised by van Wilgenburg and colleagues (2013) namely M-CSF and IL-3 (Figure 3.1). With both the GMP (CD34<sup>+</sup>/CD45<sup>+</sup>) and monocyte (CD34<sup>low</sup>/CD45<sup>+</sup>/CD11b<sup>+</sup>) cells being further differentiated into microglial-like cells in chapter 5. Figure 4.1 provides an overview of the differentiation strategy used and illustrates the time course, the stepwise changes in culture conditions as well as the transformation in cell morphology within these cultures as differentiation proceeds.

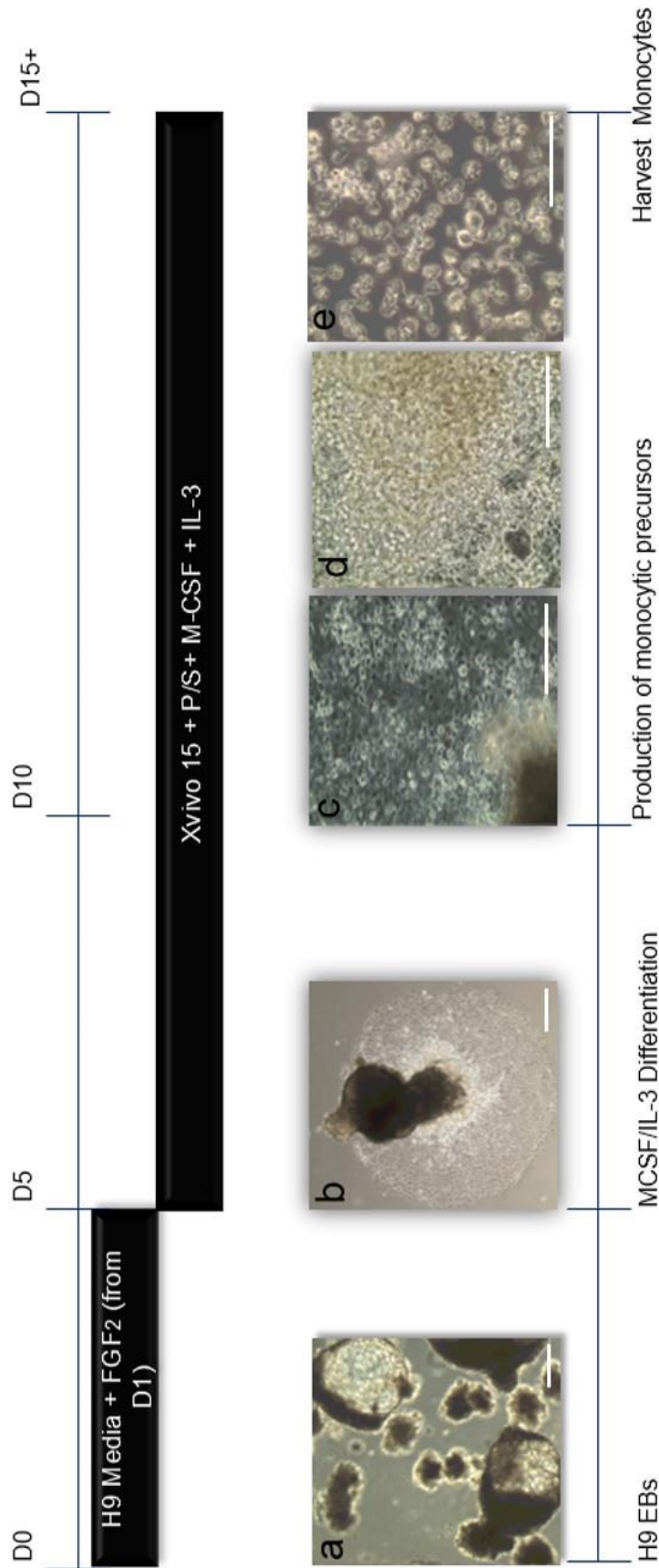


**Figure 4.1. Schematic Representation of the Differentiation Protocol**

Embryoid bodies (EBs) were formed in human ES cell culture medium with FGF2 for 4 days, with many forming cystic regions (a). EBs were transferred to 6-well tissue culture plate in XVIVO Factory medium supplemented with M-CSF and IL-3. Under these conditions EBs adhered to the culture surface and begin to spread (b). As the factories continue to differentiate there is the formation of phase bright cells (c), which subsequently increase in number (c). From day 15 (D15) these phase bright cells are shed from their factory colonies allowing them to be harvested from the supernatant (e).

Scale Bars Represent 50µM

##### 4.2 THE NON-HAEMATOPOIETIC NATURE OF HESCS

---

Since pluripotent cells are prone to spontaneous differentiation to derivatives of the three germ layers, endoderm, ectoderm and mesoderm the outcome of directed differentiation is dependent on maintaining a high standard of pluripotency in the starting hESC population. The quality of the H9 hESCs was assayed through immunocytochemistry for the expression of the standard pluripotency markers OCT4, SSEA4, NANOG and SOX2 (Figure 4.2). Staining was evident for all markers over the whole of all colonies, confirming that conditions were optimal for maintaining a pluripotent stem cell state. Staining for the transcription factors OCT4, SOX2 and NANOG was restricted to the nucleus, and staining for the surface antigen SSEA4 was constrained to the plasma membrane.

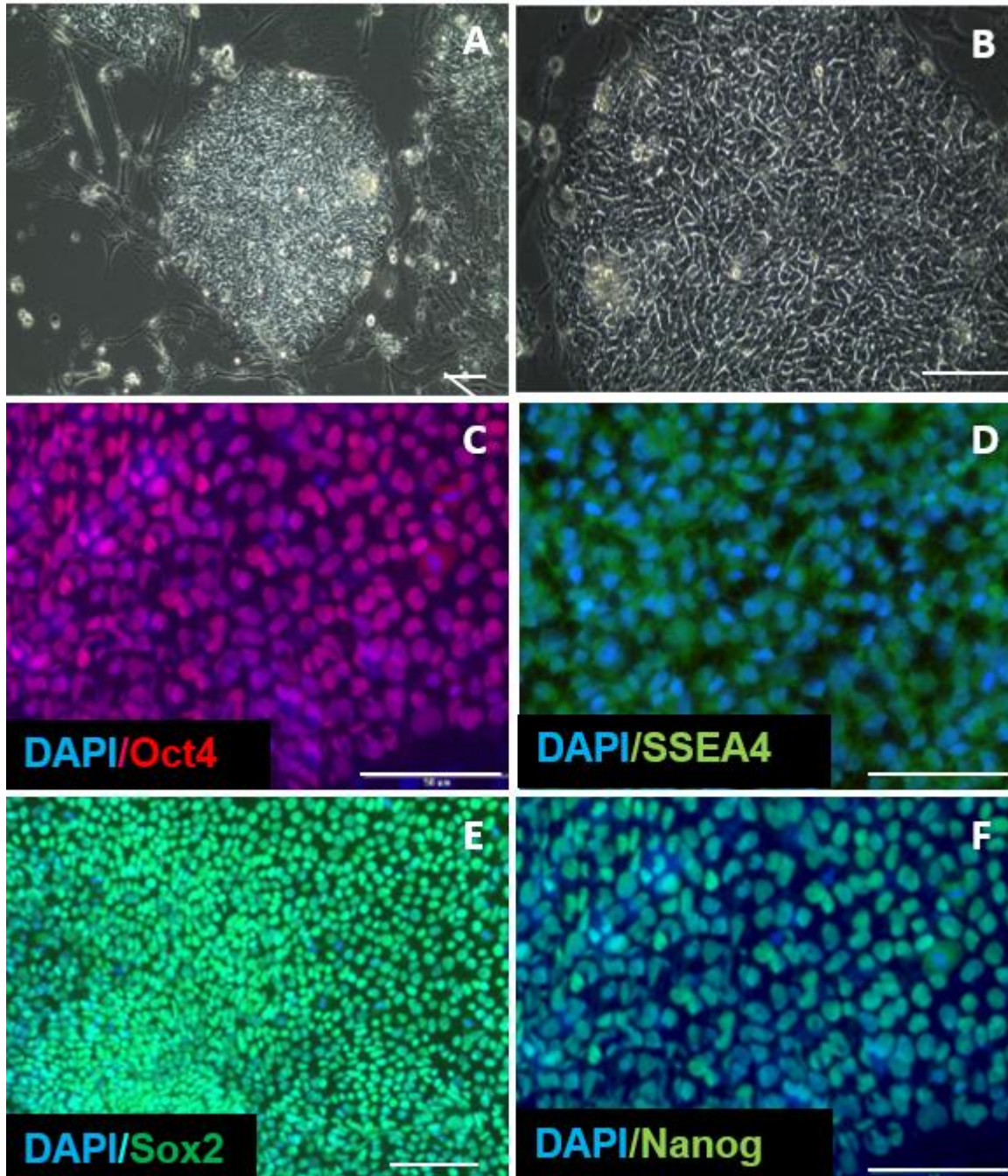


**Figure 4.2. The pluripotency of H9 Human Embryonic Stem Cells**

H9 colonies (A and B) had the morphology of pluripotent cells, compact colonies of uniform cells with a defined perimeter. The pluripotency of the H9 cells was examined through immunocytochemistry using Oct4 (C), SSEA4 (D), Sox2 (E) and Nanog (F). All cells were positive for these markers over the entire colony and are thus deemed to be pluripotent.

Scale bars represent 50um

Markers used to follow haematopoietic lineage commitment during hESCs differentiation were also analysed by flow cytometry and were confirmed to be negative in the starting H9 population. These included CD34, CD45 and CD11b. CD34 is a marker for HSCs, CD45 is a marker for leukocytes and CD11b is a marker for lineage committed monocytes (Figure 4.3). The data showed that hESCs are not innately haematopoietic with the percentage positive cells for each antibody being; 1.27% CD34+, 1.58% CD45+ and 2.41% CD11b+. The low percentages of positively stained cells could be due to background as no staining was evident when immunocytochemistry was carried out with the same antibodies. These data substantiate that the cells are pluripotent and not committed to a haematopoietic fate prior to the onset of differentiation.

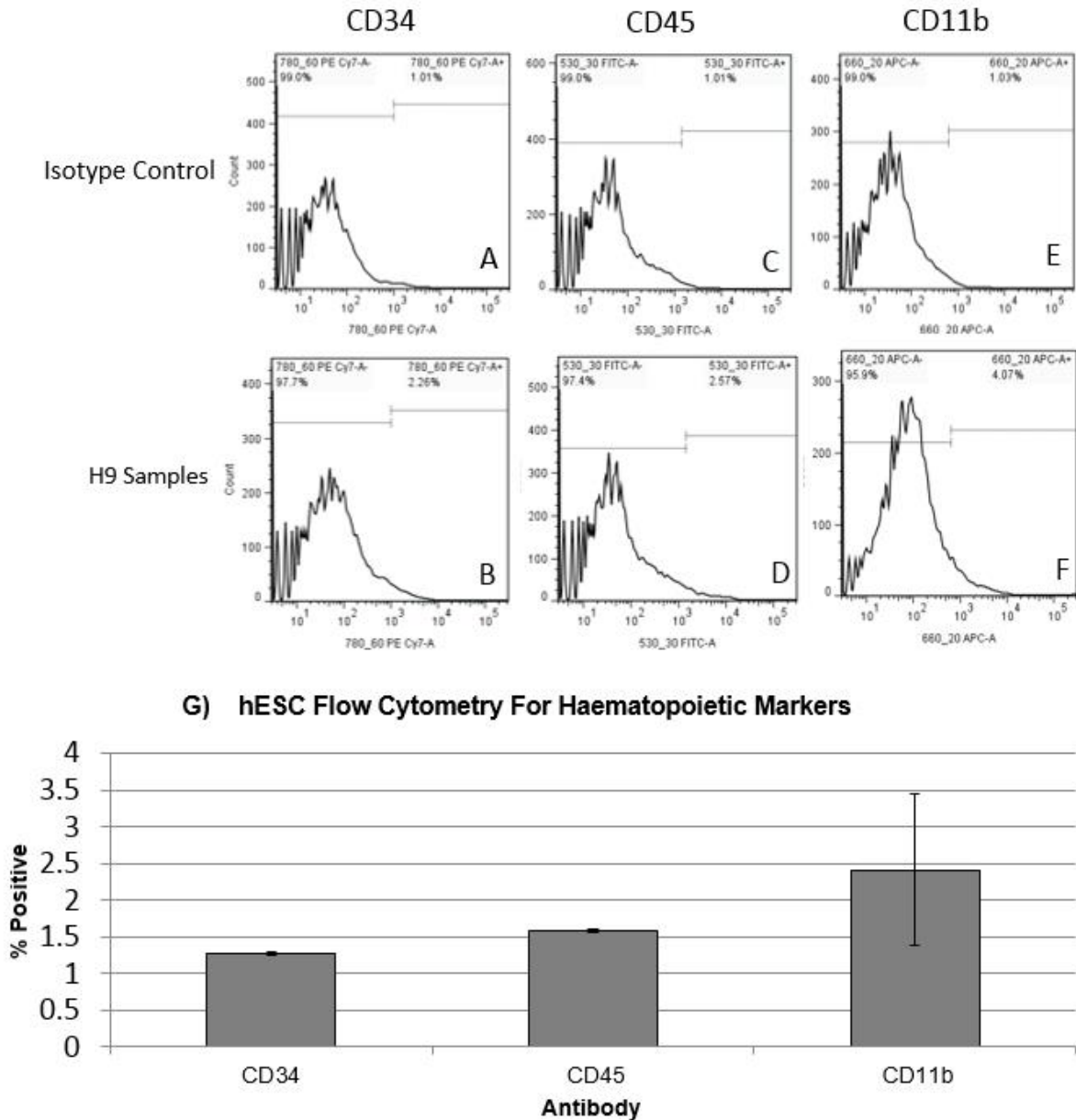


**Figure 4.3. The non-haematopoietic nature of H9 Human Embryonic Stem Cells**

Undifferentiated hESCs were assayed for their expression of the haematopoietic markers by flow cytometry. A and D show the unstained control and the CD34 stained sample respectively. CD45 staining was carried out (B) alongside its unstained control (E). The final marker assayed was CD11b (C) against its unstained control sample (F). A graph showing the average percentage positive cells in three biological replicates is shown in G.

### 4.3 THE MONOCYTE PRODUCING COLONIES

---

Directed differentiation of H9 hESCs to monocytes was achieved in two stages; (1) the formation of cystic EBs and (2) the adherence of the cystic EBs to tissue culture plastic for the production of monocytes into the culture supernatant (factory colonies). The commitment of the EB and factory colony cells to the mesoderm lineage from their pluripotent precursors was monitored through QRT-PCR using markers of pluripotency, mesoderm and neural filament; Nanog, Brachyury and Nestin, respectively (Figure 4.4). ANOVA for the comparison of the means showed that there was a statistically significant difference between them [ $F(2,18)=199.3$ ,  $p<0.0001$ ]. The post hoc Bonferroni test showed that Brachyury was increased in the EB ( $M=75.95$ ,  $SD=6.908$ ) compared to the factory colonies ( $M=0.3981$ ,  $SD=0.026$ ). Both Nestin and Nanog were similar, with no significant difference, in both EBs (Nestin ( $M=1.293$ ,  $SD=0.292$ ), Nanog ( $M=0.03401$ ,  $SD=0.029$ )) and factory colonies (Nestin ( $M=0.3321$ ,  $SD=0.103$ ), Nanog ( $M=0.0003523$ ,  $SD=0.0000418$ )).

This means that there is a loss of pluripotency on EB formation, which is sustained throughout the culture of the factory colonies. The mesoderm marker brachyury is increased during the day 4 EB stage, where production of all three germ layers is expected, but decreased in the factory colony stage where there should be the loss of general germ layer markers and the expression of the more specific haematopoietic ones.

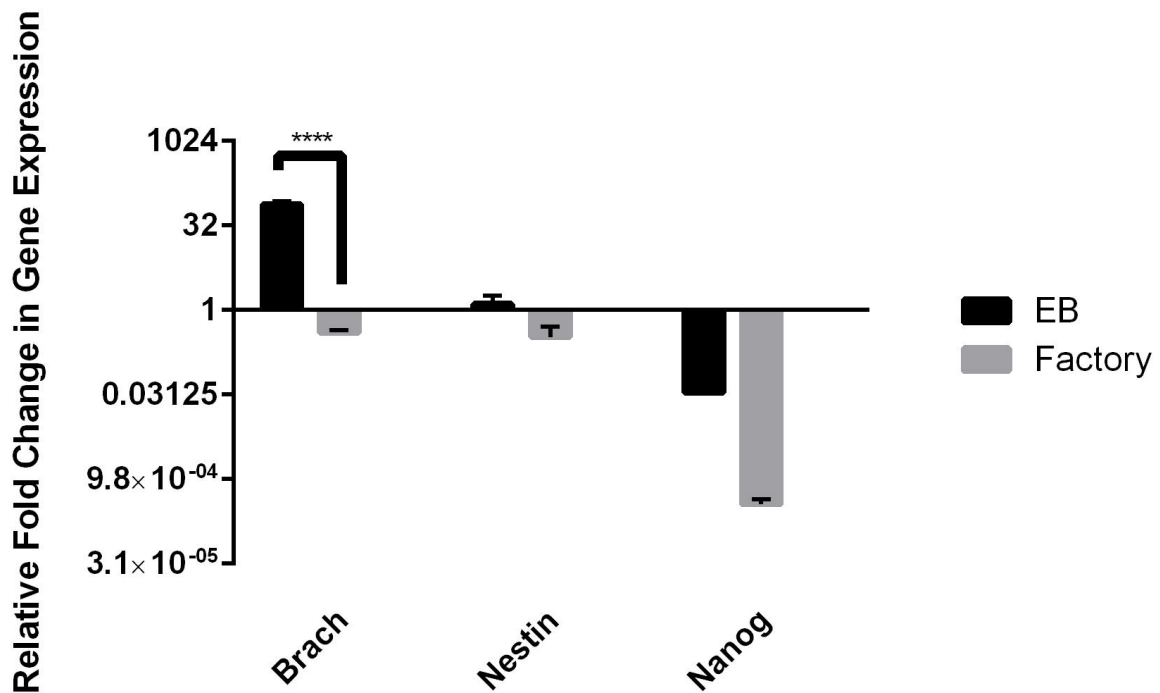


**Figure 4.4. Commitment of EBs and Factory Colonies to the Mesoderm Lineage**

Day 4 EBs are committed to the mesoderm lineage, revealed by a 76-fold increase in Brachyury expression compared to the undifferentiated hESCs. Nanog expression was decreased by 96.5% of that in hESCs revealing a loss of pluripotency and self-renewal capacity. Nestin, neural filament marker, expression remained unchanged. Day 12 factory colonies were shown to have around 0% less expression of the general mesoderm marker, Brachyury and nestin, whilst expression of nanog was decreased by 99.9% compared to the hESCs.

QRTPCR data is normalised to  $\beta$ -Actin over 3 technical replicates of 3 biological replicates

Asterisks denote statistical significance; \*  $\leq 0.05$ , \*\*  $\leq 0.01$ , \*\*\*  $\leq 0.001$ , \*\*\*\*  $\leq 0.0001$

To assess the developmental changes that occur in the EB and factory colonies expression of both early and late haematopoietic genes were also analysed by QRT-PCR relative to both hESCs and THP1 monocytes, as shown in Figure 4.5 (A and B, respectively). Relative to hESCs there is a statistical difference between the means of EB and factory colony gene expression [ $F(1,24)=233.0$ ,  $p<0.0001$ ]. Bonferroni multiple comparisons test showed that although decreased in the factory colonies, FLK1 and RunX1 expression was not statistically different to that of the EBs. The increased expression of PU.1 and CD34 in the factory colonies was also shown to not be statistically significant. There were significant increases in the expression of CD45 and CD11c in factory colonies (CD45 (M=55.43, SD=4.438), CD11c (M=15.32, SD=0.403)) compared to the levels in the EBs (CD45 (M=8.804, SD=3.780), CD11c (M=0.7188, SD=0.0645)). A comparison of the mean gene expression of EBs and Factory cells relative to THP1 monocytes was analysed by ANOVA and showed a significant difference between the fold change of the expressed genes at the two time points [ $F(2,36)=6.258$ ,  $p=0.0046$ ]. Post hoc comparisons of the means by the Bonferroni test showed that, with the exception of FLK1, the expression of all other genes were not significantly different in the EB stage compared to the factory stage. For FLK1, expression was increased in the factory stage (M=5.262, SD=0.177) compared to the EB stage (M=4.131, SD=0.664). Although the remaining genes were not statistically different the trend implies an increase in expression in the day 12 factory colonies compared to the day 4 EBs. This indicates that the factory colonies are beginning to differentiate towards leukocyte production.

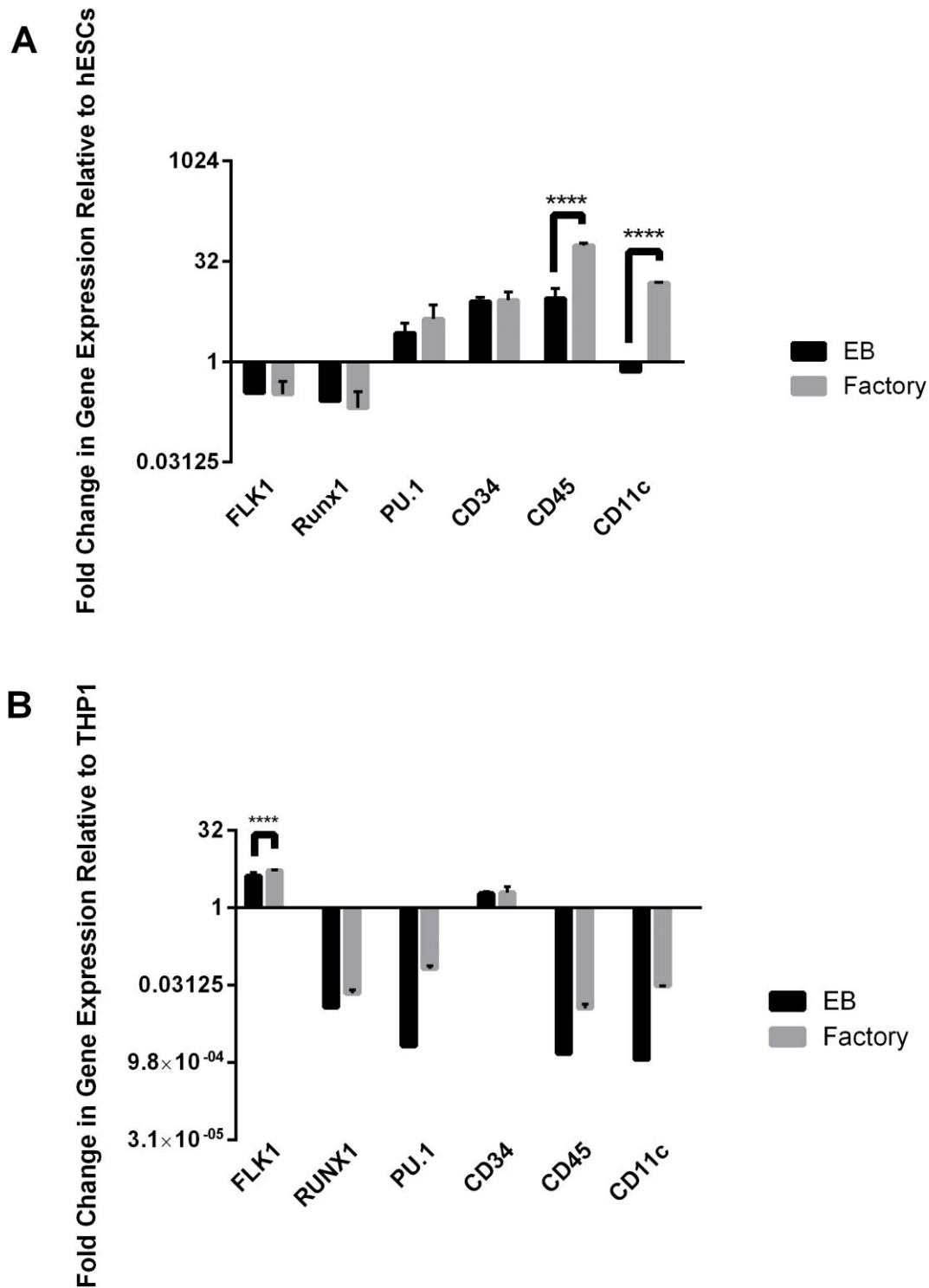


**Figure 4.5. Haematopoietic Gene Expression in EBs and Factory Cells**

(A) Gene expression relative to hESCs reveals a significant increase in the expression of CD45 and CD11c in the factory cells (CD45 (M=55.43, SD=4.438), CD11c (M=15.32, SD=0.403)) compared to the EBs (CD45 (M=8.804, SD=3.780), CD11c (M=0.7188, SD=0.0645)).

(B) Relative to THP1 monocytes there is an increase in the expression of FLK1 in the factory stage (M=5.262, SD=0.177) compared to the EB stage (M=4.131, SD=0.664).

QRTPCR data is normalised to  $\beta$ -Actin over 3 technical replicates of 3 biological replicates

Asterisks denote statistical significance; \*  $\leq 0.05$ , \*\*  $\leq 0.01$ , \*\*\*  $\leq 0.001$ , \*\*\*\*  $\leq 0.0001$

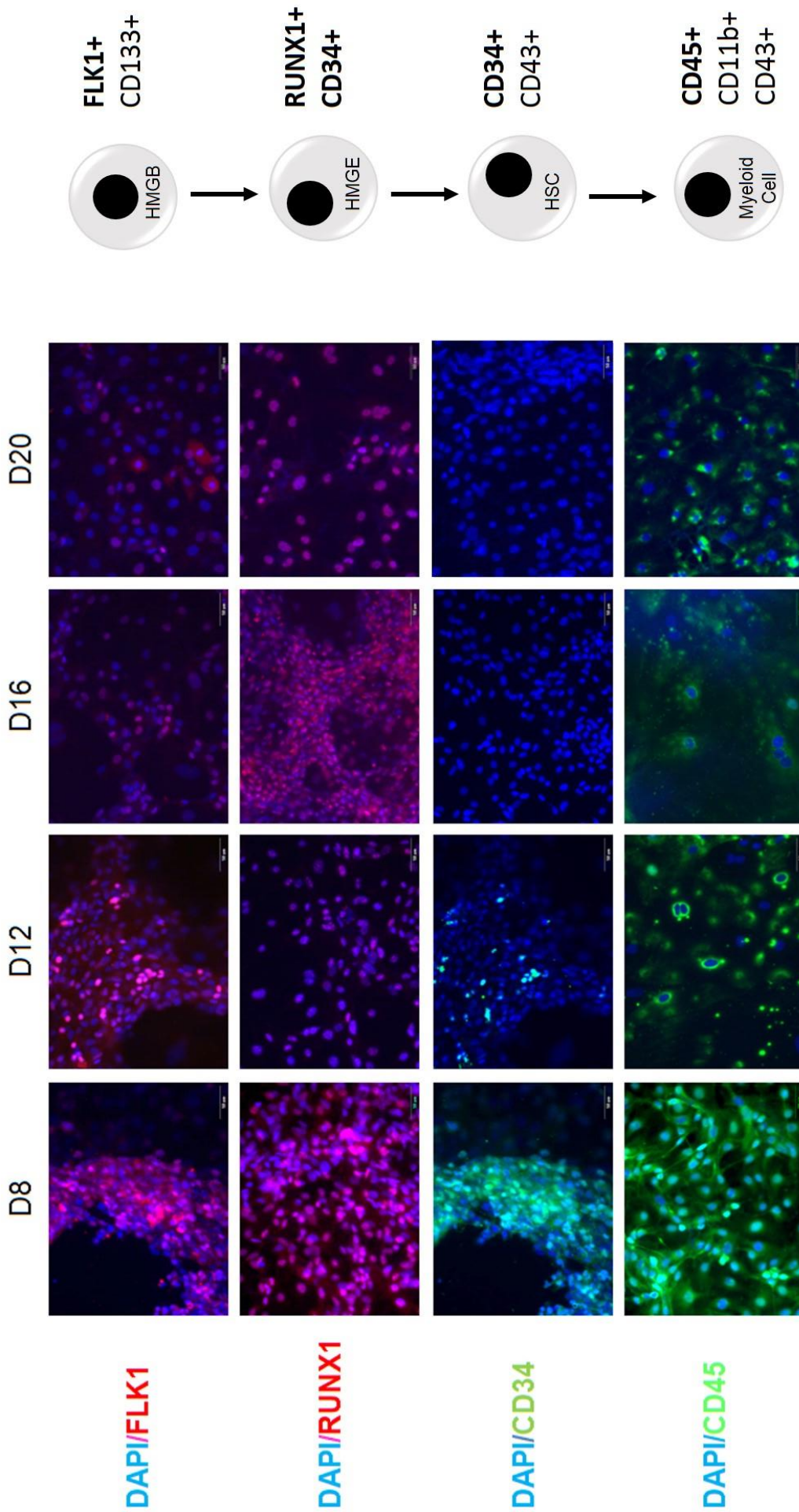
The adherent factory colonies were assayed for the presence of PU.1, FLK1 and RUNX1, markers of early haematopoietic precursors along with later markers of haematopoiesis; CD34 and CD45 (Figure 4.6). The adherent factory colony cells showed evidence of staining for PU.1 from day 8 through to day 20, although the location of the staining trafficked between the cytoplasm and the nucleus, which would be a way of controlling the dose response required for haematopoiesis. Nuclear staining for PU.1 was evident at day 12, which corresponded with the onset of the downstream marker CD45 staining the membrane. Upstream of PU.1 is the definitive haematopoietic marker, RUNX1, staining for which was high from day 8 and maintained throughout the differentiation. Maintenance of RUNX1 was expected as *in vivo* RUNX1 is expressed at some level in all haematopoietic cells, with the exception of erythrocytes (North et al. 2004). FLK1, a marker of primitive hematopoiesis and the haemangioblast, stained most positively between day 8 and day 12, after which the presence of staining decreased. CD34 expression was also shown to occur only to day 12. This could indicate a ‘budding off’ of CD34+ cells in a similar fashion to those of the embryonic blood islands.

**Figure 4.6. Primitive and definitive haematopoiesis in EBs and Factory colonies (Overleaf)**

Haematopoietic markers analysed every 4 days from day 8 (D8) to day 20 (D24). PU.1 staining was evident from D8 and maintained to D20 at low levels, where it cycled from cytoplasm to nucleus. Samples were positively stained for FLK1 from D8 onwards. High levels of RUNX1 staining were observed throughout the time course. The haematopoietic stem cell marker, CD34, was only observed by immunohistochemistry to D12. CD45; leukocyte marker, expression is seen truly as a membrane bound receptor from D12, after which expression is decreased. The right panel shows a schematic representation of the differentiation of haematopoietic cells from the Haemangioblast (HMGB) or FLK1+ primitive haematopoietic precursor to the RUNX1+ definitive haematopoietic cell (haemogenic endothelium (HMGE)). The cells then enter haematopoiesis as the CD34+ haematopoietic stem cell (HSC) and proceed through to a CD45+ myeloid cell.

Scale bars represent 50µm

4. M-CSF/IL-3 Directed Differentiation



#### 4.4 ES-DERIVED MONOCYTES

---

The non-adherent cells shed into the culture supernatant from the monocyte factories were harvested and examined microscopically using both histological and immunological techniques to assay cell morphology and the expression of CD34, CD45 and CD11b (Figure 4.7 a-c). Haematoxylin staining of the ES-derived monocytes (ESdM) revealed a uniform population of large cells (~20 $\mu$ m) with a large nuclei and nucleoli, and abundant granular cytoplasm. Immunocytochemistry revealed cells positive for all three haematopoietic markers CD34, CD45 and CD11b. The level of CD34 staining inferred of the presence of GMP cells, whilst the CD11b staining indicated that monocytes were also present, meaning that the ESdM cultures comprised mixed populations of cells at various stages in myeloid haematopoiesis.

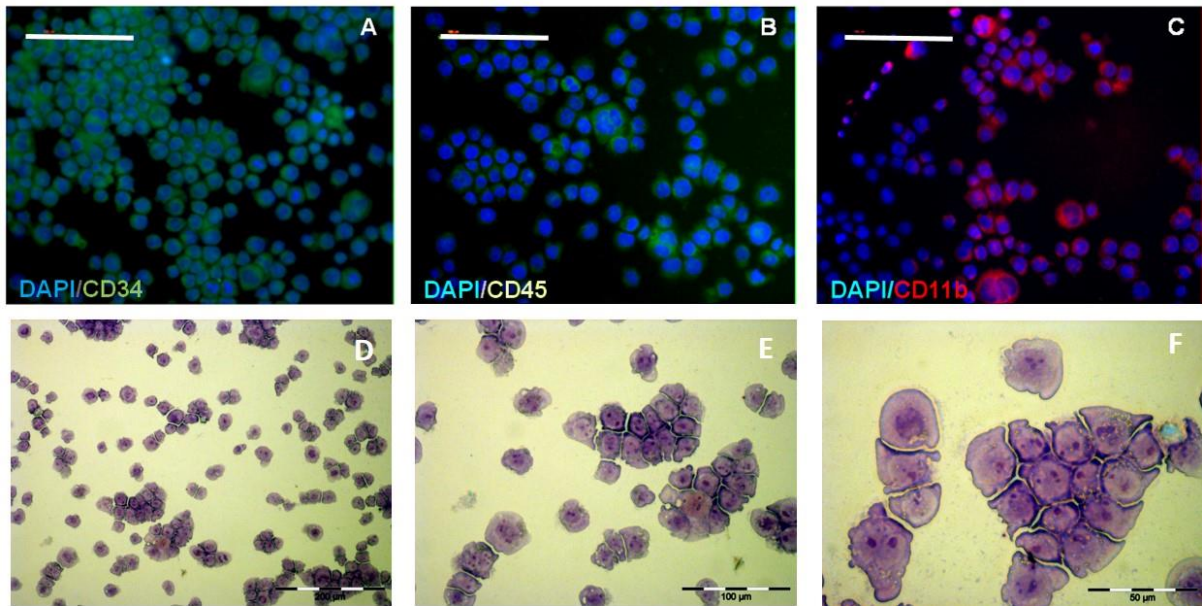


**Figure 4.7. Haematopoietic Marker Expression and Morphology**

Immunocytochemistry was carried out on cytocentrifuged cells for the haematopoietic markers CD34 (A), CD45 (B) and CD11b (C) and they were stained histologically with Haematoxylin for morphological analysis (D – F).

Scale bars represent 100µm (A-C), 200µm (D), 100µm (E), 50µm (F)

Haematopoietic gene expression in ESdM cells was examined by QRTPCR (Figure 4.8), and the levels compared to those seen in THP1 monocytes and through ANOVA were shown to have no significant difference between the means [ $F(1,2)=3.065$ ,  $p=0.221$ ]. The only significant difference between the ESdM and THP1 lays with the expression of CD11c, which is increased in the ESdM ( $M=1.371$ ,  $SD=0.114$ ). Although expressed in monocytes, CD11c is more highly expressed in microglia and dendritic cells and this marginal increase on expression could indicate that the cells have a more microglial nature.

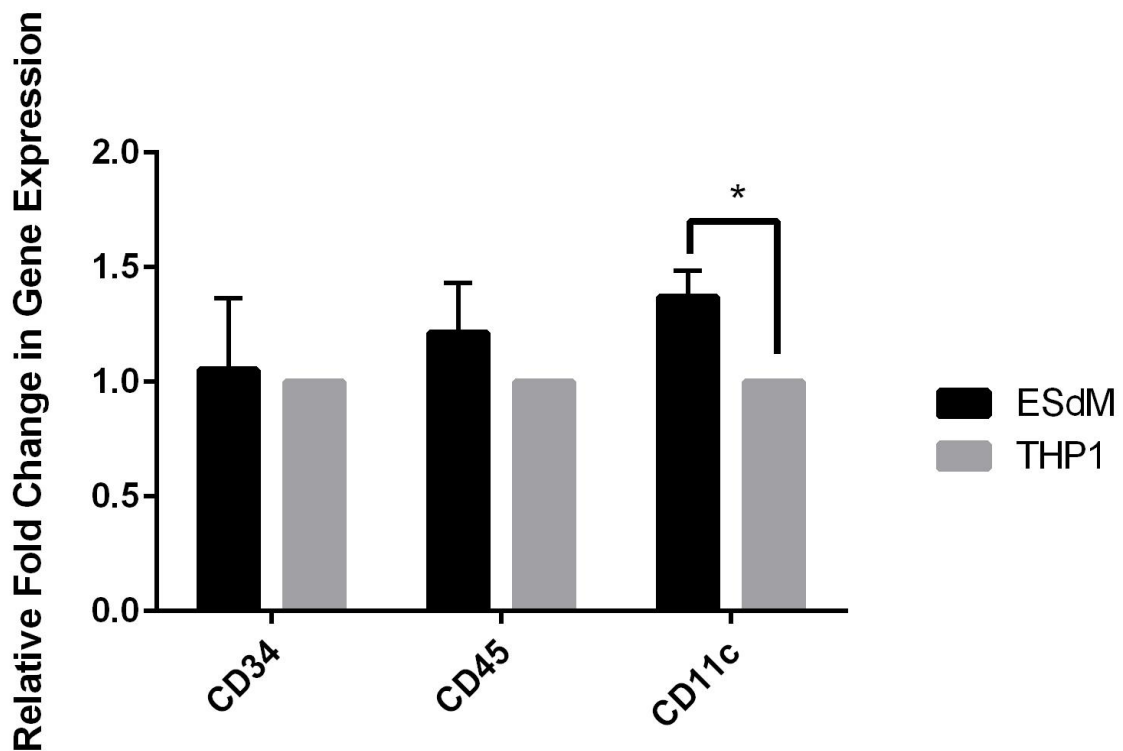


**Figure 4.8. Comparison of haematopoietic Gene Expression in ESdM and THP1 cells**

Overall comparison of the means by ANOVA, showed no statistical difference [ $F(1,2)=3.065$ ,  $p=0.221$ ]. A statistically significant difference was seen in the levels of CD11c with expression increased in ESdM cells ( $M=1.371$ ,  $SD=0.114$ ).

QRTPCR data was normalised to  $\beta$ -Actin and taken from 3 technical replicates of 3 biological replicates

Asterisks denote statistical significance; \*  $\leq 0.05$ , \*\*  $\leq 0.01$ , \*\*\*  $\leq 0.001$ , \*\*\*\*  $\leq 0.0001$

#### 4. M-CSF/IL-3 Directed Differentiation

The non-adherent cells were also characterized by flow cytometry using the same three markers to quantify the percentage of cells that were haematopoietic, leukocytic and monocytic. To optimize the FACs protocol and antibodies a primary blood mononuclear cell sample was used (Figure 4.9).

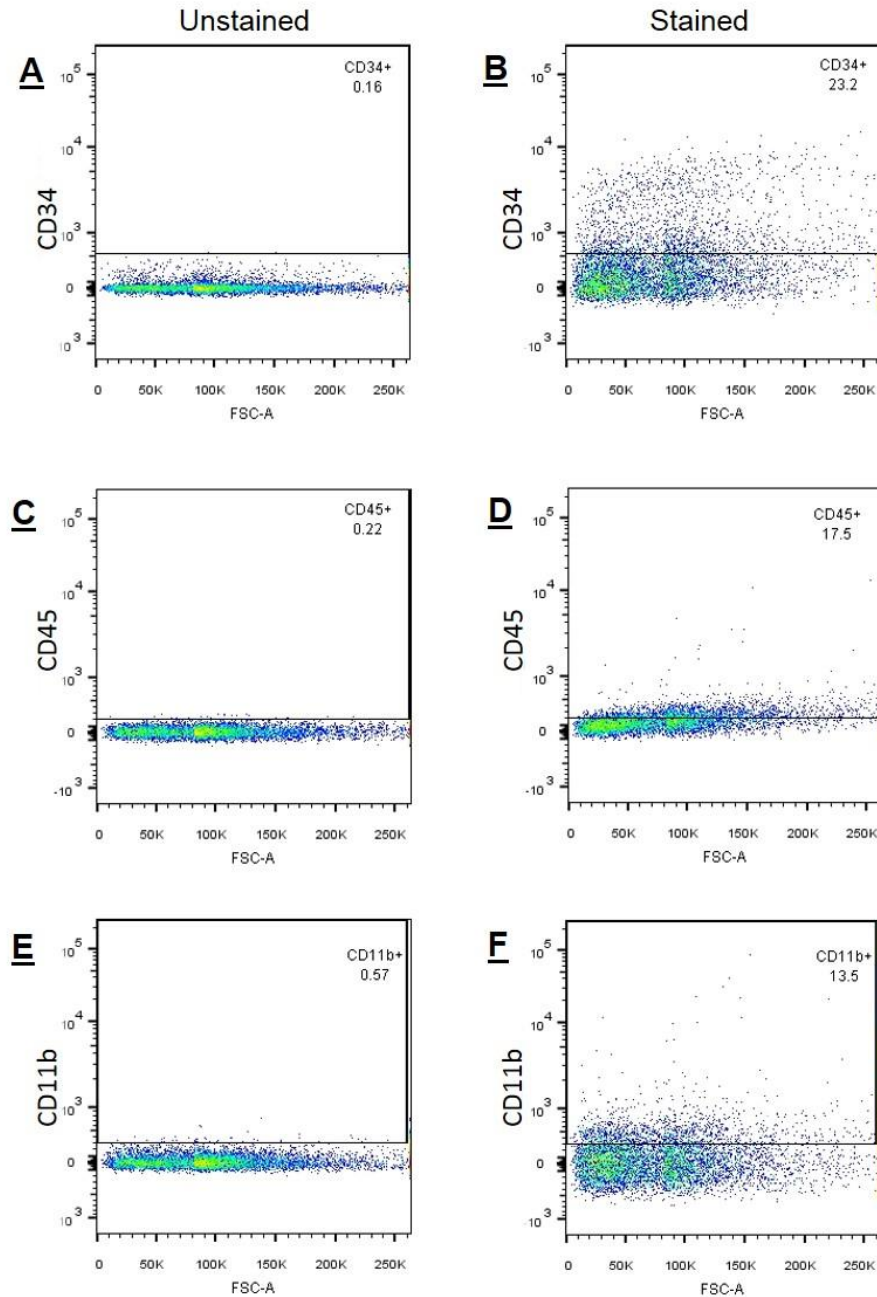


**Figure 4.9 Optimisation of the FACs protocol**

Control primary blood mononuclear cells (PBMCs) were used to optimise the FACs protocol for the conjugated antibodies, CD34 (A/B), CD45 (C/D) and CD11b (E/F). This showed a population of CD34+ cells of 23.2%, 17.5% of the cells were CD45+ and CD11b+ cells accounted for 13.5% of PBMCs

When the non-adherent cells, produced from the adherent factory colonies were stained and analysed by flow cytometry it revealed a small population of CD34+ (<5%) early haematopoietic progenitors, and a larger population of CD45 (16.4%) and a population of 7% of CD11b positive cells, indicating differentiation to yield more committed monocyte-like cells (Figure 4.10).

Triple staining the supernatant with antibodies against CD34, CD45 and CD11b and assessing their co-staining by flow cytometry (Figure 4.11), showed that there was a CD34+/CD45+ population of over 47.6% and a committed monocyte, CD45+/CD11b+, population of 37.6%. Co-staining of the early HSC marker, CD34, and the late monocyte marker, CD11b, resulted in a smaller population of around 17%.

This suggests that there is again a mixed population of GMP (CD34+/CD45+) precursors as well as committed monocytes (CD45+/CD11b+). From the single staining experiments it also appears that the supernatant also contains cells transitioning through haematopoiesis and as such fall outside of these defined stages, only CD34+ or just CD45+.

#### 4. M-CSF/IL-3 Directed Differentiation

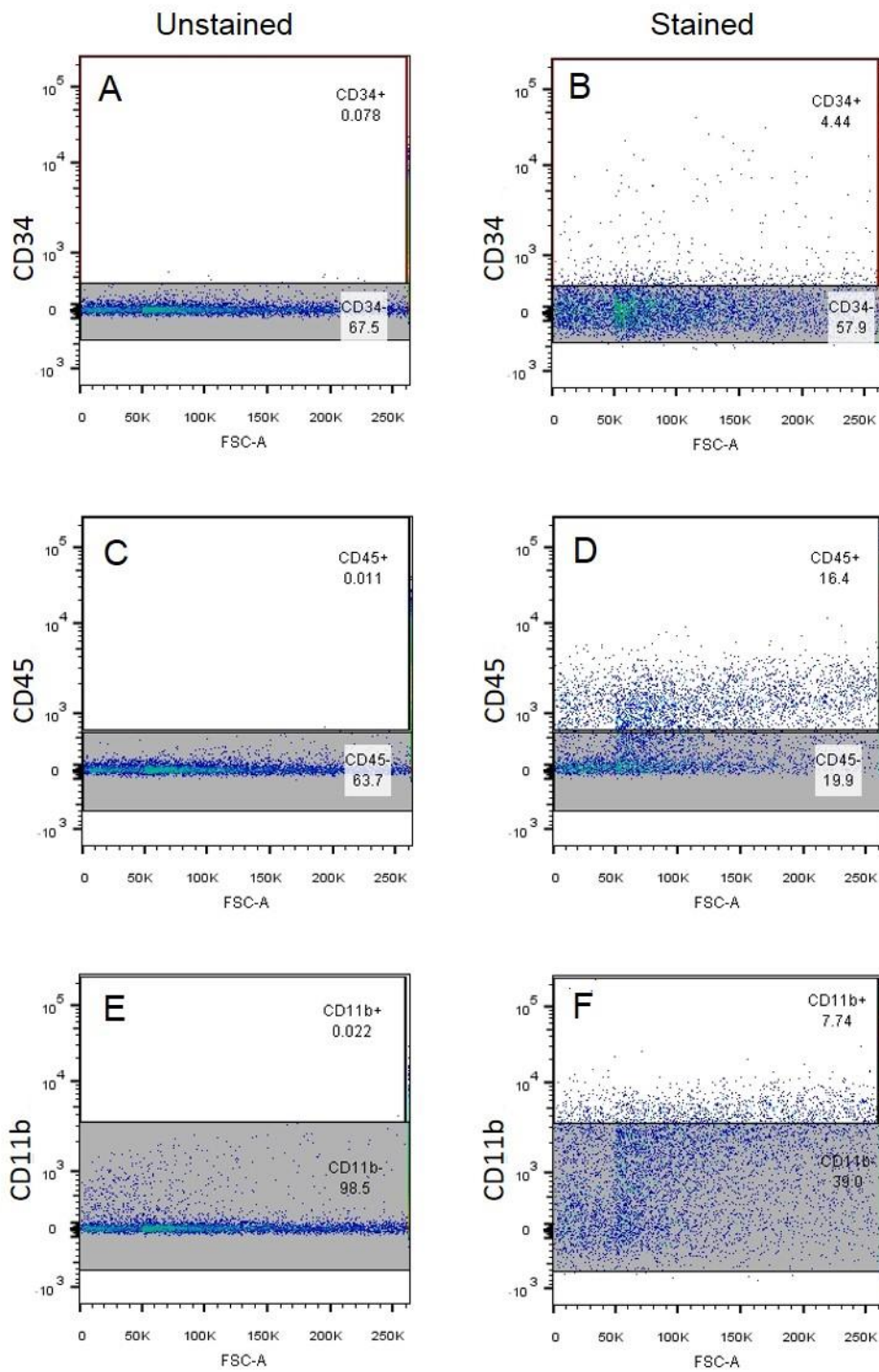


**Figure 4.10. Quantification of the Haematopoietic Population of Supernatant Cells**

Flow cytometry of the supernatant cells using the haematopoietic markers; CD34 (A/B), CD45 (C/D) and CD11b (E/F) and their dot plots for the unstained (left) and stained (right) samples, representative of three individual experiments, show that there is a mixed population of GMP cells (4.44% CD34+) and monocytes (16.4% CD45+ / 7.77% CD11b+) within the supernatant.

#### 4. M-CSF/IL-3 Directed Differentiation

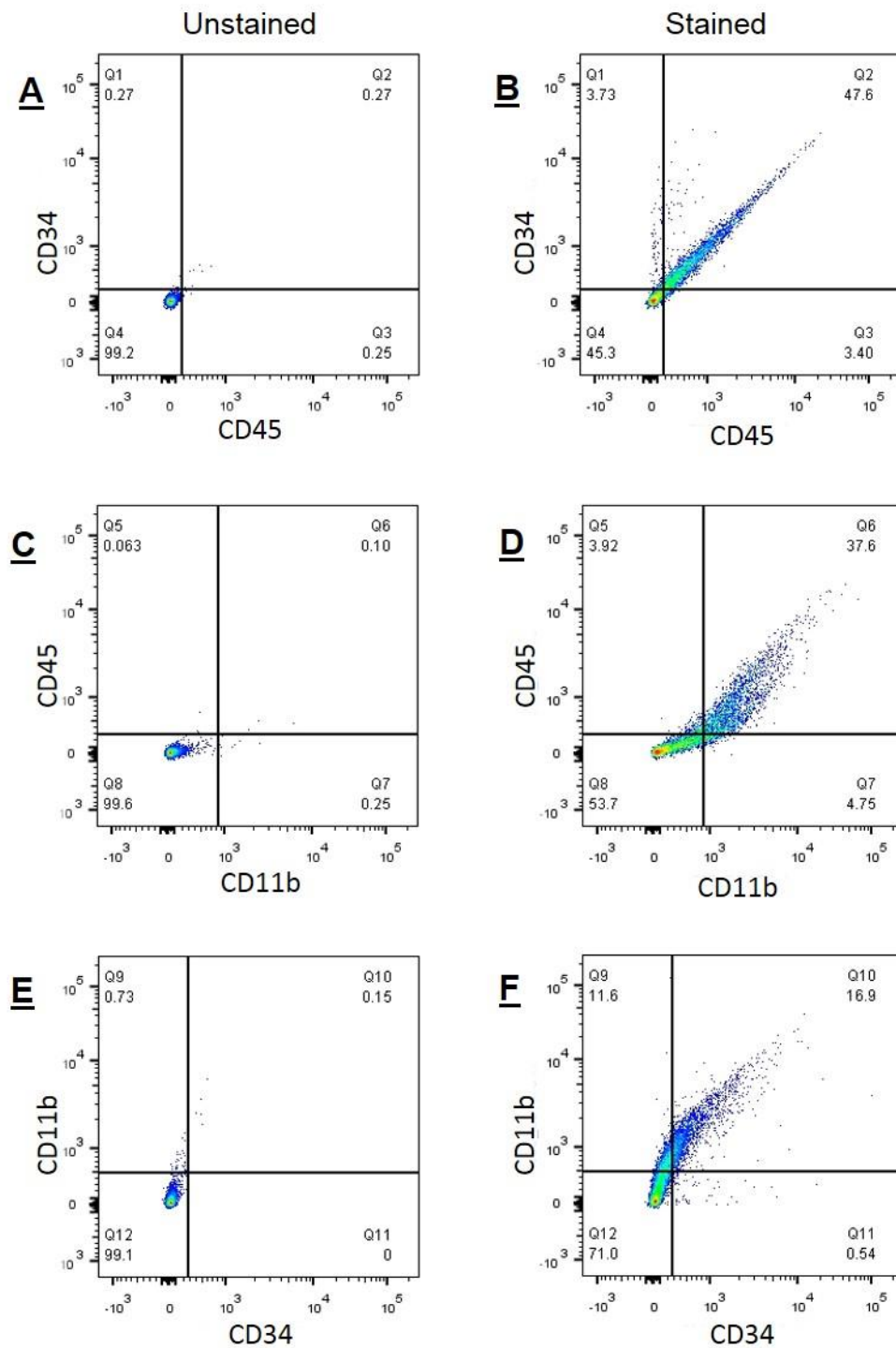


**Figure 4.11. Quantification of the Co-Expression of Haematopoietic Markers in Supernatant Cells**

Co-expression of CD34/CD45 (A/B), CD45/CD11b (C/D) and CD11b/CD34 (E/F) for the unstained (left) and stained (right) supernatant samples, representative of two individual experiments, show that there is a GMP CD34<sup>+</sup>/CD45<sup>+</sup> population (upper right quadrant) of 47.6%, a 37.6% population of CD45<sup>+</sup>/CD11b<sup>+</sup> cells and a large CD11b<sup>+</sup>/CD34<sup>+</sup> (16.9%).

#### 4.5 FUNCTIONALITY OF ES-DERIVED MONOCYTES

The functionality of the ES-derived cells was examined using a phagocytosis assay. Time-lapse microscopy and flow cytometry were used to visualize and quantify the uptake of fluorescent *E.Coli* bioparticles (Figure 4.12). For time lapse microscopy the suspended monocytes were first attached to glass coverslips using fibronectin for several hours prior to onset of the experiment. Cells were visualised by live staining with Cy5-conjugated anti-CD45 antibody to mark the perimeter of the cells and Hoescht 33342 to track cell nuclei and were analysed for uptake and cytoplasmic localisation of Alexa Fluor® 594-labelled *E.Coli* beads.

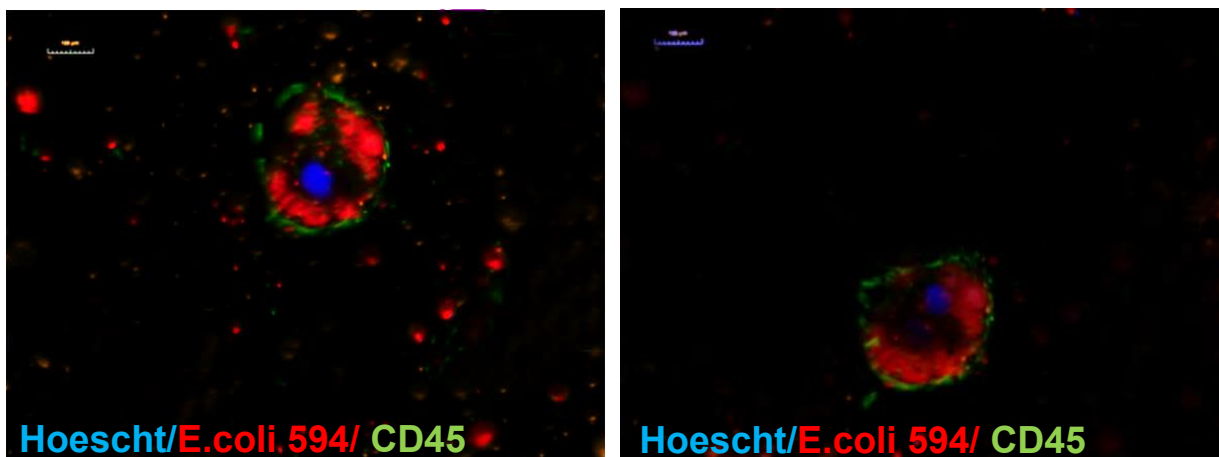


**Figure 4.12 Phagocytosis of *E.coli* Bioparticles**

Two examples of live CD45 immunofluorescent (green), Hoescht 33342 (blue) stained ES-derived monocytes, with uptake and cytoplasmic concentration of Alexa Fluor® 594 *E.coli* bioparticles (red) following a 60 minute monocyte/*E.Coli* biopartical co-culture

Scale Bars represent 100µm

Time lapse microscopy (Figure 4.13a/b) of ESdM showed that after eighteen minutes of incubation with the opsonised *E.Coli* bioparticles, the ESdM began to send out cytoplasmic extensions to surround the labeled bioparticles, twenty minutes later these projections would meet to encapsulate the particles and around 5 minutes post encapsulation the extended cytoplasmic processes began to retract followed by

internalisation of the beads approximately 40 minutes after addition of the particles, which then moved to a more central location within the cell after 60 minutes of incubation.

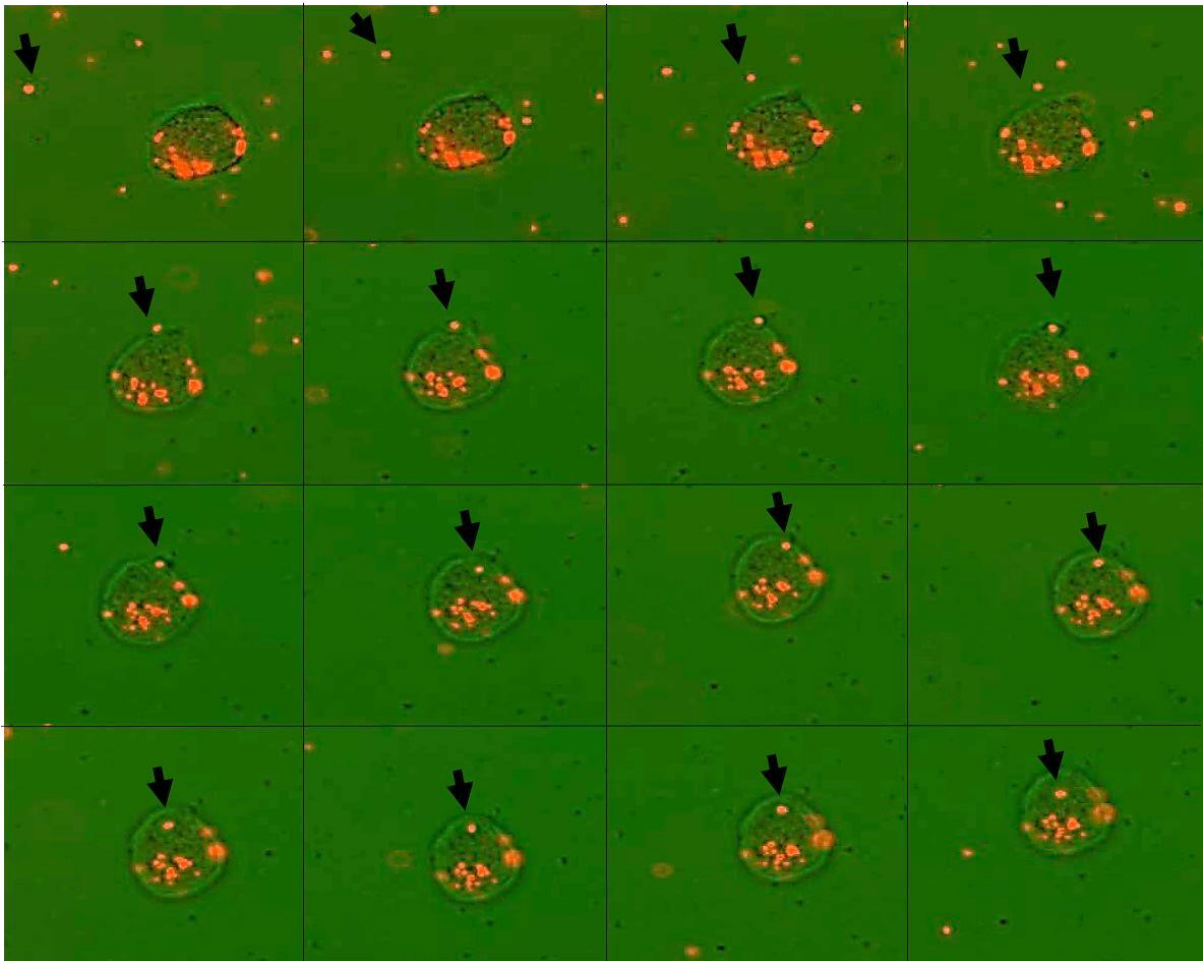


**Figure 4.13a. Time Lapse Microscopy of *E.coli* Bioparticle Phagocytosis in ESdM (Example 1)**

Images shown are taken every 3 minutes over a period of a 60 minute incubation, starting at 6 minutes. The arrow highlights the movement of a specific bead during the time course. This shows that after 18 minutes cytoplasmic extensions form to surround the bead, which retract upon internalisation after around 40 minutes. The bead then moves within the cell to a central location by the end of the incubation period.

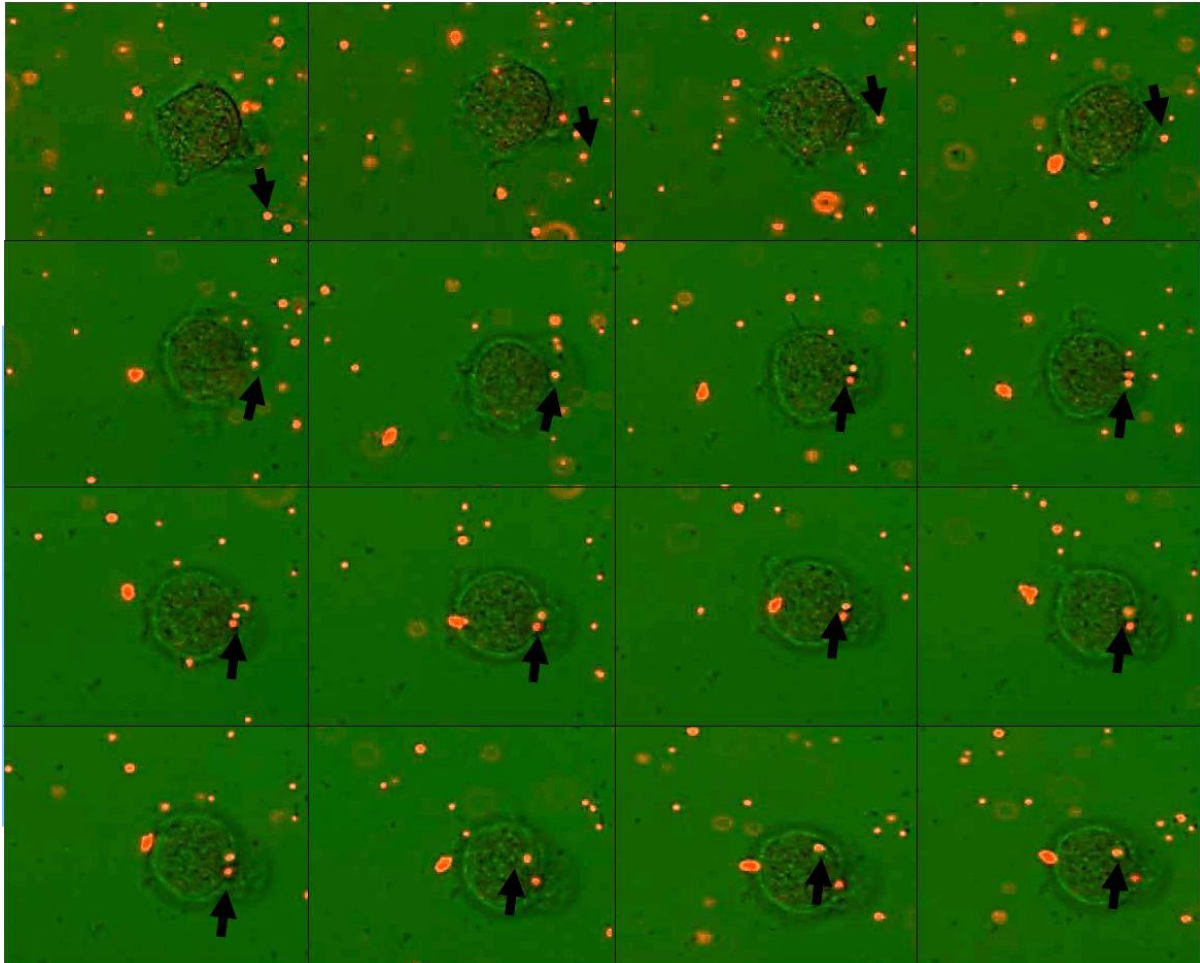


**Figure 4.13b. Time Lapse Microscopy of *E.coli* Bioparticle Phagocytosis in ESdM (Example 2)**

Images shown are taken every 3 minutes over a period of a 60 minute incubation, starting at 6 minutes. The arrow highlights the movement of a specific bead during the time course. This shows that after 18 minutes cytoplasmic extensions form to surround the bead, which retract upon internalisation after around 40 minutes. The bead then moves within the cell to a central location by the end of the incubation period.

Flow Cytometry of the resting, unstimulated, cells showed that there was a basal capacity of around 35% for phagocytosis in the control THP1 monocyte cell line and 27% in the ES-derived monocytes after a 60 minute incubation with opsonized Alexa Fluor® 594-labelled *E.Coli* beads (Figure 4.14).

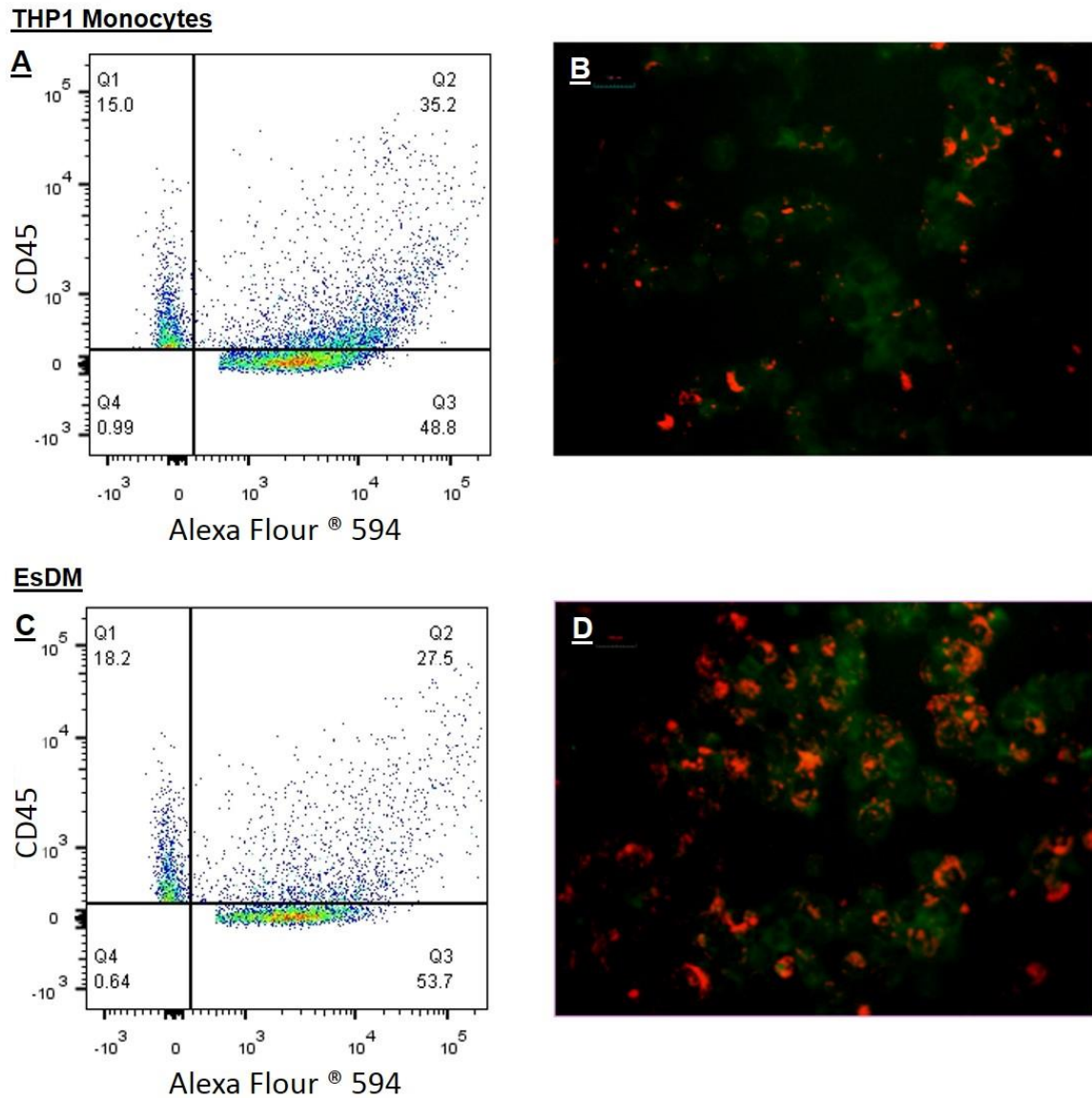


**Figure 4.14. Time Lapse Microscopy of *E.coli* Bioparticle Phagocytosis in ESdM**

Flow cytometry showed that when resting the THP1 cell line (A and B) were showed a phagocytic capacity of around 35% which compared well to the ES-derived monocytes (C and D) with a 27% capacity

#### 4.6 DATA SUMMARY

---

We have shown that H9 hESCs expressing the pluripotency markers Oct4, SSEA4, nanog and Sox2 do not express markers used to signify commitment to a haematopoietic fate. H9 cells underwent hematopoietic differentiation under the direction of the cytokines M-CSF and IL-3. Cultures progressed through differentiation of mesoderm cells in the EB stage, followed by PU.1 expression in the monocyte producing factories and ultimately produce a non-adherent cells positive for CD45 and CD11b, characteristic of monocytes. These ESdMs were also shown to be functional through their ability to successfully phagocytose *E.coli* bioparticles in a capacity that was similar to those of the human monocytic cell line THP-1. As such the method described here is capable of producing ES-derived monocytes from a H9 cell line as well as for the cell lines used during publication of the protocol by van Wilgenburg et al. (2013).

#### 4.7 DISCUSSION

---

FLK1 and RUNX1 are classic markers for the haemangioblast and primitive or definitive embryonic hematopoietic cells prerequisites for the hematopoietic stem cell (Lacaud et al. 2002). Downstream of RUNX1 is the transcription factor PU.1 that is vital for both the onset of hematopoiesis and the terminal differentiation of monocytes (Huang et al. 2008). RUNX1 is also able to bind to CD34 downstream regulatory elements, increasing CD34 expression (Levantini et al. 2011). Although the presence of RUNX1 and PU.1 in the factory cells concurs with the proposed differentiation scheme for monocyte development, the lack of CD34 in the factories is unexpected since CD34 precursors are required for the onset of haematopoiesis. However, CD34+ cells do subsequently appear in the non-adherent population, which is in keeping with the accepted differentiation scheme proposed for monocyte development; namely that RUNX1 expression in definitive haematopoietic cells results in an increase in PU.1 expression and the onset of haematopoiesis, leading to the formation of CD34+ HSCs. PU.1 expression is evident only at low levels at the HSC stage but increases as the cells progress through haematopoiesis and become committed to a monocytic fate.

The observation that the adherent factory colony cells, even at late stages, do not show significant expression of CD34, but the non-adherent population do, suggests that the factory cells act in a similar way to the embryonic blood islands where the CD34+ HSCs 'bud off' from the islands into the primitive circulatory system, explaining their absence in the adherent culture. The factory colonies are composed of cells of several different morphologies, which could be explained through their formation. The factory colonies arise from the attachment of an EB to the tissue culture plastic. Although EB differentiation in the protocol used is biased towards

mesoderm, EBs are nevertheless complex developmental entities composed of cell derivatives from all three germ layers; the outer primitive endoderm, the mesoderm and the inner ectoderm and it is from the mesoderm cells that blood islands are formed and subsequently give rise to the non-adherent myeloid cells (Dang et al. 2002).

Positivity for CD34+ and CD11b+ expression on cells within the non-adherent population is suggestive of both GMP and monocyte differentiation, representing cells that are at different stages of haematopoietic commitment. This could be due to asynchrony in differentiation resulting from differential exposure of cells within EBs to cytokines. In three dimensional EB cultures cells in the centre respond to signal from a different microenvironment than those at the exterior. As such this may account for asynchrony in differentiation as well as some diversity in lineage specification.

Changes in the profile of marker expression map well onto changes expected for monocyte differentiation. As cultures progressed through haematopoiesis CD34 expression was lost and CD45 and CD11b were up-regulated. This progression was seen by flow cytometry and corroborated by QRT-PCR.

A hallmark function of monocytes is phagocytosis. Importantly, time-lapse microscopy showed that differentiated CD45+ monocytes showed efficient phagocytosis of aggregated E.Coli particles. This was proven by flow cytometry, which showed that the phagocytic capacity of the ESdMs was similar to that of the THP-1 monocytic cell line. When un-stimulated, approximately 30% of both ESdM and THP1 populations showed phagocytosis.

---

## 5. DIFFERENTIATION OF ES-DERIVED MONOCYTES TO MICROGLIAL-LIKE CELLS

---

---

### 5.1 INTRODUCTION

---

Microglia infiltrate the CNS early in development where they proliferate *in situ* expressing an ameboid phenotype, visible from the second trimester until birth, where they then differentiate into the immune dampened ramified phenotype (Cuadros and Navascués 1998). It has been suggested that there is a microglial niche that enables self-renewal since the BBB, in young healthy individuals, provides an obstacle to recruitment of new microglia from their haematopoietic precursors (Davoust et al. 2008).

In cases where microglial load and thus apoptosis increases, due to infection and inflammation, the compromised BBB allows recruitment of new cells from the blood. This phenomenon was illustrated by Djukic et al. (2006), who showed that under pathological conditions monocytes are recruited to the CNS by secretion of CXCL2 and CXCL8 from the CNS resident microglia. These infiltrating monocytic cells were observed to integrate into the pool of brain microglia gaining both microglial morphology and functionality and eventually becoming indistinguishable from the established ramified microglia.

Monocyte descendants range from common macrophages to more specialised dendritic cells and microglia. The reason for their diverse differentiation potential is due to the constitution and milieu of their target organ, macrophages differentiate

within the majority of tissues, whereas dendritic cells are found only in tissues that contact the external environment and microglia only differentiate once a monocyte crosses the blood brain barrier and is within the CNS.

Much work has been carried out into the soluble or non-diffusable factors that play a role in microglial development. The focus of this work has been on the release of cytokines from surrounding astrocytes. The spotlight has fallen on M-CSF as a key cytokine in the maturation of microglia. It was shown by Liu et al. (1994) that obstructing the *c-fms* receptor with an antibody there was a complete inhibition of microglial ramification, which they corroborated by the use of Hebimycin A, a tyrosine kinase inhibitor, which blocked the *c-fms* cascade and thus cell ramification. Depletion of the CSF-1 receptor, the product of the *c-fms* gene, but not the loss of M-CSF lead to a decrease in almost 50% of microglia meaning that there must be an alternative ligand for CSF-1R in the brain (Greter et al. 2012). This was identified as IL-34 by Greter et al. (2012) and work by Ohgidani et al. (2014) showed that IL-34, which is released from neurons, in combination with GM-CSF was more successful at differentiating microglial-like cells from human peripheral blood cells than GM-CSF together with the original ligand, M-CSF.

Another key difference between monocytes and microglia is the presence of outwardly rectifying K<sup>+</sup> channels. Schilling et al. (2001) showed that TGF $\beta$  signaling was required for the increase in these channels which, along with M-CSF, is released from astrocytes. The proliferation of microglia is also under the control of astrocytes. It was found that soluble GM-CSF results in the formation of a rod shaped cell, which is indicative of proliferation (Suzumura et al. 1991).

Microglial differentiation from hESCs proves to be problematic and, as of yet, remains unaccomplished. More publications have, however, been made regarding the successful differentiation of human microglia from their primary haematopoietic precursor cells. Microglia were successfully differentiated from human primary monocytes by Etemad et al. (2012) by culture in the presence of MCSF, GMCSF, NGF and CCL2 for 14 days, many of which are soluble factors released from astrocytes *in vivo*. The resultant cells were comparable to those of the HMC3 microglial cell line based on expression of surface markers, phagocytic ability and antigen presentation.

The reason for the differentiation observed by Djukic et al. (2006) could be explained by the work of Sievers et al. (1994), where monocytes from the spleen and liver were cultured both in the presence of astrocytes and in astrocyte conditioned media. They found that culturing monocytes on an astrocyte monolayer produced a ramified microglial cell. The same result was achieved in cells only exposed to astrocyte conditioned medium, which suggests that astrocytes orchestrate differentiation through the secretion of diffusible factors, most importantly M-CSF, GM-CSF and TGF- $\beta$ , into their surroundings leading to monocyte to microglial differentiation both *in vitro* and *in vivo* within the brain (Sievers et al. 1994). As such this is a route that can be exploited for *in vitro* differentiation of monocytes to microglial-like cells.

## 5.2 AIM

The previous chapters aimed to produce hES- derived monocytes for their ultimate differentiation to microglial-like cells. As described, the overexpression of PU.1, although still a possible route to monocyte differentiation, is not as well developed, nor as productive for monocyte production as the MCSF/IL-3 directed differentiation protocol described in chapter 4. Further work is required to increase the reproducibility and yield of monocytic cells using the PU.1 overexpression method. As such the monocyte to microglial-like cell differentiation in this chapter will utilise hES-derived monocytes (ESdM) from chapter 4.

Work in this chapter tested the hypothesis that astrocyte conditioned medium or astrocyte co-culture would progress the differentiation of ESdMs derived from the MCSF/IL-3 directed differentiation protocol to microglial-like cells, characterised by a combination of marker expression (IBA-1, Glut5 and CD45) and electrophysiological properties that distinguish between macrophages and microglia. Figure 5.1 summarises the differentiation strategy.

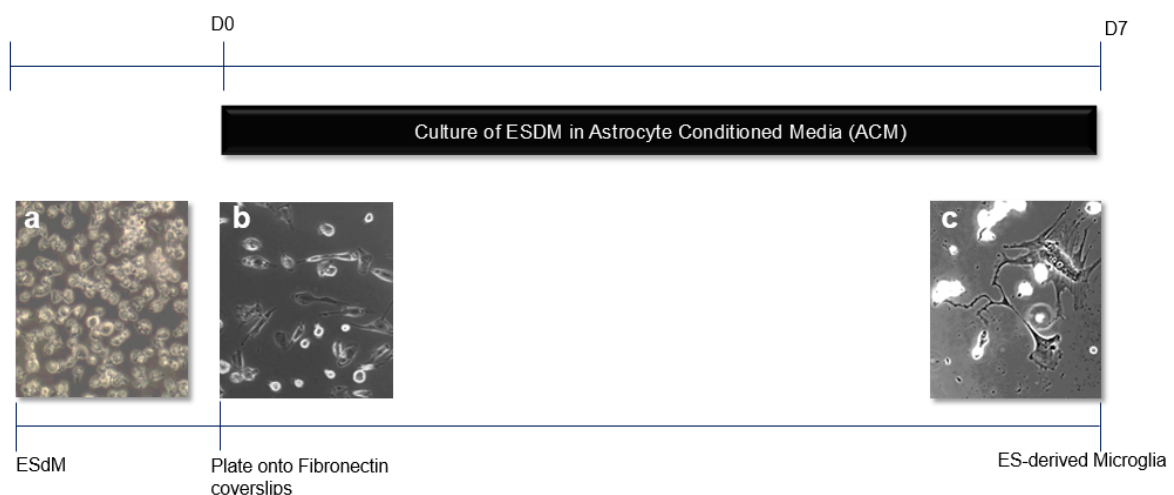


**Figure 5.1. Schematic Representation of the Differentiation Protocol**

ESdM (a) from the XVIVO factories (Chapter 4) were plated onto fibronectin coated coverslips (b) and cultured for seven days in medium conditioned by astrocytes, where they differentiate into microglia of the ramified morphology (c).

### 5.3 MONOCYTE DIFFERENTIATION TO MICROGLIAL-LIKE CELLS

---

Since brain microglia are thought to differentiate from bone marrow derived monocytes in response to signals from astrocytes (Sievers et al., 1994) we investigated the responses of ESdMs and control THP1 cells to astrocyte conditioned medium (ACM).

THP-1 cells and ESdMs were grown in fibronectin coated plates and transferred from monocyte maintenance medium to a DMEM/F12/Neurobrew21 base medium (See *Section 2.1.1*) that is routinely used for neural and astroglial cell culture, with or without conditioning from primary mouse astrocytes. After 7 days a dramatic difference in the appearance of cells cultured in ACM compared to those cultured in control medium was observed. Treatment with ACM transformed both the THP1 and ESdM monocytes to display a ramified morphology with elongated processes. Furthermore, ACM induced expression of the microglial marker IBA-1, phenotypes that were not observed in cells cultured for the same period in unconditioned control medium (Figure 5.2 A - H). Upon quantification of the IBA-1+ cells, it was shown that 88.9% of ESdMs cultured in ACM were IBA-1+ compared to just 22% in the unconditioned media. Similarly 80% of the THP-1 monocytes were IBA-1+ when cultured in ACM, whilst only 25.7% were positive for IBA-1 in the unconditioned media control.

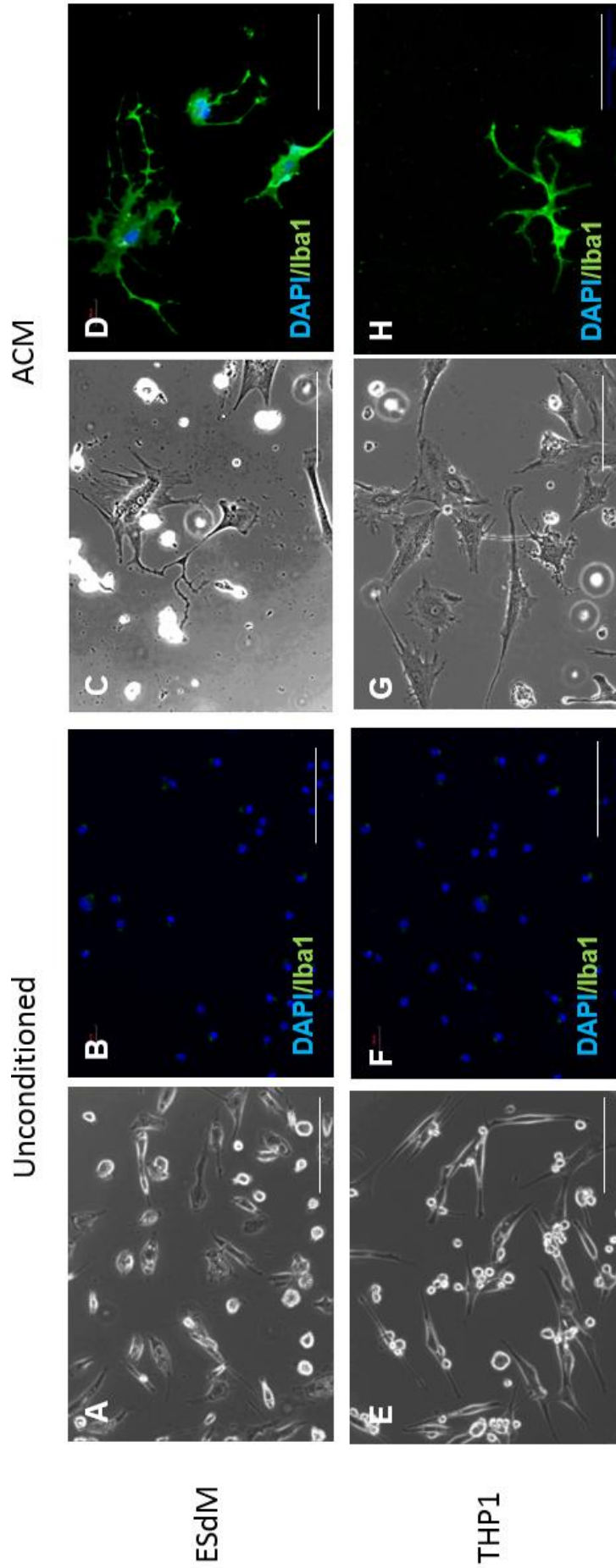


**Figure 5.2. Morphological changes of monocytes and induction of IBA-1 in response to Astrocyte Conditioned Medium**

ESdMs and THP1 cells cultured in either unconditioned medium or ACM for 7 days (A-B and C-D respectively). When cultured in ACM the cells possess microglial morphology (Phase Contrast Image C) and are positive for the microglial marker IBA-1 (D). In unconditioned medium the cells are not of a ramified morphology (Phase Contrast Image A) and show low levels of staining for IBA-1 (B). The same pattern of expression and morphology is observed in THP-1 monocytes when cultured in ACM (G and H) compared to those cultured in unconditioned medium (E and F).

Scale bars represent 100µm

It was also observed that ACM provided an apparent selection for the IBA-1+/ramified cells. Compared to the number of cells plated, approximately 17% were present at day 7 post-plating in ACM, compared to approximately 80% in unconditioned medium. It is interesting to note that the percentage survival is similar to the percentage of CD11b+ cells that were originally present within the ESdM population derived from the MCSF/IL-3 directed differentiation protocol (Figure 5.3).

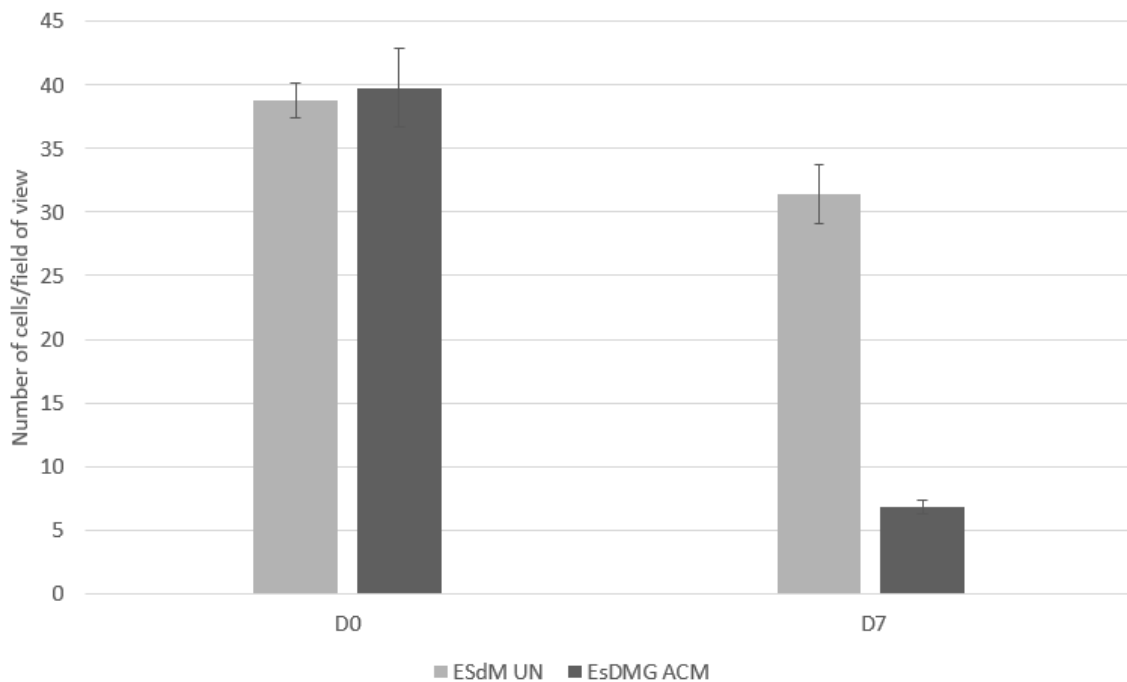


**Figure 5.3. Culture with ACM Leads to a Decrease in Cell Number in the ESdM Population**

When cultured in unconditioned media, there was maintenance of ~80% of the plated cells by day 7, none of which were IBA-1+. Conversely culturing in ACM led to a reduction in cell number, to around 17% of the starting cell number.

The loss of cells on culturing with ACM and the apparent selection for CD11b+ cells that differentiated into IBA-1+ ramified microglial-like cells led to the hypothesis that the ramified cells stopped proliferating and thus ACM promoted terminal differentiation of the cells. Evidence suggests that in order to proliferate ramified microglia must re-activate to the amoeboid form, and that such activation can be achieved by stimulation with GM-CSF (Zielasek and Hartung 1996). Immunocytochemistry for Ki67, a marker of the active phases of the cell cycle and so proliferation, was carried out on EsdM cultured in ACM for 7 days supplemented with either 5µg or 50µg GM-CSF and compared to the unstimulated cells (Figure 5.4). It was found that in the unstimulated cells, only 3% of the IBA-1+ cells stained for Ki67 (Figure 5.4 A). Upon stimulation with 5µg GM-CSF there was staining within the nuclei of the 69% of the IBA-1+ cells, and some were seen to be in the process of mitosis (Figure 5.4 B). Stimulation with 50µg GM-CSF also resulted in Ki67+/IBA-1+ cells, but less frequently with only 18% of the total number of cells staining positively for both markers (Figure 5.4 C).

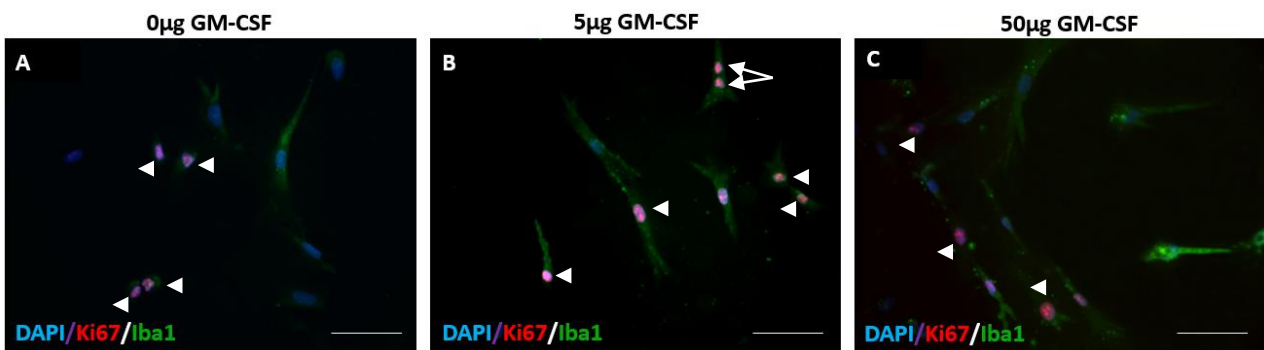


**Figure 5.4. GM-CSF promotes proliferation in ESdM Cultured in ACM**

(A) Unstimulated, IBA-1+, cells lacked nuclear Ki67 staining, whilst (B) stimulation with 5µg GM-CSF led to the re-entry of the IBA-1+ cells to the cell cycle and the presence of Ki67. (C) Addition of 50µg GM-CSF led Ki67 staining within the nuclei of the IBA-1+ cells. Arrow heads indicate Ki67+ cells, Arrows indicate mitotic cells.

Scale Bars represent 100µm

Since IBA-1 can be expressed in both microglia and activated macrophages, the resultant cells from the ACM and control cultures were also stained at day 7 for CD45 and Glut5. CD45 is a marker of leukocytes, it is highly expressed in monocytes and macrophages but is only expressed at very low levels in microglia with the ramified phenotype (Sedgwick et al. 1991). Glut5 is a highly selective marker for microglia and can be used to discriminate against even perivascular macrophages (Kettenmann et al. 2011). Thus ramified microglia can be defined as CD45<sup>low</sup>/Glut5<sup>+</sup>. Use of CD45 and Glut5 confirmed the microglial-like phenotype of the IBA-1<sup>+</sup> cells induced by treatment with ACM (Figure 5.5). After treatment with ACM both ESdM and control THP1 cells showed robust Glut5 staining (88.5% and 88.9% of total cells, respectively), with only 32.5% of EsdMs and 37% of THP-1 monocytes positive for CD45 (Figure 5.5 A - D). This contrasted with the reciprocal pattern of high CD45 and low Glut5 staining seen in cells cultured in unconditioned medium (Figure 5.5 E - H). In detail, unconditioned media resulted in 13.6% of EsdMs and 8.3% of THP-1 monocytes staining for Glut5, whilst 95.3% of EsdMs and 90.5% of THP-1 monocytes were positive for CD45. The staining also illustrates the morphological changes associated with ACM culture. In unconditioned medium the membrane staining of CD45 shows that both ESdM and THP1 cells are, without exception, round with low complexity. Whereas Glut5 staining in ACM treated cultures shows more complex cell morphologies that are elongated with process formation, typical of microglia.

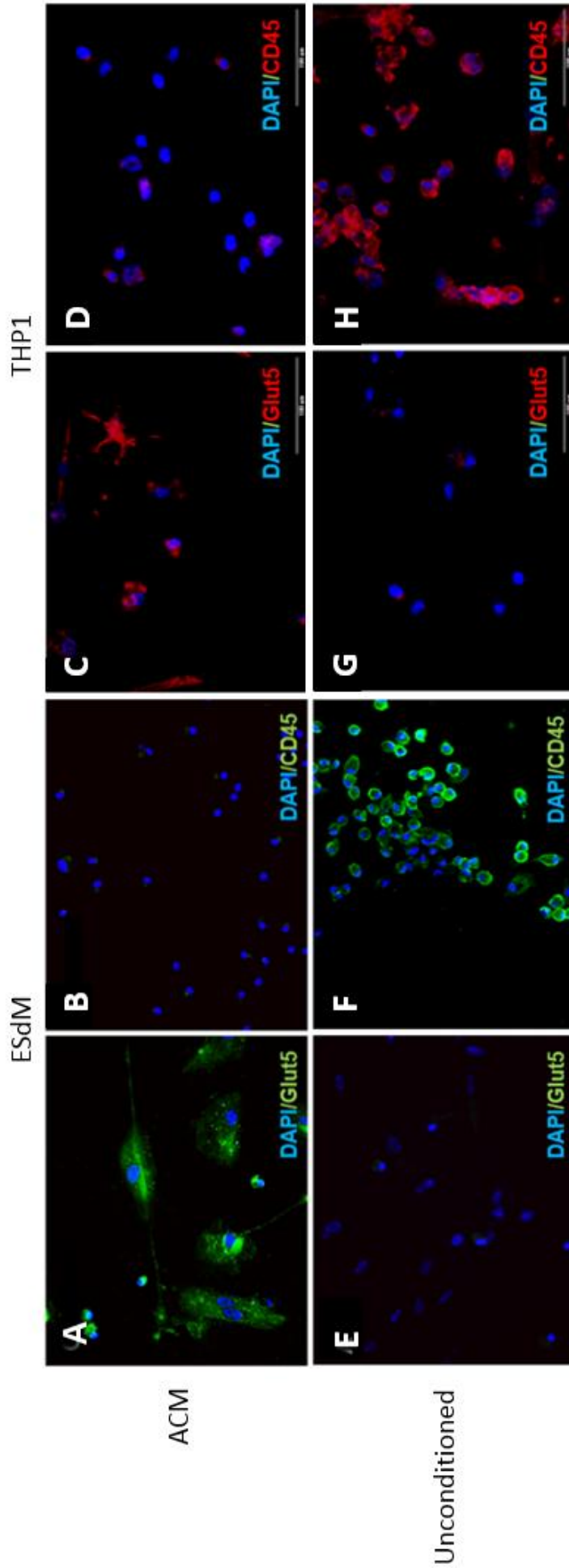


**Figure 5.5. Marker Expression of Monocytic Cells in ACM vs. Unconditioned Media**

(A) ESdM stained positively for Glut5 after culturing for 7 days in ACM. (B) In ACM there was little staining evident for CD45 after 7 days. (C) THP1 monocytes cultured in ACM for 7 days and stained positively for Glut5. (D) After 7 days in ACM THP1 stained only marginally for CD45. (E) When cultured in unconditioned media for 7 days there was no staining for GLUT5 in the ESdM cells. (F) Conversely there was positive staining for CD45 in ESdM cells maintained in unconditioned medium. (G) THP1 cells in unconditioned medium showed little staining for GLUT5. (H) The monocytic nature of THP1 cells was maintained and evident through the large proportion of CD45+ cells when cultured in unconditioned medium for 7 days.

Scale bars represent 100µm

The microglial-like cells generated from culture in ACM were also analysed by QRT-PCR for the expression of microglial genes, with gene expression levels compared to those in unconditioned media and relative to those present in THP-1 monocytes (Figure 5.6 A and B). ANOVA was used to compare the gene expression of cells cultured in ACM for 7 days to those cultured in the unconditioned media and it showed a significant difference for both the control cell line, THP1 monocytes, [ $F(1,12)=1203$ ,  $p<0.0001$ ] and for the EsdM [ $F(1,12)=60.71$ ,  $p<0.0001$ ].

Bonferroni's multiple comparison test for THP1 monocytes in ACM compared to those in unconditioned media showed that there was no significant change in the levels of CD45 or IBA-1 although the trend implied that CD45 expression had decreased in ACM culture and IBA-1 expression had increased. There was also no significant difference in the expression of TREM-2 or CD11c between the culture conditions. Surprisingly there was deemed to be no significant decrease in the expression of the monocyte specific marker NG2 upon culture in ACM (THP1(M=1.337, SD=0.371), THP1MG (M=49.86, SD=0.0001)). As expected the microglial specific marker CD80 was increased upon culture in ACM (THP1 (M=0.9323, SD=0.091), THP1MG (M=49.86, SD=2.2410)).

When the same comparison was carried out to compare EsdM cultured in ACM to those cultured in unconditioned media it showed that there was a similar, insignificant, trend for decreased CD45 and increased IBA-1. Here there was, as expected, a significant decrease in the levels of the monocyte marker NG2 when cells were cultured in ACM (EsdM (M=32.68, SD=1.218), EsdMG (M=0.7646, SD=0.093)). This corresponded with an increase in CD80 expression post culture in ACM (EsdM (M=0.1785, SD=0.099), EsdMG (M=29.00, SD=4.880)). CD11c is expressed on both monocytes and microglia, with the greatest expression observed

in the latter. After 7 days in ACM there was an increase in CD11c expression (EsdM (M=0.06338, SD=0.056), EsdMG (M=8.352, SD=0.049)). TREM2, being a myeloid receptor, is apparent on all myeloid cells but in this case culture in ACM caused a large increase in expression of over 42-fold (EsdM (M=16.82, SD=0.977), EsdMG (M=59.04, SD=9.026)).

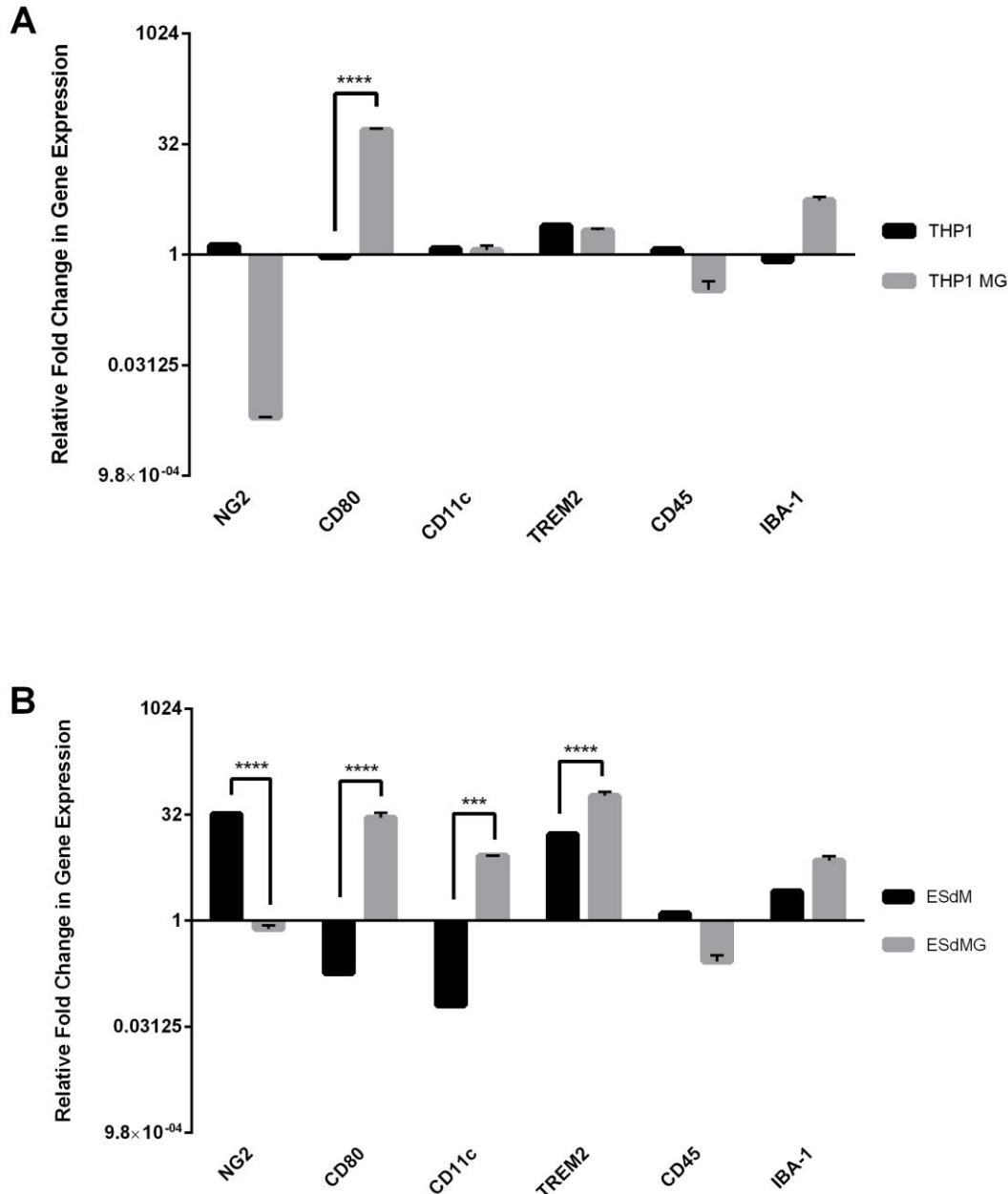


**Figure 5.6. Expression of Microglia Specific Genes**

(A) THP1 cells were cultured for seven days in either astrocyte conditioned medium (THP1MG) or unconditioned base medium (THP1). The microglial gene CD80 was shown to be significantly increased upon culture in ACM (THP1 (M=0.9323, SD=0.091), THP1MG (M=49.86, SD=2.241)). The changes in expression for the other measured genes did not show a significant difference between culture media. The trend did indicate that there was a decrease in monocytic genes (NG2 and CD45).

(B) EsDM cells were also cultured for seven days in either astrocyte conditioned medium (EsdMG) or unconditioned base media (EsdM). There was a significant decrease in NG2 expression upon ACM culture (EsdM (M=32.68, SD=1.218), EsDMG (M=0.7646, SD=0.093)), and an increase in CD80 (EsdM (M=0.1785, SD=0.099), EsDMG (M=29.00, SD=4.880)), CD11c (EsdM (M=0.06338, SD=0.056), EsDMG (M=8.352, SD=0.049)) and TREM2 (EsdM (M=16.82, SD=0.977), EsDMG (M=59.04, SD=9.026)) expression.

QPCR data is normalised to  $\beta$ -Actin with data obtained from 3 technical replicates of 3 biological replicates

Asterisks denote statistical significance; \*  $\leq 0.05$ , \*\*  $\leq 0.01$ , \*\*\*  $\leq 0.001$ , \*\*\*\*  $\leq 0.0001$

#### 5.4 ELECTROPHYSIOLOGICAL PROFILE OF ES-DERIVED MICROGLIAL-LIKE CELLS

---

Previous work has determined that microglia express a distinctive profile of electrophysiological activity (Kettenmann et al. 1993; Kettenmann et al. 2011). The most characteristic and distinctive channel possessed by microglia is an inwardly rectifying  $K^+$  channel, which is not present in any other myeloid lineage cell (Kettenmann et al. 1993). The presence and activity of the  $K_{ir}$  channel can be induced in monocytes and macrophages by co-culture with astrocytes and astrocytic factors released into conditioned medium (Schmidtmayer et al. 1994). Attachment of microglia to a substratum also induces a change in the ion channel profile, with the appearance of voltage gated  $K^+$  channels (McLarnon et al. 1997). The presence of a voltage-gated sodium channel is also expected, this is suggested to be due to the expression of NaV1.5 or NaV1.6 channels (Black and Waxman 2012).

$Na^+$  and  $K^+$  channel expression was investigated using whole-cell patch clamp electrophysiology (Figure 5.7). By utilising a voltage step protocol from -170mV to +60mV after clamping at -70mV and using whole cell patch clamps to record the data, the family of currents generated show the presence of large inward currents with the addition of some outward or voltage gated events (Figure 5.7B).

When these data were investigated via mean current density versus voltage plots, there was evidence to suggest that the majority of cells possessed inwardly rectifying  $K^+$  channels, confirmed by the reversal potential of around -80mV (Figure 5.7C). The lack of plateau subsequent to this, expected if only  $K_{ir}$  channels were present, would suggest that there was also the presence of voltage-gated  $K^+$  channels in the EsdMG when attached to coverslips with fibronectin and cultured in ACM. As

mentioned, attachment to a substrate has been shown to induce the activity of  $K_v$  channels (McLarnon et al. 1997).

$Na_v$  channels are also thought to be present in microglia, and are to be linked to the activation state of the cell. Of the cells investigated, around 50%, showed a mean-current density versus voltage plot that resembled that of voltage-gated sodium channels (Figure 5.7 D). The reversal potential in this case was around +20mV, although large error bars were present, possibly due to a highly variable intracellular sodium concentration between the tested cells.

The membrane capacitance of cells is relative to the cell surface area and thus size of the cell. Microglia are thought to have smaller membrane capacitance than neurons but a similar capacitance to macrophages. The capacitance of the EsdMG subsequent to culture in ACM for 7 days (Table 5.1) was, on average,  $34.34 \pm 2.48$  pF ( $n=14$ ), an expected value for microglial cells. If we assume  $1\mu\text{F}/\text{cm}^2$ , this means that the average area under the patch clamp was  $3434.26 \pm 247.94\mu\text{m}^2$ .

**Table 5.1 EsDMG Membrane Capacitance Values**

The membrane capacitance of the ESdMG was on average  $34.34 \pm 2.48$  pF. Assuming  $1\mu\text{F}/\text{cm}^2$ , the average area under patch clamp was  $3434.46 \pm 247.94\mu\text{m}^2$ .

<i>Membrane Capacitance (pF)</i>							
	Cell1	Cell 2	Cell 3	Cell 4	Cell 5	Average	SEM
Rep 1	31.37	40.16	58.47	34.31	-	41.08	6.078
Rep 2	30.45	20.25	25.55	36.91	-	28.29	3.549
Rep 3	24.69	35.65	37.87	34.8	36	33.8	2.618
Av. Capacitance (pF)						34.34	2.48
Av. Area ( $\mu\text{m}^2$ )						3434.46	247.94

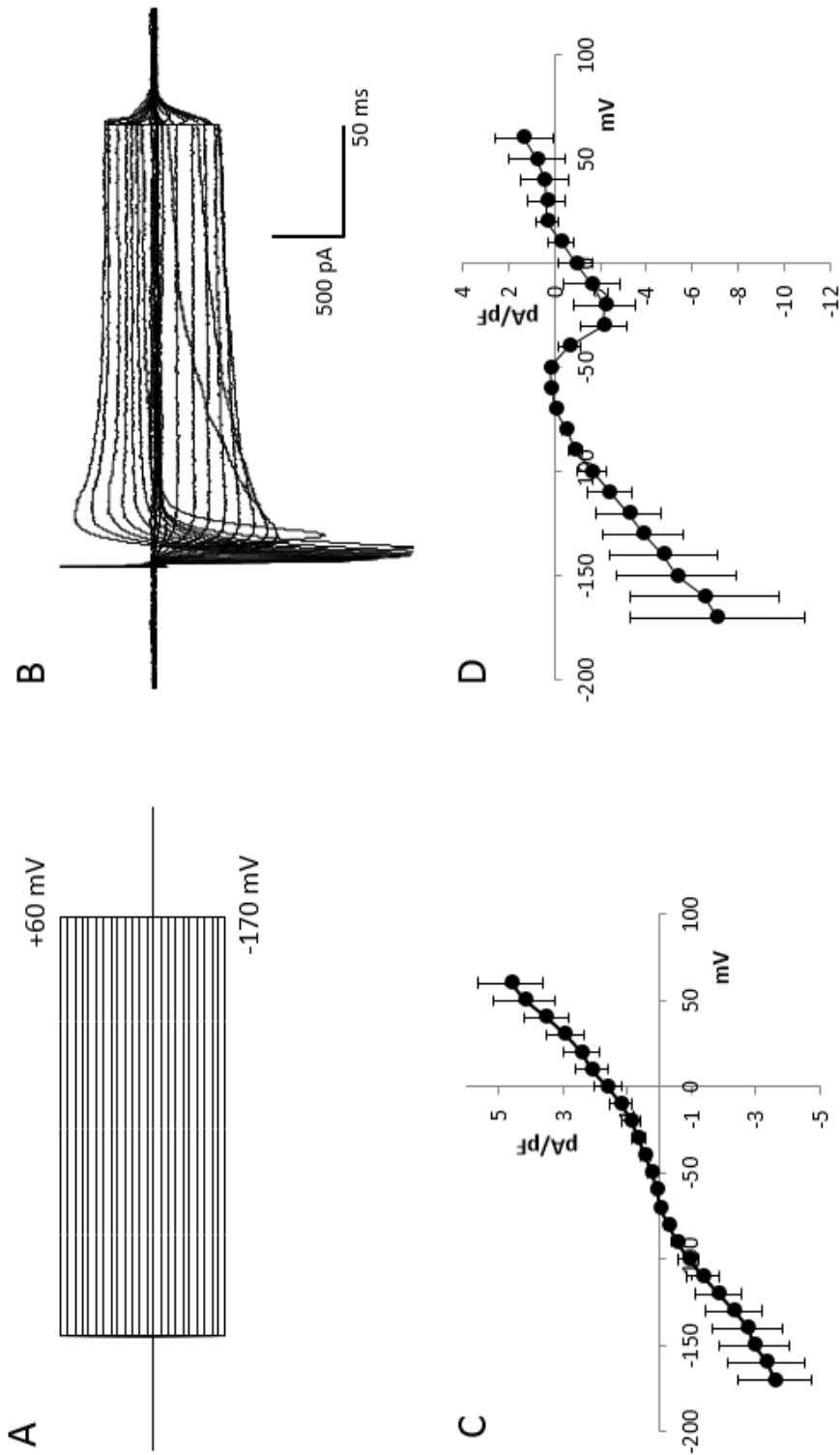


**Figure 5.7. Electrophysiological properties of ES-derived Microglia**

(A) Voltage step protocol used for all whole cell patch clamp recordings, cells were clamped at -170mV and stepped from -170mV to +60mV in 10mV increments. (B) Exemplar family of currents generated using the voltage step protocol showing large inward currents and several outward current events. (C) Mean current-density versus voltage plots for cells showing  $K^+$  channels ( $n=9$ ), the reversal potential at -80mV is suggestive of  $K_{ir}$  channels, whilst there is no plateau subsequent to the reversal potential, which suggests the presence of outward  $K_v$  channels. (D) Mean current-density versus voltage plots for cells with  $Na^+$  currents ( $n=4$ ), around half of the analysed cells showed typical  $Na^+$  currents with a reversal potential of +20mV.

To quantify the expression of selected ion channels, QRT-PCR was performed for Kir2.1, Nav1.5 and Nav1.6 and expression was compared in ACM and in the unconditioned base medium relative to THP1 monocytes (Figure 5.8). ANOVA showed that there was a significant difference in the means depending on culture media [ $F(3,24)=94.65$ ,  $p<0.0001$ ]. For THP1 monocytes, culture in ACM promoted the expression of both Kir2.1 (THP1 (M=0.1600, SD=0.053) THP1MG (M=2.770, SD=0.665)) and Nav1.6 (THP1 (M=0.2533, SD=0.029), THP1MG (M=1.983, SD=0.340)). Culture conditions seemed to not have an effect on the levels of Nav1.5, as there was no significant difference in expression.

The same was true of the EsDM, ACM culture lead to an increase in both Kir2.1 (EsDM (M=0.2267, SD=0.006), EsDMG (M=6.843, SD=0.930)) and Nav1.6 (EsDM (M=1.953, SD=0.741), EsDMG (M=4.320, SD =0.902)). Again culture in ACM had no effect on the expression of Nav1.5.

Kir2.1 channels are prevalent in microglia and is expressed less in monocytes and macrophages, and as such is a good marker for microglial functionality. Thus the increase in their expression after culture in ACM is indicative of the formation of microglial-like cells. Voltage gated Na<sup>+</sup> channels are also expressed in microglia, of the two most likely candidates found within the literature, Nav1.6 was most highly expressed in cells cultured in ACM for seven days, whilst Nav1.5 expression was illustrated to be down-regulated in all cells regardless of conditioning relative to the maintained THP1 monocytes and thus not responsible for the Nav-type traces witnessed by the electrophysiology.

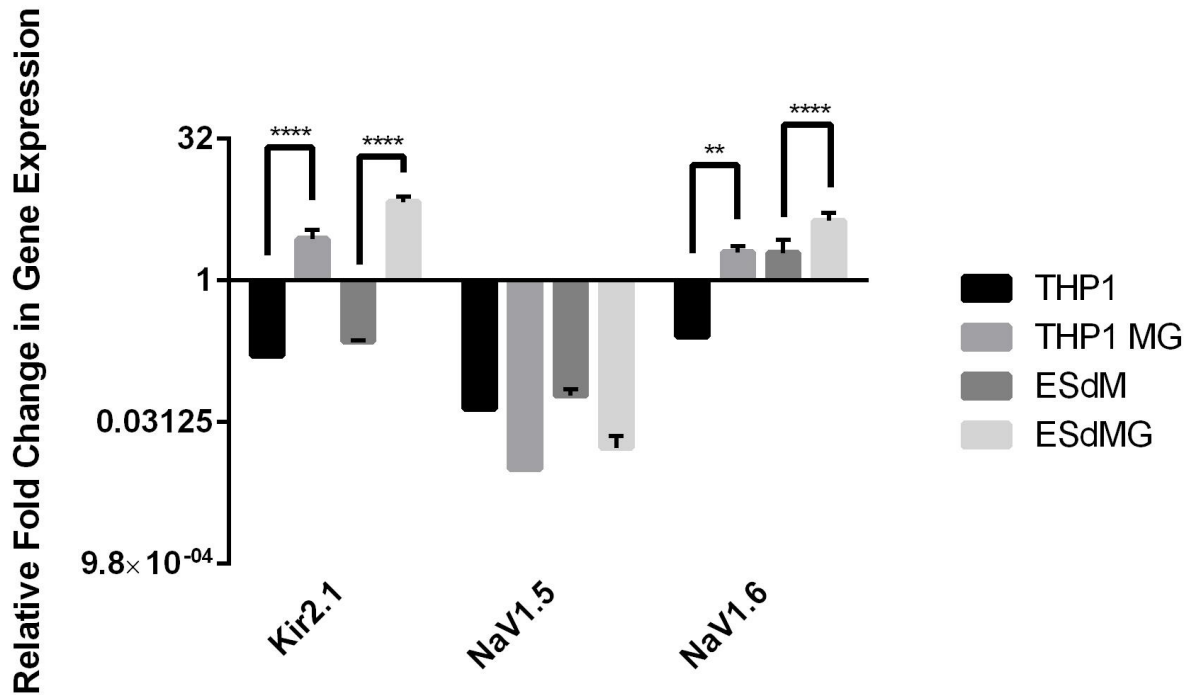


### Figure 5.8. Expression of Ion Channels in Microglia

ES derived monocytes (ESdM) and THP1 cells were cultured for seven days in either conditioned medium (-MG) or unconditioned medium. Kir2,1 is upregulated in both THP1MG and EsdMG after culture in ACM, similarly Nav1.6 is also increased after seven days in ACM. Nav1,5 remains constant, regardless of conditioning, and is downregulated relative to THP1 monocytes in maintenance media.

QPCR data is normalised to  $\beta$ -Actin with data obtained from 3 technical replicates of 3 biological replicates.

Asterisks denote statistical significance; \*  $\leq 0.05$ , \*\*  $\leq 0.01$ , \*\*\*  $\leq 0.001$ , \*\*\*\*  $\leq 0.0001$

### 5.5 FUNCTIONALITY OF ES-DERIVED MICROGLIAL-LIKE CELLS

---

To determine whether the microglial-like cells produced by culture of ESdMs in ACM were could be activated, cultures were incubated with amyloid  $A\beta_{(1-42)}$  or the reverse control peptide  $rA\beta_{(42-1)}$  for 120 minutes. The results were consistent with the hypothesis that ramified microglia on  $A\beta_{(1-42)}$  incubation would re-activate to the ameboid form and phagocytose the peptide (Figure 5.9 A-D). This was not seen to the same extent when incubated with the control. Although the cells do not become ameboid and are not activated there is staining for  $A\beta$  on the membrane of the cell. In the unconditioned control,  $A\beta$  staining is seen around the nucleus, which could indicate phagocytosis by the CD45+ cells that this culture produces. There is no such staining evident on the  $rA\beta$  treated cells. Preliminary sholl analysis of the ACM cultured cells (Figure 5.9 E) shows that ramified cells are around 200 $\mu$ m in length prior to  $A\beta$  treatment. Upon treatment of these cells with  $rA\beta_{(1-42)}$  has little effect on the cell length, but there is a trend for a decreased number of processes. Conversely treatment of ACM cultured cells with  $A\beta_{(1-42)}$  resulted in a dramatically reduced cell length, by 35%, due to the retraction of processes as the ramified quiescent cell is re-activated to the phagocytic ameboid form.

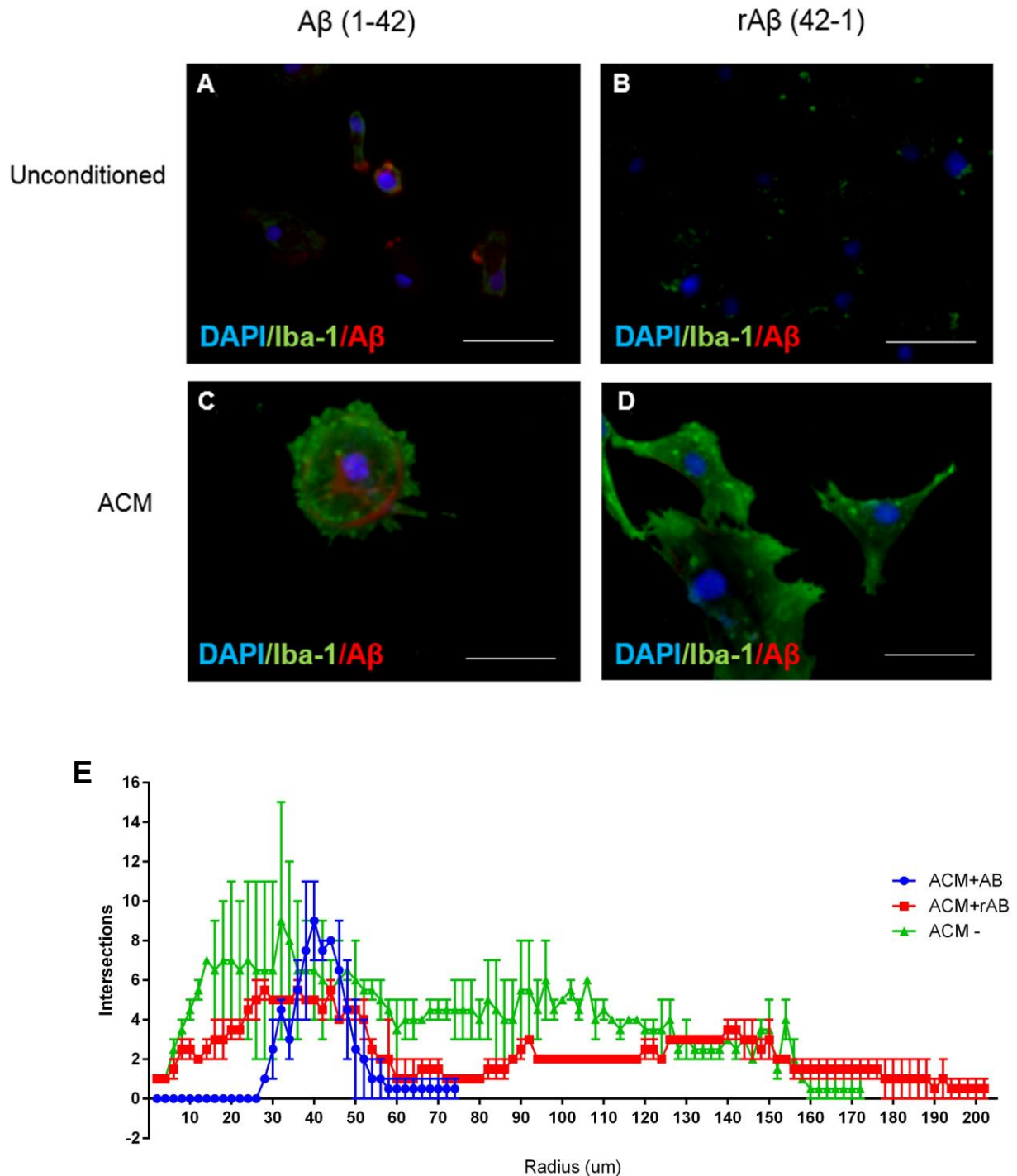


**Figure 5.9. Activation of ES-derived Microglia by Amyloid  $\beta$**

The ES-derived monocytes cultured in unconditioned medium and subjected to incubation with either  $A\beta_{(1-42)}$  (A) or the control peptide (B) remain IBA-1 negative, with no morphological changes. Monocytes cultured in ACM for 7 days and subjected to a 120 minute incubation with  $A\beta_{(1-42)}$  show IBA-1 positivity with a rounded, ameboid, phenotype and internalization of  $A\beta$  (C). When incubated with the control peptide, the cells remain IBA-1 positive but do not take on the ameboid form (D). Preliminary sholl analysis shows that treatment of ACM cultured cells with  $rA\beta_{(42-1)}$  makes little difference in the length of the microglial-like cells when compared to untreated cells ACM cultured cells (E). Incubation of ACM cultured cells with  $A\beta_{(1-42)}$  reduces cell length by over a third as processes retract (E).

Scale bars represent 50 $\mu$ m

The morphological changes witnessed through the immunocytochemistry, should be accompanied by changes in the expression and release of cytokines. To corroborate this, EsdMG and EsdM were collected post incubation with either  $A\beta_{(1-42)}$  or the control  $rA\beta_{(42-1)}$  and tested for changes in mRNA levels of cytokines through QRT-PCR relative to THP1 monocytes in maintenance media (Figure 5.10). ANOVA was used to compare the means, which showed a significant difference between them [ $F(3,12)=259.1$ ,  $p<0.0001$ ]. Bonferroni multiple comparison test showed that there was no significant difference in the expression of  $TNF\alpha$  regardless if cell type or  $A\beta_{(1-42)}$  addition.

IL-1 $\beta$  expression in EsdM treated with  $A\beta_{(1-42)}$  was increased compared to EsdMG treated with  $A\beta_{(1-42)}$  (EsdM (M=17.37, SD=1.556), EsdMG (M=9.268, SD=0.279)). IL-1 $\beta$  was decreased in EsdMG when treated with the reverse peptide  $rA\beta_{(42-1)}$  (EsdMG+A $\beta$  (M=9.268, SD=0.279), EsdMG+rA $\beta$  (M=1.368, SD=0.080)). IL-1 $\beta$  was similarly reduced in the EsdM when treated with the reverse peptide compared to treatment with  $A\beta_{(1-42)}$  (EsdM+A $\beta$  (M=17.37, SD=1.556), EsdM+rA $\beta$  (M=3.128, SD=0.490)). Comparing the effect of  $rA\beta_{(42-1)}$  on EsdMG and EsdM there was an increase in expression of IL-1 $\beta$  in EsdM +  $rA\beta_{(42-1)}$  (EsdMG+A $\beta$  (M=1.368, SD=0.080), EsdM+rA $\beta$  (M=3.128, SD=0.490)).

Between both the cell types, the EsdM monocytes show the greatest increases in cytokine levels when  $A\beta_{(1-42)}$ . There was a less pronounced effect on the levels of cytokines in EsdMG when treated with  $A\beta_{(1-42)}$ .

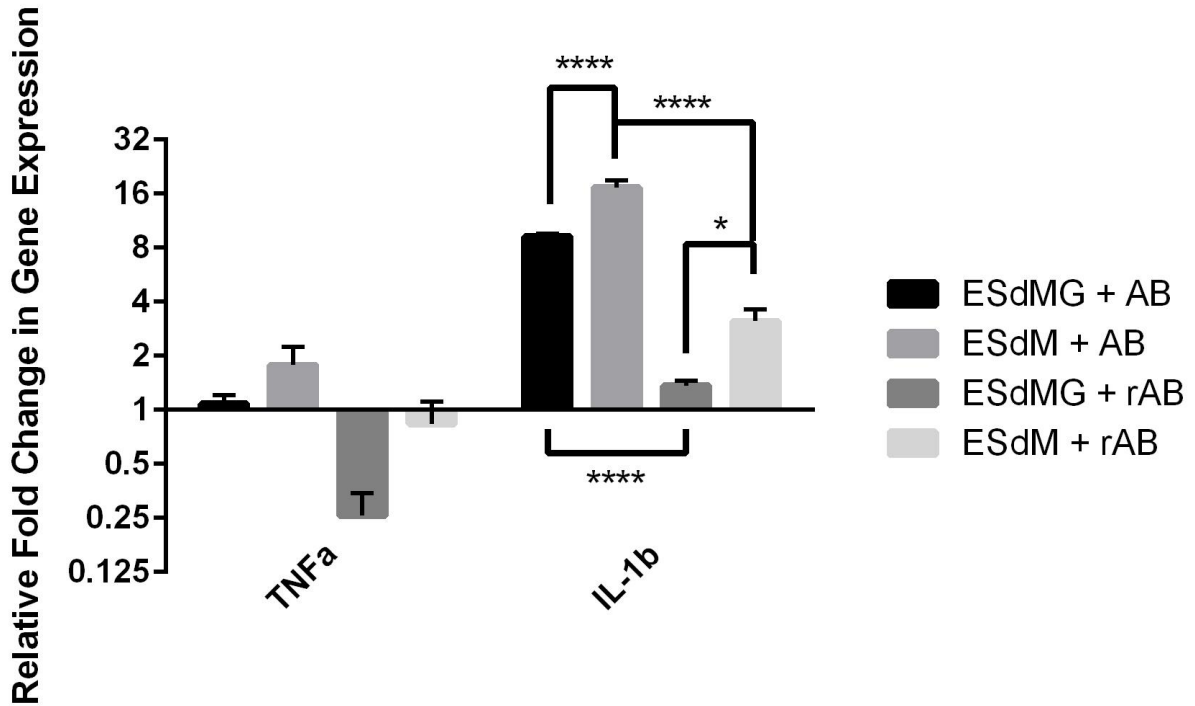


**Figure 5.10. Levels of Cytokine mRNA Post Incubation with A $\beta$**

ES derived microglia (ESdMG) or ES derived monocytes (ESdM) were incubated with either 5 $\mu$ g/ml AB<sub>(1-42)</sub> or an equal concentration of the control rAB<sub>(42-1)</sub>. There was no statistical difference in the expression of TNF $\alpha$  on addition of AB<sub>(1-42)</sub>. IL-1 $\beta$  was increased in EsdM+A $\beta$  compared to EsdMG+A $\beta$  (EsdM (M=17.37, SD=1.556), EsdMG (M=9.268, SD=0.279)). When treated with the reverse peptide both EsdMG and EsdM were decreased compared to the AB<sub>(1-42)</sub> treated cells. The effect of treatment with rAB<sub>(42-1)</sub> on the cells resulted in the decreased IL-1 $\beta$ , but of the two cell types the greatest expression was observed in the EsdM monocytes.

QPCR data is normalised to  $\beta$ -Actin with data obtained from 3 technical replicates of 3 biological replicates

Asterisks denote statistical significance; \*  $\leq 0.05$ , \*\*  $\leq 0.01$ , \*\*\*  $\leq 0.001$ , \*\*\*\*  $\leq 0.0001$

The cytokine release from the cells was also assayed by collecting the supernatant post incubation with both  $A\beta_{(1-42)}$  and the control,  $rA\beta_{(42-1)}$ , and analysing through immunoblotting techniques (Figures 5.11-5.14).

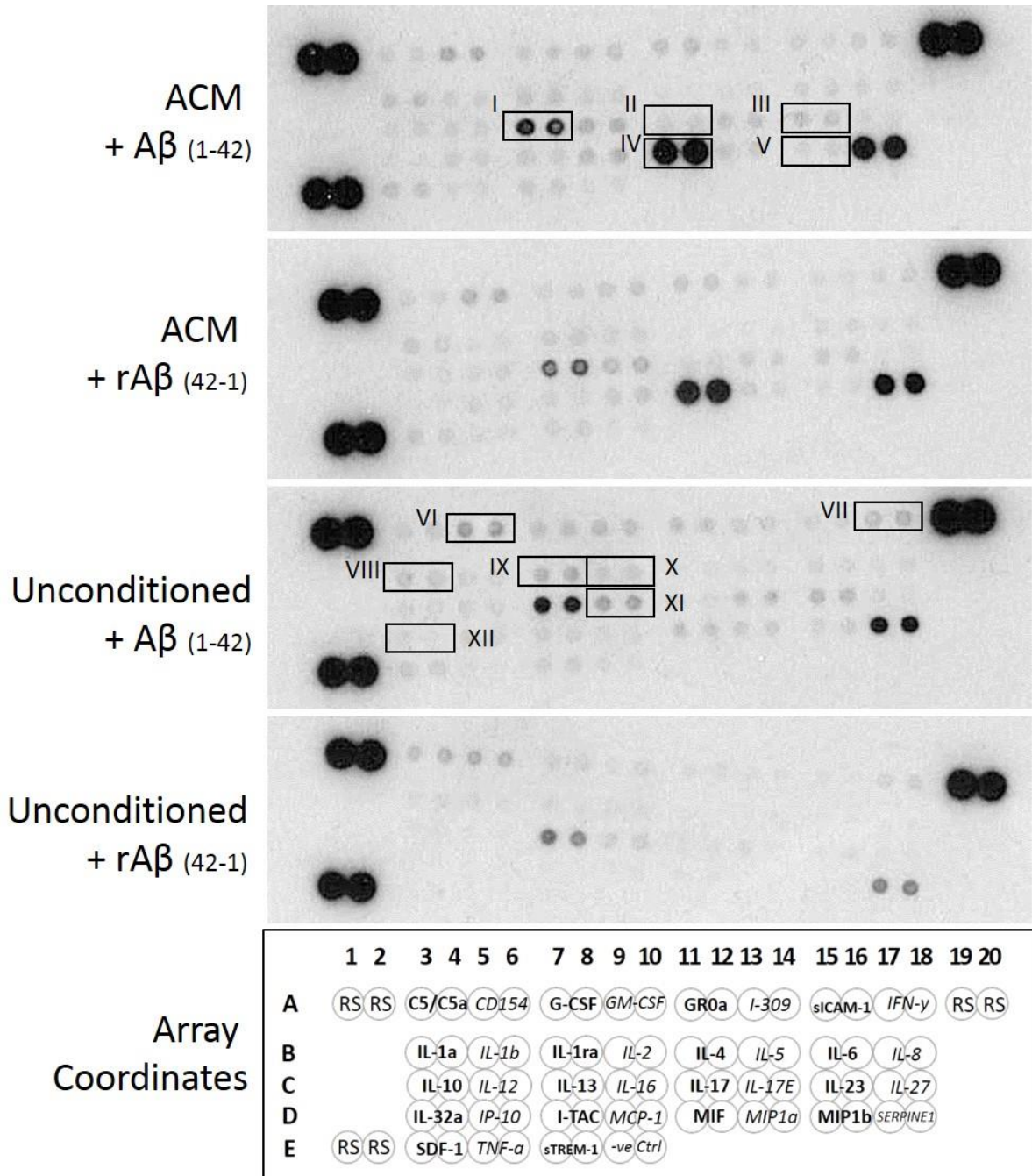


**Figure 5.11. Cytokine Secretion post AB Incubation**

The dot blot was carried out for ESdMG in ACM or ESdM in unconditioned media. All cells were treated with either  $A\beta_{(1-42)}$  or  $rA\beta_{(42-1)}$ . Major differences are highlighted by white rectangles; IL-13 (I), IL-17 (II), IL-27 (III), MIF (IV) and SERPINE1 (V) in cells cultured with ACM on addition of  $A\beta$  and CD154 (VI), IFN- $\gamma$  (VII), IL-1 $\alpha$  (VIII), IL-1ra (IX), IL-2 (X), IL-16 (XI), and IL-32a (XII) in cells cultured in unconditioned media with the addition of  $A\beta$ .

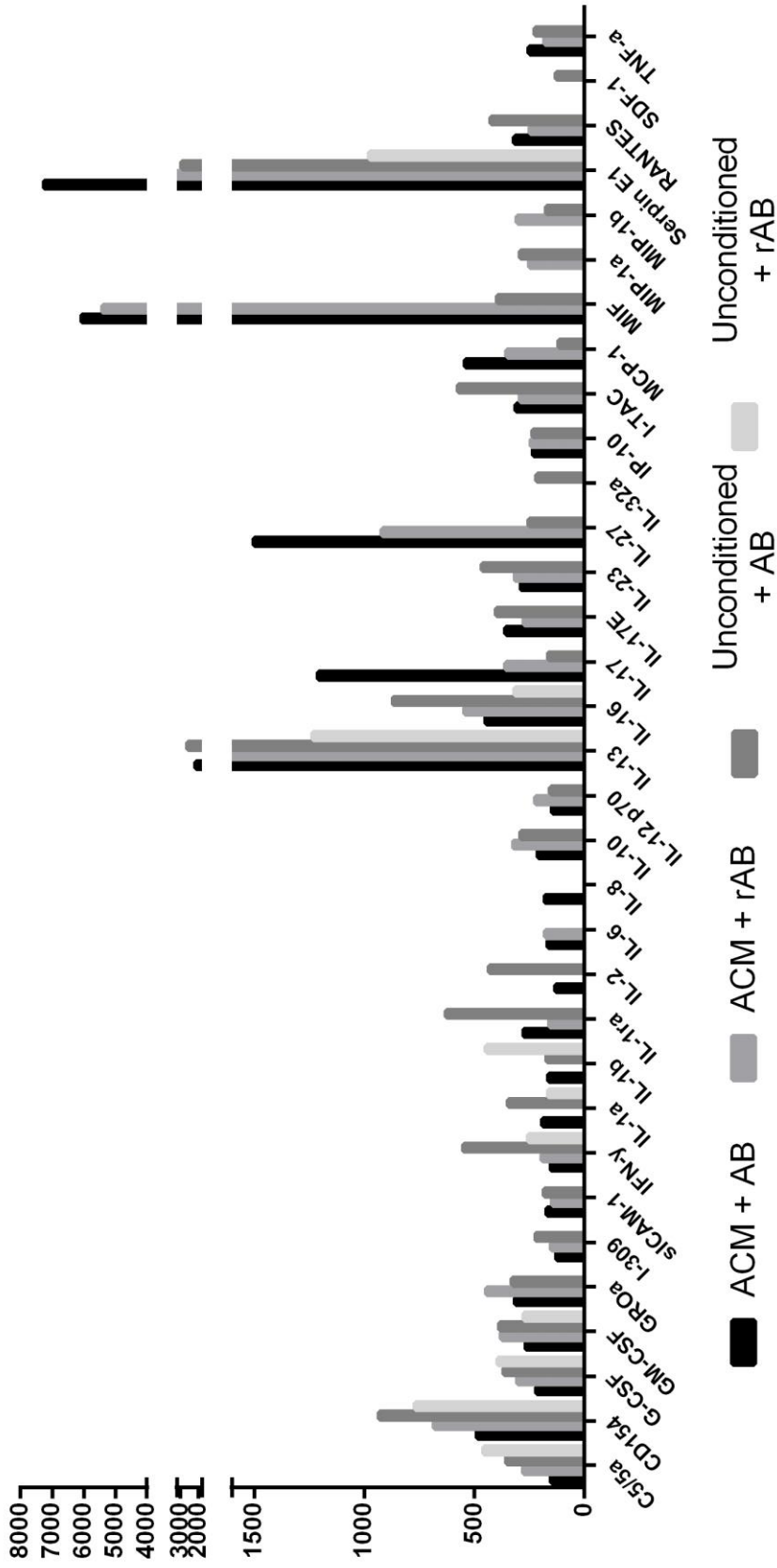


**Figure 5.12. Cytokine Secretion post AB Incubation**

The dot blot was carried out for ESdMG in ACM or ESdM in unconditioned media. All cells were treated with either  $A\beta_{(1-42)}$  or  $rA\beta_{(42-1)}$ . It showed increased IL-13, -17 and -27 (anti-inflammatory cytokines) in ESdMG in ACM treated with  $A\beta_{(1-42)}$ . Pro-inflammatory cytokines (IL-1ra, -2, -16 and -23) where shown to be increased in ESdM in unconditioned medium when treated with  $A\beta_{(1-42)}$ .

The cytokine array (Figure 5.11/5.12) showed that when ESdMG in ACM are incubated with  $A\beta_{(1-42)}$ , there was an increase in the levels of MIF and SERPIN E1 along with increases in the levels of several interleukins; IL-13, IL-17 and IL-27. When EsdM, cultured in the unconditioned base media, were treated with  $A\beta_{(1-42)}$  there was an increase in the levels of CD154, IFN- $\gamma$ , IL-1 $\alpha$  along with IL-1 $\alpha$ , IL-2, IL-16 and IL-32 $\alpha$ . This shows that the EsdMG were behaving in a anti-inflammatory manner, whilst the EsdM, being monocytic, were pro-inflammatory.

The chemokine array (Figure 5.13/5.14) showed that post incubation with  $A\beta_{(1-42)}$ , there was an increase in the levels of secreted CCL21 and CCL19 in EsdMG cultured in ACM. There was also an increase in CXCL4 levels along with an increase in IL-8 secretion seen in these cells. Secretion of CXCL5 and IL-16 was increased in those cells cultured in unconditioned medium and incubated with  $A\beta$ . Again suggesting an anti-inflammatory nature in the EsdMG and a pro-inflammatory nature in the EsdM monocytes.

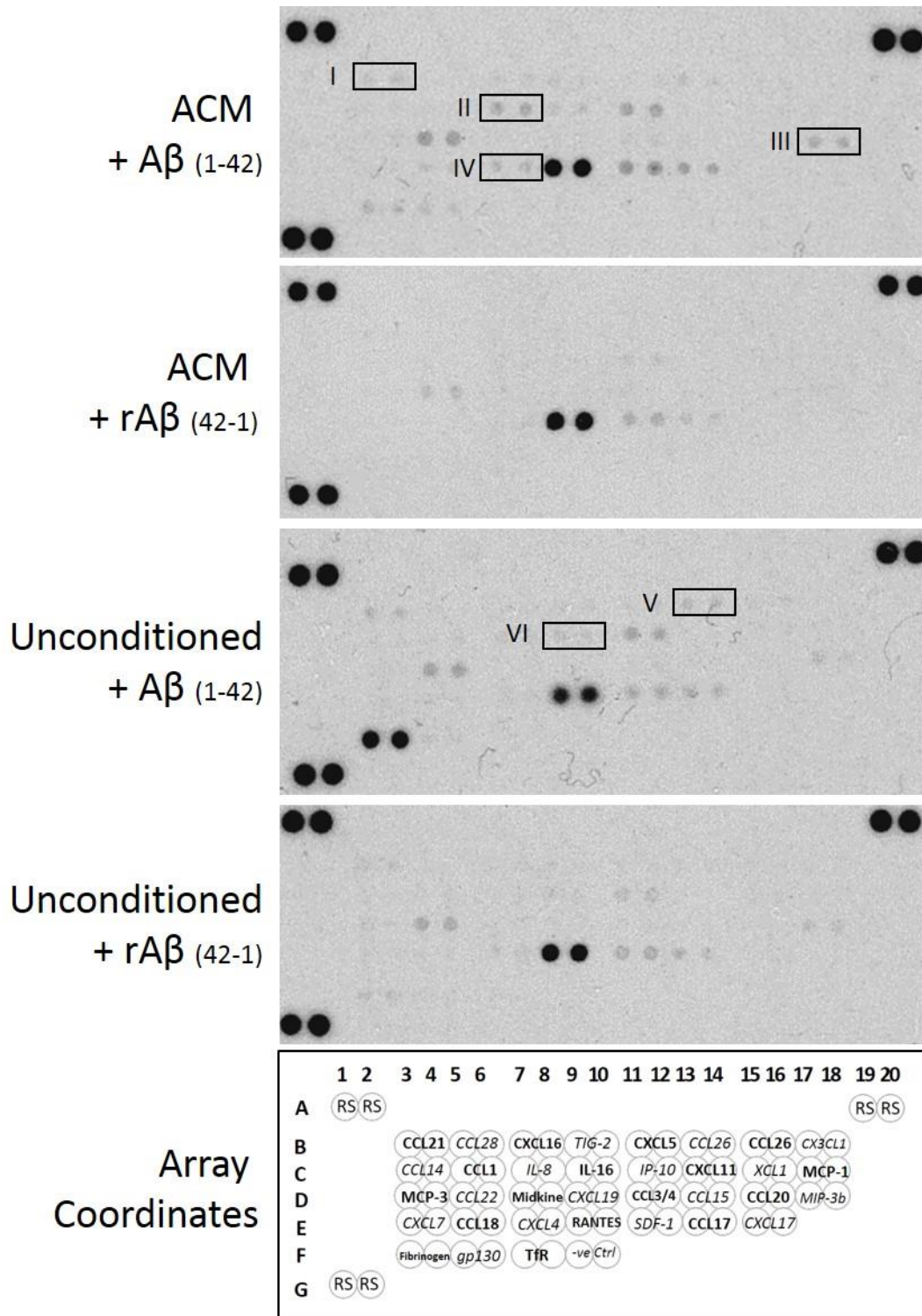


**Figure 5.13. Chemokine Secretion post AB Incubation**

The dot blot was carried out for ESdMG in ACM or ESdM in unconditioned media. All cells were treated with either A $\beta$ <sub>(1-42)</sub> or rA $\beta$ <sub>(42-1)</sub>. Major differences are highlighted by the black rectangles; CCL21(I), IL-8 (II), CCL19 (II), CXCL4 (IV) in cells cultured with ACM and on the addition of A $\beta$  and CCL26 (V), IL-16 (VI) in cells cultured in unconditioned media upon the addition of A $\beta$ .

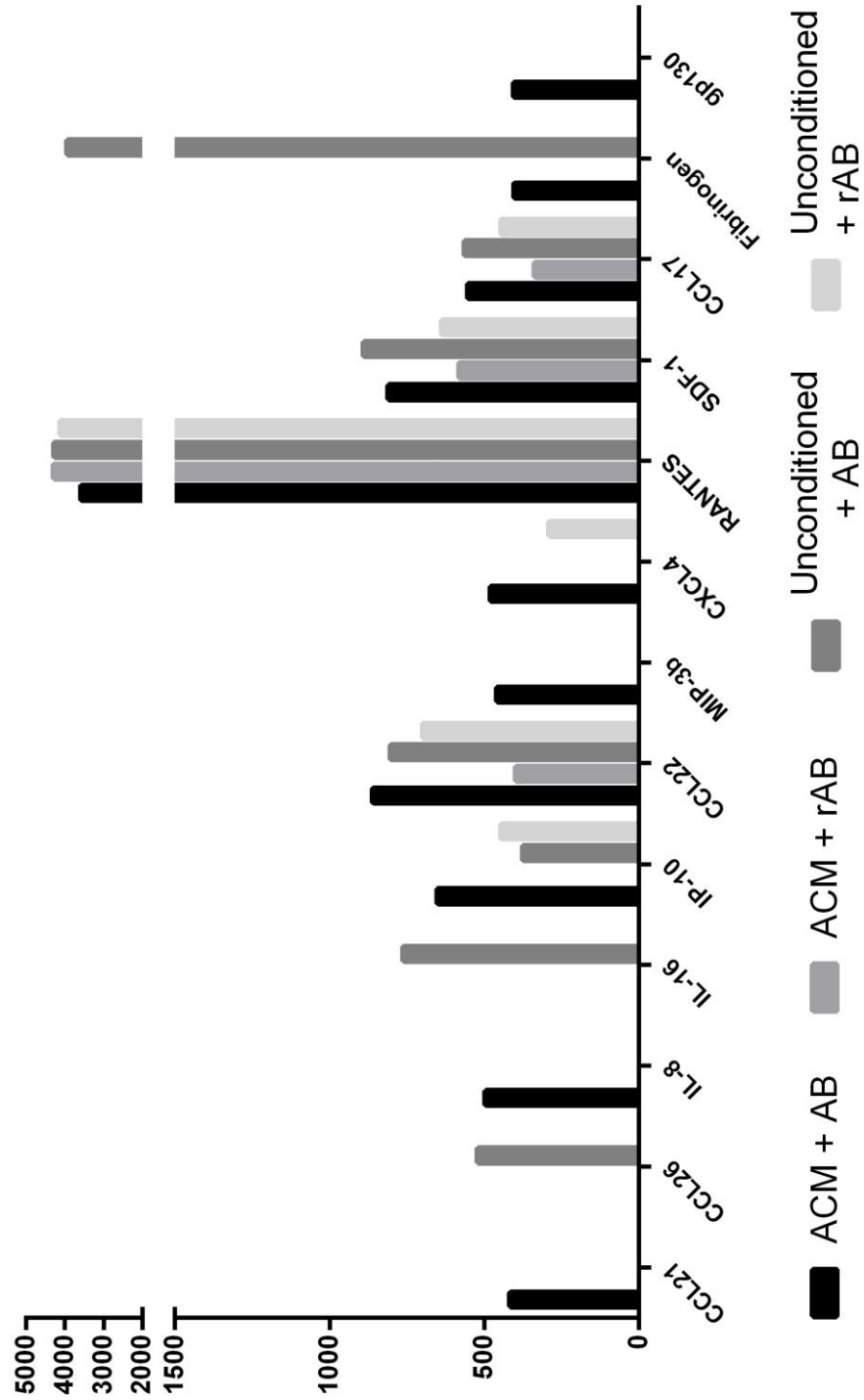


**Figure 5.14. Chemokine Secretion post AB Incubation**

The dot blot was carried out for ESdMG in ACM or ESdM in unconditioned media. All cells were treated with either  $A\beta_{(1-42)}$  or  $rA\beta_{(42-1)}$ . When ESdMG were treated with  $A\beta_{(1-42)}$  there was an increase in CCL21, CCL19, CXCL4 and IL-8. ESdM in unconditioned medium had increased levels of CXCL5 and IL-16 on incubation with  $A\beta_{(1-42)}$ .

---

## 5.6 DATA SUMMARY

---

We showed that EsdMs that were cultured in ACM for seven days differentiated into ramified microglial-like cells. This resulted in the formation of IBA-1+/Glut5+/CD45<sup>low</sup> cells, which were not produced when culturing in unconditioned control medium (IBA-1-/Glut5-/CD45<sup>high</sup>). These ramified microglial-like cells were susceptible to stimulation by GM-CSF, which increased the rate of proliferation.

The microglial-like cells were further characterised by QRT-PCR for microglial and monocytic genes, which showed low expression of monocytic genes NG2 and CD45, but increased expression of microglial gene, CD80, whilst there was also expression of TREM2 and IBA-1 in all cell types.

Electrophysiological experiments showed that there was the presence of both inwardly rectifying and voltage gated potassium channels and voltage gated sodium channels in the resting H9-derived cells. The membrane capacitance, and thus cell surface area, was consistent with values gained in prior published experiments. Together this data reveals that the cells differentiated in ACM are of a microglial-like nature.

Further functional experiments showed that the ramified cells were capable of becoming activated to the amoeboid form on incubation with AB<sub>(1-42)</sub>, which was not seen when incubated with the reverse control peptide. Under these conditions the ESdMG also secreted cytokines and chemokines, although here the profile would suggest that the EsdMG were anti-inflammatory in nature, rather than the pro-inflammatory nature expected in the case of AD.

## 5.7 DISCUSSION

---

This work showed that monocytes derived from H9 hESCs are able to differentiate into microglial-like cells in the presence of astrocytes but we also see the same differentiation with only astrocyte conditioned media.

Since monocytes can differentiate into microglia in medium only conditioned by astrocytes and do not require a physical astrocyte presence, this shows that monocytes require cues from their surrounding milieu to differentiate. As mentioned previously and in the works of Sievers et al. (1994) these factors are likely to be M-CSF, GM-CSF and TGF- $\beta$ . The differentiation shown here occurs within just seven days, whereas protocols using a defined medium with additional growth factors, such as that of Etemad et al. (2012), takes twice as long. This is most likely due to the astrocytic secretion of all the required cytokines at the correct concentration, initiating an efficient differentiation.

Clearly microglia and macrophages are intricately linked and thus specific markers to differentiate between both populations are difficult to find. Even the routinely used IBA-1 falls short in this application since it is also expressed by activated macrophages. Here we used a combination of IBA-1, the more specific Glut5 and CD45. This showed that under the influence of ACM monocytes differentiate into microglial-like cells. It was noted that only around 17%, the level of CD11b<sup>+</sup> cells in the ESdM supernatant, remained after 7 days of ACM culture. This suggests that only committed monocytes (CD11b<sup>+</sup>) and not their GMP precursors (CD34<sup>+</sup>/CD45<sup>+</sup>) are able to differentiate into microglial-like cells.

To ultimately distinguish between these cell types electrophysiology was used to show the presence of inwardly rectifying K<sup>+</sup> channels with the absence of outward

currents, this observation concurs with the published findings from Kettenman et al. During the recording there was also evidence of the presence of a voltage gated sodium channel, such channels seen in the work of Anderson et al. (2006).

Membrane capacitance is proportional to the surface area of the cell under the patch clamp. Reports of microglial capacitance range from,  $46 \pm 2\text{pF}$  and  $18 \pm 6\text{pF}$  and culture in ACM has been shown to lead to increases in membrane capacitance in the order of around  $9\text{pF}$ , due to increased ramification (Toulme and Khakh 2012; Boucsein et al. 2000; Klee et al. 1999). The average capacitance of the EsdMG was  $34.34 \pm 2.48\text{pF}$ , and thus a value expected for microglial cells.

Activation of microglia from the immune dampened ramified cell to the phagocytic ameboid cell in the presence of  $A\beta$  is determined by engagement of the  $fA\beta$  receptor complex along with the activation of ion channels and transporters. The  $fA\beta$  receptor complex is comprised of CD36, CD47 and integrin  $\alpha_6 \beta_1$ , which is able to initiate a cascade involving the Src kinases Lyn and Syk, followed by ERK and then p38 map kinase to lead to the secretion of  $IL-1\beta$  and phagocytosis of the  $A\beta$  (Bamberger et al. 2003; Koeingsknecht-Talboo and Landreth 2005). De-ramification is in part due to the osmotic potential of the cell, which is tightly regulated by ion channels and transporters. Non-selective cation channels within the cell body enable the entry of cations that results in the entry of water and the swelling of the cell body. Conversely there is an efflux of  $KCl$  through  $Cl^-/K^+$  co-transporters localized on the processes, which causes efflux of water and their retraction to the ameboid phenotype.  $A\beta$  itself is regarded by many as a regulator of voltage-gated potassium and calcium channels in neurons. Plant et al. (2006) show that  $AB$  acts as a chaperone of  $KV4$  subunits to the plasma membrane to result in an increased A-type current. Although this work is focused upon neurons, microglia also possess  $KV$  channels, which are

up-regulated during activation with A $\beta$ . Upon staining ESdMG for A $\beta$  after incubation there is evidence of intra-membrane staining, which could be linked to the chaperoning role proposed by Plant et al. (2006).

The ESdMG show the presence of Kir2.1 and NaV1.6 whilst they have very little expression of NaV1.5 channels. NaV1.5 has been the focus of voltage gated sodium channel work in human microglia in recent years but it has been noted that their appearance is activation dependent (Nicholson and Randall 2009). Since the microglial-like cells cultured here are of the immune dampened ramified form, it is perhaps fitting that there is little activity from these channels.

Associated with IL-1 $\beta$  is the NF $\kappa$ B pathway, where a positive feedback system is instigated with NF $\kappa$ B acting as the transcription factor for the production of yet more IL-1 $\beta$ . In this pathway TNF- $\alpha$  also plays a role, through a very similar positive feedback mechanism. Both IL-1 $\beta$  and TNF- $\alpha$  can, through this signaling cascade, lead to the degradation of the cell. TNF- $\alpha$  production is also stimulated by IFN- $\gamma$  secretion, which effects the cell through a JAK/STAT mediated pathway involving STAT1a and inducing several genes, not just TNF- $\alpha$ , but also IL-1, IL-3, G-CSF and GM-CSF along with a positive feedback system for IFN- $\gamma$  expression (Benveniste and Benos 1995).

Secretion of all three of these cytokines can have detrimental effects on the survival of surrounding cells, causing the initiation of their own NF $\kappa$ B pathway and cell degradation, a vicious cycle that leads to a region of inflammation and in the case of microglia and the brain, loss of the surrounding neuron population. This is seen in neurodegeneration and in particular AD, where the decrease in brain volume is substantial.

Activation of microglia is dependent upon the level of tPA, an enzyme required for the conversion of Plasminogen to plasmin. In this regard the increased levels of MIF and SERPIN E1 witnessed in the array would suggest that the A $\beta$ <sub>(1-42)</sub> is not acting in a neurotoxic manner, but instead is in the case of MIF retarding neuronal death and enhancing axonal regeneration whilst transforming ramified microglia to the ameboid form. Infusion of MIF into mouse brain prior to excitotoxin – induced neuronal death was shown to protect neurons against the damage. SERPIN E1, an inhibitor of both tPA and uPA increases the migratory ability of microglia and modulates phagocytosis, whilst inhibiting microglial activation through the tPA pathway. Plasmin, a broad spectrum protease, is able to degrade A $\beta$  and promote non-amyloidogenic cleavage to sAPP $\alpha$ . Thus tPA inhibition through SERPIN E1, which is increased in both AD patients and through direct AB injection in murine models, results in AB accumulation and the formation of senile plaques and ghost tangles.

Several interleukins were shown to be increased in the ESdMG cultures on addition of A $\beta$ . IL-13 secretion was increased on addition of A $\beta$  and has been shown to induce death of activated microglia through the enhancement of COX-2 expression and PGE(2) production. This fits with the degradation of microglia that have phagocytosed A $\beta$ , to prevent further inflammation. IL-17 was shown to be increased dramatically in ESdMG cultures on addition of A $\beta$ . IL-17 was shown to be increased in the ESdMG cultures with A $\beta$  addition, whilst very little was released by the ESdMG stimulated with the reverse peptide. This increase is similar to published results, where unstimulated microglia produced no IL-17, whilst the increase in the stimulated microglia also lead to the increased expression of anti-inflammatory proteins, NGF, BDNF and GDNF. Finally IL-27 secretion was up-regulated in cells treated with A $\beta$ . IL-27 inhibits A $\beta$  degradation and enhances its retention once

phagocytosed by microglia. It has also been shown that IL-27 inhibits OSM-mediated TNF- $\alpha$  and iNOS expression in microglia.

This reveals that the ESdMG although functional are not neurotoxic, from their activation being inhibited, the increased anti-inflammatory proteins that result from the secretion of the specific interleukins that were up-regulated, to the increase in cell death that results from increased COX-2 expression.

This could be due to the A $\beta$  incubation time being too short, so that there was little time for neurotoxic behaviours to develop, the microglial-like cells were not pre-conditioned to react in a cytotoxic manner or it could be due to the ESdMG being immature and acting more like fetal microglia than the aged microglia that are found in AD brains.

The second array highlighted several differences in chemokines secreted by ESdMG when treated with AB compared to those secreted by ESdM. Of note are the chemokines that are involved in homing and chemotaxis; CCL21 and MIP-3b (CCL19). These are up-regulated in ESdMG after incubation with AB and microglia have been shown to have increased migration to these chemokines when TREM2 is stimulated. TREM2, a risk factor gene in AD, controls phagocytosis and the production of pro-inflammatory mediators. Stimulation increases phagocytosis and decreases pro-inflammatory mediators. CXCL4 has also been shown to be involved in chemotaxis of microglia, which requires CXCR3. CXCL4 has also been shown to decrease facial nerve regeneration and increase the severity of disease in stroke models when exogenously applied. In monocytes there is an increase in phagocytic ability in response to CXCL4 but it was shown to be decreased in microglia, along with a decrease in NO production. CXCL4 is not found in ramified microglia and is

not found within neurons or astrocytes. IL-8 was shown to be increased in ESdMG incubated with AB. Studies suggest that IL-8 causes an increase in COX-2 and is produced in response to pro-inflammatory stimuli, such as LPS or A $\beta$ . IL-8 is also functional in microglial chemotaxis. Together this again suggests that the ESdMG, although functional, are not centres of inflammation when incubated with A $\beta$ .

There are four proteins that are present on both the cytokine and chemokine array, but their expression differs between each array. IL-8 is only present in the EsdM cultured in ACM and incubated with A $\beta$ . It has a pixel density of around 250 in the cytokine array, whereas the chemokine array showed IL-8 pixel density to be doubled. IL-16 is present in all conditions in the cytokine array but only present in EsdM cultured in unconditioned media and treated with A $\beta$  in the chemokine array, but all densities are less than 1000. IP-10 is not present in the unconditioned media group treated with rA $\beta$  in the cytokine array but is present in all other conditions. In the chemokine array IP-10 is absent from the ACM + A $\beta$  group. For both arrays the pixel densities are less than 600. Finally SDF-1 is present only in the unconditioned + A $\beta$  group in the cytokine array, but is present in all conditions in the chemokine array, with densities far below 1000.

This could be attributed to many factors including; the supernatants being taken from different wells. We know that the EsDM population is a mixed one and although ACM seemingly provides a selection for IBA-1+ cells, there could be different cell types, at various stages of differentiation contained within each well that could lead to differences in protein secretion. The differences between arrays could also be attributed to potential differences in the protein concentration within each sample, although a constant volume, 250 $\mu$ l, of supernatant was added to each array membrane it does not necessarily follow that there is a consistent protein

concentration and there is no way in which to normalise for such differences. Finally the differences in the density of these spots are small and they arise from weak spots that could result in less accuracy during the analysis, especially after background subtraction.

The levels of GM-CSF from the cytokine array were similar for both treatments with both cell types. GM-CSF is considered to be one of the major factors released by astrocytes that directly influences microglial phenotype and proliferation. To enable the true effect of  $A\beta_{(1-42)}$  stimulation to be deduced a media only control would need to be included for both arrays. But from the data currently available we concluded that the microglial-like cells resultant from the differentiation in ACM are anti-inflammatory in nature, whereas those in unconditioned media have a pro-inflammatory nature.

Thus we have shown a method for the differentiation of functional microglial-like cells from an ES-derived monocyte, which displays the correct phenotype and gene expression, ion channel activation and cytokine secretion can be induced through the incubation of such cells with  $A\beta$ .

---

## 6. GENERAL DISCUSSION

---

The work presented here focused upon the development of an efficient, reproducible protocol for the generation of microglial-like cells from hESCs. At the time of onset of the study there were no published protocols available for hESC differentiation to microglia, but innovative work in mouse models had yielded several routes; namely 'reprogramming' adult neural stem cells by Forsberg et al. (2008) and growth factor directed differentiation from mESCs (Napoli et al. 2009). We show that functional microglial-like cells can be produced in relatively large numbers without the need of feeder layers or large quantities of growth factors from hESCs. These ES-derived cells can then be used in *in vitro* modelling of disease or utilised in functional and cell therapy experiments.

---

### 6.1 MONOCYTE DIFFERENTIATION

---

---

#### 6.1.1 PU.1 OVEREXPRESSION

---

Exogenous over-expression of PU.1 in hESC-derived NSCs produced GFP+/CD11b+ cells. CD11b is required as a component of the leukocyte adhesion and migration complex and as such is a marker for myeloid cells and in particular monocytes, macrophages and microglia (Strauss-Ayali et al. 2007). This would suggest that PU.1 does promote the differentiation of neuronal precursors to a myeloid lineage, however, the resulting cells lacked the ability to phagocytose *E. coli* bioparticles nor did they possess the ability to respond to secreted factors in the ACM and differentiate to microglia.

At physiological levels PU.1 is vital throughout haematopoiesis to promote terminal differentiation to monocytes (see Figure 1.2). PU.1 antagonises GATA-1 to enable myeloid lineage fate determination over a lymphoid fate, and high doses of PU.1 are required to promote the formation of CFU-M over CFU-G (Mak et al. 2011). Overexpression of PU.1 in haematopoietic precursors would override the antagonistic unbias of haematopoiesis and would favour the differentiation of monocytes. In terms of the 're-programming' carried out in chapter 3; neural precursors, with their substantial nuclear plasticity, hold great potential for re-programming to any cell type including iPSCs and monocytes with the introduction of only one important exogenous gene, Oct4 or PU.1 respectively (Kim et al. 2009).

PU.1 is bound by and targets many other proteins, including CBP, HDAC1, RUNX1 and PU.1 itself (Takahashi 2011). CBP is required for early phagocytosis and activation of macrophages to the M1 state (Yamamoto et al. 1999). Overexpression of PU.1 could lead to the sequestration of CBP leading to a reduction in both phagocytosis and classical activation. PU.1 is able to form a complex with HDAC1 which has been shown to have a down regulating effect on the expression of other TFs, including c-MYC (Kihara-Negishi et al. 2001). This could be extended to enable us to theorise that other genes, required for phagocytosis and differentiation to microglia, could also be affected. RUNX1 has been shown to be in a negative feedback loop with PU.1 and RUNX1 expression is required for both myeloid and microglial development. If the level of overexpression is the root cause of the lack of function witnessed, the fact that PU.1 is able to bind to itself to increase expression would mean that any inhibition caused would be exacerbated.

Expression of interferon regulatory factor 8 (IRF8) could be used to address their lack of differentiation to microglia. Kierdorf et al. (2013) reported that

microgliogenesis is a process that requires expression of both PU.1 and IRF8 and the heterodimeric complex that they form. IRF8 has also been implicated in mononuclear phagocyte development from myeloid precursors as such lack of IRF8 expression in the produced cells could explain both their lack of phagocytic capacity and their inability to differentiate to microglia (Marquis et al. 2011).

To combat these issues the vector could be re-designed to include a Cre/LoxP system to enable exogenous PU.1 expression to be stopped subsequent to the lineage switch allowing endogenous expression to continue and thus permit downstream processes to occur as intended.

Although the lack of function could also be explained through the integration of plasmid DNA into a gene vital for phagocytosis and or differentiation to microglia. This could be avoided by targeting the vector to integrate into the genome by recombination. On the whole this protocol, with slight alterations in the plasmid design could show promise for the production of monocytes through lineage switching or from iPSCs without the need for numerous growth factors.

---

### 6.1.2 MCSF/IL3 DIRECTED DIFFERENTIATION

---

The protocol set out in chapter 4 resulted in the formation of a mixed haematopoietic population consisting of cells positive for the haematopoietic stem cell marker CD34 as well as more committed myeloid lineage cells, CD45+, and monocytes; CD11b+. These latter, differentiated cells were also deemed functional through their ability to phagocytose *E. coli* microbeads.

Monocytes are classified as CD45+/CD11b+, whilst lymphocytes are CD45+/CD11b- and microglia can be described as CD45<sup>low</sup>/CD11b+. QPCR of both the factory colonies and the resultant supernatant cells also showed expression of CD11c at

similar levels to the THP1 control. CD11c expression is most common in non-lymphoid tissues in particular dendritic cells of the small intestine and skin but it is also expressed in monocytes and macrophages. Dendritic cells and monocytes do have a common precursor, but have strikingly different morphologies. Dendritic cells have branched projections that function to increase the surface area of the cell to enable antigen processing and presentation (Patterson et al. 1991). Monocytes on the other hand, do not bear such processes and are on the whole spherical, with few membrane ruffles. It is based on this morphological difference that we can confirm that the cells that result from this protocol are indeed monocytic rather than dendritic.

Phagocytosis, is a function of many white blood cells including monocytes. As such phagocytosis was used as a marker of functionality of the ES-derived monocytes (ESdM). It was shown that the percentage of cells that had phagocytosed the *E.coli* biobarticles were similar to that of the monocytic cell line THP-1. Although the percentage was only around 30% this was slightly greater than a characteristic value for unstimulated cells (Baqui et al. 1998). Stimulation with LPS or IFN- $\gamma$  would have shown an increase in phagocytosis (Suzumura et al. 1991), which if the process was repeated, could be included to further reveal the functionality of the cells produced in response to interferons and endotoxins.

Van Wilgenburg and colleagues (2013) have previously used this protocol, with some variations, to generate monocytes from the Hues2 hES cell line along with multiple iPSC lines. We now show that the protocol is also functional with the H9 cell line. The resultant ESdM are numerous, express the correct profile of markers and most importantly are shown to be functional through their ability to phagocytose. Thus this protocol has the potential to function with AD iPSCs to produce patient and or disease specific cells.

## 6.2 MONOCYTE DIFFERENTIATION TO MICROGLIAL-LIKE CELLS

---

### 6.2.1 ASTROCYTE CONDITIONED MEDIA (ACM)

---

Upon culturing the ESdM in ACM for seven days, there was down regulation of the leukocyte marker, CD45, with the appearance of IBA-1, GLUT5 and CD80 and a resultant ramified morphology. The resultant cells were able to phagocytose A $\beta$ <sub>(1-42)</sub>, which also resulted in a morphological adaptation to the ameboid phenotype. Functionality of these cells was also shown through their cytokine expression and release along with their electrophysiological properties. The differentiation of these cells in ACM is suggested to be due to the simultaneous presentation of M-CSF, GM-CSF and TGF- $\beta$  secreted by astrocytes (Schilling et al. 2001).

Ramification of microglia results in a down regulation of markers associated with immunity, instead focus is transferred to their surveying functions. The use of IBA-1 as a marker for microglia is useful when confined to the parameter of the brain but, outside of the CNS IBA-1 expression is seen in other cells such as activated macrophages (Imai et al. 1996). Thus the use of other markers for microglia are required to endorse the differentiation scheme for microglial-like cell production. Another marker of interest in microglial identification is GLUT5, which is able to distinguish even peripheral macrophages from the target microglial cells (Sasaki et al. 2003; Kettenmann et al. 2011). CD80, although not exclusively expressed in microglia, is only expressed at low levels in monocytes. Differential expression can thus be utilised along with the additional markers to enable a confirmation upon cell type. The marker profile of the ESdM subsequent to culture with ACM is thus comparable to that of microglia.

Under normal physiological conditions ramified microglia survey the environment and are activated upon uncovering a stimulus; cell debris, protein or foreign body.

Activation results in a retraction of cytoplasmic processes to the cell body and the formation of the characteristic ameboid cell, capable of engulfing and removing potentially toxic bodies. Such a process occurs on detection of A $\beta$  fibrils, resulting in their phagocytosis. Phagocytosis of A $\beta$  was shown to occur when incubated with the ESdM subsequent to their culture in ACM. Along with their capacity for phagocytosis the ramified cells were also shown to undergo a morphological change to an ameboid phenotype, where the processes had retracted and the cells were largely spherical. This indicates that resultant ESdMGs would be functional in the desired AD model as they possess the ability to recognise and engulf A $\beta$ <sub>(1-42)</sub>.

Microglia have a unique electrophysiological profile, most pronounced in murine and rodent cells. There is an absence of outwardly rectifying K<sup>+</sup> currents with only inwardly rectifying K<sub>ir</sub> currents visible, microglia are the only myeloid lineage cell to display such electrophysiology (Kettenmann et al. 1993). This is the polar opposite to the profile of macrophages and as such serves as an ideal marker to differentiate between the two closely related cell types. The profile for human microglial cells is more complicated as they show both inward and outward K<sup>+</sup> currents as well as voltage-gated Na<sup>+</sup> currents and these currents can be induced through the presence of astrocytes (Schmidtmayer et al. 1994). The currents recorded in the ESdMG were comparable with those recorded by Schmidtmayer and colleagues (1994), when differentiating monocytes and macrophages to microglia through astrocyte co-culture. Schilling et al. (2001) also showed that culture of the BV-2 murine microglial cell line in ACM led to an up-regulation of outward K<sup>+</sup> channels, which would also explain the activity from the outward K<sup>+</sup> channels witnessed within the patch clamp experiments with the ESdMG cells.

Chemokine and cytokine secretion from ESdMG after incubation with A $\beta$ <sub>(1-42)</sub> showed that these, non-AD microglial-like cells would promote axonal regeneration and reduce cell death, instead of acting in a neurotoxic manner, which is likely to be the case in AD-derived cells. As such these ESdMG are not classically activated (M1), but are of the M2 phenotype, which is neuroprotective (Lewis et al. 2012). TREM2 is an AD risk factor gene that is expressed on microglia, its physiological function inhibits inflammation and promotes phagocytosis, it would follow that TREM2 could promote M2 activation over the neurotoxic M1 activation (Guerreiro et al. 2013). Its loss of function in AD could result in a greater number of classically activated M1 microglia and inflammation. If the protocol was repeated with iPSCs from patients with an AD TREM2 variant, it may be expected to show the opposite cytokine profile and thus M1 activation.

---

## 6.3 LEGITIMACY OF STUDY

---

### 6.3.1 DIFFERENTIATION STRATEGY

---

Is the differentiation of hESCs to microglial-like cells, via monocytes, a valid differentiation strategy?

Microglia are derived from myeloid precursors in early development which infiltrate the CNS prior to the formation of the BBB proper. These cells proliferate *in situ* and further differentiate to the immune dampened ramified cells to form the resident microglial population (Perry et al. 1985; Davis et al. 1994).

Monocytes can also be recruited from the bone marrow under pathological stresses, where the BBB loses integrity. The *in vivo* differentiation of microglia during development would suggest that they are of myeloid origin and as with all monocyte

derived cells, the environment within which the cells reside impact on further differentiation (Cuadros and Navascués 1998).

Monocytes in the bone marrow become tissue macrophages with very different properties dependent on location from osteoclasts in the bone to Kupffer cells in the liver. Dendritic cells are specialised for mucosa and epidermis, whilst microglia are generated from the same precursors but are specialised for the CNS, the differentiation of which occurs subsequent to crossing the BBB. As such the only scheme suitable for microglial differentiation would require a monocytic step, followed by a period of time in an environment similar to that of the CNS to enable final differentiation to microglia.

Aside from the *in vivo* differentiation scheme, there have been previous studies in published works that are able to create microglia from monocytes, using environmental stimuli to direct differentiation. Forsberg et al. (2008) were able to create murine monocytes and transplant them into the brain, where they differentiated and became indistinguishable from the resident microglial population. Sievers et al. (1994) also showed that the presence of factors released from astrocytes were capable of differentiating blood and splenic monocytes into microglia. Thus to take a two-step approach to the differentiation scheme, hESCs to monocytes and then monocytes to microglia is the most feasible option in producing hES-derived microglial-like cells.

---

### 6.3.2 MICROGLIAL MARKERS

---

As mentioned microglia are closely related and function similarly to monocytes and macrophages, which means that specific microglial markers are rare. Microglia are still identified using a marker profile rather than the use of an absolute microglial

marker. The suggested profile is CD68+, CD45<sup>low</sup>, CD11c<sup>high</sup>, MHC-II+, CD14-, IBA-1+. There are numerous other markers that show differential expression between monocytes/macrophages and microglia, such as; CD80, NG2, LN, peroxidase and Ki-67. There is also the use of GLUT5, a marker found to be more specific than IBA-1 toward microglia in the confines of the brain. Thus the profile used here to differentiate between microglial-like cells and monocytes is CD45<sup>low</sup>, CD11c<sup>high</sup>, NG2<sup>low</sup>, CD80<sup>high</sup>, IBA-1+, TREM2+, GLUT5+.

It is with the use of these various markers that microglia can be positively identified from their close relatives, the monocyte. This study has incorporated the use of many of these markers as well as using functional and morphological data to enable a satisfactory identification of the cells resulting from the differentiation as microglial-like cells.

---

### 6.3.3 THP1 MONOCYTIC CELLS AS A CONTROL CELL LINE

---

The THP1 cell line was established in 1980 from the culture of a 1-year old Japanese boy suffering with acute monocytic leukemia by Tschিয়া et al. (1980). The group showed that the cell line was monocytic in nature via function and marker expression, characteristics that remained true when cultured for over a year. Two decades later cytogenetic analysis of the THP-1 cell line by Odero et al. (2000), revealed that the cells were near diploid but they were karyotypically abnormal, including trisomy 8 and monosomy 10. This means that the expression of particular genes in THP1 cells, especially those located on chromosome 8 and 10 will differ from the expression of those same genes in karyotypically normal cells and thus the differentiation potential may also vary. This could be combated by the use of other control cell lines together with the THP1 cells to validate the results.

---

### 6.3.4 THE EFFECT OF NEUROBREW 21 IN THE ACM

---

NeuroBrew 21 is an optimised form of B27, a supplement used during neuronal differentiations and used here within the ACM (Chen et al. 2008). It should be noted that there are several components of NeuroBrew 21 that could, if in the correct concentration, have an effect on functionality of both microglia and A $\beta$  upon such cells.

The first component listed is bovine albumin, which has been shown to increase expression and secretion of pro-inflammatory cytokines such as IL-1 $\beta$  and TNF- $\alpha$  (Zhao et al. 2009). Microglial activation by albumin is unsurprising since a breakdown in the BBB would lead to the influx of albumin and the resultant microglial activation is anticipated in such a situation. There is also high homology between the mammalian albumins, so bovine albumin would have a similar effect on human microglia as human albumin. Albumin can also play a role in preventing the aggregation of A $\beta$  via its physiological chaperone role, decreasing the cytotoxic effects since microglia are only able to respond to fibrillary A $\beta$  (Finn et al. 2012).

Albumin has also been associated with enhancing superoxide production in cultured microglia (Si et al. 1997), which leads to the next component of NeuroBrew 21; superoxide dismutase (SOD). Extracellular SOD, an enzyme that partitions toxic O $_2^{\cdot-}$  into the less harmful H $_2$ O $_2$  or conventional O $_2$  has been implicated in the activation of microglia to the cytotoxic phenotype, whilst an excess of SOD1 has been shown to protect against A $\beta$  toxicity (Roberts et al. 2013; Celsi 2004). Conversion of H $_2$ O $_2$  into water and oxygen is catalysed by Catalase, which protects cells from the harmful actions of hydrogen peroxide. Catalase can also inhibit the proliferative response of microglia to IL-1 $\beta$  and TNF- $\alpha$  since this response is governed by the release of hydrogen peroxide from NADPH oxidase (Mander et al. 2006). With regards to A $\beta$ ,

A $\beta$  is able to bind to catalase and thus inhibit the break-down of H<sub>2</sub>O<sub>2</sub>, which is able to contribute to A $\beta$  toxicity (Milton et al. 1999).

The glutathione within the NeuroBrew 21 supplement is an anti-oxidant and plays a role in protecting cells from reactive oxygen species, which are produced during cell stress (Hirrlinger et al. 2000). Excess glutathione could also lead to an increase in the generation of plasmin, since glutathione and tPA are intricately linked. Since plasmin degrades A $\beta$ , lessening A $\beta$  load, glutathione provides protection from the effects of A $\beta$  (Lasierra-Cirujeda et al. 2013). Oxidative stress due to A $\beta$  can also be diminished by L-Carnitine, the precursor to Acetyl-CoEnzyme A and another component of NeuroBrew 21, which functions through a buffering system and via the maintenance of ATP levels (Dhitavat et al. 2002).

NeuroBrew 21 also contains steroid hormones, of note are corticosterone and progesterone. Corticosterone has the ability to inhibit both the synthesis and secretion of TNF $\alpha$  and through this action has an anti-inflammatory effect (Jacobsson et al. 2006). Similarly progesterone is deemed an anti-inflammatory agent and has been shown to inhibit microglial proliferation in microglial only cultures (Ganter et al. 1992).

Finally, vitamins A and E are also contained within the NeuroBrew 21 supplement. Vitamin A, or retinol, suppresses the production of IL-6, a plaque promoting cytokine, in astrocytes and microglia. Vitamin A also functions to inhibit the nuclear translocation of NF $\kappa$ B leading to the suppression of TNF- $\alpha$  and iNOS production in activated microglia (Shudo et al. 2009). Vitamin E,  $\alpha$ -tocopherol, decreases the levels of COX-2 and PGE(2) and through its activation of Protein Phosphatase 2 in

microglial cells enables the silencing of the NF $\kappa$ B signalling cascade (Egger et al. 2003).

Although these components of NeuroBrew 21 are, on the whole, able to promote an anti-inflammatory nature in microglia and decrease the cytotoxicity of A $\beta$ . The concentrations of each component are not sufficient to interfere with the differentiation of the microglial-like cells nor have an effect on the outcome of A $\beta$  treatment, but it is important to be aware of their presence within the ACM.

---

#### 6.4 IMPACT OF STUDY

---

Prior to the onset of this study there were no published protocols to enable the differentiation of microglia from human pluripotent cells although protocols did exist for the generation of microglia from mESCs, thus the impact of the study is vast, and holds great potential for both AD and many other CNS disorders.

From hES-derived microglia we can study the function of microglia in response to A $\beta$ , in exceptional detail whilst limiting the number of animal models or using precious primary cell samples. A plentiful supply of microglial-like cells can be produced via this protocol and thus numerous possibilities to study the effect A $\beta$  has on cell activation. This can then be extended with the use of AD IPS, with common variants of the recently discovered risk factor genes, like TREM2, to enable a better understanding of the gene function in the disease.

The protocol could also be used to create a co-culture model of AD, using AD iPSC-derived neurons and microglia. Such a model would provide insight into the effect microglia have on neurons during disease progression under certain conditions, such as A $\beta$  load and hypoxia. The model could provide a good substitute to animal models for early drug screening, to lessen the burden on animal usage on drugs that

simply will not work. The use of iPSCs could eventually lead to patient specific models of the disease and thus tailor made treatments dependent on their genetic constitution.

Microglia are not just implicated in the progression of AD, but also play a role in multiple sclerosis (MS), Parkinson's Disease (PD), HIV associated neurocognitive disorder (HAND) and even OCD. The development of a protocol to differentiate numerous numbers of microglia and microglia from patient specific cells will inevitably lead to progress being made in these other CNS diseases. For these diseases, as in AD, IPS models of the brain could be developed for use in both understanding the disease and drug discovery. In HAND for example, there have been moves made to try and target microglia to protect them from HIV. The techniques and genes required for protection could thus be optimised on ES-derived cells, without the need to sacrifice animals or again use valuable primary cells.

One of the underlying mechanisms of AD disease progression is neuroinflammation caused by microglia that, through the process of aging and the accumulation of risk factors, become neurotoxic and deregulated. Age will also increase the permeability of the BBB enabling easier entry for cells, and as such cell therapy could be a useful route for AD treatment. Although there will never be ablation of the endogenous neurotoxic cells, the incorporation of new, healthy, phagocytic cells could be enough to regain control of the inflammation by an increase in phagocytosis of debris and plaques.

Transplantation of microglia has been completed successfully in rat models of stroke where there was an improvement in the disease phenotype and behaviour (Narantuya et al. 2010). This protocol could be harnessed for said therapy, since

there are no contaminants from feeder layers, such as OP9 for haematopoietic differentiation, when using iPSCs. Aside from their obvious uses in AD, microglia harness the ability to traverse the BBB, which together with the ability to be created from patient specific cells, means that they hold great potential to be used for gene delivery to the CNS. The future of cell transplantation into human patients is uncertain, whether the transplanted cells will do more harm than good is still not fully understood, but should cell transplantation be a possibility in the near future this protocol could be harnessed to enable transplantation of patient-specific microglia that could be genetically modified if necessary to combat disease caused by the resident microglial population.

#### 6.5 FURTHER WORK

---

Further work would initially include experiments that focus on the functional aspects of microglia in response to A $\beta$ , such as the electrophysiological changes that occur on activation, as well as migration experiments towards A $\beta$ , as microglia do toward A $\beta$  plaques *in vivo*, to prove that the differentiated cells are capable of functioning in the same way as endogenous microglia.

Then the focus would be on the conditioned media, and the identification of the components secreted by astrocytes that are vital for monocyte to microglial differentiation. Would the base media with the addition of TGF- $\beta$ , M-CSF (or IL-34) and GM-CSF alone or in combination promote the same differentiation as witnessed by the astrocyte conditioned media? Would this defined media prevent any batch to batch variation as is problematic with conditioning? Would neuron conditioned media also promote such differentiation and if so would the resultant microglia function in a similar manner?

The differentiation could then be expanded to include more cell lines, especially those from AD patients with genetic variants of the genes involved in immunity identified in the recent GWAS studies; TREM2, INPP5D, HLA-DRB1 and HLA-DRB5. Any loss of function of these genes would result in alterations in the behaviour of the endogenous microglial population. Creating IPS derived microglia with these mutations would enable a better understanding of the role these mutations play in inflammation and thus AD progression.

The ultimate aim would be to develop an *in vitro* AD model to enable the effect of microglia on all cell types in the brain to be studied in relative ease under numerous conditions, without requiring such a dependence on animal models. *In vitro* brain models created with iPSCs containing genetic variants of interest where neurons and microglia are able to interact would allow for an insight into how afflicted cells behave in a system. It is known that neuronal loss occurs during AD, with such a model the loss of neurons could be observed and the mechanism more greatly understood through MAP2 staining techniques, live/dead or MTT assays. The addition of A $\beta$  is thought to increase the resting calcium level and will give an enhanced response to EAAs via Ca<sup>2+</sup> homeostasis destabilisation, which could be examined through calcium imaging techniques.

Electrophysiologically, neurons from AD brains show inhibition of both glutamate and potassium receptors that could be observed through patch clamping experiments. The non-AD microglia in this system would show an increase in A $\beta$  phagocytosis and then, to limit inflammation, should undergo apoptosis thus decreasing the viability of the microglia in the model. The variant cells would possibly show less phagocytosis, less apoptosis and thus more inflammation leading to a greater loss of neuronal

cells.

---

## 7. REFERENCES

---

- Alexopoulou, A.N., Couchman, J.R. and Whiteford, J.R. 2008. The CMV early enhancer/chicken beta actin (CAG) promoter can be used to drive transgene expression during the differentiation of murine embryonic stem cells into vascular progenitors. *BMC cell biology* 9, p. 2.
- Alliot, F., Godin, I. and Pessac, B. 1999. Microglia derive from progenitors, originating from the yolk sac, and which proliferate in the brain. *Brain research. Developmental brain research* 117(2), pp. 145–52.
- Bamberger, M.E., Harris, M.E., McDonald, D.R., Husemann, J. and Landreth, G. 2003. A cell surface receptor complex for fibrillar B-Amyloid mediates microglial activation. *The Journal of neuroscience : the official journal of the Society for Neuroscience* 23, pp. 2665–22674.
- Baqui, A.A.M., Meiller, T.F., Turng, B., Kelley, J.I. and Falker, W.A. 1998. Functional Changes In Thp-1 Human Monocytic Cells after Stimulation with Lipopolysaccharide of Oral Microorganisms and Granulocyte Macrophage Colony Stimulating Factor. *Immunopharmacology and Immunotoxicology* 20(4), pp. 493–518.
- Black, J. a and Waxman, S.G. 2012. Sodium channels and microglial function. *Experimental neurology* 234(2), pp. 302–15.
- Boucsein, C., Kettenmann, H. and Nolte, C. 2000. Electrophysiological properties of microglial cells in nomral and pathologic rat brain slices. *European Journal of Neuroscience* 12(6), pp. 2049–2058.
- Boya, J., Calvo, J. and Prado, A. 1979. The origin of microglial cells. *Journal of Anatomy* 129, pp. 177–186.
- Bronner-Fraser, M. and Fraser, S. 1997. Differentiation of the Vertebrate Neural Tube. *Current Opinion in Cell Biology* 9, pp. 885–891.
- Brustle, O., Jones, K.N., Learish, R.D., Karram, K., Choudhary, K., Wiestler, O.D., Duncan, I.D. and McKay, R.D. 1999. Embryonic stem cell - derived glial precursors; a source of myelinating transplants. *Science* 285, pp. 754–756.
- Brustle, O., Spiro, A.C., Karram, K., Choudhary, K., Okabe, S. and McKay, R.D. 1997. In vitro-generated neural precursors participate in mammalian brain development. *Proceedings of the National Academy of Sciences of the United States of America* (94), pp. 14809–14814.
- Bushong, E. a, Martone, M.E. and Ellisman, M.H. 2004. Maturation of astrocyte morphology and the establishment of astrocyte domains during postnatal hippocampal development. *International journal of developmental neuroscience : the*

*official journal of the International Society for Developmental Neuroscience* 22(2), pp. 73–86.

Butovsky, O., Talpalar, A.E., Ben-Yaakov, K. and Schwartz, M. 2005. Activation of microglia by aggregated beta-amyloid or lipopolysaccharide impairs MHC-II expression and renders them cytotoxic whereas IFN-gamma and IL-4 render them protective. *Molecular and cellular neurosciences* 29(3), pp. 381–93.

Cajal, S.R. 1913. Contribucion al conocimiento de la neuroglia del cerebro human. *Trab. del Lab. de Invest. Biol* 11, p. 254.

Celsi, F. 2004. Overexpression of superoxide dismutase 1 protects against  $\beta$ -amyloid peptide toxicity: effect of estrogen and copper chelators. *Neurochemistry International* 44(1), pp. 25–33.

Cerretti, D.P. 1988. Human macrophage colony stimulating factor: alternative RNA and protein processing from a single gene. *Molecular Immunology* 25, pp. 761–770.

Chadwick, K., Wang, L., Li, L., Menendez, P., Murdoch, B., Rouleau, A. and Bhatia, M. 2003. Cytokines and BMP-4 promote hematopoietic differentiation of human embryonic stem cells. *Blood* 102(3), pp. 906–15.

Chambers, S.M., Fasano, C. a, Papapetrou, E.P., Tomishima, M., Sadelain, M. and Studer, L. 2009. Highly efficient neural conversion of human ES and iPS cells by dual inhibition of SMAD signaling. *Nature biotechnology* 27(3), pp. 275–80.

Chan, H.. and Bonini, N.M. 2000. Drosophila models of human neurodegenerative disease. *Cell Death and Differentiation* 7(11), pp. 1075 – 1080.

Chan, W.Y., Kohsaka, S. and Rezaie, P. 2007. The origin and cell lineage of microglia: new concepts. *Brain research reviews* 53(2), pp. 344–54.

Chen, S.K., Tvrdik, P., Peden, E., Cho, S., Wu, S. and Spangrude, G. 2010. Hematopoietic origin of pathological grooming in HoxB8 mutant mice. *Cell* 141, pp. 775–785.

Chen, Y., Stevens, B., Chang, J., Milbrandt, J., Barres, B. a and Hell, J.W. 2008. NS21: re-defined and modified supplement B27 for neuronal cultures. *Journal of neuroscience methods* 171(2), pp. 239–47.

Cleveland, D.W., Hwo, S.Y. and Kirschner, M.W. 1977. Purification of Tau, a microtubule-associated protein that induces assembly of microtubules from purified tubulin. *Journal of molecular biology* 116, pp. 207–225.

Comery, T.A., Martone, R.L., Aschmies, S., Atchison, K.P., Diamantidis, G., Gong, X., Zhou, H., Kreft, A.F., Pangalos, M.N., Sonnenberg-Reines, J., Jacobsen, J.S. and Marquis, K.L. 2005. Acute Y-Secretase Inhibition Improves Contextual Fear Conditioning in the Tg2576 Mouse Model of AD. *Journal of Neuroscience* 28, pp. 8898–8902.

- Costa, M.R., Gotz, M. and Berninger, B. 2010. What determines neurogenic competence in glia? *Brain research reviews* 63, pp. 47 – 59.
- Cuadros, M. a and Navascués, J. 1998. The origin and differentiation of microglial cells during development. *Progress in neurobiology* 56(2), pp. 173–89.
- Dahéron, L., Opitz, S.L., Zaehres, H., Lensch, W.M., Andrews, P.W., Itskovitz-eldor, J. and Daley, Q. 2013. Stem Cells. , pp. 770–778.
- Dakic, A., Wu, L. and Nutt, S.L. 2007. Is PU.1 a dosage-sensitive regulator of haemopoietic lineage commitment and leukaemogenesis? *Trends in immunology* 28(3), pp. 108–14.
- Dang, S.M., Kyba, M., Perlangeiro, K., Daley, G.Q. and Zandstra, P.W. 2002. Efficiency of Embryoid Body Formation and Haematopoietic Development from ESC in Different Culture Systems. *Biotechnology and Bioengineering* 78(4), pp. 442 – 453.
- Davis, E.J., Foster, T.D. and Thomas, W.E. 1994. Cellular forms and functions of brain microglia. *Brain research bulletin* 34(1), pp. 73–8. Available at: <http://www.ncbi.nlm.nih.gov/pubmed/8193937>.
- Davoust, N., Vuillat, C., Androdias, G. and Nataf, S. 2008. From bone marrow to microglia: barriers and avenues. *Trends in immunology* 29(5), pp. 227–34. Available at: <http://www.ncbi.nlm.nih.gov/pubmed/18396103> [Accessed: 13 March 2012].
- Deeks, S.G. 2011. HIV infection, inflammation, immunosenescence and aging. *Annual Reviews in Medicine* 62, pp. 141–155.
- Dhitavat, S., Ortiz, D., Shea, T. and Rivera, E. 2002. Acetyl-L-Carnitine Protects Against Amyloid-Beta Neurotoxicity: Roles of Oxidative Buffering and ATP Levels. *Neurochemical Research* 27(6), pp. 501–505.
- Dodart, J.-C., Bales, K.R., Gannon, K.S., Greene, S.J., DeMattos, R.B., Mathis, C., DeLong, C. a, Wu, S., Wu, X., Holtzman, D.M. and Paul, S.M. 2002. Immunization reverses memory deficits without reducing brain Abeta burden in Alzheimer's disease model. *Nature neuroscience* 5(5), pp. 452–7.
- Doestsh, F. 2003. The Glial Identity of Neural Stem Cells. *Nature Neuroscience* 6(11), pp. 1127–1134.
- Egger, T., Schuligoi, R., Wintersperger, A., Amann, R., Malle, E. and Sattler, W. 2003. Vitamin E (α-tocopherol) attenuates cyclo-oxygenase 2 transcription and synthesis in immortalized murine BV-2 microglia. *Biochemical Journal* 370, pp. 459–467.
- Etemad, S., Zamin, R.M., Ruitenber, M.J. and Filgueira, L. 2012. A novel in vitro human microglia model: Characterization of human monocyte-derived microglia. *Journal of neuroscience methods*.

- Evans, M.J. and Kaufman, M.H. 1981. Establishment in culture of pluripotential cells from mouse embryos. *Nature* 292(9), pp. 154–156.
- Evseenko, D., Zhu, Y., Schenke-layland, K., Kuo, J., Latour, B., Ge, S. and Scholes, J. 2010. Mapping the first stages of mesoderm commitment during differentiation of human embryonic stem cells. *Proceedings of the National Academy of Sciences of the United States of America* 107(31), pp. 13742–13747.
- Findeis, M.A. 2007. The role of amyloid beta peptide 42 in Alzheimer's disease. *Pharmacology and Therapeutics* 116, pp. 266–286.
- Finn, T.E., Nunez, A.C., Sunde, M. and Easterbrook-Smith, S.B. 2012. Serum albumin prevents protein aggregation and amyloid formation and retains chaperone-like activity in the presence of physiological ligands. *The Journal of biological chemistry* 287(25), pp. 21530–40.
- Flower, R.J. and Rothwell, N.J. 1994. Lipocortin-1: cellular mechanisms and clinical relevance. *Trends in pharmacological sciences* 15(3), pp. 71–6.
- Forsberg, M., Carlén, M., Meletis, K., Yeung, M.S.Y., Barnabé-Heider, F., Persson, M. a a, Aarum, J. and Frisé, J. 2008. Efficient reprogramming of adult neural stem cells to monocytes by ectopic expression of a single gene. *Proceedings of the National Academy of Sciences of the United States of America* 107(33), pp. 14657–61.
- Fredoroff, S. 1995. Development of Microglia. In: Kettenmann, H. and Ransom, B. R. eds. *Neuroglia*. Oxford University Press, New York, pp. 162–181.
- Freed, C.R. and Greene, P.E. 2001. Transplantation of Embryonic Dopamine Neurons for Severe Parkinson's Disease. 344(10), pp. 710–719.
- Freed, C.R., Greene, P.E., Breeze, R.E., Tsai, W.Y., DuMouchel, W., Kao, R., Dillion, S., Winfield, H., Culver, S., Trojanowski, J.Q., Eidelberg, D. and Fahn, S. 2001. Transplantation of embryonic dopamine neurons for severe Parkinson's disease. *New England Journal of Medicine* 344, pp. 710–719.
- Freundel, G. 1992. Interleukin 3: from colony-stimulating factor to pluripotent immunoregulatory cytokine. *International Journal of Immunopharmacology* 14, pp. 421–430.
- Ganter, S., Northoff, H. and Mannel, D. 1992. Growth Control of Cultured Microglia. 230.
- Ginhoux, F., Greter, M., Leboeuf, M., Nandi, S., See, P., Gokhan, S., Mehler, M.F., Conway, S.J., Ng, L.G., Stanley, E.R., Samokhalov, I.M. and M., M. 2010. Fate mapping analysis reveals that adult micoglia derive from primitive macrophages. *Science* 330(6005), pp. 841–845.
- Greter, M., Lelios, I., Pelczar, P., Hoeffel, G., Price, J., Leboeuf, M., Kündig, T.M., Frei, K., Ginhoux, F., Merad, M. and Becher, B. 2012. Stroma-derived interleukin-34

controls the development and maintenance of langerhans cells and the maintenance of microglia. *Immunity* 37(6), pp. 1050–60.

Griciuc, A., Serrano-pozo, A., Parrado, A.R., Lesinski, A.N., Asselin, N., Mullin, K., Hooli, B., Choi, S.H., Hyman, B.T. and Tanzi, R.E. 2014. Alzheimer's Disease Risk Gene CD33 Inhibits Microglial Uptake of Amyloid Beta. *Neuron* 78(4), pp. 631–643.

Guerreiro, R., Wojtas, A., Bras, J., Carrasquillo, M., Rogaeva, E., Majounie, E., Cruchaga, C., Sassi, C., Kauwe, J.S.K., Younkin, S., Hazrati, L., Collinge, J., Pocock, J., Lashley, T., Williams, J., Lambert, J.-C., Amouyel, P., Goate, A., Rademakers, R., Morgan, K., Powell, J., St George-Hyslop, P., Singleton, A. and Hardy, J. 2013. TREM2 variants in Alzheimer's disease. *The New England journal of medicine* 368(2), pp. 117–27.

Guillemin, G.J. and Brew, B.J. 2004. Microglia, macrophages, perivascular macrophages and pericytes : a review of function and identification. *Journal of leukocyte Biology* 75(3), pp. 388–397.

Hanisch, U.-K. and Kettenmann, H. 2007. Microglia: active sensor and versatile effector cells in the normal and pathologic brain. *Nature neuroscience* 10(11), pp. 1387–94.

Hansen, D. V, Lui, J.H., Parker, P.R.L. and Kriegstein, A.R. 2010. Neurogenic radial glia in the outer subventricular zone of human neocortex. *Nature* 464(7288), pp. 554–561.

Hao, C., Richardson, A. and Fedoroff, S. 1991. MACROPHAGE-LIKE CELLS ORIGINATE FROM NEUROEPITHELIUM IN CULTURE : CHARACTERISATION and PROPERTIES OF THE MACROPHAGE-LIKE cells. *International journal of developmental neuroscience : the official journal of the International Society for Developmental Neuroscience* 9(1).

Heneka, M.T. 2006. Inflammation in Alzheimer's disease. *Clinical Neuroscience Research* 6, pp. 247–260.

Heneka, M.T., Rodríguez, J.J. and Verkhratsky, A. 2010. Neuroglia in neurodegeneration. *Brain research reviews* 63(1-2), pp. 189–211.

Hirrlinger, J., Gutterer, J., Kussmaul, L., Hamprecht, B. and Dringen, R. 2000. Microglial cells in culture express a prominent glutathione system for the defense against reactive oxygen species. *Developmental Neuroscience* 22(5-6), pp. 384–392.

Huang, G., Zhang, P., Hirai, H., Elf, S., Yan, X., Chen, Y., Koschmieder, S., Okuno, Y., Dayaram, T., Grownwy, J.D., Shivdasani, R., Gilliland, D.G., Speck, N.A., Nimer, S. and Tenen, D.G. 2008. PU.1 is a major downstream target of AML1 (RunX1) in adult mouse hematopoiesis. *Nature Genetics* 40, pp. 51–60.

Ihne, J.N. 1992. Interleukin-3 and hematopoeisis. *Chemical Immunology* 51, pp. 65–106.

- Imai, Y., Iyata, I., Ito, D., Ohsawa, K. and Kohsaka, S. 1996. A novel gene *iba1* in the major histocompatibility complex class III region encoding an EF hand protein expressed in a monocytic lineage. *Biochemical and biophysical research communications* 224(3), pp. 855–62.
- Ito, D., Imai, Y., Ohsawa, K., Nakajima, K., Fukuuchi, Y. and Kohsaka, S. 1998. Microglia-specific localisation of a novel calcium binding protein, *Iba1*. *Brain research. Molecular brain research* 57(1), pp. 1–9.
- Jacobsson, J., Persson, M., Hansson, E. and Rönnbäck, L. 2006. Corticosterone inhibits expression of the microglial glutamate transporter GLT-1 in vitro. *Neuroscience* 139(2), pp. 475–83.
- James, D., Levine, A.J., Besser, D. and Hemmati-Brivanlou, A. 2005. TGFb/activin/nodal signaling is necessary for the maintenance of pluripotency in human embryonic stem cells. *Development* 132, pp. 1273–1282.
- Jordan, F.L. and Thomas, W.E. 1988. Brain macrophages: questions of origin and interrelationship. *Brain research reviews* 13, pp. 165–178.
- Karlsson, K.R., Cowley, S., Martinez, F.O., Shaw, M., Minger, S.L. and James, W. 2008. Homogeneous monocytes and macrophages from human embryonic stem cells following coculture-free differentiation in M-CSF and IL-3. *Experimental hematology* 36(9), pp. 1167–75.
- Kettenmann, H., Banati, R. and Walz, W. 1993. Electrophysiological behavior of microglia. *Glia* 7(1), pp. 93–101.
- Kettenmann, H., Hanisch, U., Noda, M. and Verkhratsky, A. 2011. Physiology of Microglia. , pp. 461–553.
- De Keyser, J., Mostert, J.P. and Koch, M.W. 2008. Dysfunctional astrocytes as key players in the pathogenesis of central nervous system disorders. *Journal of the neurological sciences* 267(1-2), pp. 3–16.
- El Khoury, J. and Luster, A.D. 2008. Mechanisms of microglia accumulation in Alzheimer's disease: therapeutic implications. *Trends in pharmacological sciences* 29(12), pp. 626–32.
- Kierdorf, K., Erny, D., Goldmann, T., Sander, V., Schulz, C., Perdiguero, E.G., Wieghofer, P., Heinrich, A., Riemke, P., Hölscher, C., Müller, D.N., Luckow, B., Brouwer, T., Debowski, K., Fritz, G., Opdenakker, G., Diefenbach, A., Biber, K., Heikenwalder, M., Geissmann, F., Rosenbauer, F. and Prinz, M. 2013. Microglia emerge from erythromyeloid precursors via Pu.1- and Irf8-dependent pathways. *Nature neuroscience* 16(3), pp. 273–80.
- Kihara-Negishi, F., Yamamoto, H., Suzuki, M., Yamada, T., Sakurai, T., Tamura, T. and Oikawa, T. 2001. In vivo complex formation of PU.1 with HDAC1 associated with PU.1-mediated transcriptional repression. *Oncogene* 20(42), pp. 6039–47.

- Killackey, H.P. 1984. Glia and the elimination of transient cortical projections. *Trends in neurosciences* 7, pp. 2225 – 226.
- Kim, J.B., Sebastiano, V., Wu, G., Araúzo-Bravo, M.J., Sasse, P., Gentile, L., Ko, K., Ruau, D., Ehrich, M., van den Boom, D., Meyer, J., Hübner, K., Bernemann, C., Ortmeier, C., Zenke, M., Fleischmann, B.K., Zaehres, H. and Schöler, H.R. 2009. Oct4-induced pluripotency in adult neural stem cells. *Cell* 136(3), pp. 411–9.
- Kim, J.H., Auerbach, J.M., Rodriguez-Gomez, J.A., Velasco, I., Gavin, D., Lumelsky, N., Lee, S.H., Nguyen, J., Sanchez-Pernaute, R., Bankiewicz, K. and McKay, R.D. 2002. Dopamine neurons derived from embryonic stem cells function in an animal model of Parkinson's disease. *Nature* 418, pp. 50–56.
- Kim, S.U. and de Vellis, J. 2005. Microglia in health and disease. *Journal of neuroscience research* 81(3), pp. 302–13.
- Kim, S.W., Fitzgerald, M.L., Kang, K., Okuhira, K., Bell, S.A., Manning, J., Koehn, S.L., Lu, N., Moore, K.J. and Freeman, M.W. 2005. Abca7 null mice retain normal macrophage phosphatidylcholine and cholesterol efflux activity despite alterations in adipose mass and serum cholesterol levels. *Journal of Biological Chemistry* 280, pp. 3989–3995.
- Kitamura, T., Miyake, T. and Fujita, S. 1984. Genesis of resting microglia in the gray matter of mouse hippocampus. *Journal of Comparative Neurology* 226, pp. 421–433.
- Klee, R., Heinemann, U. and Eder, C. 1999. Voltage-Gated Proton Currents in Microglia of Distinct Morphology and Functional State. *Neuroscience* 91(4), pp. 1415–1424.
- Klemsz, M.J., McKercher, S.R., Celada, a, Van Beveren, C. and Maki, R. a 1990. The macrophage and B cell-specific transcription factor PU.1 is related to the ets oncogene. *Cell* 61(1), pp. 113–24.
- Koeingsknecht-Talboo, J. and Landreth, G. 2005. Microglial Phagocytosis Induced by Fibrillar B-Amyloid and IgGs are Differentially Regulated by Proinflammatory Cytokines. *The Journal of neuroscience : the official journal of the Society for Neuroscience* 25, pp. 8420–8249.
- Kroon, E., Martinson, L., Kadoya, K., Bang, A., Kelly, O., Eliazer, S., Young, H., Richardson, M., Smart, N., Cunningham, J., Aqulnick, A., D'Amour, K., Carpenter, M. and Baetge, E. 2008. Pancreatic endoderm derived from human embryonic stem cells generates glucose-responsive insulin-secreting cells in vivo. *Nature Biotechnology* 26(4), pp. 443–452.
- Lacaud, G., Gore, L., Kennedy, M., Kouskoff, V., Kingsley, P., Hogan, C., Carlsson, L., Speck, N., Palis, J. and Keller, G. 2002. Runx1 is essential for hematopoietic commitment at the hemangioblast stage of development in vitro. *Blood* 100(2), pp. 458–66.

LaFerla, F.M., Green, K.N. and Oddo, S. 2006. Intracellular amyloid-B in Alzheimer's disease. *Nature reviews. Neuroscience* 8, pp. 499–509.

Lambert, J.C., Ibrahim-Verbaas, C. a, Harold, D., Naj, a C., Sims, R., Bellenguez, C., DeStafano, a L., Bis, J.C., Beecham, G.W., Granier-Boley, B., Russo, G., Thorton-Wells, T. a, Jones, N., Smith, a V, Chouraki, V., Thomas, C., Ikram, M. a, Zelenika, D., Vardarajan, B.N., Kamatani, Y., Lin, C.F., Gerrish, a, Schmidt, H., Kunkle, B., Dunstan, M.L., Ruiz, a, Bihoreau, M.T., Choi, S.H., Reitz, C., Pasquier, F., Cruchaga, C., Craig, D., Amin, N., Berr, C., Lopez, O.L., De Jager, P.L., Deramecourt, V., Johnston, J. a, Evans, D., Lovestone, S., Letenneur, L., Morón, F.J., Rubinsztein, D.C., Eiriksdottir, G., Sleegers, K., Goate, a M., Fiévet, N., Huentelman, M.W., Gill, M., Brown, K., Kamboh, M.I., Keller, L., Barberger-Gateau, P., McGuinness, B., Larson, E.B., Green, R., Myers, a J., Dufouil, C., Todd, S., Wallon, D., Love, S., Rogaeva, E., Gallacher, J., St George-Hyslop, P., Clarimon, J., Lleo, a, Bayer, a, Tsuang, D.W., Yu, L., Tsolaki, M., Bossù, P., Spalletta, G., Proitsi, P., Collinge, J., Sorbi, S., Sanchez-Garcia, F., Fox, N.C., Hardy, J., Deniz Naranjo, M.C., Bosco, P., Clarke, R., Brayne, C., Galimberti, D., Mancuso, M., Matthews, F., Moebus, S., Mecocci, P., Del Zompo, M., Maier, W., Hampel, H., Pilotto, a, Bullido, M., Panza, F., Caffarra, P., Nacmias, B., Gilbert, J.R., Mayhaus, M., Lannefelt, L., Hakonarson, H., Pichler, S., Carrasquillo, M.M., Ingelsson, M., Beekly, D., Alvarez, V., Zou, F., Valladares, O., Younkin, S.G., Coto, E., Hamilton-Nelson, K.L., Gu, W., Razquin, C., Pastor, P., Mateo, I., Owen, M.J., Faber, K.M., Jonsson, P. V, Combarros, O., O'Donovan, M.C., Cantwell, L.B., Soininen, H., Blacker, D., Mead, S., Mosley, T.H., Bennett, D. a, Harris, T.B., Fratiglioni, L., Holmes, C., de Bruijn, R.F., Passmore, P., Montine, T.J., Bettens, K., Rotter, J.I., Brice, a, Morgan, K., Foroud, T.M., Kukull, W. a, Hannequin, D., Powell, J.F., Nalls, M. a, Ritchie, K., Lunetta, K.L., Kauwe, J.S., Boerwinkle, E., Riemenschneider, M., Boada, M., Hiltunen, M., Martin, E.R., Schmidt, R., Rujescu, D., Wang, L.S., Dartigues, J.F., Mayeux, R., Tzourio, C., Hofman, a, Nöthen, M.M., Graff, C., Psaty, B.M., Jones, L., Haines, J.L., Holmans, P. a, Lathrop, M., Pericak-Vance, M. a, Launer, L.J., Farrer, L. a, van Duijn, C.M., Van Broeckhoven, C., Moskvina, V., Seshadri, S., Williams, J., Schellenberg, G.D. and Amouyel, P. 2013. Meta-analysis of 74,046 individuals identifies 11 new susceptibility loci for Alzheimer's disease. *Nature genetics* 45(12), pp. 1452–8.

Lasierra-Cirujeda, J., Coronel, P., Aza, M. and Gimeno, M. 2013. Beta-amyloidolysis and glutathione in Alzheimer ' s disease. *Journal of Blood Medicine* 4, pp. 31–38.

Lee, S.H., Lumelsky, N., Studer, L., Auerbach, J.M. and McKay, R.D. 2000. Efficient generation of midbrain and hindbrain neurons from mouse embryonic stem cells. *Nature biotechnology* 18(6), pp. 675–9.

Lehnardt, S. 2010. Innate immunity and neuroinflammation in the CNS: the role of microglia in Toll-like receptor-mediated neuronal injury. *Glia* 58(3), pp. 253–63.

Levantini, E., Radomska, H.S., Hetherington, C.J., Alberich-Jorda, M., Amabile, G., Zhang, P., Gonzalez, D.A., Zhang, J., Basseres, D.S., Wilson, N.K., Koschmieder, S., Huang, G., Zhang, D.E., Ebralidze, A.K., Bonifer, C., Okuno, Y., Gottgens, B. and Tenen, D.G. 2011. RUNX1 regulates the CD34 gene in haematopoietic stem cells by

mediating interactions with a distal regulatory element. *EMBO* 30(119), pp. 4059–4070.

Levenberg, S., Golub, J.S., Amit, M., Itskovitz-Eldor, J. and Langer, R. 2002. Endothelial cells derived from human embryonic stem cells. *Proceedings of the National Academy of Sciences of the United States of America* 99, pp. 4391–4396.

Lewis, C.-A., Manning, J., Rossi, F. and Krieger, C. 2012. The Neuroinflammatory Response in ALS: The Roles of Microglia and T Cells. *Neurology research international* 2012, p. 803701.

Liang, J., Takeuchi, H., Jin, S., Noda, M., Li, H., Doi, Y., Kawanokuchi, J., Sonobe, Y., Mizuno, T. and Suzumura, A. 2010. Glutamate induces neurotrophic factor production from microglia via protein kinase C pathway. *Brain research* 1322, pp. 8–23.

Lim, W.F., Inoue-Yokoo, T., Tan, K.S., Lai, M.I. and Sugiyama, D. 2013. Hematopoietic cell differentiation from embryonic and induced pluripotent stem cells. *Stem cell research & therapy* 4(3), p. 71.

Ling, E.A., Kaur, C. and Wong, W.C. 1982. Light and electron microscopic demonstration of non-specific esterase in ameboid microglial cells in the corpus callosum in postnatal rats: a cytochemical link to monocytes. *Journal of Anatomy* 135, pp. 385 – 394.

Link, C.D. 2005. Invertebrate models of Alzheimer's disease. *Genes, brain, and behavior* 4(3), pp. 147–56.

Liu, W., Brosnan, C.F., Dickson, D.W. and Lee, S.C. 1994. Short Communication Macrophage Colony-Stimulating Factor Mediates Human Fetal Central Nervous System Culture. 145(1), pp. 48–53.

Livak, K.J. and Schmittgen, T.D. 2001. Analysis of relative gene expression data using real-time quantitative PCR and the 2<sup>-Delta Delta C(T)</sup> Method. *Methods (San Diego, Calif.)* 25(4), pp. 402–8.

Loh, Y.-H., Wu, Q., Chew, J.-L., Vega, V.B., Zhang, W., Chen, X., Bourque, G., George, J., Leong, B., Liu, J., Wong, K.-Y., Sung, K.W., Lee, C.W.H., Zhao, X.-D., Chiu, K.-P., Lipovich, L., Kuznetsov, V. a, Robson, P., Stanton, L.W., Wei, C.-L., Ruan, Y., Lim, B. and Ng, H.-H. 2006. The Oct4 and Nanog transcription network regulates pluripotency in mouse embryonic stem cells. *Nature genetics* 38(4), pp. 431–40.

Mak, K.S., Funnell, A.P.W., Pearson, R.C.M. and Crossley, M. 2011. PU.1 and Haematopoietic Cell Fate: Dosage Matters. *International journal of cell biology* 2011, p. 808524.

Mander, P.K., Jekabsone, a. and Brown, G.C. 2006. Microglia Proliferation Is Regulated by Hydrogen Peroxide from NADPH Oxidase. *The Journal of Immunology* 176(2), pp. 1046–1052.

- Maniatis, T., Fritsch, E.F. and Sambrook, J. 1982. *Molecular Cloning: A Laboratory Manual*. Cold Spring Harbor Laboratory.
- Manz, M.G., Miyamoto, T., Akashi, K. and Weissman, I.L. 2002. Prospective isolation of human clonogenic common myeloid progenitors. *Proceedings of the National Academy of Sciences of the United States of America* 99(18), pp. 11872–7.
- Marquis, J.-F., Kapoustina, O., Langlais, D., Ruddy, R., Dufour, C.R., Kim, B.-H., MacMicking, J.D., Giguère, V. and Gros, P. 2011. Interferon regulatory factor 8 regulates pathways for antigen presentation in myeloid cells and during tuberculosis. *PLoS genetics* 7(6), p. e1002097.
- Martin, C., Ingersoll, S.A. and Martin, B.K. 2007. Transcriptional control of the C3a receptor gene in glial cells: dependence upon AP-1 but not Ets. *Molecular Immunology* 44, pp. 703–712.
- Martin, G.R. 1981. Isolation of a pluripotent cell line from early mouse embryos cultured in medium conditioned by teratocarcinoma stem cells *Developmental Biology* : 78(12), pp. 7634–7638.
- Mattson, M.P. 2000. Apoptosis in neurodegenerative disorders. *Nature reviews. Molecular cell biology* 1(2), pp. 120–9.
- McGeer, P.L., Schulzer, M. and McGeer, E.G. 1996. Arthritis and anti-inflammatory agents as possible protective factors for Alzheimer's disease: a review of 17 epidemiologic studies. *Neurology* 47(2), pp. 425–432.
- McGrath, K.E. and Palis, J. 2005. Hematopoiesis in the yolk sac: more than meets the eye. *Experimental hematology* 33(9), pp. 1021–1028.
- McIvor, Z., Hein, S., Fiegler, H., Schroeder, T., Stocking, C., Just, U. and Cross, M. 2003. Transient expression of PU.1 commits multipotent progenitors to a myeloid fate whereas continued expression favors macrophage over granulocyte differentiation. *Experimental hematology* 31(1), pp. 39–47.
- McLarnon, J.G., Xu, R., Lee, Y.B. and Kim, S.U. 1997. Ion channels of human microglia in culture. *Neuroscience* 78(4), pp. 1217–28.
- Merkle, F.T. and Alvarez-Buylla, A. 2006. Neural stem cells in mammalian development. *Current opinion in cell biology* 18(6), pp. 704–9.
- Merrill, J.E. 1987. Macrogliia : neural cells responsive to lymphokines and growth fadors. 8(5), pp. 146–150.
- Metcalf, D. 1992. Synergistic suppression: anomalous inhibition of the proliferation of factor-dependent hamopoietic cells by combination of two colony-stimulating factors. *Proceedings of the National Academy of Sciences of the United States of America* 89, pp. 2819–2823.

- Milton, N.G.N., Campus, R.F., Street, R.H. and Nw, L. 1999. Amyloid-B binds catalase with highaffinity and inhibits hydrogen peroxide breakdown. *Biochemical Journal* 296, pp. 293–296.
- Min, J.Y., Yang, Y., Converso, K.L., Liu, L., Huang, Q., Morgan, J.P. and Xiao, Y.F. 2002. Transplantation of emryonic stem cells improves cardiac function in postinfarcted rats. *Journal of Applied Physiology* 92, pp. 288–296.
- Mineur, Y.S., McLoughlin, D., Crusio, W.E. and Sluyter, F. 2005. Genetic Mouse Models of Alzheimer’s Disease. *Neural Plasticity* 12(4), pp. 299–310.
- Moore, M.A.S. and Metcalf, D. 1970. Ontogeny of the haematopoietic system: yolk sac origin in vivo and in vitro colony forming cells in the developing mouse embryo. *British Journal of Haematology* 18, p. 279.
- Napoli, I., Kierdorf, K. and Neumann, H. 2009. Microglial precursors derived from mouse embryonic stem cells. *Glia* 57(15), pp. 1660–71.
- Narantuya, D., Nagai, A., Sheikh, A.M., Masuda, J., Kobayashi, S., Yamaguchi, S. and Kim, S.U. 2010. Human Microglia Transplanted in Rat Focal Ischemia Brain Induce Neuroprotection and Behavioral Improvement. *PLoS ONE* 5(7), p. e11746.
- Navascués, J., Cuadros, M.A. and Almendros, A. 1996. Development of microglia: Evidence from studies in the avain central nervous system. In: Ling, E. A., Tan, C. K., and Tan, C. B. . eds. *Topical Issues in Microglial Research*. Singapore: Singapore Neuroscience Assosication, pp. 43–64.
- Neher, J.J., Neniskyte, U., Zhao, J.-W., Bal-Price, A., Tolkovsky, A.M. and Brown, G.C. 2011. Inhibition of microglial phagocytosis is sufficient to prevent inflammatory neuronal death. *Journal of immunology (Baltimore, Md. : 1950)* 186(8), pp. 4973–83.
- Neumann, J., Gunzer, M., Gutzeit, H.O., Ullrich, O., Reymann, K.G. and Dinkel, K. 2006. Microglia provide neuroprotection after ischemia. *FASEB journal : official publication of the Federation of American Societies for Experimental Biology* 20(6), pp. 714–6.
- Nicholson, E. and Randall, a D. 2009. Na(v)1.5 sodium channels in a human microglial cell line. *Journal of neuroimmunology* 215(1-2), pp. 25–30.
- Niwa, H., Burdon, T., Chamber, I. and Smith, A. 1998. Self-renewal of pluripotent embryonic stem cells is mediated via activation of STAT3. *Genes and Development* 12, pp. 2048–2060.
- Odero, M., Zeleznik-Le, N., Chinwalla, V. and Rowley, J. 2000. cytogenetic and molecular analysis of the acute monocytic leukemia cell line THP-1 with an MLL-AF9 translocation. *Genes, Chromosomes and Cancer* 29(4), pp. 333–338.
- Ohgidani, M., Kato, T. a, Setoyama, D., Sagata, N., Hashimoto, R., Shigenobu, K., Yoshida, T., Hayakawa, K., Shimokawa, N., Miura, D., Utsumi, H. and Kanba, S.

2014. Direct induction of ramified microglia-like cells from human monocytes: dynamic microglial dysfunction in Nasu-Hakola disease. *Scientific reports* 4, p. 4957.
- Orlovskaya, I., Schraufstatter, I., Loring, J. and Khaldoyanidi, S. 2008. Hematopoietic differentiation of embryonic stem cells. *Methods (San Diego, Calif.)* 45(2), pp. 159–67.
- Palis, J., Robertson, S., Kennedy, M. and Al, E. 1999. Development of erythroid and myeloid progenitors in the yolk sac and embryo proper of the mouse. *Development* 126, p. 5073.
- Palis, J. and Yoder, M.C. 2001. Yolk-sac hematopoiesis : The first blood cells of mouse and man. 29, pp. 927–936.
- Parakalan, R., Jiang, B., Nimmi, B., Janani, M., Jayapal, M., Lu, J., Tay, S.S.W., Ling, E.-A. and Dheen, S.T. 2012. Transcriptome analysis of amoeboid and ramified microglia isolated from the corpus callosum of rat brain. *BMC neuroscience* 13(1), p. 64.
- Parpura, V., Basarsky, Trent, A., Liu, F., Jeftinija, K., Jeftinija, S. and Haydon, Philip, G. 1994. Glutamate-mediated astrocyte-neuron signalling. *Nature* 369, pp. 744 – 747.
- Patterson, S., Gross, J., Bedford, P. and Knight, S.C. 1991. Morphology and phenotype of dendritic cells from peripheral blood and their productive and non-productive infection with human immunodeficiency virus type 1. *Immunology* 72(3), pp. 361–7.
- Perry, V.H., Hume, D.. and Gordon, S. 1985. Immunohistochemical localization of macrophages and microglia in the adult and developing mouse brain. *Neuroscience* 15(2), pp. 313 – 326.
- Pittman, A.M., Fung, H.-C. and de Silva, R. 2006. Untangling the tau gene association with neurodegenerative disorders. *Human molecular genetics* 15 Spec No(2), pp. R188–95.
- Priller, C., Bauer, T., Mitteregger, G., Krebs, B., Kretzschmar, H. a and Herms, J. 2006. Synapse formation and function is modulated by the amyloid precursor protein. *The Journal of neuroscience : the official journal of the Society for Neuroscience* 26(27), pp. 7212–21.
- Priller, J., Flugel, A., Wehner, T., Boentert, M., Haas, C.A., Prinz, M., Fernandez-Klett, F., Prass, K., Bechmann, I., de Boer, B.A., Frotscher, M., Kreutzberg, G.W., Persons, D.A. and Dirnagl, U. 2001. Targeting gene-modified hematopoietic cells to the central nervous system: use of green fluorescent protein uncovers microglial engraftment. *Nature Medicine* 7(12), pp. 1356–1361.
- Putnam, A.J. and Mooney, D.J. 1996. Tissue Engineering using synthetic extracellular matrices. *Nature Medicine* 2, pp. 824–826.

- Rambaldi, A., Young, D.C. and Griffin, D. 1987. Expression of the M-CSF (CSF-1) gene by human monocytes. *Blood* 69, pp. 1409–1413.
- Ray, D., Culine, S., Tavittain, A. and Moreau-Gachelin, F. 1990. The human homologue of the putative proto-oncogene Spi-1: characterisation and expression in tumors. *Oncogene* 5(5), pp. 663–668.
- Reed-Geaghan, E.G., Savage, J.C., Hise, A.G. and Landreth, G. 2009. CD14 and toll-like receptors 2 and 4 are required for fibrillar AB-stimulated microglial activation. *The Journal of neuroscience : the official journal of the Society for Neuroscience* 29, pp. 11982–11992.
- Rezaie, P. and Male, D. 2002. Differentiation, Ramification and Distribution of microglia within the Central Nervous System Examined. *Neuroembryology and Aging* 1(1), pp. 29–43.
- Del Rio-Hortega, P. 1919. El “tercer element” de los centros nerviosos. I. La microglia en estado normal. II. Intervencion de la microglia an los procesos patologicos (Celulas en bastoncito y cuerpo granulo-adiposos). III. Naturaleza probable de la microglia. *Bol. Soc. Espan. Biol* 9, pp. 68–120.
- Del Rio-Hortega, P. 1932. Microglia. In: Penfield, W. ed. *Cytology and Cellular Pathology of the Nervous System*. New York: Paul B. Hoeber, pp. 483 – 534.
- Roberts, K., Zeineddine, R., Corcoran, L., Li, W., Campbell, I.L. and Yerbury, J.J. 2013. Extracellular aggregated Cu/Zn superoxide dismutase activates microglia to give a cytotoxic phenotype. *Glia* 61(3), pp. 409–19.
- Rosenthal, S.L. and Kamboh, M.I. 2014. Late-Onset Alzheimer’s Disease Genes and the Potentially Implicated Pathways. *Current genetic medicine reports* 2, pp. 85–101. Available at:
- Rushton, D.J., Mattis, V.B., Svendsen, C.N., Allen, N.D. and Kemp, P.J. 2013. Stimulation of GABA-induced Ca<sup>2+</sup> influx enhances maturation of human induced pluripotent stem cell-derived neurons. *PloS one* 8(11), p. e81031.
- Saijo, K. and Glass, C.K. 2011. Microglial cell origin and phenotypes in health and disease. *Nature reviews. Immunology* 11(11), pp. 775–87.
- Sasaki, A., Horikoshi, Y., Yokoo, H., Nakazato, Y. and Yamaguchi, H. 2003. Antiserum against human glucose transporter 5 is highly specific for microglia among cells of the mononuclear phagocyte system. *Neuroscience letters* 338(1), pp. 17–20.
- Sasaki, K. and Matsamura, G.A. 1986. Haematopoietic cells of the yolk sac and the liver in mouse embryo: a light and electron microscopical study. *Journal of Anatomy* 148, p. 87.
- Schiegelmich, T., Henke, K. and Peri, F. 2011. Microglia in the developing brain: from immunity to behavior. *Current Opinion in Neurobiology* 21, pp. 5–10.

- Schilling, T., Nitsch, R., Heinemann, U., Haas, D. and Eder, C. 2001. Astrocyte-released cytokines induce ramification and outward K<sup>+</sup> channel expression in microglia via distinct signalling pathways. *European Journal of Neuroscience* 14(3), pp. 463–473.
- Schmidtmayer, J., Jacobsen, C., Miksch, G. and Sievers, J. 1994. Blood monocytes and spleen macrophages differentiate into microglia-like cells on monolayers of astrocytes: membrane currents. *Glia* 12(4), pp. 259–67.
- Sedgwick, J.D., Schwender, S., Imrich, H., Dörries, R., Butcher, G.W. and ter Meulen, V. 1991. Isolation and direct characterization of resident microglial cells from the normal and inflamed central nervous system. *Proceedings of the National Academy of Sciences of the United States of America* 88(16), pp. 7438–42.  
Available at:  
<http://www.pubmedcentral.nih.gov/articlerender.fcgi?artid=52311&tool=pmcentrez&endertype=abstract>.
- Shudo, K., Fukasawa, H., Nakagomi, M. and Yamagata, N. 2009. Towards Retinoid Therapy for Alzheimer ' s Disease. , pp. 302–311.
- Si, Q., Nakamura, Y. and Kataoka, K. 1997. Albumin enhances superoxide production in cultured microglia. *Glia* 21(4), pp. 413–418.
- Sievers, J., Parwaresch, R. and Wottge, H.U. 1994. Blood monocytes and spleen macrophages differentiate into microglia-like cells on monolayers of astrocytes: morphology. *Glia* 12(4), pp. 245–58.
- Simard, a R., Soulet, D., Gowing, G., Julien, J.P. and Rivest, S. 2006. Bone Marrow-Derived Microglia Play a Critical Role in Restricting Senile Plaque Formation in Alzheimer's Disease. *Neuron* 49, pp. 489–502.
- Sporle, R. and Schughart, K. 1997. Neural Tube Morphogenesis. *Current Opinion in Genetics and Development* 7, pp. 507 – 512.
- Strauss-Ayali, D., Conrad, S.M. and Mosser, D.M. 2007. Monocyte subpopulations and their differentiation patterns during infection. *Journal of leukocyte biology* 82(2), pp. 244–52.
- Strazza, M., Pirrone, V., Wigdhal, B. and Nonnemacher, M.R. 2011. Breaking down the barrier: the effects of HIV-1 on the blood-brain barrier. *Brain research* 1399, pp. 96–115.
- Sumi, S.M., Bird, T.D., Nochlin, D. and Raskind, M.A. 1992. Familial presenile dementia with psychosis associated with cortical neurofibrillary tangles and degeneration of the amygdala. *Neurology* 42(1), pp. 120 – 127.
- Sun, Y.E., Martinowich, K. and Ge, W. 2003. Making and repairing the mammalian brain - signaling toward neurogenesis and gliogenesis. *Seminars in Cell and Developmental Biology* 14, pp. 161–168.

- Suzuki, A., Raya, A., Kawakami, Y., Morita, M., Matsui, T., Nakashima, K., Gage, F.H., Rodriguez-Esteban, C. and Belmonte, J.C.I. 2006. Nanog binds to Smad1 and blocks bone morphogenetic protein-induced differentiation of embryonic stem cells. *Proceedings of the National Academy of Sciences of the United States of America* 103(27), pp. 10294–10299.
- Suzumura, a, Marunouchi, T. and Yamamoto, H. 1991. Morphological transformation of microglia in vitro. *Brain research* 545(1-2), pp. 301–6.
- Takahashi, K., Tanabe, K., Ohnuki, M., Narita, M., Ichisaka, T., Tomoda, K. and Yamanaka, S. 2007. Induction of pluripotent stem cells from adult human fibroblasts by defined factors. *Cell* 131(5), pp. 861–72.
- Takahashi, S. 2011. *Myeloid Leukemia - Basic Mechanisms of Leukemogenesis*. December, . Koschmieder, S. ed. InTech.
- Tanaka, R., Komine-Kobayashi, M., Mochizuki, H., Yamada, M., Furuya, T., Migita, M., Shimada, T., Mizuno, Y. and Urabe, T. 2003. Migration of enhanced green fluorescent protein expressing bone marrow-derived microglia/macrophage into the mouse brain following permanent focal ischemia. *Neuroscience* 117(3), pp. 531–539.
- Tanzi, R.. and Bertram, L. 2001. New Frontiers in Alzheimer's Disease Genetics. *Neuron* 32, pp. 181–184.
- Thomson, J.A., Itskovitz-Eldor, J., Shapiro, S.S., Waknitz, M.A., Swiegiel, J.J., Marshall, V.S. and Jones, J.M. 1998. Embryonic Stem Cell Lines Derived from Human Blastocysts. *Science* 282, pp. 1145–1147.
- Toulme, E. and Khakh, B.S. 2012. ImagingP2X4 Receptor Lateral Mobility in Microglia: REGULATION BY CALCIUM AND p38 MAPK. *The Journal of Biological Chemistry* 287(18), pp. 14734–14748.
- Tschiya, S., Yamabe, M., Yamaguchi, Y., Kobayashi, Y., Konno, T. and Tada, K. 1980. Establishment and characterisation of a human acute monocytic leukemia cell line (THP-1). *International journal of cancer* 26(2), pp. 171–176.
- Vilhardt, F. 2005. Microglia: phagocyte and glia cell. *The International Journal of Biochemistry and Cell Biology* 37, pp. 17–21.
- Virchow, R. 1846. uber das granuliert ansehen de Wandungen der Gehirnventrikel. *Allg Z Psychiat* 3, pp. 242–250.
- Walton, M.R., Gibbons, H., MacGibbon, G. a, Sirimanne, E., Saura, J., Gluckman, P.D. and Dragunow, M. 2000. PU.1 expression in microglia. *Journal of neuroimmunology* 104(2), pp. 109–15.
- Van Wilgenburg, B., Browne, C., Vowles, J. and Cowley, S. a 2013. Efficient, long term production of monocyte-derived macrophages from human pluripotent stem cells under partly-defined and fully-defined conditions. *PloS one* 8(8), p. e71098.

- Williams, R.L., Hilton, D.J., Pease, S., Wilson, T.A., Stewart, C.L., Gearing, D.P., Wagner, E.F., Metcalf, D., Nicola, N.A. and Gough, N.M. 1988. Myeloid leukaemia inhibitory factor maintains the developmental potential of embryonic stem cells. *Nature* 336, pp. 684–687.
- Wisniewski, T. and Konietzko, U. 2008. Amyloid-B immunisation of Alzheimer's disease. *Lancet Neurology* 7(9), pp. 805–811.
- Yamamoto, H., Kihara-Negishi, F., Yamada, T., Hashimoto, Y. and Oikawa, T. 1999. Physical and functional interactions between the transcription factor PU.1 and the coactivator CBP. *Oncogene* 18(7), pp. 1495–501.
- Yang, Z.F., Poon, R.T., Luo, Y., Cheung, C.K., Ho, D.W., Lo, C.M. and Fan, S.T. 2004. Up-Regulation of Vascular Endothelial Growth Factor (VEGF) in Small-for-Size Liver Grafts Enhances Macrophage Activities through VEGF Receptor 2-Dependent Pathway. *The Journal of Immunology* 173(4), pp. 2507–2515.
- Yokomizo, T., Hasegawa, K., Ishitobi, H., Osato, M., Ema, M., Ito, Y., Yamamoto, M. and Takahashi, S. 2008. Runx1 is involved in primitive erythropoiesis in the mouse. *Blood* 111(8), pp. 4075–80.
- Zhao, T., Xia, Y., Li, L., Zhu, G., Chen, S., Feng, H. and Lin, J. 2009. Bovine serum albumin promotes IL-1beta and TNF-alpha secretion by N9 microglia cells. *Neurological Sciences* 30(5), pp. 379–383.
- Zielasek, J. and Hartung, H.P. 1996. Molecular mechanisms of microglial activation. *Advances in neuroimmunology* 6(2), pp. 191–22.

---

# APPENDICES

---

---

## APPENDIX I

---

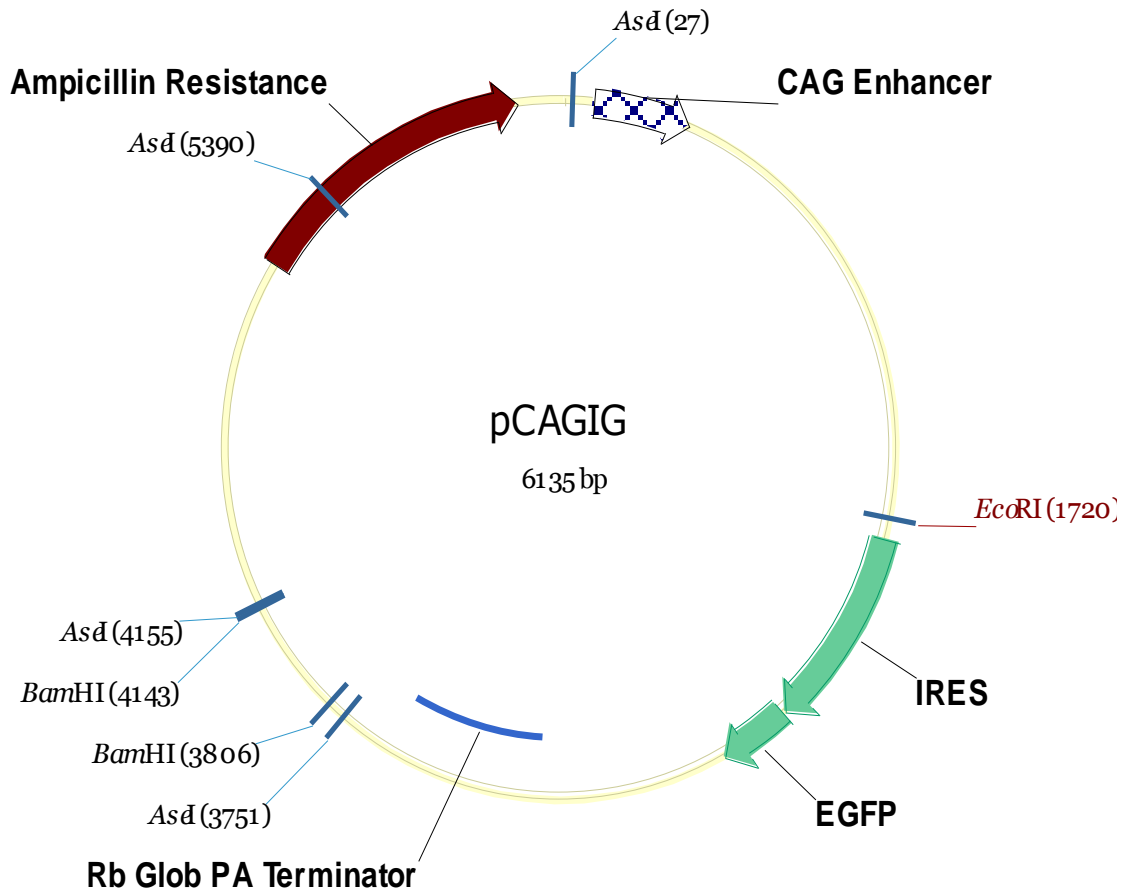
---

### I.I PU.1 SEQUENCED REGION (825BP)

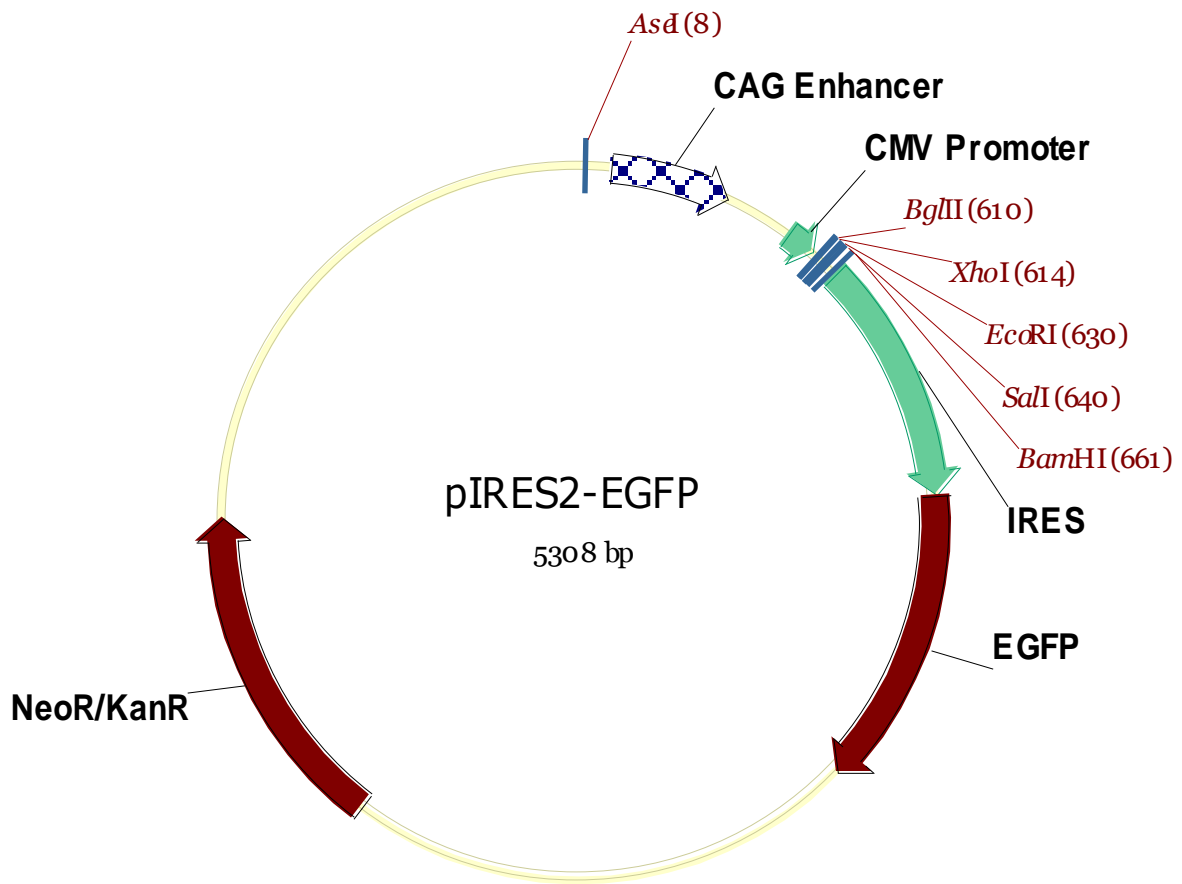
---

**GGATCCATGTTACAGGCGTGCAAAATG**gaagggtttcccctcgtccccctccatcagaagacctggt  
gccctatgacacggatctataccaacgcCAAacgcacgagtattaccctatctcagcagtgatgggg  
agagccatagcgaccattactgggacttccacccccaccacgtgcacagcgagttcgagagcttcgcc  
gagaacaacttcacggagctccagagcgtgcagcccccgagctgcagcagctctaccgccacatgga  
gctggagcagatgcacgtcctcgatacccccatgggtgccaccccatcccagtcttggccaccaggtct  
cctacctgccccggatgtgcctccagtacccatccctgtcccagcccagcccagctcagatgaggag  
gagggcgagcggcagagcccccaactggaggtgtctgacggcgaggcggatggcctggagcccggg  
tgggctcctgcctggggagacaggcagcaagaagaagatccgctgtaccagttcctggtggacctgc  
tccgcagcggcgacatgaaggacagcatctggtgggtggacaaggacaaggcaccttccagttctcg  
tccaagcacaaggaggcgctggcgcaccgctggggcatccagaagggaaccgcaagaagatgacct  
ccagaagatggcgcgcgcgctgcgcaactacggcaagacgggaggtcaagaaggtgaagaagaagc  
tcacctaccagttcagcggcgaagtgctgggcccgggggcctggccgagcg**GCGCCACCCGCCAC**  
**TGAGGATCC**

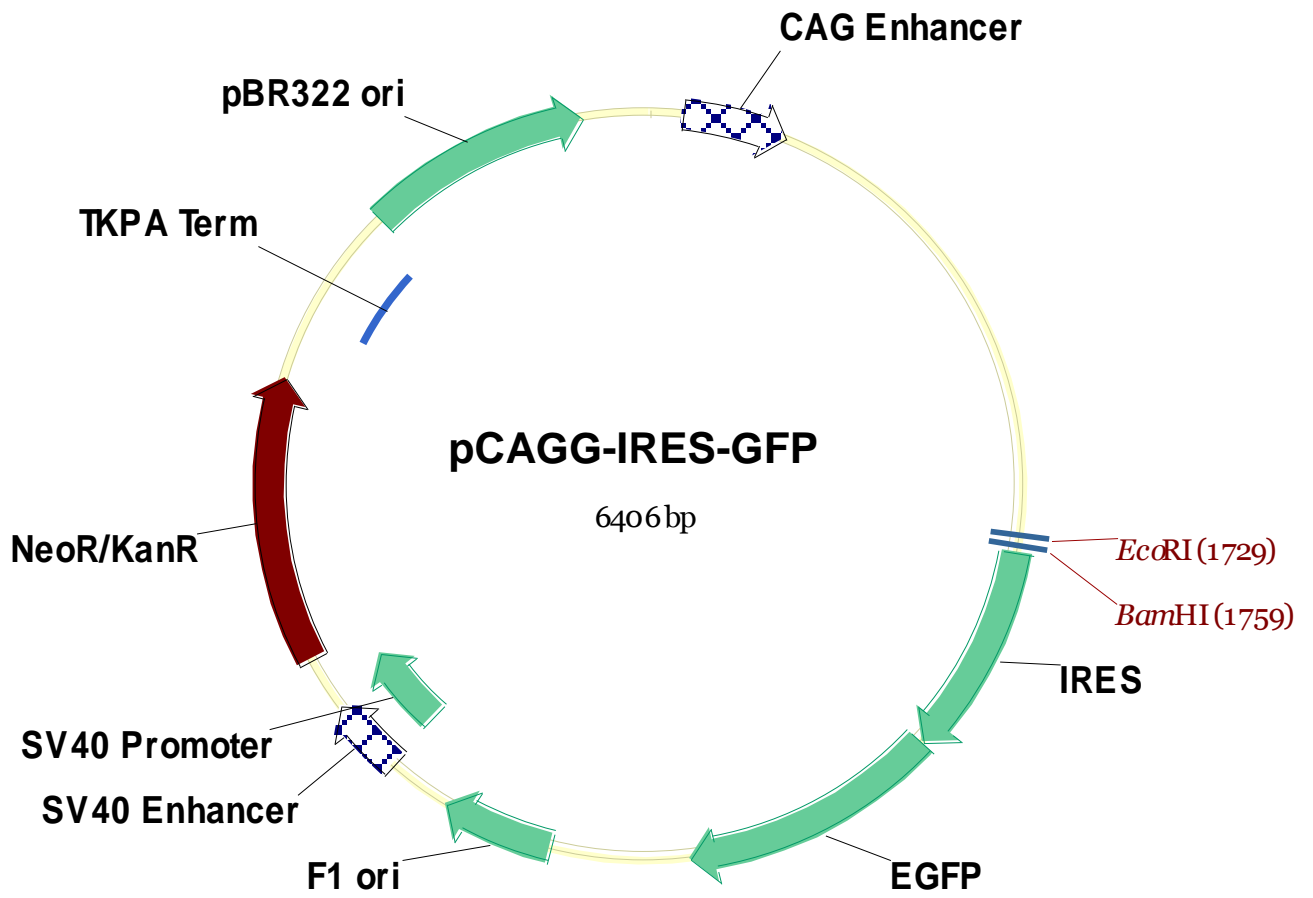
I.II PCAGIG



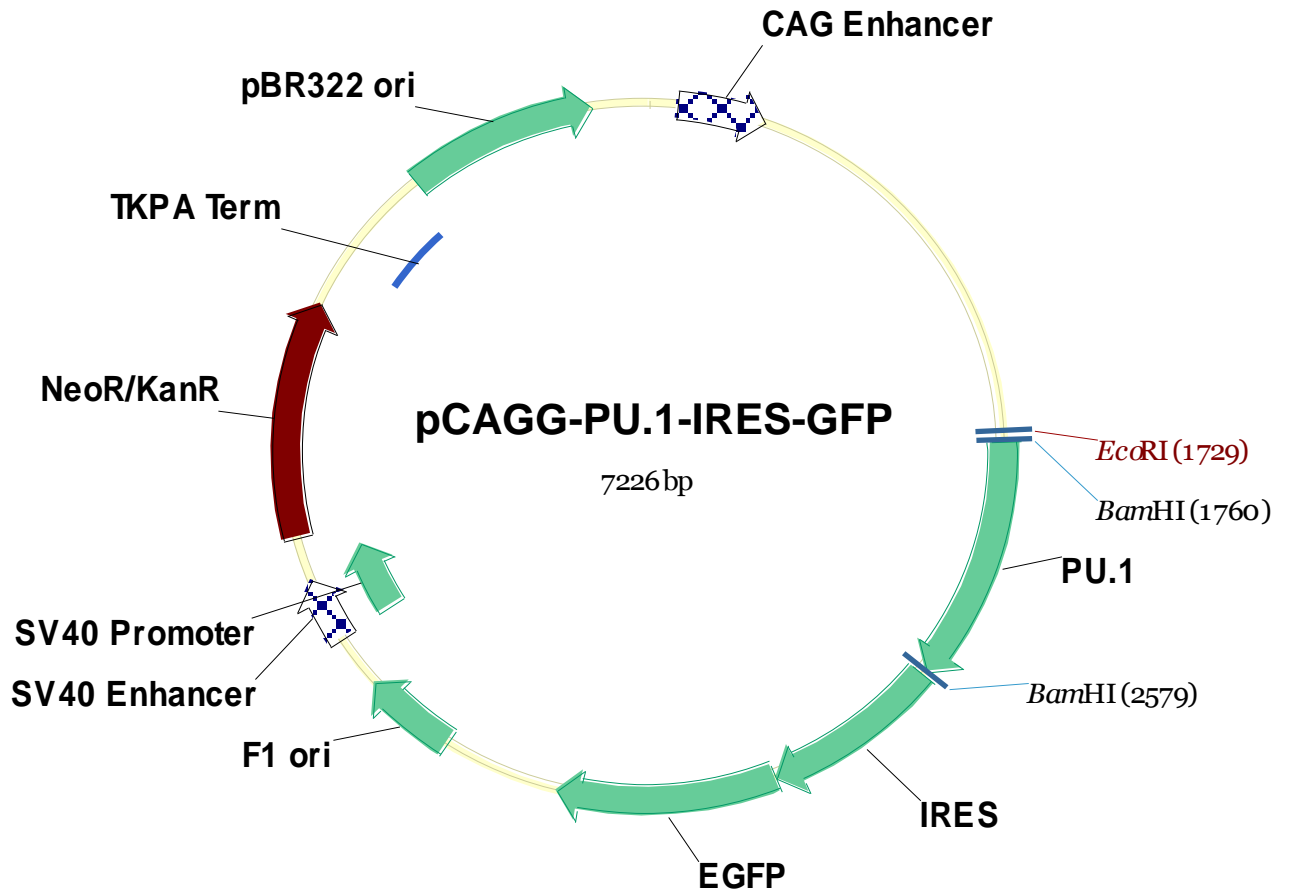
I.III PIRES2-EGFP



I.IV PCAGG-IRES-GFP



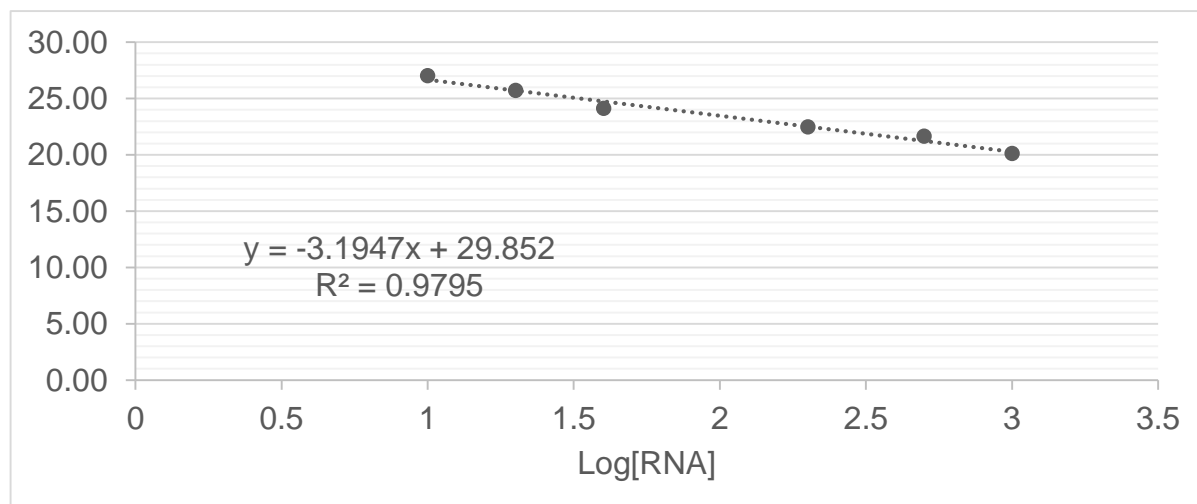
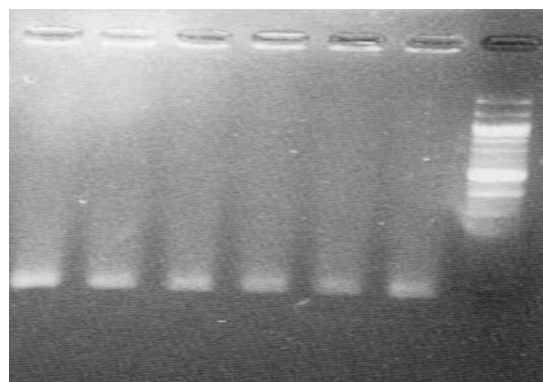
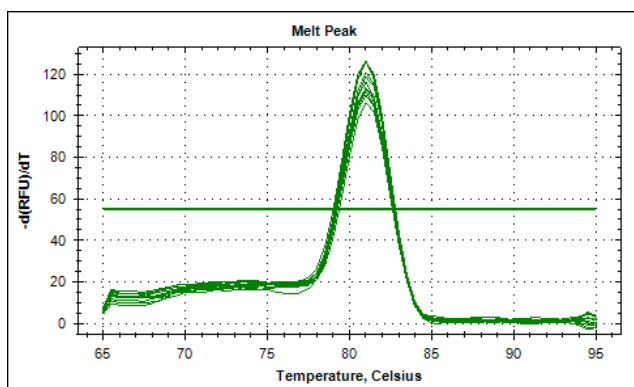
I.V PCAGG-PU.1-IRES-GFP



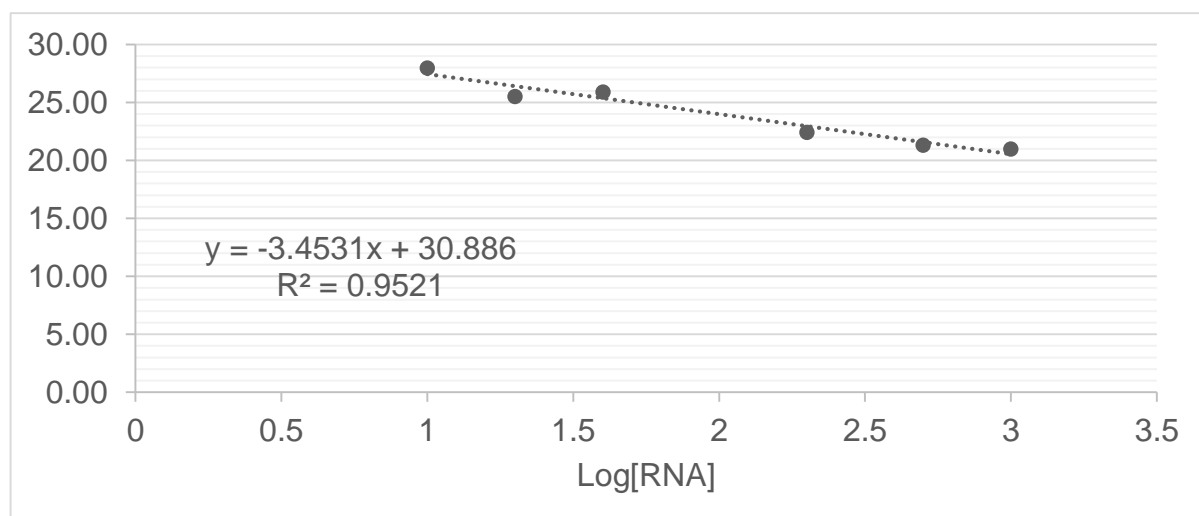
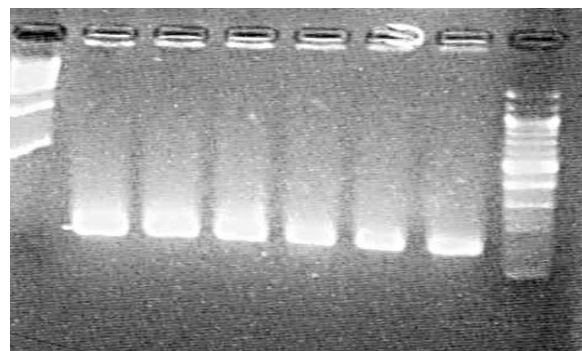
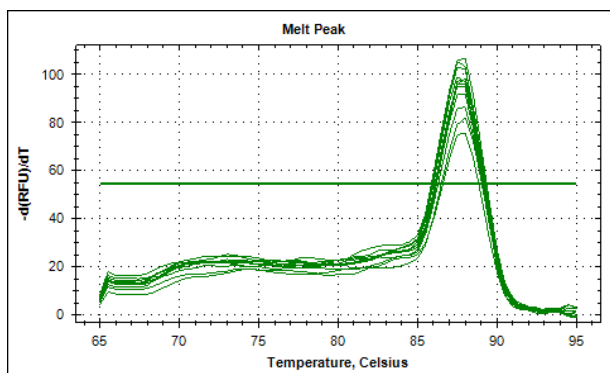
APPENDIX II

II.I QPCR PRIMER DATA SHEETS

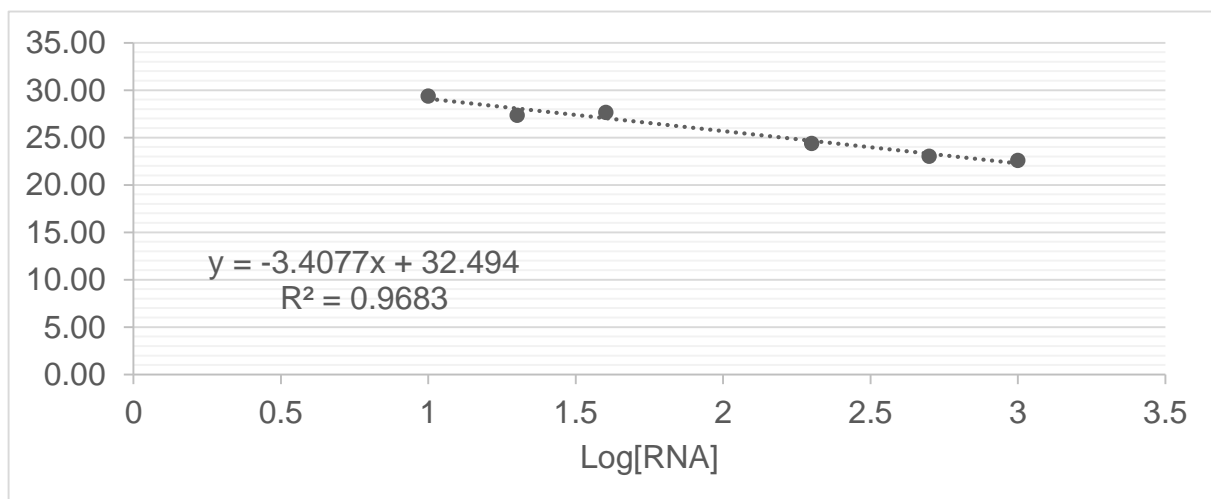
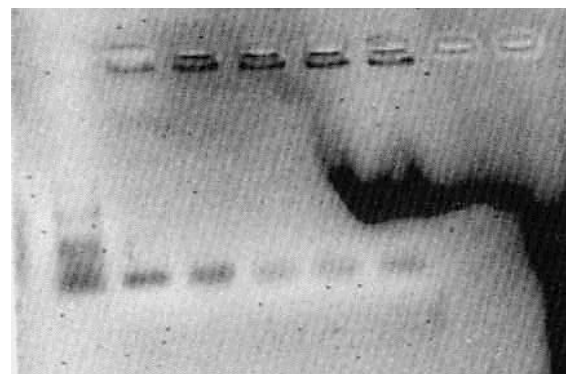
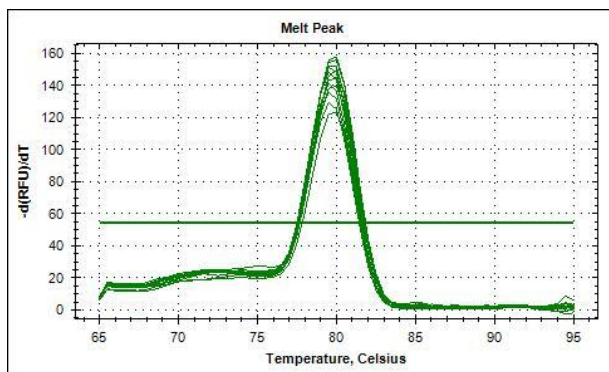
RUNX1	
Accession Number	NM_001754.4
Forward Sequence (5'→3')	CTGCCCATCGCTTTCAAGGT (20)
Tm (°C)	59.4
GC content	55%
Reverse Sequence (5'→3')	GCCGAGTAGTTTTTCATCATTGCC (23)
Tm (°C)	60.6
GC content	47.8%
% Efficiency	105.5%



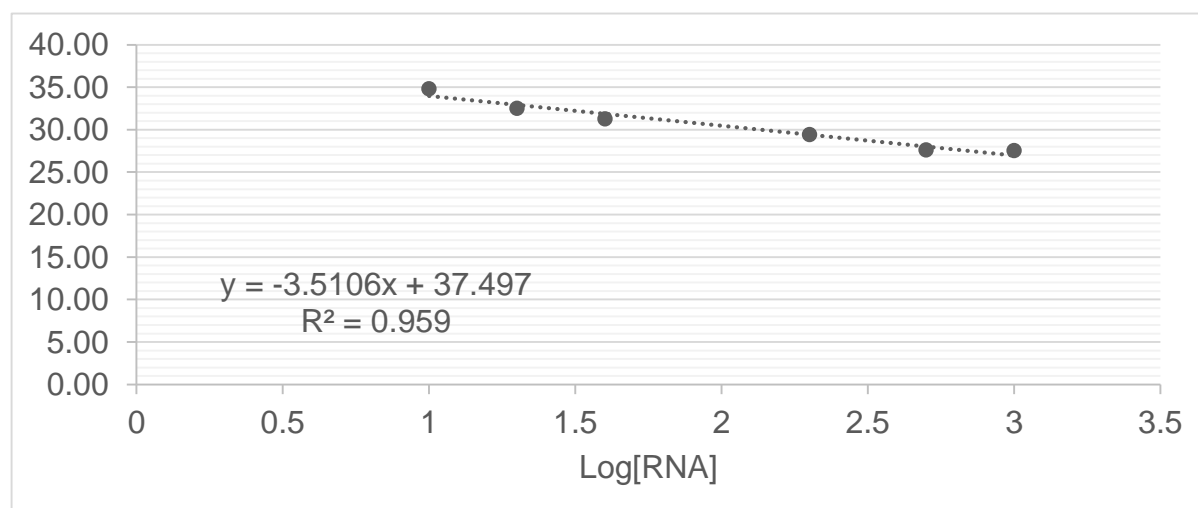
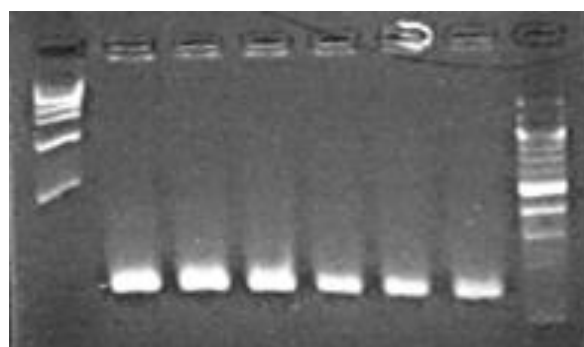
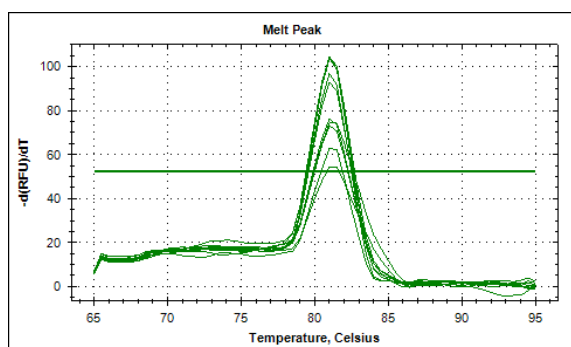
PU.1	
Accession Number	NM_001080547.1
Forward Sequence (5'→3')	CCAGCTCAGATGAGGAGGAG (20)
Tm (°C)	61.4
GC content	60%
Reverse Sequence (5'→3')	CAGGTCCAACAGGAACTGGT (20)
Tm (°C)	59.4
GC content	55%
% Efficiency	94.8%



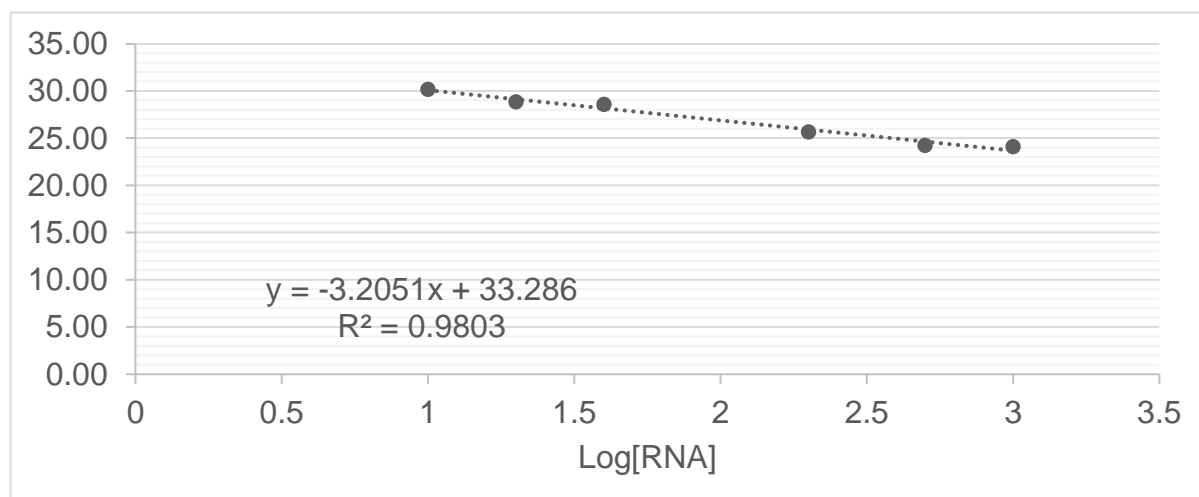
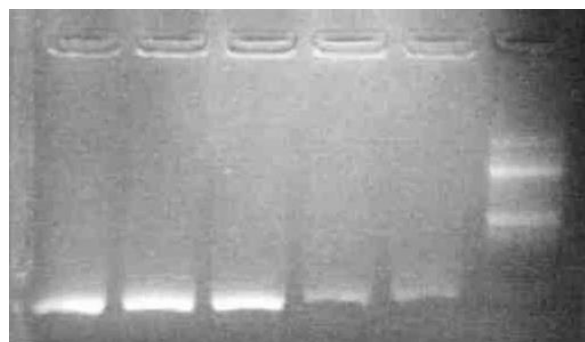
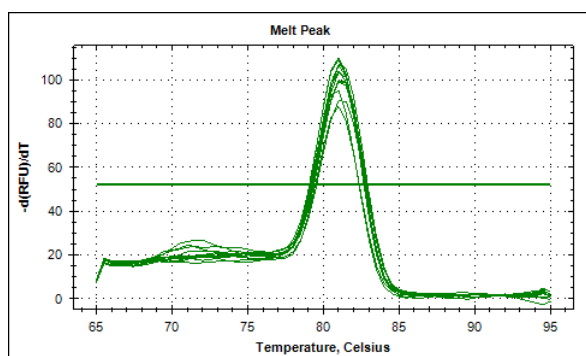
IBA-1	
Accession Number	NM_001623.3
Forward Sequence (5'→3')	GCTGAGCTATGAGCCAAACC (20)
Tm (°C)	59.4
GC content	55%
Reverse Sequence (5'→3')	TCATCCAGCCTCTCTTCCTG (20)
Tm (°C)	59.4
GC content	55%
% Efficiency	96.5%



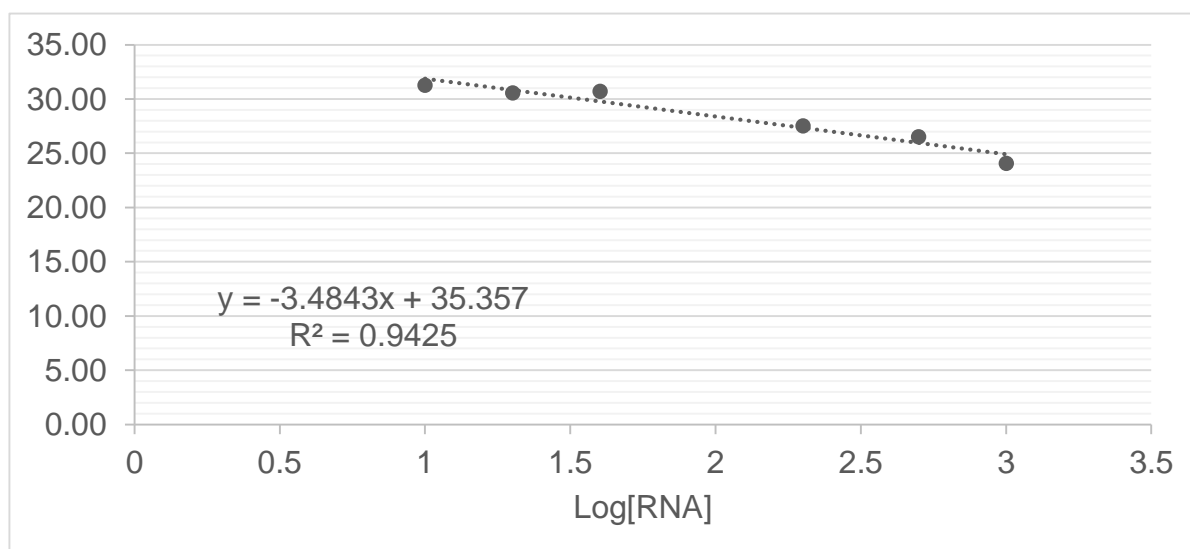
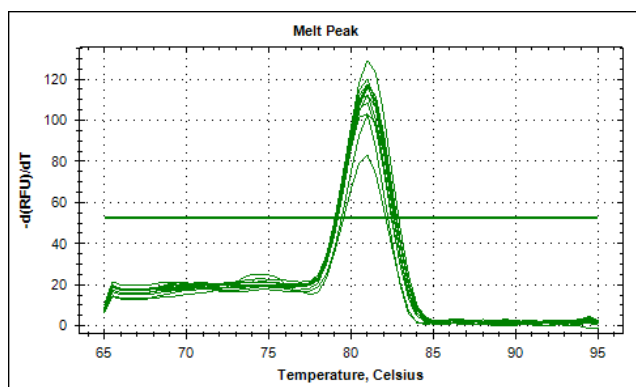
CD45	
Accession Number	NM_002838.4
Forward Sequence (5'→3')	CATTTGGCTTTGCCTTTCTG (20)
T <sub>m</sub> (°C)	55.3
GC content	45%
Reverse Sequence (5'→3')	TTCTCTTCAAAGGTGCTTGC (21)
T <sub>m</sub> (°C)	55.9
GC content	42.9%
% Efficiency	92.7%



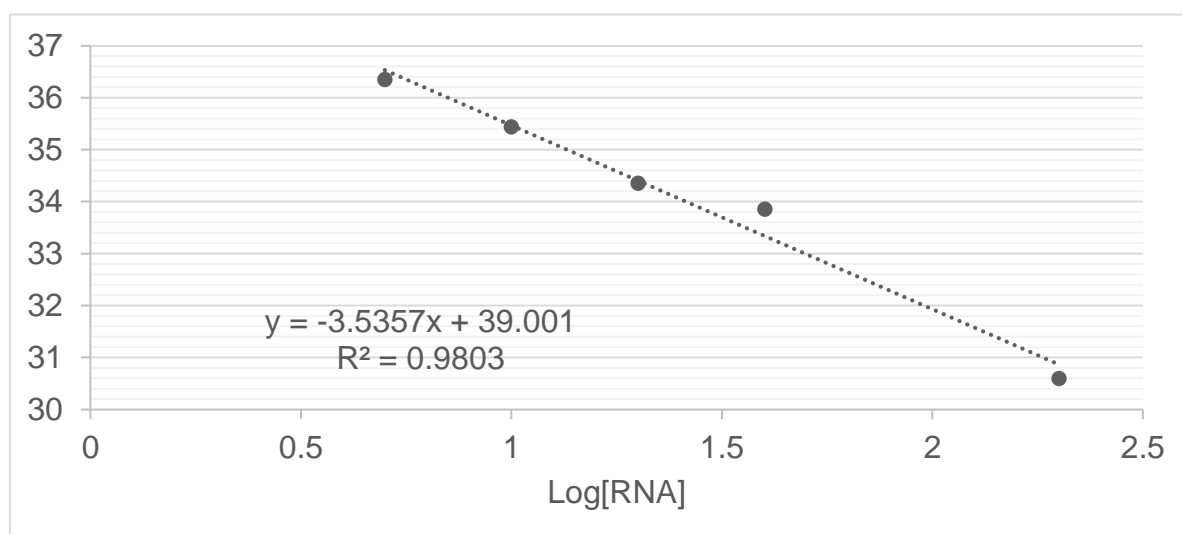
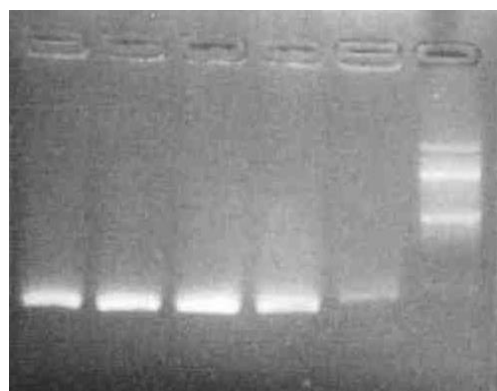
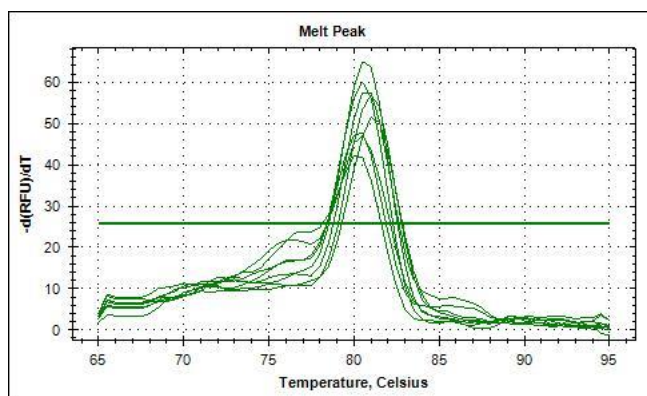
IL-1 $\beta$	
Accession Number	NM_000576.2
Forward Sequence (5'→3')	ACAGATGAAGTGCTCCTTCCA (21)
Tm (°C)	57.9
GC content	47.6%
Reverse Sequence (5'→3')	GTCGGAGATTCGTAGCTGGAT (21)
Tm (°C)	59.8
GC content	52.4%
% Efficiency	105%



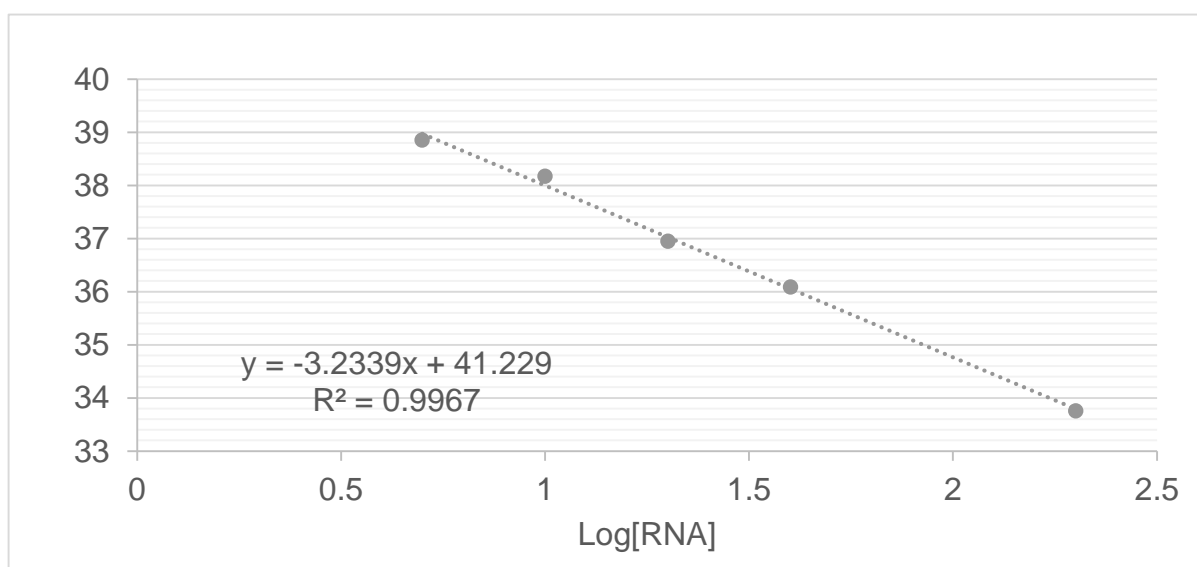
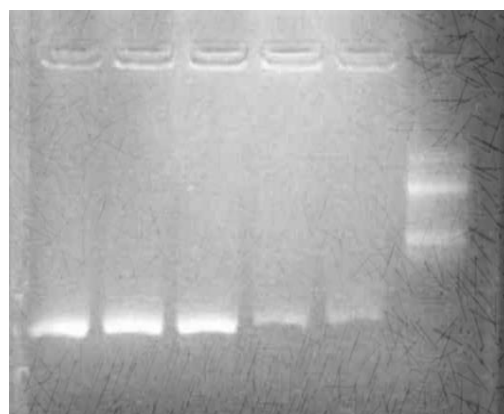
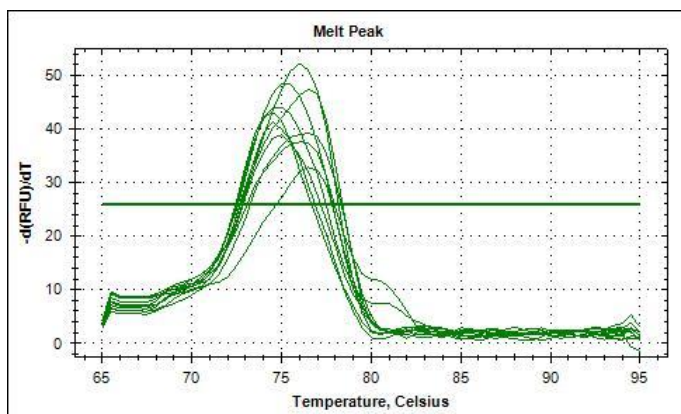
TNF-α	
Accession Number	NM_000594.3
Forward Sequence (5'→3')	CCCAGGGACCTCTTCTCTAATC (21)
Tm (°C)	61.8
GC content	57.1%
Reverse Sequence (5'→3')	ATGGGCTACAGGCTTGTCCT (21)
Tm (°C)	55.9
GC content	33.3%
% Efficiency	93.64%



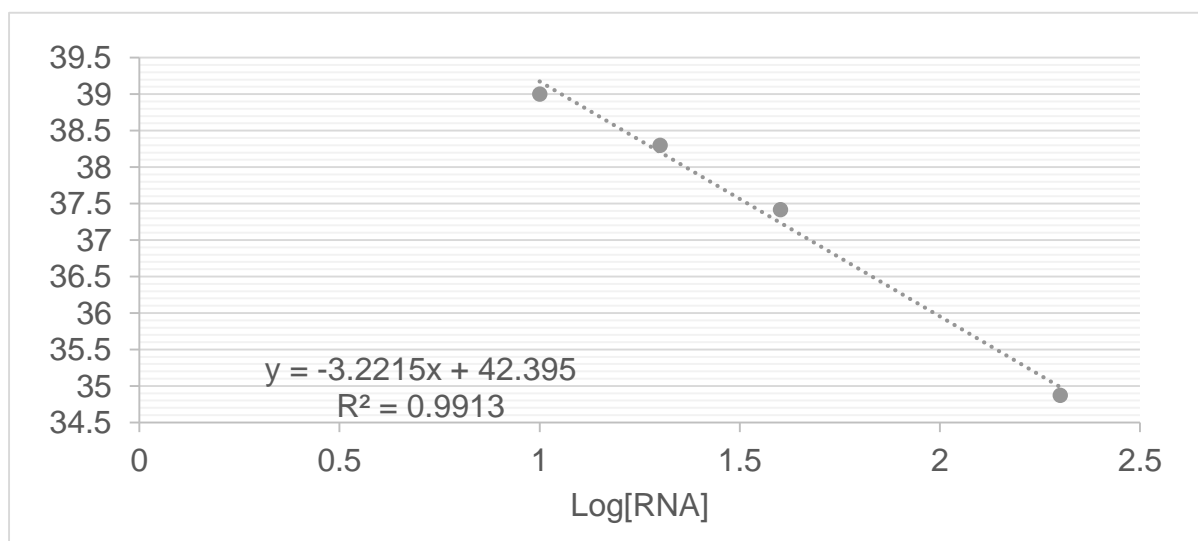
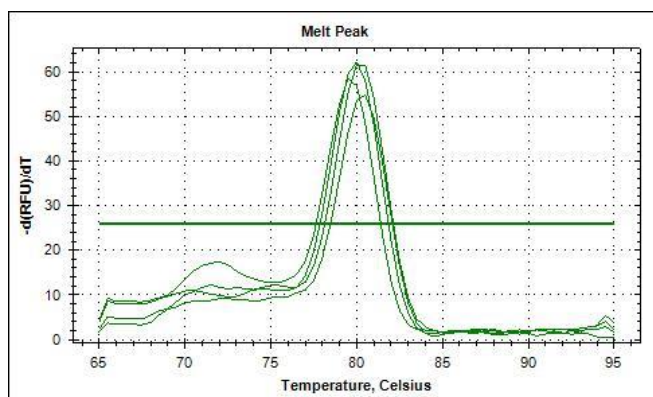
NaV1.5	
Accession Number	NM_198056.2
Forward Sequence (5'→3')	CATTTTCAGGGCTGAAGACCA
Tm (°C)	57.3
GC content	50%
Reverse Sequence (5'→3')	GGCAGAAGACTGTGAGGACC
Tm (°C)	61.4
GC content	60%
% Efficiency	91.7%



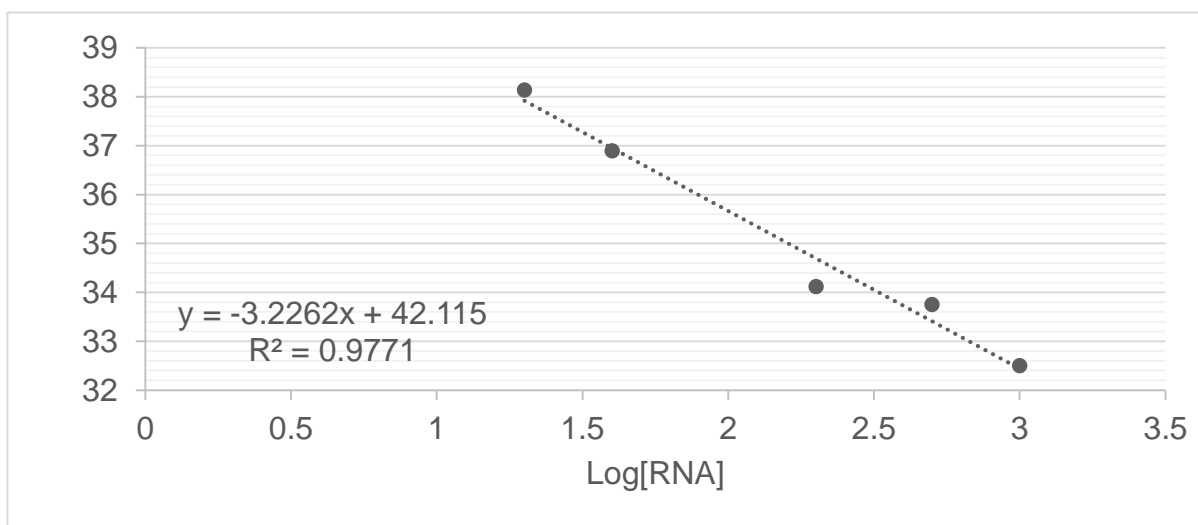
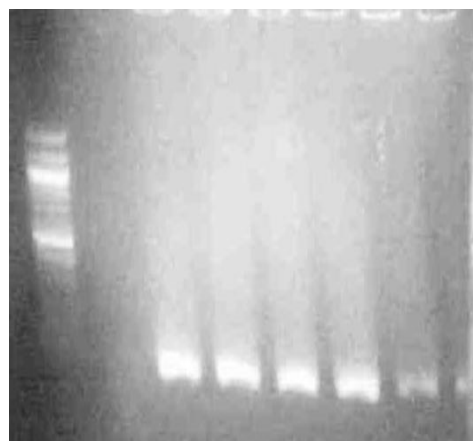
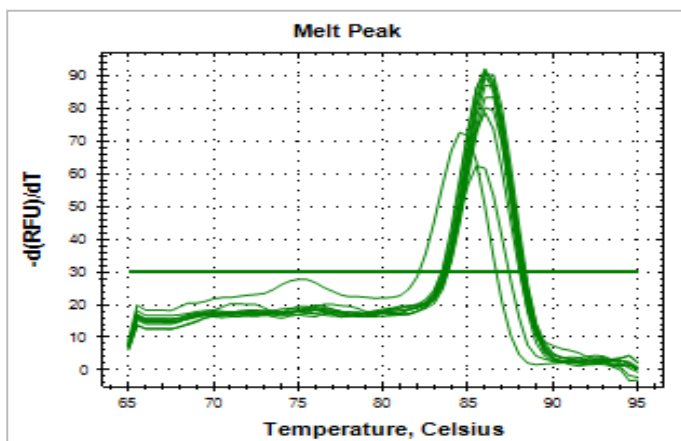
NaV1.6	
Accession Number	NM_014191.3
Forward Sequence (5'→3')	GGCAATGTTTCAGCTCTACGC
Tm (°C)	59.8
GC content	52.4%
Reverse Sequence (5'→3')	ATTGTCTTCAGGCCTGGGATT
Tm (°C)	59.8
GC content	47.6%
% Efficiency	103.8%



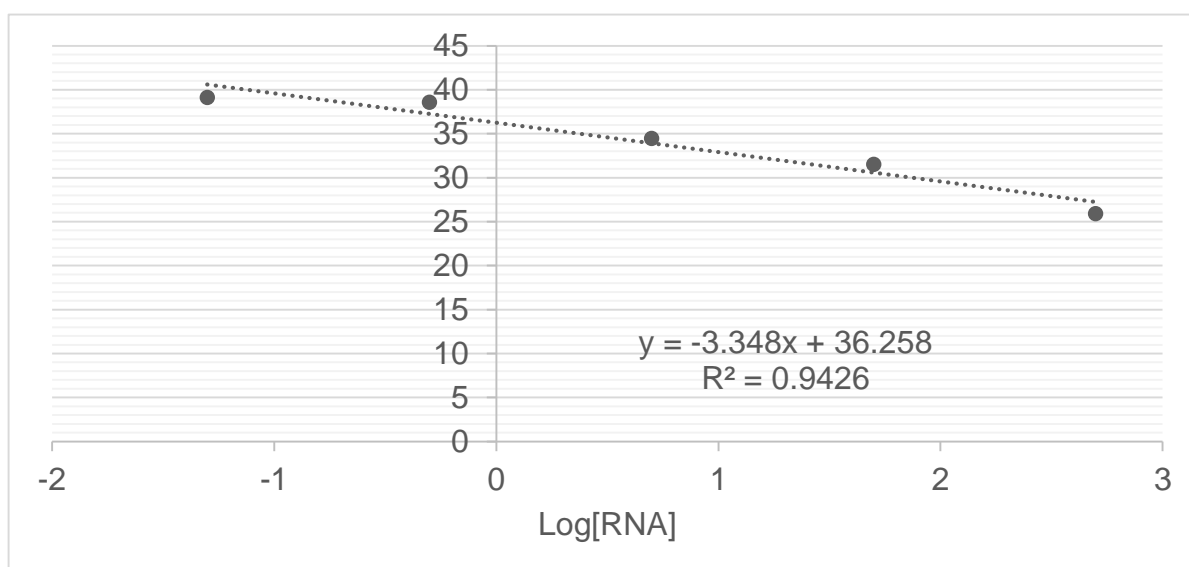
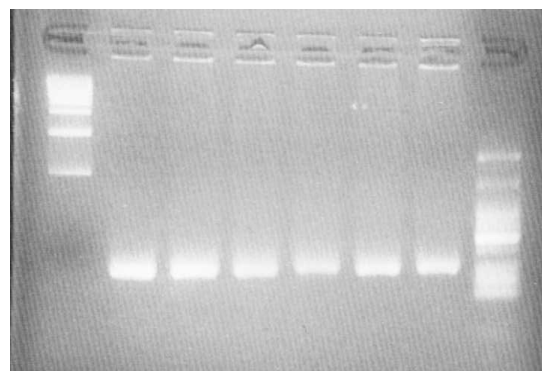
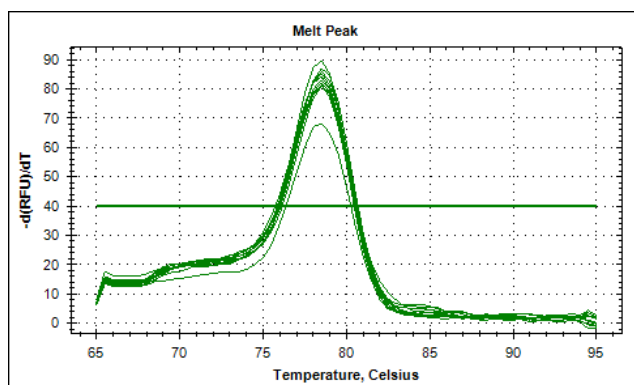
Kir2.1	
Accession Number	NM_000891.2
Forward Sequence (5'→3')	GGTTTGCTTTGGCTCAGTCG
T <sub>m</sub> (°C)	59.4
GC content	55%
Reverse Sequence (5'→3')	GAACATGTCCTGTTGCTGGC
T <sub>m</sub> (°C)	59.4
GC content	55%
% Efficiency	104.4%



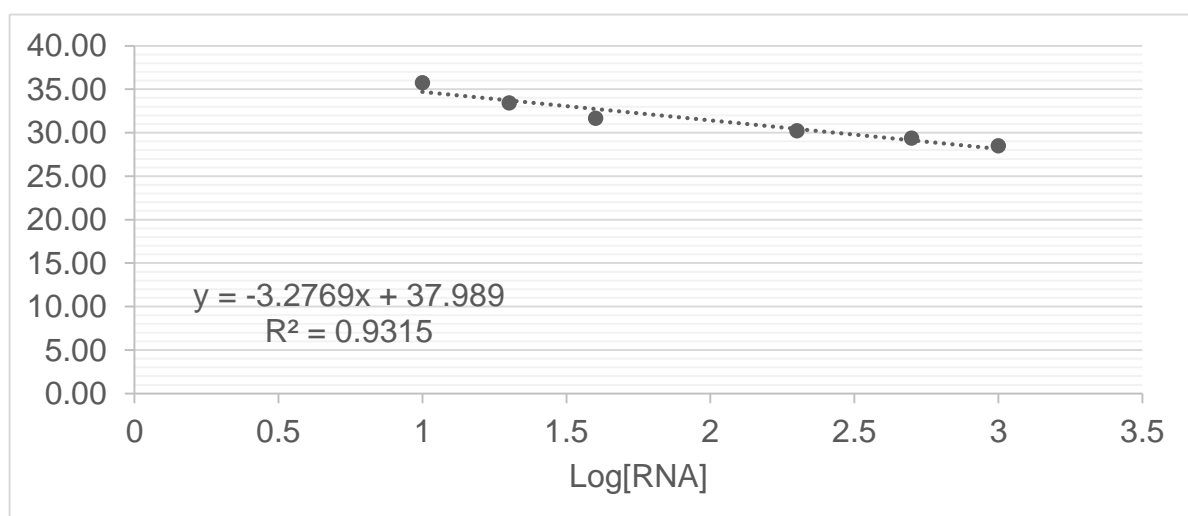
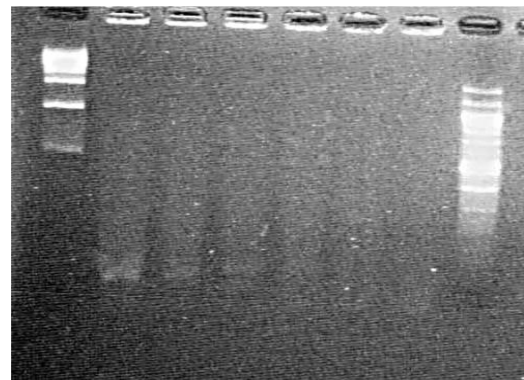
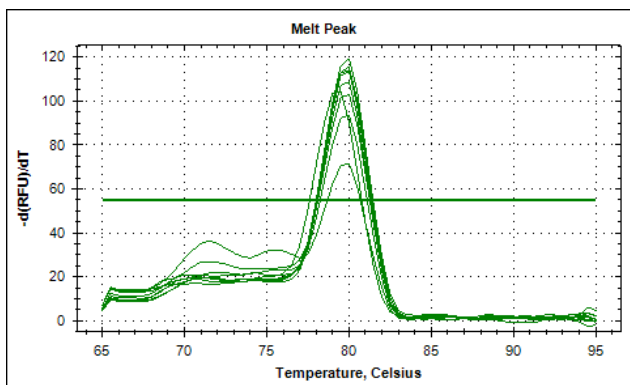
CD34	
Accession Number	NM_001025109.1
Forward Sequence (5'→3')	CTTTC AACCACTAGCACTAGCC (22)
Tm (°C)	60.3
GC content	50%
Reverse Sequence (5'→3')	TGCCCTGAGTCAATTTCACTTC (22)
Tm (°C)	58.4
GC content	45.5%
% Efficiency	104.15%



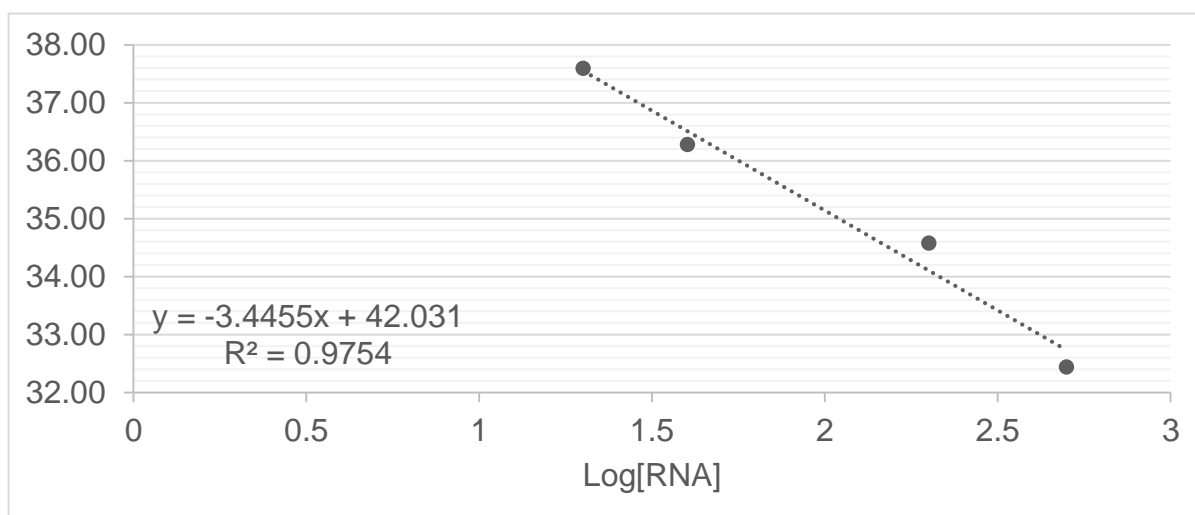
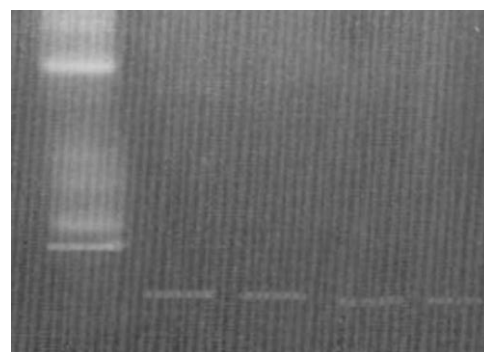
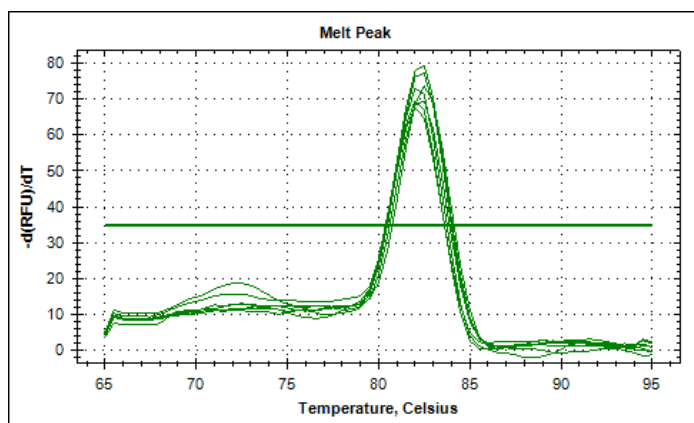
TREM2	
Accession Number	NM_018965.3
Forward Sequence (5'→3')	CTGGAGATCTCTGGTCCCC (20)
Tm (°C)	61.4
GC content	60%
Reverse Sequence (5'→3')	AGAAGGATGGAAGTGGGTGG (20)
Tm (°C)	59.4
GC content	55%
% Efficiency	98.9%



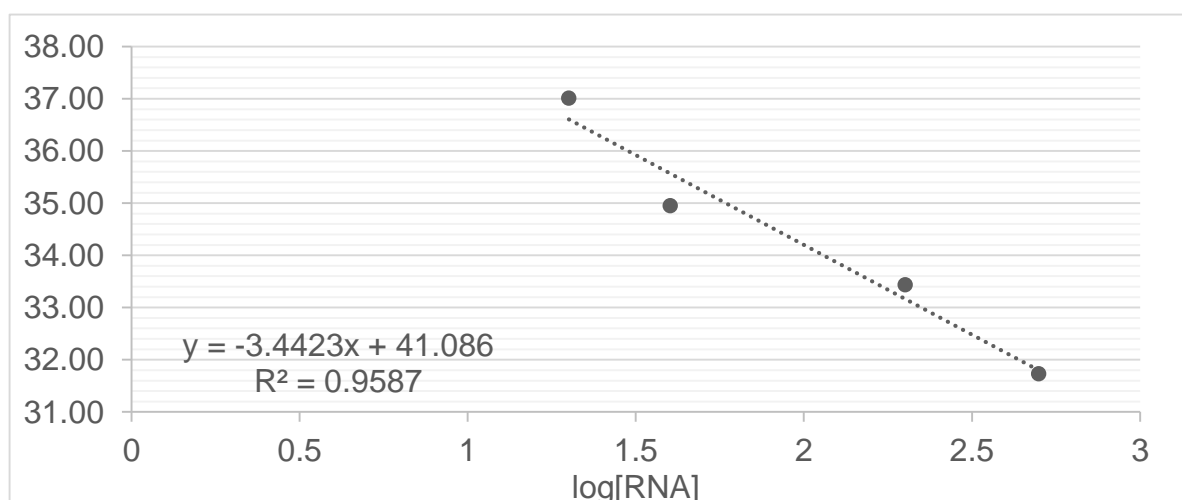
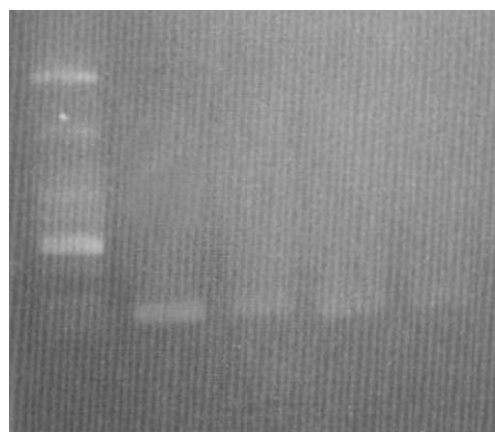
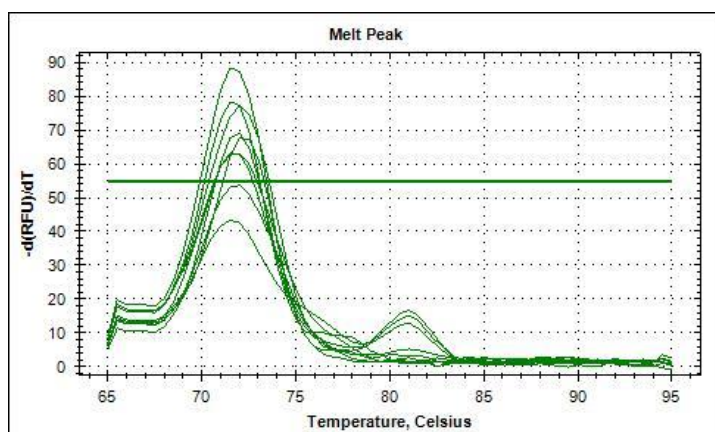
FLK1	
Accession Number	NM_001025366.2
Forward Sequence (5'→3')	GGCCCAATAATCAGAGTGGCA (21)
Tm (°C)	59.8
GC content	52.4%
Reverse Sequence (5'→3')	CCAGTGTCAATTCGATCACTTT (23)
Tm (°C)	59.8
GC content	43.5%
% Efficiency	101.9%



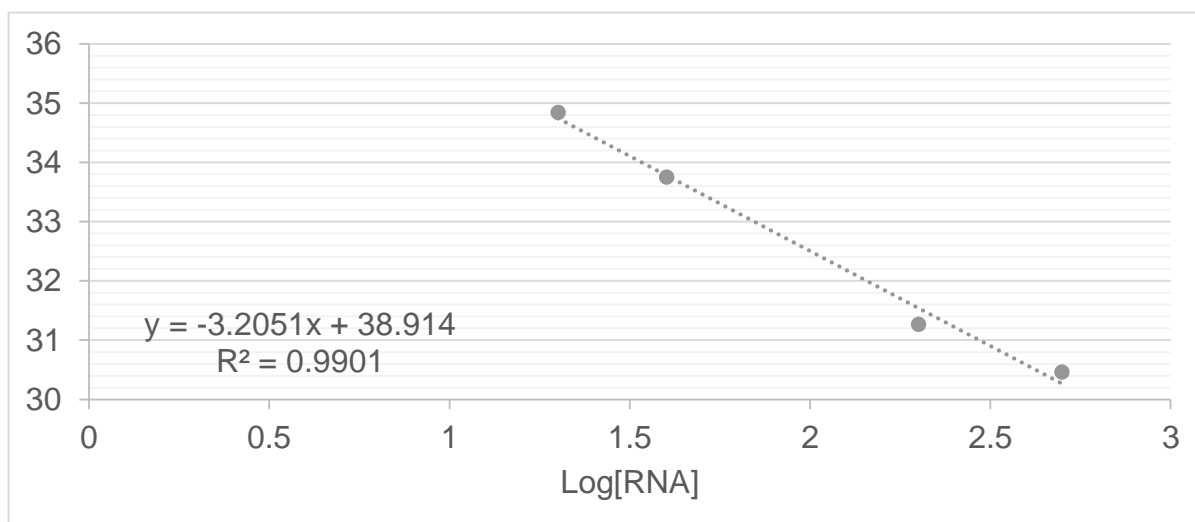
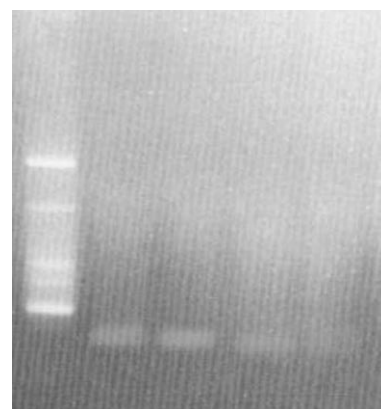
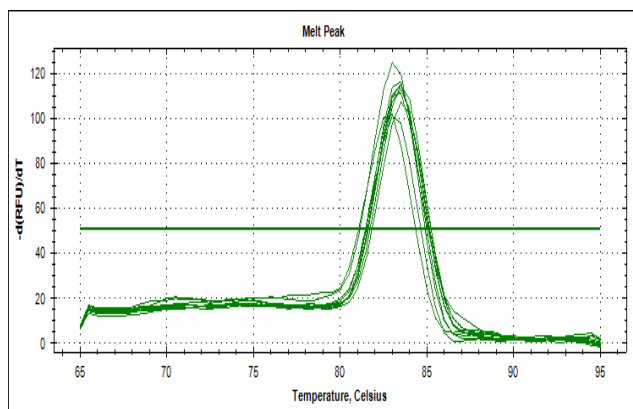
CD11c	
Accession Number	NM_00128675.1
Forward Sequence (5'→3')	GGAAGACCCTTCTCCAAGC (20)
T <sub>m</sub> (°C)	59.4
GC content	55%
Reverse Sequence (5'→3')	CAGAGGAGCTGACAGCCTTC (20)
T <sub>m</sub> (°C)	61.4
GC content	60%
% Efficiency	95.1%



CD80	
Accession Number	NM_005191.3
Forward Sequence (5'→3')	AGGGAACATCACCATCCAAG (20)
Tm (°C)	57.3
GC content	50%
Reverse Sequence (5'→3')	CAAACCTCGCATCTACTGGCA (20)
Tm (°C)	57.3
GC content	50%
% Efficiency	95.2%



NG2	
Accession Number	NM_001897.4
Forward Sequence (5'→3')	AGAAGCAAGTGCTCCTCTCG (20)
Tm (°C)	59.4
GC content	55%
Reverse Sequence (5'→3')	CCACTCAGCAGTCAGACCCT (20)
Tm (°C)	61.4
GC content	60%
% Efficiency	105%



<b>B-Actin</b>	
Accession Number	NM_001101.3
Forward Sequence (5'→3')	CCCAGCACAATGAAGATCAA (20)
T <sub>m</sub> (°C)	55.2
GC content	45%
Reverse Sequence (5'→3')	ACATCTGCTGGAAGGTGGAC (20)
T <sub>m</sub> (°C)	59.4
GC content	55%
% Efficiency	109%

